

USAAMRDL-TR-76-4

12



VALIDATION OF THE ROTORCRAFT FLIGHT SIMULATION
PROGRAM (C81) FOR ARTICULATED ROTOR HELICOPTERS
THROUGH CORRELATION WITH FLIGHT DATA

AD A 025934

United Technologies Corporation
Sikorsky Aircraft Division
Stratford, Connecticut 06602



May 1976

Final Report for Period June 1974 - January 1976

Approved for public release;
distribution unlimited.

Prepared for

EUSTIS DIRECTORATE

U. S. ARMY AIR MOBILITY RESEARCH AND DEVELOPMENT LABORATORY
Fort Eustis, Va. 23604

**Best
Available
Copy**

EUSTIS DIRECTORATE POSITION STATEMENT

This report provides an independent evaluation of the C-81 Rotorcraft Flight Simulation Computer Program as applied to articulated rotors. The version of C-81 evaluated did not, however, include the variable induced-velocity tables or permit precise location of flap and lag hinges considered potentially significant for rotor loads prediction. Results of this contract are being combined with results from similar contracts and in-house efforts to identify the strong and weak areas of C-81 prediction capability, and to establish a state-of-the-art position with regard to the global computer program concept for helicopter analysis. The results of this effort, while not exhaustive, are believed to be technically sound and within the originally intended scope.

Mr. G. Thomas White of the Technology Applications Division, Aeromechanics Area, served as Project Engineer for this investigation.

DISCLAIMERS

The findings in this report are not to be construed as an official Department of the Army position unless so designated by other authorized documents.

When Government drawings, specifications, or other data are used for any purpose other than in connection with a definitely related Government procurement operation, the United States Government thereby incurs no responsibility nor any obligation whatsoever; and the fact that the Government may have formulated, furnished, or in any way supplied the said drawings, specifications, or other data is not to be regarded by implication or otherwise as in any manner licensing the holder or any other person or corporation, or conveying any rights or permission, to manufacture, use, or sell any patented invention that may in any way be related thereto.

Trade names cited in this report do not constitute an official endorsement or approval of the use of such commercial hardware or software.

DISPOSITION INSTRUCTIONS

Destroy this report when no longer needed. Do not return it to the originator.

Unclassified

SECURITY CLASSIFICATION OF THIS PAGE (When Data Entered)

REPORT DOCUMENTATION PAGE		READ INSTRUCTIONS BEFORE COMPLETING FORM
1. REPORT NUMBER USAAMRD-TR-76-4	2. GOVT ACCESSION NO.	3. RECIPIENT'S CATALOG NUMBER
4. TITLE (and Subtitle) VALIDATION OF THE ROTORCRAFT FLIGHT SIMULATION PROGRAM (C81) FOR ARTICULATED ROTOR HELICOPTERS THROUGH CORRELATION WITH FLIGHT DATA		5. TYPE OF REPORT & PERIOD COVERED Final Report June 74-Jan 76
7. AUTHOR(s) S. J. Briczinski		6. PERFORMING ORG. REPORT NUMBER DAAG02-74-C-0046
9. PERFORMING ORGANIZATION NAME AND ADDRESS United Technologies Corporation Sikorsky Aircraft Division Stratford, Connecticut 06602		10. PROGRAM ELEMENT, PROJECT, TASK AREA & WORK UNIT NUMBERS 62208A 1F262208AH90 01 010 EK
11. CONTROLLING OFFICE NAME AND ADDRESS Eustis Directorate U.S. Army Air Mobility Research and Development Laboratory Fort Eustis, VA 23604		12. REPORT DATE May 1976
14. MONITORING AGENCY NAME & ADDRESS (if different from Controlling Office) DH-1-F-262208-111-76		13. NUMBER OF PAGES 155
		15. SECURITY CLASS. (of this report) Unclassified
16. DISTRIBUTION STATEMENT (of this Report) Approved for public release; distribution unlimited.		15a. DECLASSIFICATION/DOWNGRADING SCHEDULE
17. DISTRIBUTION STATEMENT (of the abstract entered in Block 20, if different from Report)		
18. SUPPLEMENTARY NOTES		
19. KEY WORDS (Continue on reverse side if necessary and identify by block number) Rotorcraft Flight Simulation Program C81, Validation for Articulated Rotor Helicopter, Correlation with Test Data		
20. ABSTRACT (Continue on reverse side if necessary and identify by block number) The Rotorcraft Flight Simulation Program C81 (Version AGAJ74) was run, simulating a wide variety of flight conditions, in order to gather data for comparison to flight test data and data originating from other analyses, to determine the accuracy with which the C81 program predicts various characteristics of articulated rotor helicopters. The C81 input data were prepared, modeling the H-53 and S-67 helicopters, and runs were made to obtain trim, performance, stability, time history response, and rotor loads data predictions.		

323800

Unclassified

SECURITY CLASSIFICATION OF THIS PAGE(When Data Entered)

The results of this study of the application of C81 to articulated rotor helicopters pointed out severe limitations to its application to rotors with any significant blade parameter discontinuities. Even under most favorable circumstances, this study did not indicate any significant increase in accuracy over other methods available for handling the disciplines covered by C81. While the ability to treat performance, stability and control, and rotor loads all within the same program has some advantages, in this case the advantages appear to be offset by excessive running times required for performance and maneuver response problems which normally can be handled by much simpler and quicker running programs.

Unclassified

SECURITY CLASSIFICATION OF THIS PAGE(When Data Entered)

PREFACE

The work reported herein was performed by the Sikorsky Aircraft Division of United Technologies Corporation for the U. S. Army Air Mobility Research and Development Laboratory under Contract DAAJ02-74-C-0046. Technical monitor for the contract was Mr. G. Thomas White of USAAMRDL. Sikorsky Aircraft personnel contributing to this program included Messrs. B. Campbell, A. Day, K. Hansen, R. Studwell, R. Johnston, R. Sopher, R. Blackwell, and D. Cooper.

TABLE OF CONTENTS

	<u>Page</u>
PREFACE.	3
LIST OF ILLUSTRATIONS.	5
LIST OF TABLES	10
INTRODUCTION	11
PROGRAM IMPLEMENTATION	12
PROGRAM INPUT DATA PREPARATION	14
METHOD OF CORRELATION AND DESCRIPTION OF TEST DATA	15
TRIM CORRELATION - RESULTS AND DISCUSSION.	17
PERFORMANCE CORRELATION - RESULTS AND DISCUSSION	22
STABILITY CORRELATION - RESULTS AND DISCUSSION	26
TIME HISTORY CORRELATION - RESULTS AND DISCUSSION.	31
ROTOR LOADS CORRELATION - RESULTS AND DISCUSSION	36
DISCUSSION OF GENERAL PROGRAM CHARACTERISTICS.	42
CONCLUSIONS.	46
RECOMMENDATIONS.	48
REFERENCES	49
LIST OF SYMBOLS.	154

LIST OF ILLUSTRATIONS

<u>Figure</u>		<u>Page</u>
1	CH-53A Articulated-Rotor Helicopter.	76
2	S-67 Articulated-Rotor Helicopter.	77
3	C81 Level Flight Trim vs Airspeed, Compared With Flight Test Data for the CH-53D at 35,000 Lb, Forward FSCG = 328 (100% N_r , h_d = 2000 Ft) . . .	78
4	C81 Level Flight Trim vs Airspeed, Compared With Flight Test Data for the CH-53D at 35,000 Lb, Mid FSCG = 336 (100% N_r , h_d = 2000 Ft)	80
5	C81 Level Flight Trim vs Airspeed, Compared With Flight Test Data for the CH-53D at 35,000 Lb, Aft FSCG = 352 (100% N_r , h_d = 2000 Ft)	82
6	C81 Level Flight Trim vs Airspeed, Compared With Flight Test Data for the S-67 at 16,500 Lb, Mid FSCG = 272 (104% N_r , h_d = 3000 Ft)	84
7	C81 Level Flight Trim vs Airspeed, Compared With Flight Test Data for the S-67 at 17,300 Lb, Forward FSCG = 253 (104% N_r , h_d = 3000 Ft) . . .	87
8	C81 Sideward Flight Trim vs Airspeed, Compared With Flight Test Data for the CH-53D at 42,000 Lb, Forward FSCG = 328 (100% N_r , h_d = 0 Ft).	90
9	C81 Rearward Flight Trim vs Airspeed, Compared With Flight Test Data for the CH-53D at 46,000 Lb, Forward FSCG = 328.3 (104% N_r , h_d = 2000 Ft) . .	92
10	C81 Hover Gross Weight vs Power Requirement, Compared With Flight Test Data for the CH-53A at 105% N_r and at Standard Sea Level Conditions (FSCG = 336)	94
11	C81 Level Flight Power Requirement vs Advance Ratio, Compared With Flight Test Data for the CH-53A at 42,000 Lb, 105% N_r , h_d = 2130 Ft (FSCG = 328, C_W = 0.0088).	95
12	C31 Level Flight Power Requirement vs Advance Ratio, Compared With Flight Test Data for the S-67 at 16,500 Lb, 102.5% N_r , h_d = 0 Ft (FSCG = 272.3, C_W = 0.00505)	96

<u>Figure</u>		<u>Page</u>
13	C81 Level Flight Power Requirement vs Advance Ratio, Compared With GRP Analysis and Flight Test Data for the CH-53A at 42,000 Lb, 105% N_r , $h_d = 2130$ Ft (FSCG = 328, $C_w = 0.0088$)	97
14	C81 Prediction of Main Rotor Thrust Coefficient vs Power Coefficient, Compared With Whirl Stand Test Data for the CH-53D Main Rotor Out of Ground Effect, at 100% N_r , and at Standard Sea Level Conditions.	98
15	C81 Prediction of Tail Rotor Thrust Coefficient vs Power Coefficient, Compared With Whirl Stand Test Data for the CH-53A Tail Rotor Out of Ground Effect, at 100% N_r , and at Standard Sea Level Conditions.	99
16	C81 Maximum Rate of Climb Performance vs Airspeed, Compared With Flight Test Data for the HH-53C at 35,000 Lb at Various Density Altitudes (100% N_r , FSCG = 340)	100
17	C81 Maximum Rate of Descent in Autorotation vs Airspeed, Compared With Flight Test Data for the HH-53C at 35,000 Lb, 100% N_r , $h_d = 4500$ Ft (FSCG = 340)	101
18	C81 Main Rotor and Body Root Locus, Compared With GENHEL Analysis Data for the CH-53A in Hover (33,500 Lb, FSCG = 348)	102
19	C81 Main Rotor and Body Root Locus, Compared With GENHEL Analysis Data for the CH-53A at 100 Kt (33,500 Lb, FSCG = 348)	103
20	C81 Main Rotor and Body Root Locus, Compared With GENHEL Analysis Data for the CH-53A at 150 Kt (33,500 Lb, FSCG = 348)	104
21	C81 Prediction of Time to Double Amplitude and Period of Phugoid Modes, Compared With GENHEL Data for the CH-53A at Various Speeds (33,500 Lb, FSCG = 348)	105
22	C81 Body Root Locus Compared With Flight Test System-Identified Data for the CH-53A at 100 Kt (35,000 Lb, FSCG = 352)	106
23	C81 Body Root Locus Compared With Flight Test System-Identified Data for the CH-53A at 150 Kt (35,000 Lb, FSCG = 352)	107

<u>Figure</u>		<u>Page</u>
24	C81 Body Root Locus Compared With Flight Test Time-History-Fitted Data for the S-67 at 100 Kt (14,800 Lb, FSCG = 276)	108
25	C81 Body Root Locus Compared With Flight Test Time-History-Fitted Data for the S-67 at 140 Kt (14,800 Lb, FSCG = 276)	109
26	C81 Body Root Locus Compared With Flight Test Time-History-Fitted Data for the S-67 at 180 Kt (14,800 Lb, FSCG = 276)	110
27	C81 Maneuver Response Time History Comparison With Flight Test Data for the CH-53A at 100 Kt, Following a Forward Stick Pulse Input (33,539 Lb, FSCG = 347.7)	111
28	C81 Maneuver Response Time History Comparison With Flight Test Data for the HH-53C in Hover, Following a Forward Stick Pulse Input (31,000 Lb, FSCG = 328)	114
29	C81 Maneuver Response Time History Comparison With Flight Test Data for the HH-53C in Hover, Following a Right Lateral Stick Pulse Input (31,000 Lb, FSCG = 328)	117
30	C81 Maneuver Response Time History Comparison With Flight Test Data for the HH-53C in Hover, Following a Left Pedal Pulse Input (31,000 Lb, FSCG = 328)	120
31	C81 Maneuver Response Time History Comparison With Flight Test Data for the HH-53C in Hover, Following an Aft Stick Step Input (31,000 Lb, FSCG = 328)	123
32	C81 Maneuver Response Time History Comparison With Flight Test Data for the HH-53C in Hover, Following a Right Lateral Stick Step Input (31,000 Lb, FSCG = 328)	126
33	C81 Maneuver Response Time History Comparison With Flight Test Data for the HH-53C in Hover, Following a Right Pedal Step Input (31,000 Lb, FSCG = 328)	129
34	C81 Maneuver Response Time History Comparison With Flight Test Data for the HH-53C at 113 Kt, Following a Forward Stick Step Input (41,000 Lb, FSCG = 328)	132

<u>Figure</u>		<u>Page</u>
35	C81 Maneuver Response Time History Comparison With Flight Test Data for the HH-53C at 113 Kt, Following a Left Lateral Stick Step Input (41,000 Lb, FSCG = 328)	135
36	C81 Maneuver Response Time History Comparison With Flight Test Data for the HH-53C at 113 Kt, Following a Right Pedal Step Input (41,000 Lb, FSCG = 328)	138
37	C81 Solutions of Blade Beamwise Bending Moment vs Span at $\psi_{MR} = 60$ Deg as Functions of Mode Shape, Hinge Offset, and Mass Distribution for the CH-53A in Hover at 32,550 Lb.	141
38	C81 Solutions of Blade Chordwise Bending Moment vs Span at $\psi_{MR} = 60$ Deg as Functions of Mode Shape, Hinge Offset, and Mass Distribution for the CH-53A in Hover at 32,550 Lb.	142
39	C81 Rotor Loads Solution of Blade Steady Beamwise Bending Moment vs Span, Compared With Flight Test and Y200 Analysis Data for the CH-53A at 159 Kt, 33,070 Lb (103% N_r , $h_d = 3000$ Ft, FSCG = 336, Level Flight)	143
40	C81 Rotor Loads Solution of Blade Vibratory Beamwise Bending Moment vs Span, Compared With Flight Test and Y200 Analysis Data for the CH-53A at 159 Kt, 33,070 Lb (103% N_r , $h_d = 3000$ Ft, FSCG = 336, Level Flight)	144
41	C81 Rotor Loads Solution of Harmonic Content of Blade Vibratory Beamwise Bending Moment at Approxi- mately 80% Blade Span, Compared With Flight Test and Y200 Analysis Data for the CH-53A at 159 Kt, 33,070 Lb (103% N_r , $h_d = 3000$ Ft, FSCG = 336, Level Flight)	145
42	C81 Rotor Loads Time History Solution of Total Blade Beamwise Bending Moment at Approximately 80% Blade Span, Compared With Flight Test and Y200 Analysis Data for the CH-53A at 159 Kt, 33,070 Lb (103% N_r , $h_d = 3000$ Ft, FSCG = 336, Level Flight)	146
43	C81 Rotor Loads Solution of Blade Steady Chordwise Bending Moment vs Span, Compared With Flight Test and Y200 Analysis Data for the CH-53A at 159 Kt, 33,070 Lb (103% N_r , $h_d = 3000$ Ft, FSCG = 336, Level Flight)	147

<u>Figure</u>		<u>Page</u>
44	C81 Rotor Loads Solution of Blade Vibratory Chordwise Bending Moment vs Span, Compared With Flight Test and Y200 Analysis Data for the CH-53A at 159 Kt, 33,070 Lb (103% N_r , h_d = 3000 Ft, FSCG = 336, Level Flight)	148
45	C81 Rotor Loads Solution of Harmonic Content of Blade Vibratory Chordwise Bending Moment at Approximately 55% Blade Span, Compared With Flight Test and Y200 Analysis Data for the CH-53A at 159 Kt, 33,070 Lb (103% N_r , h_d = 3000 Ft, FSCG = 336, Level Flight)	149
46	C81 Rotor Loads Time History Solution of Total Blade Chordwise Bending Moment at Approximately 55% Blade Span, Compared With Flight Test and Y200 Analysis Data for the CH-53A at 159 Kt, 33,070 Lb (103% N_r , h_d = 3000 Ft, FSCG = 336, Level Flight)	150
47	C81 Rotor Loads Solution of Blade Steady Torsional Moment vs Span, Compared With Flight Test and Y200 Analysis Data for the CH-53A at 159 Kt, 33,070 Lb (103% N_r , h_d = 3000 Ft, FSCG = 336, Level Flight)	151
48	C81 Rotor Loads Solution of Blade Vibratory Torsional Moment vs Span, Compared With Flight Test and Y200 Analysis Data for the CH-53A at 159 Kt, 33,070 Lb (103% N_r , h_d = 3000 Ft, FSCG = 336, Level Flight)	152
49	C81 Rotor Loads Solution of Harmonic Content of Blade Vibratory Torisonal Moment at Approximately 15% Blade Span, Compared With Flight Test and Y200 Analysis Data for the CH-53A at 159 Kt, 33,070 Lb (103% N_r , h_d = 3000 Ft, FSCG = 336, Level Flight)	153

LIST OF TABLES

<u>Table</u>		<u>Page</u>
I	Basic Aircraft Descriptive Data	52
II	C81 Input Listing for H-53.	54
III	C81 Input Listing for S-67.	56
IV	C81 Preloaded 0012 Airfoil Data	58
V	Sikorsky Version of 0012 Airfoil Data in C81 Format.	60
VI	H-53 Aeroelastic Blade Data Used in C81	62
VII	S-67 Aeroelastic Blade Data Used in C81	64
VIII	C81 Program Validation Data Cases	66
IX	CH-53A Trim at 100 Kt, 33,500 Lb, 348 FSCG, Calculated by the C81 and the GENHEL Analyses .	69
X	Coordinated Turn Trim for the CH-53D at 46,000 Lb, 328.3 FSCG, 104% N_T , Test Data Comparison to C81 Analysis.	70
XI	Rotor and Body Stability Derivatives for the CH-53A at 100 Kt, 33,500 Lb, 348 FSCG, Obtained From the C81 and the GENHEL Analyses .	71
XII	Body Stability Derivatives for the CH-53A at 100 Kt, 33,500 Lb, 348 FSCG, Obtained From the C81 and the GENHEL Analyses.	73
XIII	CH-53A Main Rotor Blade Flapping Mode Shapes and Mass Distributions Used In Investigatory C81 Rotor Loads Solution Runs	74
XIV	Comparison of C81 Main Rotor Trim Parameters for Free Aircraft and Shaft-Fixed Solutions With Flight Test Data for the CH-53A With Neutral (336 FSCG) Center of Gravity Location .	75

INTRODUCTION

The Rotorcraft Flight Simulation Program C81 is a modular computer program capable of performing performance, stability, and rotor loads solutions. This complex and comprehensive program may be operated in a variety of ways. Data input and selection of user options determine the degree of interaction between the different analyses offered by the program, and determine the complexity of each of the major sections of the program. The C81 essentially utilizes the modular concept of programming the different major analyses comprising a global program package. The program is described in some detail in References 1 through 3.

The C81 program was developed by the Bell Helicopter Company, and has been made available to the rotorcraft industry by the U. S. Army. Although used and validated mostly with helicopters with teetering rotor systems, the program is also intended for modeling helicopters with articulated or hingeless rotors. At the request of the U. S. Army Air Mobility Research and Development Laboratory, Eustis Directorate, this study was conducted by Sikorsky Aircraft to validate the C81 program for use with articulated rotor helicopters.

This report describes the comparison of the C81 program with test data. Correlation results are presented and discussed for the H-53 (S-65) and S-67 aircraft. The usefulness of the C81 program as an articulated rotor helicopter design tool is evaluated based on the correlation data gathered in the study. This report also provides constructive criticism of those areas of the program needing improvement to increase accuracy.

Both the Sikorsky H-53 and the Sikorsky S-67 aircraft represent single-rotor helicopters with anti-torque tail rotors. The main rotors of these aircraft are fully articulated, employing blade flapping and lagging (hunting) hinges. The twin turbine engine H-53 is basically a transport helicopter, although it has also been used for a number of other purposes. Many production versions of the H-53 exist, but the basic characteristics of these versions are quite similar. Figure 1 is a drawing of the CH-53A. The twin turbine engine S-67 demonstrator aircraft was designed as a high-speed derivative of the Sikorsky S-61 (SH-3D) helicopter. Wings could be attached to the sponsons for additional lift and attachment points for armament. Figure 2 is a drawing of the S-67. Principal dimensions and general data for the H-53 and S-67 aircraft are presented in Table I.

PROGRAM IMPLEMENTATION

The Eustis Directorate provided Sikorsky Aircraft with a copy of the 300K (300,000) bytes of core storage rendition of the Rotorcraft Simulation Program C81, Version AGAJ74. This version of the program was adapted for use on the contractor's IBM 370/155 computer system. The 300K core version of the C81 program differs from the full size 600K core version of the program primarily in the number of input data tables that may be loaded into the program. Rotor-induced velocity of the rotor wake acting at aerodynamic surfaces cannot be loaded into the smaller 300K version of the program. These phenomena are described instead by analytic expressions in the version of the C81 used in this correlation study. Whereas the 600K version of the C81 provides for up to five airfoil data tables to be loaded into the program to describe the aerodynamic characteristics of rotor blades or aerodynamic surfaces, the 300K version of the C81 has room for only two such tables.

No major problems were encountered in converting the IBM 360-65 copy of the program for operation on the IBM 370/155 computer system. The program was initially compiled using a G2 compiler. Later, in an effort to reduce the running time of the program, it was re-compiled using the H2 (H - extended) compiler. (The running time requirement is discussed in the General Program Characteristics section of this report.)

A number of check cases were provided by USAAMRDL to determine if the C81 program had been converted properly to the IBM 370/155 system. The check cases included: (1) a quasi-static trim followed by a quasi-static maneuver of approximately two seconds duration for the AH-1G; (2) a quasi-static trim followed by a time-variant trim and maneuver of approximately four seconds duration for the AH-1G with an automatic-pilot feedback; and (3) a quasi-static trim and stability solution of a modified UH-1D/H deck which analytically simulated an articulated rotor helicopter. The input data for these cases were loaded into the IBM 370 version of the C81 and the program was executed. The solutions were compared with the check case solutions provided by the Eustis Directorate. The correlation of these three check cases was discussed in detail with the contract technical representative at Fort Eustis; the printout for check case 1 was delivered to the Eustis Directorate as required by contract. With the exception of the portion of the time history maneuver response which followed the activation of the Automatic Pilot routine, all portions and options of the C81 program investigated by the check cases at the contractor's facilities yielded the same results as those provided by the Eustis Directorate. The only inconsistency involved the Automatic Pilot routine and was explained as an error or modification in the routine. But, since the Automatic Pilot routine

would not be needed for the planned correlation study, it was decided that the C81 program had been made properly operational at the contractor's facilities.

About midway through the C81 prediction/correlation effort, a CALCOMP plotting system was installed at the contractor's facilities and was interfaced with the C81 program which possesses a CALCOMP plotting capability. The CALCOMP routine was used to plot some of the time histories that were run in the correlation effort. An evaluation of the C81 CALCOMP routine can be found in the Discussion of General Program Characteristics section of this report.

PROGRAM INPUT DATA PREPARATION

Rotor blade airfoil data, aerodynamic data, blade bending mode shape data, and all other necessary aircraft characteristic data required as input to the C81 program were prepared for the H-53 (S-65) and S-67 single-rotor helicopters. The H-53 and S-67 input data for the C81 program were drawn from References 4 through 9. Some of the basic data from these references were manipulated as required to present them in a form compatible with the C81 program. The digital computer program AS812A, written in the PL/I computer language, was obtained from the Eustis Directorate and used to convert fuselage wind tunnel data into aerodynamic input data for the C81 for the H-53 and S-67 aircraft. An existing in-house Sikorsky digital computer program was used to calculate the blade normal mode shapes. These data, in turn, were manipulated by hand to prepare them for the C81 input format. A short FORTRAN program was written to convert existing airfoil data from the Sikorsky input format to an input format compatible with the C81. Appropriate airfoil data were then converted for the correlation effort. The Sikorsky airfoil data converted for use with the C81 program consisted of data which were smoothed to best fit a number of sets of raw data obtained from many wind tunnel tests of each airfoil section under consideration. Comments regarding the C81 input format and problems encountered while preparing data for input into the C81 program are presented in the Discussion of General Program Characteristics section and other related sections.

Tables II through VII are listings from the C81 program of the basic inputs, airfoil data, and blade aeroelastic data for the H-53 and S-67 aircraft which were used in the majority of the C81 runs conducted as part of the correlation effort. When any input datum is related to a problem or an inadequacy in the C81 program, the datum is described in sufficient detail in the appropriate sections of the report.

METHOD OF CORRELATION AND DESCRIPTION OF TEST DATA

The validation of the C81 program was accomplished through comparison of test data with the data calculated by the C81 rotorcraft analysis. For each correlation case investigated, helicopter speed, weight loading, and control inputs were loaded into the C81 to best duplicate the conditions flown in the test program. The C81 and test data correlation results were drawn on to evaluate the accuracy of the C81 program in modeling articulated helicopter static and dynamic flight characteristics.

Flight test and whirl stand test data used in the correlation effort were selected based on confidence in the accuracy of the data as well as the ease of accessibility. The test data represented cases chosen to exercise the three major portions of the C81: trim, stability and control, and maneuver. Where available, results from other digital rotorcraft analyses were also used for comparison with the C81 program.

The major prediction efforts conducted under this study are more specifically defined by five types of data comparisons:

- (1) Trim
- (2) Performance
- (3) Stability (roots and derivatives)
- (4) Time history (helicopter response characteristics)
- (5) Rotor loads

Table VIII lists all of the conditions under these five areas that were successfully executed by the C81 program, producing data for the correlation study. The reports from which the data were selected, against which the C81 is compared, are listed in the reference section. Pertinent test and analytic data from these sources and the corresponding C81 data appear in the following sections of this report.

The test data used in the correlation effort were taken from Reference 7 and from References 9 through 16. The trim data from References 9 and 10, and the unpublished S-67 trim data are raw flight test data. The unpublished S-67 performance data and the forward speed performance data from Reference 12 also are raw flight test data. The hover performance data from Reference 12 are test data which have been analytically fitted and extrapolated from raw flight test data. The main rotor and tail rotor whirl stand data are refined from raw test stand data to reflect standard sea level conditions. The climb and autorotation test data from Reference 14 are refined from

raw flight test data to reflect consistency in atmospheric conditions. The root locus data from References 15 and 16 have been processed from smoothed time history flight test data. All time history and rotor loads data from References 7, 11, 14, and 16 have been filtered to remove high frequency noise content from the flight test data. All test data selected here for correlation purposes are of high accuracy within each specific data type (trim, performance, response, and rotor loads).

Contract schedule and budget restrictions dictated the number of C81 runs made during the study. (Approximately 260 exploratory and data runs were made.) All C81 program updates and modifications specified by the program developer, through USAAMRDL, for the AGAJ74 version were incorporated in any H-53 and S-67 data runs. Flight conditions that were attempted but not run successfully (and therefore not listed in Table VIII) are discussed in the following sections. Those flight conditions in Table VIII that were run with only moderate success or with great difficulty are also elaborated on in the following sections.

The following sections of the report group the results and evaluation of the C81 comparative study according to the major analyses conducted by the C81 program. Any noteworthy characteristics of the C81 experienced while running or analyzing particular aspects of the program are described in the appropriate sections. Good and poor characteristics of the C81 that have been discovered in this correlation effort are discussed. The activation or deactivation of levels of program sophistication or the selection of program options is defined or explained when necessary. Also, a section of this report is devoted to discussion of general program input, operational, and output characteristics that are not specifically related to one of the five basic types of program analyses under investigation.

TRIM CORRELATION - RESULTS AND DISCUSSION

The general trim solution of the C81 program is of great interest, because practically every type of analysis offered by the program begins by calculating the trim conditions of the rotorcraft. In computing data cases for the articulated rotor correlation, a few problems were experienced pertaining to trim iteration solutions. These occasionally experienced difficulties are discussed first.

Although the version of the C81 program used in this validation study contained its own table of 0012 airfoil data, another table was prepared in the C81 input format based on 0012 airfoil data existing at the contractor's facility. Also converted for input to the C81 program was a table of modified 0011 airfoil data, intended for use in modeling the H-53 aircraft. Often initial efforts to trim the H-53, modeled by the C81, would not succeed, even following as many as 50 trim iterations. Study of the trimming routine partial derivative matrix revealed that the main rotor moments were oscillating by repeatedly identical values, above the trim tolerance loaded into the program. When the contractor's version of 0012 airfoil data was used, occasionally the same problem would occur. When the C81 version of 0012 airfoil data was substituted in an otherwise identical case, trims were always successfully obtained, even though differences in the two sets of 0012 data were apparently negligible. In order to run the program as efficiently as possible, and because H-53 flight characteristics were shown not to be highly influenced by the differences in 0011 and 0012 airfoil data, the C81 version of the airfoil data was used exclusively during the remainder of the correlation study. Although it was not determined why the use of only the C81-supplied airfoil data guaranteed successful convergence of trim rotor moments, a possible explanation may be that the airfoil angle-of-attack and Mach number increments selected for loading the airfoil data table at high angles of attack are more critical than originally thought. Tables IV and V may be used to compare the 0012 airfoil data supplied within the C81 program to the 0012 airfoil data prepared for the C81 from Sikorsky data tables for this airfoil. The C81-supplied 0012 data tables were used in modeling the S-67 by the C81 program in order to avoid re-experiencing trimming difficulties similar to those encountered with the H-53 simulation.

In rare instances it was not possible to trim the helicopter while fixing either the roll or yaw angle at a specific value. This situation was experienced while trying to trim the S-67 at a 1.5-deg yaw angle. The C81 would not trim the helicopter for either + 1.5 deg yaw, yet it trimmed successfully at a zero yaw angle. Side force and yawing moment were not different enough between these different yaw conditions to account for the experienced trim difficulties.

For certain flight conditions, the C81 trim routine appeared to be very sensitive to the input starting values of control position, particularly the pedal setting. For some runs, the trim routine successively modified the control input in the wrong direction, without being able to correct itself within the given number of trim iterations, and thus failed to trim. This situation occurred quite frequently when the C81 attempted coordinated turns, and occasionally occurred when the C81 attempted various other flight conditions.

Sometimes the main rotor flapping angles a_1 and b_1 were

printed out as asterisks (*) in the time-variant trim solution. Experience running the program indicated that this occurred whenever the value of XIT(2) (the rotor azimuth increment during the time-variant trim), was not small enough to allow at least ten calculations per highest blade bending mode frequency. This characteristic was observed a number of times even though the user's manual claims that the C81 will calculate and substitute the proper value for the parameter XIT(2) if an improper value is loaded into the program. The lack of a solution for a_1 or

b_1 in a time-variant trim prevents the program from proceeding to following stacked cases (if requested).

In isolated cases, when at least five bending modes were input for a quasi-static/time-variant trim search, the time-variant rotor flapping angles printed out were asterisks. There probably was not enough memory storage for the program (particularly if there had been a high number of rotor blades), so that some values were overwritten, thus contaminating portions of the solution.

Another general trim problem concerned stacking cases using different numbers of rotor elastic modes. The C81 would not converge on a quasi-static trim if the preceding case was a quasi-static trim for a condition using a higher number of elastic modes. Most likely, some residual variables in the trim solution of the preceding case associated with the blade mode shapes were not zeroed out before the C81 began the unsuccessful case.

Turning now to the specific trim conditions that were studied, the bulk of the C81 trim data cases that were run requested the quasi-static trim option and were run with only two main rotor elastic modes (hinged rigid flapping and lagging). Initial C81 runs that were made to investigate the effects of five, four, or two rotor normal modes showed that the number of modes had little influence on trim values of aircraft attitudes, control positions, or flapping. Most pertinent trim parameters are held constant within the C81 when going from a

quasi-static to a time-variant trim solution. Investigatory runs showed negligible variation in trim parameters between the quasi-static/time-variant pairs of solutions. Yawed flow and unsteady aerodynamics also proved to have negligible effect.

Figures 3, 4, and 5 show the trim pitch attitude control angle versus speed for the CH-53D modeled by the C81, compared to flight test data at three center-of-gravity positions. The collective pitch calculated by the C81 is typically higher than that indicated by flight test data throughout the speed range, except at high speeds, where it is lower. The difference in tail rotor pitch between the test data and the values predicted by the C81 reflects the inability of the C81 to model the delta-3 (flap/pitch) coupling of the tail rotor blades of the CH-53D. The delta-3 was loaded into the program input, but the program solution was identical to a case run using no delta-3. The delta-3 causes the effective blade pitch to be lower than the pitch impressed by the control system. The test data are impressed control system inputs; the values calculated by the C81 are effective pitch angles.

Figure 6 shows S-67 trim data versus speed for mid center-of-gravity loading, while Figure 7 shows other trim parameters for the S-67 at the forward center of gravity. Both figures contain flight test and C81 predicted data. The fuselage angle-of-attack correlation in Figure 6 illustrates a C81 program deficiency in that the influence of the rotor-induced velocity on the fuselage is not calculated. Also, the lack of such a downwash calculation certainly has some influence on the accuracy of prediction of the required thrust and main rotor collective blade pitch.

In general, the data of Figures 6 and 7 indicate that the prediction of aircraft attitude and cyclic control angles by the C81 becomes less accurate at increasing forward speeds. The program solution of roll attitude in particular seems to be overly sensitive. Similar to the CH-53D level-flight correlation of Figures 3, 4, and 5, the S-67 level-flight correlation indicates that the C81 predicts lower collective pitch requirements at high speed than are indicated by the flight test data. The rotor aerodynamic characteristics at high local blade angles of attack may not be calculated with sufficient accuracy by the C81. Unlike the CH-53D correlation, the S-67 data comparison shows the required C81 trim collective pitch at low and moderate speeds to be lower than the test values. The wing of the S-67 may be carrying too much lift in these C81 simulations. Similar to the CH-53D correlation, the S-67 tail rotor pitch requirement predicted by the C81 differs somewhat from the flight test data due to the delta-3 hinge. For the S-67, another contribution to the difference in tail rotor pitch may be due to a less than accurate calculation of the force produced by the highly effective vertical tail of this helicopter.

The prediction of the S-67 pitch attitude and longitudinal cyclic control between 60 and 100 kt forward speed, seen in Figure 7 describes an unusual trend in the values predicted by the C81 program. The jump in these data might suggest a severe discontinuity in either the fuselage aerodynamic data or the airfoil data inputs; however, no such discontinuity was discovered upon examination of these data tables. A possible explanation for this isolated trim characteristic may lie in the aerodynamic calculations of the wing or horizontal tail within the C81 program.

Inconsistencies between C81 and test trim parameters are influenced by the aerodynamic characteristics of the fuselage. The fuselage aerodynamics within the C81 are represented by analytic expressions, which are third-order functions of angle of attack and sideslip. When these C81 input data were derived from existing wind tunnel map data, experience showed that the C81 input data could not represent even small variations from smooth, relatively simple curves in the aerodynamic forces and moments plotted against angle of attack or sideslip, even though such variations were often present in the wind tunnel data. Therefore, the fuselage aerodynamic data used by the C81 were not as accurate as the available wind tunnel map data.

A C81 run was set up with inputs corresponding to conditions previously used to model the CH-53A helicopter at 100 kt on the Sikorsky General Helicopter Simulation Program, GENHEL. (The GENHEL program is described in References 17 and 18.) Table IX compares the C81 results to the trim solution of this high-speed, nonlinear hybrid computer program. Compared to the GENHEL solution, the C81 does well in matching required control settings, and has moderate success in duplicating the rotor flapping. The lack of rotor downwash acting on the fuselage in the C81 program is evident again in the data of Table IX. Studying the values in this table of the rolling and pitching moments produced by the main rotor reveals an inadequacy in the C81 rotor solution. GENHEL correctly predicts the major moment contribution about the pitch axis, while the C81 predicts a major contribution about the roll axis, which does not correspond (via the hub moment constant) to the relative magnitudes of the rotor longitudinal and lateral flapping angles prescribed by the C81. This result indicates an inadequacy in the C81 rotor analysis for predicting the precession (gyroscopic) relations of the articulated rotor. The C81 rotor analysis was originally developed specifically for a teetering rotor system.

The C81 program was exercised in sideward and rearward flight trim, and the predictions were correlated with CH-53D flight test data. The fuselage aerodynamic data were loaded into the program based on wind tunnel data and on estimates of the helicopter forces and moments in sideward and rearward flight. Since the available aerodynamic data for the CH-53D in the wind

tunnel configuration included the tail, the tail data groups were removed from the C81 input when running the sideward and rearward data cases. The test trim data and predicted C81 values for the CH-53D in sideward flight are given in Figure 8. The C81 program showed some difficulty trimming in sideward flight; it would not trim beyond 20 kt when flying to the left. The C81 results show few variations in roll attitude with sideward speed or direction; nor does the lateral cyclic control prediction match flight test very accurately. Again the C81 tail rotor pitch control is seen to be low.

Figure 9 gives the C81 trim parameters compared to test data for the CH-53D in rearward flight. Evident in these plots is the completely erroneous prediction of the amount of lateral cyclic control required to trim the model at the rearward speeds studied.

Table X contains the C81 and test data for the CH-53D in various coordinated turns in the vicinity of 75 kt. The C81 coordinated turn trims were obtained only after several attempts to run the program for this flight condition, due to difficulties in obtaining trim as described earlier. The C81 program demonstrated reasonable success in predicting the trim attitudes and the control settings in the turns, considering the program trim criticisms already described, which naturally also influence the coordinated turn trim.

The overall impression of the C81 trim analysis as applied to articulated rotor helicopters is that the program predicts trim characteristics with moderate success. The program would probably benefit from a more detailed correlation with articulated rotor helicopter trim data combined with program refinements for obtaining better correlation in those areas needing improvement (such as the analytic calculations for the aerodynamic surfaces). The C81 appears to model low-speed characteristics well, and the trim solution displays proper static stability characteristics. The C81 trim solution would be more accurate if a more accurate representation of fuselage aerodynamics than is presently available could be loaded into the program. Some program inadequacies lie in the rotor solution for the articulated system, but this problem is not entirely visible when studying only the trim analysis. The trimming routine, which brings the C81 to a trim solution, operates well in general, although there are occasional instances in which a trim solution cannot be obtained due solely to some type of inefficiency in this routine.

PERFORMANCE CORRELATION - RESULTS AND DISCUSSION

The C81 data for the performance correlation were gathered from the time-variant portion of the combined quasi-static/time-variant trim solution of the program. Most of the C81 performance data shown here were obtained from program runs utilizing four main rotor mode shapes. Preliminary runs showed little variation in power requirements between cases using four mode shapes and those using two mode shapes; typically there was also little difference in power between the quasi-static and the time-variant solutions (about one to two percent difference in each instance). Because more accuracy was expected in a time-variant solution using a greater number of blade bending modes, and because the user's manual recommended a time-variant solution when doing any detailed analysis concerned with the rotor of an articulated system, these conditions were selected when running most of the performance cases. The use of five blade bending modes was attempted in the performance runs, but this condition could not be run with any efficiency due to the problems discussed in the previous Trim Correlation section of the report. Those few cases that did run with five bending modes showed power requirements of only one to two percent difference from the requirements established from cases using four bending modes. The drag coefficient of the blade spar inboard of the airfoil section was maintained at the same constant value for all conditions run in the performance analysis.

The main rotor shaft horsepower required in hover predicted by the C81 trim analysis for various CH-53A gross weights is compared to appropriate test data in Figure 10. In hover, the power requirement predicted by the quasi-static and by the time-variant portions of the combined quasi-static/time-variant C81 trim analysis are identical. The data of Figure 10 show that the C81 calculates less power required to hover at a given helicopter gross weight than is established by the flight test data.

The main rotor power coefficient versus tip speed ratio for the CH-53A predicted by both the quasi-static and the time-variant portions of the C81 trim analysis at forward speed is compared to appropriate test data in Figure 11. Both portions of the C81 solution are shown to provide insight into the differences in performance data obtained from the quasi-static and time-variant solutions. As anticipated, the time-variant analysis predicts higher power requirements. Both portions of the C81 trim solution predict higher main rotor horsepower than is specified by the test data, although the C81 data appear to fit the test data relatively well at moderate speeds.

Figure 12 shows the C81 quasi-static and time-variant predicted main rotor power coefficients (versus main rotor tip speed ratio)

compared to test data for the S-67 helicopter. These data illustrate that the C81 underpredicts the power requirement for the S-67 helicopter. As mentioned in the Trim Correlation section, the wings of the S-67 may be generating too much lift, causing the main rotor power requirement to be too low and thus inconsistent with the CH-53A comparison in Figure 11.

Figure 13 repeats the same C81 quasi-static performance data for the CH-53A that is shown in Figure 11 and compares it to performance data predicted for the same conditions by the Sikorsky Generalized Rotor Performance program (GRP). A description of the GRP program can be found in References 19 and 20. The quasi-static C81 solution was selected for comparison with GRP because the quasi-static analysis more closely resembles the GRP analysis (i.e., a modified single-blade analysis) than does the time-variant analysis. Both the C81 and GRP programs predict the test results with similar accuracy; for the particular test conditions representing the baseline in this comparison, the C81 predicts the moderate speed performance more accurately, while GRP predicts the performance at high speed better. The accuracy of C81 at low speed is due to the inclusion of the tip vortex correction factors in the C81 calculation of induced velocities that are employed by the C81 analysis even when tip vortex effects are not specifically modeled in the simulation.

Some main rotor and tail rotor whirl stand cases were simulated by the C81 program by setting the program logic switch IPL(1) unequal to zero. When using the reduced data deck for these runs, it was discovered that a tail rotor simulation was possible only when the tail rotor data were loaded into the main rotor data groups of the C81. The C81 program was solved for various specified blade pitch control inputs, obtaining the resulting rotor thrust values and the required rotor power for the conditions simulated. The main rotor thrust coefficient versus power coefficient for the CH-53D predicted by the C81 is compared to appropriate whirl test data in Figure 14. The data of this figure show that the power requirement predicted by the C81 loses accuracy at increasing thrust levels (corresponding to increasing blade angles of attack). The tail rotor thrust coefficient versus power coefficient for the CH-53A predicted by the C81 is compared to appropriate whirl test data in Figure 15. The thrust level for any given power predicted by the C81 for the tail rotor is higher than the measured test value of thrust. At one particular low setting of the tail rotor blade pitch (4 deg), the C81 predicted a power coefficient of 0.00038, corresponding to a thrust coefficient of 0.0098. This datum point was not consistent with the other thrust/power predictions by the C81, and was omitted from Figure 15. The cause of this one inconsistent datum point was not apparent upon examination of the C81 computer run which produced it.

A number of C81 cases were run to iterate the climb performance predicted by the program. At a given speed, cases were set up

requesting trim at different rates of climb. Maximum rate of climb at a given speed is based on available power and available collective pitch. After obtaining trims at two or three rates of climb, rate of climb versus collective pitch and versus power were plotted to determine the maximum rate of climb. This process was then repeated at a different speed. Figure 16 shows the maximum rates of climb obtained in this manner from the C81 at two altitudes compared to test data for the HH-53C. Some difficulty was experienced obtaining even a limited number of data points from the C81 because the program could not easily trim its simulated helicopter in an attempted climb. The C81 simulated trim was very sensitive in the directional degree of freedom in general, including climb runs. Stacked cases, in which only the requested rate of climb changed, were also difficult to run. Often the quasi-static portion of the trim could not be obtained successfully for a stacked case, requiring the programmer to re-run the case a number of times, varying the fixed value of either the roll or the yaw attitude until a satisfactory trim had been established.

In a manner similar to the climb performance analysis, autorotative performance data were gathered from the C81 for the HH-53C. At a given speed, cases were set up requesting trim at different rates of descent. After obtaining trims at two or three rates of descent, the rate of descent versus the collective control was plotted, and the maximum rate of descent was established based on the lowest collective pitch available for the helicopter. (The C81 predicted essentially zero main rotor torque for the runs with low collective pitch.) This process was then repeated at a different speed. The maximum rate of descent versus airspeed thus determined from the C81 is plotted in Figure 17 along with the corresponding test results. Unlike the climb cases, no difficulties were experienced in obtaining the autorotative trims. The data of Figure 17 show that the C81 is highly optimistic in predicting the autorotation performance characteristic of the helicopter.

For this study, the major prediction effort was directed within the normal flight envelopes of the subject helicopters. Simulated CH-53A pull-ups were attempted by the C81 program in an effort to obtain representative data points approaching and on the flight boundaries, and the resulting data points were to be placed on the empirically determined load factor-velocity (V-n) diagrams of Reference 21. But such data were never obtained because the C81 program could not be trimmed for any of the cases attempting maneuver trims. A number of attempts were made to obtain these maneuver trims, allowing for 40 trim iterations per case. Initial condition program inputs (particularly control settings) were varied many times without producing a successful trim. The program output for these cases gave no clear indication of what the difficulty was. The maneuver trim solution difficulties of the C81 program merit investigation because this is a desirable program capability that would be frequently

requested in a helicopter design effort. If any further correlation work is conducted with the C81 program in the future, the maneuver trim data should be gathered for comparison to flight test data provided some program improvement has been made allowing these cases to be run.

Tail rotor performance was not studied in as much detail as main rotor performance was studied because the main rotor and tail rotor solutions are essentially identical in the C81, and because tail rotor test data is not as easily accessible as main rotor test data. However, an unusual tail rotor characteristic was discovered during the course of this correlation effort. While running S-67 cases on the C81, the helicopter sometimes would not trim when the tail rotor was made to rotate in the proper direction; yet when it was allowed to rotate in the opposite sense, the otherwise identical cases trimmed successfully. Investigatory cases which trimmed when either direction of tail rotor rotation was used revealed that trim, performance, and response characteristics were hardly affected by the direction of rotation. The influence of the direction of tail rotor rotation on reaching a trim discouraged any further detailed pursuit of tail rotor performance characteristics.

Concerning the general operation of the performance analysis of the C81, the lack of rotor wake effects on the fuselage (as discussed in the Trim Correlation section) clearly subtracts from the accuracy of the helicopter performance predicted by the program. A better understanding of the performance analysis in its present form might be obtained by continued correlation with good whirl stand test data. An interactive wake routine would be needed for an accurate performance prediction for a helicopter possessing a coaxial or tandem rotor system. Although not a major criticism of the C81, the iterative method that is presently required to determine the maximum rate of climb and the autorotative rate of descent is cumbersome, requiring much interaction and plotting of data by the program user. A program modification that would iterate and interpolate within the program to determine these maximum values would be useful.

STABILITY CORRELATION - RESULTS AND DISCUSSION

The stability analysis option provided by the C81 program was used to gather roots and stability derivatives for a number of CH-53 and S-67 correlation cases. The stability analysis used by the C81 follows a quasi-static trim of the case under investigation. Choice of various program inputs and program options (number of blade bending modes, yawed flow, and unsteady aerodynamics) were found to have essentially no effect on the roots and stability derivatives calculated by the program. No difficulties related to the stability routine of the program were experienced while making the stability data runs.

The majority of the C81 stability runs were made employing ten degrees of freedom for the helicopter: six body motions, two main rotor motions, and two tail rotor motions. Figures 18, 19, and 20 compare the roots calculated by the C81 for the CH-53A at three airspeeds (hover, 100 kt, 150 kt) to the roots calculated by the Sikorsky GENHEL program for the corresponding conditions. The linear model derived from the GENHEL analysis employs nine degrees of freedom: six body and three main rotor motion (including the coning degree of freedom). The roots for this model are shown in Figures 18, 19, and 20, and the six body and two main rotor roots from the C81 were selected and shown for comparison in these figures. The roots originating from the GENHEL model, in Figures 18, 19, and 20, were derived from linear derivative models, which were obtained from GENHEL by using a system identification (parameter identification) technique described in Reference 15. Past experience has shown that the body roots associated with the nine degrees-of-freedom system identified linear models are very similar to the roots associated with linear models derived by the familiar perturbation technique.

Figures 18, 19, and 20 indicate that the C81 roots associated with the main rotor degrees of freedom are of a considerably lower frequency than the GENHEL rotor roots. The exact implications of this characteristic are not clear in a general "complete-helicopter" analysis due to the short period of these roots, but the magnitude of the difference in the frequencies of the rotor roots implies that some accuracy is lost in modeling the articulated rotor with the existing rotor description used by the C81.

Figures 18, 19, and 20 show that the characteristics of the Dutch roll mode and the phugoid mode predicted by the C81 differ noticeably from those characteristics predicted by GENHEL. The periods of the Dutch roll modes of the two analyses are considerably different. Figure 20 shows that GENHEL models a phugoid mode that has become aperiodic at 150 kt. This characteristic is not shown by the C81 model. The C81 predicts an

aperiodic instability in hover, which is not evident in the GENHEL linear model, which can be seen in Figure 18. The period and the time to double amplitude for the phugoid mode of the CH-53A, taken from the data of Figures 18, 19, and 20, are shown in Figure 21 for the C81 and the GENHEL root locus solutions. Figures 18, 19, and 20 illustrate that, in general, the characteristics of the linear models derived from the C81 do not match the characteristics of the linear models derived from the GENHEL program.

The stability derivatives gathered from the C81 for the CH-53A (weighing 33,500 lb with a 348-inch fuselage station center-of-gravity location) at 100 knots are listed in matrix form in Table XI, having been normalized by mass and appropriate moments of inertia. Therefore, the body, rotor force, and moment variations in the table are expressed as accelerations. Also listed in Table XI, in parentheses, are the corresponding derivatives identified from the GENHEL program for those degrees of freedom that are common to the two analytic helicopter model programs. The derivatives for the main rotor coning degree of freedom derived from GENHEL are also shown for completeness. Appropriate sign convention changes have been made to maintain consistency between the two sets of derivatives. The roots associated with the linear models described in this matrix of stability derivatives are those given in Figure 19. The stability derivatives listed in Table XI show what these expressions look like for the ten degrees-of-freedom model derived from the nonlinear C81 helicopter representation and from the nine degrees-of-freedom model derived from the nonlinear GENHEL helicopter representation. Both derivative models have independent rotor degrees of freedom that remain constant as each body degree of freedom is allowed to vary independently. These linear derivative models are not comprised of the stability derivatives which have been more frequently experienced in the past; i.e., body derivatives with respect to the body parameters, for which the rotor has been allowed to respond to and to retrim before being included in the calculation of the body derivatives.

Table XII lists the stability derivatives for the same flight condition, but this time corresponding to the six degrees-of-freedom linear model in which the rotor is not treated as having independent degrees of freedom. The derivatives derived from the GENHEL program are shown in parentheses. These terms were determined from GENHEL by using the familiar perturbation technique. No means exists for extracting such a set of stability derivatives from the AGAJ74 version of the C81, so the C81 derivatives listed in Table XII were derived from the ten degrees-of-freedom C81 derivatives listed in Table XI. This was done in the following manner. Assuming a unit perturbation in one body variable (while all other variable changes were fixed at zero), the four rotor equations were solved for four unknowns: main rotor and tail rotor fore/aft and lateral flapping

angles. Each flapping acceleration and rate was assumed to be zero while solving the set of four equations in order to simulate the retrimmed rotor conditions for the given body variable perturbation. After the flapping angles were solved for the body variable perturbation, these flapping angles were multiplied by the appropriate body degree-of-freedom derivative with respect to the appropriate flapping angle. For each body degree of freedom, the resulting contributions for each flapping angle change were then added to the body degree-of-freedom derivative with-respect-to the body variable that had been perturbed with unity magnitude. These sums yield the stability derivatives for the six body degrees of freedom for the body variable being perturbed. The same process was then repeated for a different body variable until the matrix of Table XII was completed.

The method used to calculate stability derivatives for the six degrees-of-freedom linear model from the C81 ten degrees-of-freedom derivatives is only an approximation of the actual helicopter dynamics occurring after some small perturbation. The C81 program should be modified to provide accurate stability derivatives for a helicopter with an articulated rotor when it is not desired to treat the rotor as having independent degrees of freedom. There is enough confidence in the concept used here to approximate the C81 six degrees-of-freedom stability derivatives to permit these data to be compared to the corresponding derivatives derived from the GENHEL program, in an effort to determine what portions of the C81 description of an articulated helicopter need further investigation or improvement.

The important stability derivatives for describing helicopter stability characteristics modeled by the C81 were selected from Table XII and were compared to corresponding derivatives obtained from GENHEL. Derivatives that showed more than small differences from each other were studied to determine what might be responsible for these differences. Insight gained from all other C81 correlation efforts (trim, performance, time histories, and rotor loads) were applied in this stability study, and references to the higher degrees-of-freedom derivatives of Table XI were made whenever these more specific (but less familiar) derivatives could assist in the analysis.

The lack of a routine for calculating the influence of rotor downwash on the fuselage, and the accuracy lost by representing the fuselage aerodynamics by an analytic expression rather than by wind tunnel map data have some influence on the discrepancies seen in the C81 calculation of X-force with vertical velocity and Z-force with longitudinal velocity derivatives of Tables XI and XII. The pitching moment with vertical velocity is also a function of the aerodynamic characteristics of the fuselage. The orientation of the rotor thrust relative to the fuselage affects all of the major longitudinal stability derivatives which the C81 does not predict accurately. All those stability

derivatives that are a function of rotor thrust orientation appear to be predicted with little accuracy by the C81. The difference in signs between the C81 and GENHEL derivatives for rotor pitching moment with lateral flapping and rotor rolling moment with longitudinal flapping (see Table XI) shows an inaccuracy in rotor cross-coupling in the C81. The C81 trim solution of the rotor and the cross-coupling effects due to rotor precession calculated by the C81 program for an articulated rotor system lead to enough questions to merit a detailed investigation of all contributions to these calculations. Such an investigation should include a comparison of the various components of each rotor force and moment to the corresponding components calculated by some established baseline analysis for articulated rotors (such as the GENHEL program). This type of detailed investigation would probably require entering the C81 program and breaking the solution at various points in the programmed equations. The technique used to approximate the articulated rotor solution within the C81 should be further investigated if the C81 rotor solution in the program is subjected to detailed examination.

The damping and control power expressions from the C81 in Table XII compare well with those calculated by GENHEL except in the directional degree of freedom. The yawing moment with yaw rate derivative has the wrong sign (opposite direction), while the yawing moment with tail rotor pitch is too high as predicted by the C81. The side force and the rolling moment derivatives with respect to tail rotor pitch are also too high. The tail rotor modeled by the C81 program therefore must produce too much change in thrust in response to a change in tail rotor pitch. Other major lateral-directional derivatives that are not predicted accurately by the C81 are the rolling moment with yaw rate, and the yawing moment with lateral velocity and with roll rate. These stability derivatives are functions of the change in tail rotor thrust with sideslip and of the change in side force produced by the vertical tail with sideslip.

Some C81 stability data runs were made in order to collect CH-53D and S-67 root locus data for comparison to roots estimated from flight test data. Figures 22 and 23 show the body roots of the CH-53A at 100 kt and 150 kt obtained by system-identifying flight test data. The roots obtained from the C81 program runs simulating these same flight conditions also appear in the figures. Roots gathered by semiempirical methods show some difference from analytically derived roots. If the GENHEL set of roots from Figures 19 and 20 is compared to the two sets of roots in Figures 22 and 23, respectively (the gross weight and center-of-gravity locations of the flight conditions represented by these sets of data are slightly different), it is seen that the GENHEL roots more closely resemble the test data roots than do the C81 roots.

Few root locus data are available for the S-67 helicopter. Roots derived from test data are shown in Figures 24, 25, and 26 in order to provide some such data for the S-67 in this report. These roots were obtained by studying time history test data and measuring the frequency and period of responses to pulse input disturbances. The frequency and period information was transferred to root locus plots. Roots gathered from C81 data runs corresponding to the same flight conditions are also included in Figures 24, 25, and 26.

The stability characteristics of the C81 linear representations of the CH-53 and S-67 helicopters, as interpreted from the roots and derivatives calculated by the C81 program, can only reflect the characteristics of the nonlinear model from which the stability derivatives and roots were derived. The roots and derivatives cannot be expected to be highly accurate if some portions of the nonlinear helicopter representation need improvement. The roots and derivatives are used to indicate the areas of weakness (and strength) in the model from which they were derived. The mechanics of the stability analysis within the C81 for gathering roots and derivatives works well and relatively quickly. Besides a needed option for obtaining the stability derivatives of an articulated rotor helicopter selected without independent rotor degrees of freedom, the ability to obtain stability derivatives at any time during a time-variant maneuver solution might also prove to be a useful addition to the C81 program.

TIME HISTORY CORRELATION - RESULTS AND DISCUSSION

Maneuver cases for the H-53 and S-67 helicopters were run to demonstrate the response characteristics of the C81 modeled helicopter via the resulting time history data. Pulse, step, and other miscellaneous control inputs from reliable test data, representing a variety of selected aircraft configurations and flight conditions, were reproduced as accurately as possible and submitted as inputs into the C81 program during its maneuver mode of operation. All helicopter maneuver responses simulated by the C81 and compared to flight test data were for basic helicopter responses without stability augmentation. Experience showed that the number of main rotor bending modes used in the maneuver cases had negligible effect on response time histories; all of the time history data runs referenced in the figures were made using two main rotor normal modes (hinged rigid flapping and lagging). Most of the data cases were run using the time-variant solution of the C81, although the responses differed very little from the responses obtained from the quasi-static maneuver solution. A few time history data cases were run using the quasi-static solution in order to study the time history characteristics of the rotor flapping angles. Yawed flow was employed in all the time history data runs, although unsteady aerodynamics were requested in only a few of the runs. The effects of yawed flow and unsteady aerodynamics on the parameters under study were negligible.

Quasi-static maneuvers for the CH-53A at approximately 33,000 lb and aft center-of-gravity location were run on the C81 program at hover, 100 kt, and 150 kt to compare the resulting helicopter responses to flight test data. In particular, the rotor longitudinal and lateral flapping angle responses following longitudinal stick pulse inputs were to be compared; these angles are available only from the quasi-static solution of the C81. Few of these flapping response correlation data are shown in the report. The problem with these (and other) maneuver time history C81 runs is that immediately upon beginning the time history solution, nonzero angular accelerations are calculated by the program. Often these accelerations are of large magnitudes (up to 70 deg/sec² for one of the HH-53C cases). These erroneous inputs appear as discontinuous disturbances to the helicopter. Some cases show the helicopter responding in the wrong direction; reaction to the erroneous acceleration input completely overrides the control stick input. These initial nonzero accelerations occur frequently for both quasi-static and time-variant time history solutions. These acceleration disturbances usually occur at the very beginning of the time history solution, although in isolated instances they appeared later in the time history. For all the time history data cases that were run in this study, the helicopter was quasi-static trimmed well within a very tight tolerance, usually within 10 pounds or foot-pounds.

For this reason, and because the problem occurred for quasi-static maneuvers as well as time-variant maneuvers, the nonzero accelerations are most likely caused by a program memory location error.

The quasi-static longitudinal pulse cases, which were run on the C81 for the 33,000 lb CH-53A, typically had very poor pitch attitude and load factor responses in comparison to the test results. Figure 27 presents data from the C81 run with the least inaccurate aircraft responses, from among these CH-53A cases. Due to the inexact duplication of the helicopter response by the C81 program for this case, firm conclusions cannot be drawn on the rotor flapping response predicted by the C81. However, the resulting longitudinal flapping response predicted by the C81 for this case peaked at 2.5 deg (compared to about 1 deg from test data), while lateral flapping was cross-coupled by about 1 deg in the prediction (compared to almost zero response in the test data), as seen in Figure 27.

Noticeably absent from the C81 program output are values of the flapping and lagging angles of individual rotor blades during the time history. Even if these angles were only approximated by the blade and rotor head geometry, based on the generalized coordinates of the closest blade segment outboard of the flapping and lagging hinge locations, these data would prove useful when using the C81 to model helicopters with articulated rotor systems and should be made available from the C81.

Figures 28 through 36 show the time history responses predicted by the C81, compared to test data, for pulse and step control inputs to the HH-53C helicopter. These data are shown here even though initial nonzero angular accelerations occasionally occur in the C81 runs. All C81 accelerations at time zero in these figures are shown as zero because the program prints these zero values when beginning a maneuver. But the large nonzero value for acceleration seen at the next data point printed in the computer output (requested as early as 0.004 sec into the maneuver for some of the data runs made) indicates that an erroneous input is immediately entering the maneuver solution.

Figure 28, 29, and 30 illustrate the actual and the C81 predicted responses of the HH-53C at 31,000 lb in hover to longitudinal, lateral, and directional pulse control inputs, respectively. Figure 30 illustrate the effects of the large erroneous accelerations sustained in roll and yaw at the beginning of this C81 run. The quasi-static/time-variant trim condition solutions generated by the C81 prior to initiating the maneuvers illustrated by the time histories of Figures 29 and 30 were identical; yet the nonzero acceleration disturbance that occurred during the lateral input case was negligible in comparison to that for the pedal input case. Irregularities in the time histories of Figure 29 near 4 seconds elapsed time indicate that some extraneous

acceleration disturbance can occur at some time other than zero in the C81 maneuver solution.

The unusual behavior of the pitch acceleration, both near time zero and near three seconds, corresponding to a forward stick pulse input predicted by the C81, as seen in Figure 28, prevents any conclusions from being drawn from the data for this case. However, a divergence in yaw can be seen, and the directional degree of freedom may be highly coupled to the roll response. The data of Figure 29 indicate decent correlation between C81 and test data for a right stick pulse input except that the roll attitude response corresponding to the changes in roll rate and acceleration predicted within the program was unusual. The data of Figure 30 does not lead to any useful information about the C81 maneuver solution because of the severe initial inputs in roll and yaw accelerations.

At 31,000 lb in hover, the actual and the C81 predicted responses of the HH-53C to longitudinal, lateral, and directional step control inputs are shown in Figures 31, 32, and 33, respectively. Despite an initial roll acceleration, which was far too large, the response of the helicopter predicted by the C81 for an aft stick step input, shown in Figure 31, closely resembled the actual test response. The variation in pitch responses may have been due to a minor but erroneous biasing of pitch acceleration at time zero. In this example the coupled roll response appears to be proper, once the bias due to different trim values of roll attitude is considered. The data of Figure 32 show that the roll rate and acceleration predicted by the C81 were too large within the 2 seconds following a right stick step input. Figure 30 also indicates that the coupled pitch response to the roll input was not in the proper direction. Not much can be concluded from the data of Figure 33 about the response to a pedal step predicted by the C81 because of the large initial disturbance in yaw acceleration.

Figures 34, 35, and 36 show the actual and the C81 predicted response of the HH-53C at 41,000 lb at 113 kt to longitudinal, lateral, and directional step control inputs, respectively. The pitch acceleration predicted by the C81 for a forward stick step input, as shown in Figure 34, appears to have been delayed compared to the flight test results. The change in load factor predicted by the C81 was not as great as the change in the actual data. Figure 35, illustrating the response to a left stick step, also indicates a delay in the roll response predicted by the C81 when compared to the test data. The C81 data of Figure 36, for a right pedal step input, was contaminated by roll and yaw acceleration disturbances at about 0.5 second elapsed time, which occurred for no apparent reason.

The C81 data runs, which yield the data of Figures 28 through 36, employed a 15-degree change in main rotor azimuth between

successive program calculations during each time history solution. The C81 data plotted in these figures were drawn from the computer printouts, which requested listings of the maneuver solution only after every 60-degree change in rotor azimuth. Some CALCOMP plots were requested using a more frequent data sampling interval (every 30 degrees in azimuth). The CALCOMP plots occasionally revealed a 6/rev oscillatory content in angular accelerations during the maneuvers. This oscillatory content was not exhibited in the computer printed data because of the infrequent sampling of data.

Some S-67 time histories solved by the C81 were gathered and compared to test data, but these runs also showed high nonzero accelerations at the beginning of the computed maneuver solution. A symmetrical dive and pull-up at 180 kt was run on the C81. Comparing the program data to test data over 25 seconds of time history response showed the C81 to predict excessive pitch angles (as much as 60 deg nose down). The normal load factor and the change in airspeed solved by the C81 were also extremely inaccurate. About 30 seconds of response following an aft cyclic stick pulse input solved by the C81 were studied for the S-67 at 140 kt. These data showed roll to be highly coupled in the solution, reaching excessive roll angles (60 deg) in comparison to test data. Here, too, the load factor and airspeed responses were erroneous. The pitch response was divergent, showing no oscillatory content as seen in the test data. The root locus solution from the C81 for exactly the same aircraft configuration and flight condition (Figure 25) predicts long-term longitudinal stability characteristics different from those shown by the non-linear C81 time history solution of this data case. Another S-67 maneuver, which was simulated by the C81 at 140 kt, was a pedal doublet. Studying about 20 seconds of response showed the yaw response of the helicopter solved by the C81 to be excessive (40 deg) and divergent (unlike test data). The roll response of the helicopter was highly coupled and excessive (35 deg). The time history of the sideslip predicted by the C81 did compare well with test results. It should be remembered that the initial accelerations of the S-67 for all the cases discussed here were excessive, and this may have played a major part in the ensuing responses.

Although most of the C81 time histories gathered in this study were apparently contaminated by the unusual acceleration solutions, some data were presented and discussed in this report anyhow, when it was felt that the data might indicate characteristics of the basic C81 maneuver solution. Some of the time history data suggests that the C81 program may be moderately successful in predicting articulated rotor helicopter maneuver response characteristics. (However, the computer time required for time history solutions is excessive and is discussed in a later section of this report.) Pitch-roll coupling and yaw sensitivity appear to be areas needing improvement. Detailed quantitative

analysis of the C81 maneuver solution should be postponed until the excessive accelerations experienced in the solution are corrected or explained.

ROTOR LOADS CORRELATION - RESULTS AND DISCUSSION

Data for the C81 rotor loads correlation were collected by running C81 maneuver cases, with no disturbing inputs, for a duration equivalent to one rotor revolution, and printouts of blade moment solutions were requested after trim and periodically during the rotor revolution. A considerable effort was expended running introductory and comparative cases to determine how to best set up the cases to produce the most accurate rotor loads solutions from the C81 for an articulated rotor helicopter. After establishing criteria for selecting input data and program options, data cases were run, and C81 rotor loads data were collected for comparison to test and other analytic data. All rotor loads cases run in this study were for the CH-53A helicopter.

Comparing data from a number of C81 runs indicated that the blade moment distribution solution of this program is highly dependent upon (and far too sensitive to) the degree of accuracy used in expressing the blade normal mode shapes and mass distribution. Figure 37 shows the distribution of the blade beamwise bending moment (at 60 deg rotor azimuth location) calculated by the C81 for a number of cases. Table XIII presents the blade normal modes shapes and mass distributions used for these cases. Two mode shapes (rigid flapping and lagging) were used in each case for the CH-53A at 32,550 lb in hover. (The rigid lagging mode shapes were identical to the rigid flapping mode shapes listed in Table XIII.) Case A in the figure illustrates the solution for an ideal blade with exactly linear mode shapes (calculated to four significant figures) and uniform mass distribution. Case B is the solution for a blade which also has uniform mass distribution, but whose mode shape generalized coordinates are only approximately linear. (The inexactness of the mode shape at 5% radius for case B is the result of an attempt to accurately represent the location of the flapping hinge. This is another problem which will be discussed shortly.) Comparing the data of cases A and B in Figure 37 shows that spikes appear in the moment solution wherever the mode shape is not exact, and that the moment distribution across the blade can be biased by these discontinuities. Case C illustrates the moment distribution when exactly linear bending mode shapes are used, but when the mass distribution for the blade is nonuniform. Case C is compared to case A for this purpose.

When the C81 program is used to model a helicopter with an articulated rotor, the locations of flapping and lagging hinges are specified through the normal mode shape input data for the rotor blades. The flapping hinge offset from the center of rotation of the rotor for the CH-53A is 5.56% of the rotor radius. Due to the restriction in C81 input and program equations regarding the fixed number of blade segments (20), each

of equal length (5% radius), the exact offset for an articulated rotor may be loaded into the program only if the offset is an integer multiple of 5% radius. Cases B and D of Figure 37 illustrate unsuccessful attempts to accurately locate the true hinge offset by loading mode shapes into the program which reflect the exact location of this hinge. These cases were unsuccessful because the C81 cannot interpolate the proper offset location between blade station mode shape input data. Case D represents the moment solution when the blade input data represent the exact nonuniform mass distribution and the precise offset hinge location of the CH-53A main rotor blade.

Another problem pertaining to the flapping hinge, discovered while making these and other investigatory C81 rotor loads runs, involves the C81 solution of the bending moment at the flapping hinge. This moment should always be zero. The only condition for which the C81 would solve a zero moment at the hinge (within some computational error tolerance) was for the hinge to be located exactly at a blade segment radial station, with exactly linear blade mode shapes, and with uniform blade mass distribution (case A in Figure 37). All other cases that were run (many more than are shown in Figure 37) could produce no better an average value of hinge moment over one revolution than 1000 to 2000 in-lb.

Investigatory C81 rotor loads solution runs, which were made in addition to those included in Figure 37 showed that the number of normal mode shapes used in the runs and the forward speed of the helicopter do not affect the results seen in Figure 37 or discussed in the previous paragraphs. Properties similar to those discussed were also exhibited for the chordwise moment distribution, as shown in Figure 38.

The majority of the rotor load runs made in this study used the shaft-free solution of the C81, wherein the entire helicopter is trimmed. But the shaft-fixed solution was also investigated, though only in a few computer runs. Here the shaft angle is specified and only the rotor is trimmed, either for specified flapping angles, or for specified control angles. Table XIV presents the rotor trims obtained from various shaft-fixed solutions, compared to free aircraft (shaft-free) solutions, and to test data. These C81 solutions correlated well with test data on longitudinal flapping and control angles, although the lateral flapping and control angles predicted by the C81 were not always as accurate. The shaft-fixed solutions were obtained using two normal modes (flapping and lagging). A quasi-static trim could not be reached when shaft-fixed trims were attempted using five blade bending modes.

Runs were made using two and five normal mode shapes to compare the resulting blade bending moment distribution along the blade radius. The steady beamwise moment at the flapping hinge was

considerably smaller when two modes were used instead of five (-1600 in-lb compared to 8800 in-lb for the CH-53A at 34,120 lb and 159 kt); but the oscillatory content of bending moments was much too small everywhere else along the blade when two modes were used. The vibratory bending moments solved by the C81 when five modes were used matched test data much more closely than they did when two modes were used. Therefore, it was decided to use five mode shapes in the rotor loads data runs being compared to test and other analytic data.

The C81 data runs made for the purpose of collecting blade bending moments for comparison to test and analytic results were shaft-free solutions using five main rotor blade bending modes. Control system deformation, not explicitly available in the C81 program, was represented in the torsional bending mode shape loaded into the runs. Yawed flow and unsteady aerodynamics were included in these runs. The flapping hinge was located at 5% radius rather than 5.56% in order to avoid biasing the moment distribution, which would have occurred had an attempt been made to accurately locate the flapping hinge. The lagging hinge was located at a designated blade station for the same reason. Mode shapes were loaded into these runs as accurately as was possible, and the correct (nonuniform) blade mass distribution was used.

Three C81 rotor-load data runs were compared to test results for the CH-53A helicopter. These were for 34,120 lb in hover, 33,070 lb at 159 kt, and 40,650 lb at 137 kt (all at a neutral center of gravity). These conditions cover low and high weight, as well as hover and high speed. The C81 data gathered at 137 kt and 159 kt were also compared to analytic solutions from the Sikorsky Y200 normal modes blade aeroelastic analysis computer program. (The Y200 program is described in References 22 and 23.) The data from the Y200 runs were previously obtained in conjunction with the work of Reference 24. (Due to the solution technique used in program Y200, the rotor thrust obtained in its solutions are about 6% higher than the thrust values for the test and the C81 conditions.)

Figure 39 compares the C81 and Y200 solutions of the steady contribution of beamwise bending moment versus blade radius to test data for the CH-53A at 159 kt. The C81 more closely predicts the maximum steady beamwise bending moment. The Y200 predicts the tip-down steady moment, whereas the C81 does not. Figure 40 is similar to Figure 39 except that it compares the vibratory content of the beamwise bending moment. Here, the Y200 predicts the proper trend in the radial distribution of vibratory beamwise bending moment, while the C81 does not. Figure 41 compares the harmonic content of the vibratory beamwise bending moment near the radial station where this moment is highest. (The test and Y200 data actually correspond to 79% radius but are compared to the C81 values at 80% since the C81 program fixes, by 5% increments, the radial stations at which

bending moment data will be available.) The two programs predict low-frequency (1/rev and 2/rev) beamwise bending moment amplitudes with comparable accuracy. The Y200 program predicts the approximate amplitudes of the high-frequency beamwise bending moment components. The C81 underpredicts these vibratory components. Figure 42 compares time histories of the the total beamwise moment over one rotor revolution at the critical blade station (80% radius) from the C81, the Y200, and the flight test data. This time history is predicted accurately by the Y200 analysis. The corresponding C81 time history does not exhibit the proper phase relationship or frequency content.

The steady chordwise bending moments (versus blade radius) predicted by the C81 and the Y200 analyses are compared to the test data in Figure 43 for the CH-53A at 159 kt. The C81 approximates the radial distribution of the steady chordwise bending moment slightly better than does the Y200. Figure 44 compares vibratory chordwise bending moments solved by the C81 and the Y200 to test data. Both the C81 and the Y200 analyses underpredict the amplitude of chordwise vibratory bending moment. The C81 yields a slightly better prediction of flight test results. Taking a closer look at the vibratory component at the critical blade station, the harmonic content of the vibratory chordwise bending moment at 55% radius predicted by the C81 and the Y200 is compared to test results in Figure 45. The test data in this figure show the major fourth harmonic contribution, which is a characteristic of this CH-53A rotor blade. Although the Y200 underpredicts the magnitudes of the harmonic content, the Y200 analysis does indicate that the fourth harmonic is the major contributor to this vibratory bending moment. The C81 results do not predict this characteristic, but it should be noted here that Y200 employs a detailed variable inflow model (including interactive calculation of vortex influence on the inflow), while the C81 uses a much simpler analytic expression of inflow. The time histories of the total chordwise bending moment predicted by the C81 and the Y200 during one rotor revolution at 55% radius are compared to test data in Figure 46. As with beamwise moment, the Y200 program more accurately predicts the time history of blade chordwise bending moment than does the C81 program.

A limited number of blade torsional moment data were available for the cases studied. Figures 47 and 48 show the steady and vibratory content, respectively, of the torsional moments predicted by the C81 and the Y200, compared to CH-53A test data, for the 159 kt case. Figure 49 compares test results to the C81 and the Y200 solutions for the harmonic content of vibratory torsional moment near 15% radius. Both programs had low predictions of the high-frequency (near 6/rev) components of torsional moment associated with retreating blade stall flutter.

Similar to the rotor loads comparison just discussed for the CH-53A at 33,070 lb and 159 kt, C81 and Y200 analyses were also

run and compared to test data for the CH-53A at 137 kt, but at a higher rotor loading corresponding to 40,650 lb gross weight. With few exceptions, the C81 and the Y200 each performed in the same manner when predicting blade bending moments for the higher weight case as they did for the lower weight predictions illustrated in Figures 39 through 49. The differences in the results for the two conditions were that for the higher weight case, the C81 and the Y200 predicted almost identical steady chordwise bending moment distribution with span (both underpredicting the flight test results). The vibratory chordwise bending moments versus span predicted by these two analyses also were almost identical (and once again both underpredicted corresponding test results). For the high weight case, the vibratory torsional moment distribution with span predicted by the Y200 was slightly higher than the prediction of the C81. Both the C81 and the Y200 programs underpredicted the magnitude of vibratory torsional moments for the high thrust condition.

The C81 rotor loads solution for the CH-53A in hover (at 34,120 lb) was compared to test data in the same manner as was done at 159 kt. This comparison led to basically the same results and conclusions as were drawn from the comparison made at 159 kt. Few differences were observed between these two cases. In hover, the C81 underpredicted the steady beamwise bending moment near the blade tip and predicted far too low vibratory beamwise bending moments over the entire blade span. For this case the C81 mistakenly saw essentially only a first harmonic contribution to the vibratory beamwise bending moment, and grossly underpredicted the magnitude. In hover, the C81 underpredicted the steady chordwise bending moments over most of the blade, except at the tip where it overpredicted. For this hover case the C81 underpredicted the vibratory chordwise bending moments over the entire span of the blade and underpredicted all the harmonic components of this moment at the critical blade section.

To summarize the evaluation of the C81 program for predicting blade bending moments for an articulated rotor helicopter, the program solution is overly sensitive to variations in normal mode shapes and the mass distribution of the blade. The articulated hinges cannot be accurately located due to the fixed segment length restriction. The C81 program solved an erroneous nonzero moment solution at the hinge, and this characteristic of the solution creates some lack of confidence in bending moment solution elsewhere along the blade. In hover, the C81 underpredicts the vibratory content of blade bending moments. At high speed, with higher bending modes inputted to the program in addition to the two rigid flapping and lagging modes, the C81 generally predicts the proper magnitude of the vibratory content of bending moments, while predicting the steady contribution with only moderate success. The C81 does not predict the radial distribution of moment well where this distribution shows local peaks or sudden changes in value. Using the analytic expression

within the C81 program to model the rotor inflow, the program does not accurately recognize the proper harmonic content of the vibratory bending moments. Time histories of the blade bending moments do not show the proper frequency content and are not correctly synchronized with the rotor azimuth location of the blade.

Regarding the rotor loads input/output options of the C81, more freedom in locating blade stations at which the rotor loads can be analyzed is desirable. In addition to blade bending moments, other variables that are involved in the rotor loads analysis (such as blade stresses) should be made available to the user if these variables are accessible or computable within the existing program. The user is presently restricted in the number of times he may request the printout option which reveals the bending moments along each radial station of each blade during a time history solution; this option should be improved to allow the user to see these values as frequently as he desires during a rotor revolution following the trim solution.

DISCUSSION OF GENERAL PROGRAM CHARACTERISTICS

This section of the report discusses those C81 input, operational, output, and auxiliary program characteristics, that proved to be cumbersome or were found to need improvement. The topics discussed here were not included in previous sections of the report either because their detailed discussion was not necessary in explaining the immediate topics or because these topics apply to the C81 program in general.

The time required by the central processing unit (CPU) of the computer to execute the major analyses of the C81 program is an important characteristic of the program. The required CPU time for a solution determines the cost of the solution and therefore is a very practical consideration when evaluating the usefulness of the C81 program as an articulated rotor helicopter design tool. High CPU requirements by the C81 are particularly unacceptable if other analyses are available that provide solutions that can be obtained using less CPU time than C81. The version of the C81 programmed at Sikorsky using the HX compiler ran twice as fast as the version compiled with the G2 compiler. Virtual storage of the C81 program within the computer was used in preference over real storage so that the computer could be shared with other programs while running the C81. Typical quasi-static trims and stability analyses required about one minute of CPU time. This was found to be an acceptable requirement. Quasi-static/time-variant combined trims, however, required from four to eight minutes of CPU time. The required CPU time depends greatly on the rotor azimuth increment used in consecutive solutions within a time-variant trim or during any maneuver time history solution. CPU requirements were found to depend only slightly on other program trim routine inputs varied during the course of this study. Maneuver time histories were found to require excessive amounts of CPU time. Four seconds of time history required about 25 CPU minutes when the rotor azimuth increment of 15 degrees was used, while about 50 CPU minutes were required for the same time history when the rotor azimuth increment used was 9 degrees. In comparison, the Sikorsky GENHEL program runs fast enough to be used in a real-time simulation of helicopter maneuver responses. The time needed for the C81 time history solution did not depend greatly on whether a quasi-static maneuver or a time-variant maneuver was requested. A typical rotor loads analysis run made in this study, including a maneuver time history solution over one rotor revolution (with a 5-deg rotor azimuth increment), required about 20 minutes of CPU time. This requirement was somewhat high in comparison to the CPU requirements of the Sikorsky Y200 program for similar solutions.

Certain articulated rotor helicopter characteristics are not represented in the C81 program. The C81 model has no rotor

coning degree of freedom and therefore calculates no coning angle. There is no provision in the C81 to include a blade lag-to-pitch coupling hinge. Regarding more general helicopter and rotorcraft inputs, the C81 has no input that expresses the dynamic pressure loss at the tail rotor. The stability augmentation system and the control mixing offered in the control system input group encompasses many possible configurations; however, they are not flexible enough to allow many common, straightforward stability and mixing inputs to be represented in the program. An improvement is needed here that would allow the easy input of any stability augmentation or control mixing arrangement to the C81 rotorcraft analytic model.

Some of the necessary input data to the C81 proved to be difficult to prepare or were cumbersome or confusing to use. The fuselage aerodynamic data were converted from wind tunnel map data into input consistent with the C81 program by using the AS812A program. This program was written in PL/I language and was supplied to the contractor by the Lustis Directorate. The AS812A was developed to convert fuselage aerodynamic data into input consistent with the C81. The AS812A program was difficult to run successfully. The restrictive input data requirements of the AS812A made it necessary to load in more aerodynamic input data than were often available. The engineer was forced to estimate some bivariate aerodynamic map data to satisfy the input requirements of AS812A. This auxiliary program should have more flexible input requirements.

Another point pertaining to the fuselage aerodynamic data input of the C81 concerns the format of these data with regard to the nominal and high angle of attack equations. It is unclear what input is required for different flight conditions, particularly when also considering rearward or sideward flight conditions. A change in input format or an improved description in the user's manual of the present format would be helpful.

Regarding the normal modes input, the blade bending mode shape data inputted to the C81 first had to be derived from another source. Sikorsky program Y178 (coupled normal modes) was used to solve the normal mode shapes. It would be convenient if the mode shapes were calculated within the C81, so that the appropriate input data could be loaded into the C81 program rather than into some auxiliary program.

Some errors and inconveniences are evident in the C81 program printout and manuals. The sign of the tail rotor thrust printed in the trim output never changes, even when the tail rotor is rotated 180 deg from one side of the tail boom to the other. The printout frequently does not include titles, descriptions, or units and thus requires the program user to consult the manuals much too often. The units of some of the printed data (particularly the stability derivatives) change from place to

place in the printout. This situation would be confusing even if the units were listed in the printout.

A particularly annoying and confusing inconvenience in the program regards the different conventions used in numbering the blade stations appearing in the manuals, the printout, and the CALCOMP plots. Sometimes the blade station reference begins at the root of the blade, sometimes at the tip. References to these stations appear in many places in the program and should be made consistent. One example is that the printer plot lists the wrong blade station for the plotted rotor bending moment data calculated. Another example is the program input XMR(15), which actually specifies the blade station at which bending moments are calculated when segment numbering begins at the tip, rather than at the root as explained in the user's manual.

Another inconvenience of the C81 printout is the omission of rotor moment summaries in the force and moment summary, printed out while the trim iterations are being performed. Such information can prove to be helpful in analyzing a case for which the user is having difficulty obtaining a trim.

The engineer's manual could be more informative if it included descriptions of the entire C81 program, rather than just discussing those changes made since the program was last documented. This would eliminate the need for the curious user to consult a number of referenced reports, which are often not readily available.

The plotting routine included in the C81 program, which is interactive with the CALCOMP system, operated successfully and was interfaced with the CALCOMP hardware and software systems with little difficulty. The CALCOMP plots, which were obtained while running some of the time history data cases for this study, proved to be useful working plots and aided in the correlation effort. The CALCOMP plots as generated by the C81 routine, however, are not of report quality, and could be improved. For instance, when the user requested more than one variable to be plotted on the same graph, it was often difficult to determine which plot corresponded to which variable. Also, when it was necessary to use more than one scale for the graph when plotting more than one variable, the proper scale pertaining to each variable was not obvious. After printing the scale for the plotted variable, the pen was sometimes not commanded to be lifted from the paper before beginning the time history trace, thus producing an unwanted line on the graph. The program user does not have control of the time scale selected for the CALCOMP plots. Giving the user this option could frequently prove to be useful while gathering desired CALCOMP plots.

In concluding this discussion of the general program operating characteristics, anyone interested in using the C81 program

should be aware of the fact that the program is large and detailed, and considerable time is required to prepare input and to become familiar with the operation of the program. The associated manuals for the C81 program, standing alone, do provide enough information to allow a new user to set up and run the program without any other assistance or reference, although close coordination with the developer or major users of the program (such as the Eustis Directorate) greatly reduces the effort required by the new user in obtaining successful program runs.

CONCLUSIONS

It was found that it was possible to make the C81 program operate and converge to trim solutions for an articulated rotor helicopter and, within certain limitations, provide answers comparable to those of other analytical methods. The major limitations identified in this study of the AGAJ74 version of the C81 were:

1. Various C81 analyses (particularly time-variant trims and time history solutions) require exceptionally high computer run time. The run times cannot be substantially reduced, even when requesting minimal amounts of the available sophistication and complexity of the program analyses.
2. The C81 program trimming routine is not efficient enough to produce successful trims as frequently (i.e., few iterations) as desired in a user-oriented helicopter design tool program.
3. The general trim characteristics of articulated rotor helicopters in forward flight (with the exception of roll characteristics) are predicted with moderate success by the C81. The program does not accurately predict sideward and rearward flight trims.
4. The performance characteristics predicted by the C81 do not correlate as well as desired with test data for some conditions specified within the operational flight envelope. The required main rotor collective pitch is not predicted accurately in these circumstances. The program has difficulty solving maneuver trims (pull-ups, etc.) near flight envelope boundaries.
5. For the articulated rotor helicopter cases studied in this correlation effort, the stability characteristics predicted by the C81 program were inaccurate and generally unacceptable.
6. The dynamic response characteristics modeled by the C81 helicopter simulation show excessive pitch-roll coupling and yaw sensitivity.
7. Discontinuous pulse or step inputs in helicopter acceleration frequently occur during the solution of the C81 maneuver analysis, probably originating in the mathematics of the programming technique rather than from the governing dynamic analysis, thereby contaminating time history response data.

8. Blade bending moments solved by the C81 rotor loads analysis are too sensitive to blade mass distribution and mode shape input data.
9. In the present form of the program, the articulated hinges of the rotor cannot be accurately located in the C81 helicopter model. The existing technique for solving rotor moments within the C81 does not solve the proper bending moment at the articulated hinges.
10. The magnitudes of the steady and vibratory bending moments outboard of the articulated hinges solved by the C81 rotor loads analysis are comparable to solutions obtained from other rotor loads analyses. However, the time history solutions of these bending moments about the rotor azimuth inaccurately predict when peak values occur and inaccurately describe the frequency content of the moments.

RECOMMENDATIONS

1. The incorporation of the C81 program as an articulated rotor helicopter design tool over existing separate helicopter performance, handling qualities, and rotor loads analyses is not recommended. This recommendation is made in light of the comparison of articulated rotor helicopter characteristics as predicted by the C81 to test data and data accumulated from other analyses.
2. If the C81 program is to be maintained and improved as a general rotorcraft global program, it is recommended that this program undergo a further detailed comparison with test data, provided program improvements have been implemented that correct the problems uncovered in this study. The general trim characteristics should be checked again, and characteristics established in maneuver trims near helicopter operating boundaries should be correlated with flight test data. Performance with respect to high-speed power requirements and autorotative capabilities should be reevaluated. More accuracy in stability derivatives and root locus prediction is required. Time history response should be studied again, checking for helicopter cross-coupling effects and overall sensitivity to control inputs. Rotor moments and cross-coupling should be rechecked, as well as the time history solution of blade bending moments. To operate as an efficient and truly modular global program, it is also recommended that the running times of each of the various C81 analyses be reduced, particularly when the program options that are requested do not require high degrees of available program sophistication.

REFERENCES

1. Davis, J. M., ROTORCRAFT FLIGHT SIMULATION WITH AEROELASTIC ROTOR AND IMPROVED AERODYNAMIC REPRESENTATIONS, VOLUME I - ENGINEER'S MANUAL, Bell Helicopter Company; USAAMRDL-TR-74-10A, Eustis Directorate, U.S. Army Air Mobility Research and Development Laboratory, Fort Eustis, Virginia, June, 1974, AD 782854.
2. Davis, J. M., ROTORCRAFT FLIGHT SIMULATION WITH AEROELASTIC ROTOR AND IMPROVED AERODYNAMIC REPRESENTATION, VOLUME II - USER'S MANUAL, Bell Helicopter Company; USAAMRDL-TR-74-10B, Eustis Directorate, U.S. Army Air Mobility Research and Development Laboratory, Fort Eustis, Virginia, June, 1974, AD 782756.
3. Hsieh, P. Y., and Davis, J. M., ROTORCRAFT FLIGHT SIMULATION WITH AEROELASTIC ROTOR AND IMPROVED AERODYNAMIC REPRESENTATION, VOLUME III - PROGRAMMER'S MANUAL, Bell Helicopter Company; USAAMRDL-TR-74-10C, Eustis Directorate, U.S. Army Air Mobility Research and Development Laboratory, Fort Eustis, Virginia, June, 1974, AD 782841.
4. Gaieski, T. A., and Kreutz, F., CH-53 HELICOPTER DEMONSTRATION DATA REPORT, United Aircraft Corporation, Sikorsky Aircraft Division Report SER-65254, December, 1964.
5. Pryor, M., WIND TUNNEL TESTS OF A 4/5 SCALE MODEL OF THE HH-53C/NRS ROTODOME, United Aircraft Corporation, Sikorsky Aircraft Division Report SER-65931, July, 1970.
6. Wilson, J., and Pryor, M., WIND TUNNEL TESTS OF A 1/15 SCALE MODEL OF THE S-65, United Aircraft Corporation, Sikorsky Aircraft Division Report SER-65980, June, 1970.
7. Beno, E. A., CH-53A MAIN ROTOR AND STABILIZER VIBRATORY AIRLOADS AND FORCES, United Aircraft Corporation, Sikorsky Aircraft Division Report SER-65593, NASC Report, Naval Air Systems Command, Washington, D. C., June, 1970.
8. Gifford, J. A., ONE-TWELFTH SCALE WIND TUNNEL TESTS ON THE AH-3 (S-67) DEMONSTRATOR AIRCRAFT, United Aircraft Corporation, Sikorsky Aircraft Division Report SER-67000, April, 1970.
9. Kaplita, T. T., INVESTIGATION OF THE STABILATOR ON THE S-67 AIRCRAFT, United Aircraft Corporation, Sikorsky Aircraft Division; USAAMRDL-TR-71-55, Eustis Directorate, U.S. Army Air Mobility Research and Development Laboratory, Fort Eustis, Virginia, October, 1971, AD 735766.

10. Sandberg, T., CH-53D HANDLING QUALITIES AND DYNAMIC STABILITY TESTING PER ECP 6144, United Aircraft Corporation, Sikorsky Aircraft Division Report SER-65550, December, 1970.
11. Briczinski, S. J., and Cooper, D. E., FLIGHT INVESTIGATION OF ROTOR/VEHICLE STATE FEEDBACK, United Aircraft Corporation, Sikorsky Aircraft Division; NASA CR-132546, National Aeronautics and Space Administration and Langley Directorate, U.S. Army Air Mobility Research and Development Laboratory, Hampton, Virginia, January, 1975.
12. McGeen, D., IMPROVED ROTOR BLADE SHAKEDOWN FLIGHT TEST PROGRAM ON THE CH-53D HELICOPTER, United Aircraft Corporation, Sikorsky Aircraft Division Report SER-651127, December, 1972.
13. Lucas, J., WHIRL SUBSTANTIATION OF CH-53A ROTARY RUDDER ASSEMBLY, TEST REPORT, United Aircraft Corporation, Sikorsky Aircraft Division Report SER-65082, April, 1966.
14. Barbini, W. J., Balfe, P. J., and Lovrien Jr., C. E., CATEGORY II PERFORMANCE AND FLYING QUALITIES TESTS OF THE HH-53C HELICOPTER, U.S. Air Force Systems Command; FTC-SD-70-8, Air Force Flight Test Center, Edwards Air Force Base, California, May, 1970.
15. Molusis, J. A., ANALYTICAL STUDY TO DEFINE A HELICOPTER STABILITY DERIVATIVE EXTRACTION METHOD, VOLUME II, United Aircraft Corporation, Sikorsky Aircraft Division; NASA CR-132372, National Aeronautics and Space Administration, and Langley Directorate, U.S. Army Air Mobility Research and Development Laboratory, Hampton, Virginia, May, 1974.
16. Monteleone, R. A., INVESTIGATION OF THE MANEUVERABILITY OF THE S-67 WINGED HELICOPTER, United Aircraft Corporation, Sikorsky Aircraft Division; USAAMRDL TR-73-51, Eustis Directorate, U.S. Army Air Mobility Research and Development Laboratory, Fort Eustis, Virginia, June, 1973, AD 767559.
17. Corso, J. J., and Kaplita, T. T., GENERAL HELICOPTER SIMULATION PROGRAM, United Aircraft Corporation, Sikorsky Aircraft Division Report SER-50542, May, 1968.
18. Howlett, J. J., RSRA SIMULATION MODEL VOLUME I, MATHEMATICAL MODEL EQUATIONS, United Aircraft Corporation, Sikorsky Aircraft Division Report SER-72009, October, 1974.
19. Gerdes, W. H., and Tanner, W. H., GENERALIZED ROTOR PERFORMANCE METHOD, United Aircraft Corporation, Sikorsky Aircraft Division Report SER-50355, November, 1964.

20. Studwell, R. E., INCORPORATION OF SKEWED FLOW IN THE GENERALIZED ROTOR PERFORMANCE PROGRAM, United Aircraft Corporation, Sikorsky Aircraft Division Report SER-50773, January, 1973.
21. Kreutz, F., STRUCTURAL BUILD-UP TO CRITICAL LIMITS OF THE CH-53A HELICOPTER, United Aircraft Corporation, Sikorsky Aircraft Division Report SER-65412, April, 1967.
22. Arcidiacono, P. J., PREDICTION OF ROTOR INSTABILITY AT HIGH FORWARD SPEEDS VOLUME I, STEADY FLIGHT DIFFERENTIAL EQUATIONS OF MOTION FOR A FLEXIBLE HELICOPTER BLADE WITH CHORDWISE MASS UNBALANCE, United Aircraft Corporation, Sikorsky Aircraft Division; USAAVLABS TR 68-18A, U.S. Army Aviation Materiel Laboratories, Fort Eustis, Virginia, February, 1969, AD 685860.
23. Bergquist, R. R., and Thomas, G. C., TECHNICAL MANUAL, NORMAL MODES ROTOR AEROELASTIC ANALYSIS COMPUTER PROGRAM Y200, United Aircraft Corporation, Sikorsky Aircraft Division Report SER-50840, June, 1973.
24. Blackwell, R. H., and Commerford, G. L., INVESTIGATION OF THE EFFECTS OF BLADE STRUCTURAL DESIGN PARAMETERS ON HELICOPTER STALL BOUNDARIES, United Aircraft Corporation, Sikorsky Aircraft Division; USAAMRDL TR-74-25, Eustis Directorate, U.S. Army Air Mobility Research and Development Laboratory, Fort Eustis, Virginia, May, 1974, AD 784594.

TABLE 1. BASIC AIRCRAFT DESCRIPTIVE DATA

Basic Data	H-53	S-67
Fuselage		
Aerodynamic data reference		
Stationline, in.	336.5	267.4
Buttline, in.	0	0
Waterline, in.	161	170
Main Rotor		
Number of blades	6	5
Radius, ft	36	31
Normal tip speed, ft/sec	696	686
Blade chord, ft	2.17	1.52
Blade twist, deg	6	4
Tip sweep, deg	3	20
Articulated hinge location, ft	2	1.05
Pitch-flap coupling, deg	0	0.65
Airfoil	NACA 0011	NACA 0012 (modified)
Forward shaft tilt, deg	5	4
Location		
Stationline, in.	336.5	267.5
Buttline, in.	0	0
Waterline, in.	257.5	233
Tail Rotor		
Number of blades	4	5
Radius, ft	8	5.3
Normal tip speed, ft/sec	661	718
Blade chord, ft	1.28	0.61
Blade twist, deg	8	0
Tip sweep, deg	0	0
Articulated hinge location, ft	0.42	0.32
Pitch-flap coupling, deg	45	45
Airfoil	NACA 0012	NACA 0012 (modified)
Location		
Stationline, in.	870	711
Buttline, in.	-33	-24
Waterline, in.	272	223.5
Horizontal Tail		
Area, ft ²	40	50
Aspect ratio	2.59	4.79
Taper ratio	0.60	0.48
Incidence (leading edge up), deg	3	-3.5
Center of pressure		
Stationline, in.	846	643
Buttline, in.	60.9	0
Waterline, in.	290	150

TABLE I. - Concluded

Basic Data	H-53	S-67
Vertical Tail		
Area, ft ²	35	81
Aspect ratio	1.7	2.81
Taper ratio	0.85	0.46
Center of pressure		
Stationline, in.	812	700
Buttline, in.	0	0
Waterline, in.	228.9	206
Wing		
Span, ft	NA	27.33
Area, ft ²		98
Aspect ratio		7.15
Taper ratio		0.48
Incidence (leading edge up), deg		8
Dihedral (up), deg		10
Sweep (1/4 chord line), deg		10.75
Center of pressure (right wing)		
Stationline, in.		268
Buttline, in.		103
Waterline, in.		121
Airfoil		NACA 4412
Control System Range		
Longitudinal cyclic, deg	-8.3 to 16.2	-10 to 14
Lateral cyclic, deg	-8.6 to 3.6	-8 to 8
Collective pitch, deg	2 to 14.7	1.5 to 12.7
Tail Rotor pitch, deg	-2 to 28	-6.5 to 25
Horizontal tail incidence, deg	NA	-15.5 to 8.5
Longitudinal cyclic to horizontal tail incidence coupling, deg/deg	NA	1.0
Propulsive System		
Maximum total engine horsepower available	8000	3000
Loading Conditions		
Gross weight range, lb	21,000 to 47,000	11,000 to 18,000
Inertia range		
Roll, slug-ft ²	15,800 to 67,000	6900 to 8800
Pitch, slug-ft ²	78,000 to 335,000	53,000 to 66,000
Yaw, slug-ft ²	75,000 to 310,000	48,000 to 57,500
Roll-to-yaw, slug-ft ²	6000 to 30,000	2200 to 4700
Stationline CG range, in.	328 to 352	258 to 276

TABLE II. C81 INPUT LISTING FOR H-53

[illegible]

TABLE II. - Concluded

CH-53A STABILIZER SURFACE CONTROL HORIZONTAL						
STABILIZER NO. 1 GROUP						
40.00000	40.00000	40.00000	40.00000	40.00000	40.00000	40.00000
2.500000	1.000000	1.000000	1.000000	1.000000	1.000000	1.000000
.0	.0	.0	.0	.0	.0	.0
.0	.0	1.250000	1.500000E-01	1.250000E-02	.0	.0
1.000000	.0	.0	.0	.0	.0	.0
1.000000	1.000000	1.000000	.0	.0	.0	.0
1.000000	1.000000E-02	1.000000E-01	.0	1.000000E-02	1.000000E-04	1.000000E-04
1.000000E-01	1.000000E-01	1.000000	.0	.0	.0	.0
.0	.0	.0	.0	.0	.0	.0
CH-53A VERTICAL TAIL STABILIZER GROUP						
STABILIZER NO. 2 GROUP						
40.00000	412.1444	.0	28.9000	.0	90.0000	37.50000
1.000000	1.000000	1.000000	.0	1.550000	.0	.0
.0	.0	.0	.0	.0	.0	.0
.0	.0	.0	.0	.0	.0	.0
.0	.0	.0	.0	.0	.0	.0
1.000000	1.000000	1.000000	.0	.0	.0	.0
1.000000	.0	.0	.0	1.540000E-01	1.791000E-04	1.000000
1.000000E-01	1.551999E-01	1.4250000	.0	.0	.0	.0
.0	.0	.0	.0	.0	.0	.0
CH-53A RETRO CONTROLS GROUP						
CONTROLS GROUP						
10.00000	2.000000	12.20000	.0	.0	.0	.0
12.20000	12.20000	26.40000	.0	.0	.0	.0
12.20000	12.20000	12.20000	.0	.0	.0	.0
4.400000	12.000000	30.00000	.0	.0	.0	.0
CH-53A ITERATION LOGIC GROUP						
ITERATION GROUP						
25.00000	1.000000	1.000000	1.000000	.0	.0	.0
200.0000	200.0000	.0	.0	.0	.0	.0
200.0000	200.0000	200.0000	200.0000	200.0000	200.0000	40.00000
FLIGHT CONSTANTS GROUP						
.0	.0	1.200000	2000.000	.0	5.000000	.0
50.00000	25.00000	50.00000	43.00000	.0	.0	.0
1.700000	1.710000	.0	.0	3.0000.00	2631.000	.0
.0	.0	8000.000	13600.00	.0	.0	.0

COPY AVAILABLE TO DDC DOES NOT
PERMIT FULLY LEGIBLE PRODUCTION

TABLE III. C81 INPUT LISTING FOR S-67

INPUT DATA													
S-67 PROGRAM LOGIC GROUP													
PROGRAM LOGIC GROUP													
1	0	2	1	0	2	0	0	-1	2	0	0	0	0
2	0	1	1	2	0	0	0	0	0	0	0	0	0
1	0	1	0	0	0	0	0	0	0	0	0	0	0
S-67 MAIN ROTOR AEROELASTIC PLANE DATA													
S-67 TAIL ROTOR AEROELASTIC PLANE DATA													
S-67 FUSELAGE DATA													
FUSELAGE GROUP													
15513.00	257.4977	0.0	170.0000	272.5000	0.0	170.0000							
8200.000	51500.00	55900.00	4100.000	0.0	0.0	0.0							
10.07310	0.0	0.0	0.0	0.0	0.0	0.0							
0.597100E-01	1.415343	-0.1180000E-02	0.9659999E-03	0.1471000E-01	-0.9200000E-04	0.0							
10.14900	0.0	0.0	0.0	0.0	0.0	0.0							
0.521300E-01	0.255522	0.565000E-03	-0.1149999E-03	0.4245000E-01	0.1150000E-03	0.0							
0.122000	0.0	0.0	0.0	0.0	0.0	0.0							
0.110000	12.45562	0.0	-0.7812000E-02	-0.1109410	0.0	0.0							
0.0	0.0	0.0	0.1435200E-01	-0.1285000E-02	-0.5700000E-04	0.0							
0.008400	0.0	0.0	0.2050000E-02	0.0000000E-05	0.1250000E-02	0.0							
0.0	0.0	0.0	0.0	0.0	0.0	0.0							
0.0044125	0.0	0.0	0.0	0.0	-0.1240000E-02	0.0							
0.0	0.0	0.0	0.285513	0.7592900E-01	-0.1012700E-01	0.0							
0.135423	0.333420	-0.7454000E-02	-0.2781100	-0.1776400E-01	0.2080000E-03	0.0							
S-67 ROTOR AERODYNAMIC GROUP (MAIN AND TAIL)													
RTR AERODYNAMIC GROUP													
0.0	0.0	0.0	0.0	0.0	0.0	0.0							
0.0	0.0	0.0	0.0	0.0	0.0	0.0							
0.0	0.0	0.0	2.000000	0.0	0.0	0.0							
0.0	0.0	0.0	0.0	0.0	0.0	0.0							
0.0	0.0	0.0	0.0	0.0	0.0	0.0							
0.0	0.0	0.0	0.0	0.0	0.0	0.0							
0.0	0.0	0.0	0.0	0.0	0.0	0.0							
0.0	0.0	0.0	2.000000	0.0	0.0	0.0							
0.0	0.0	0.0	0.0	0.0	0.0	0.0							
S-67 MAIN ROTOR GROUP													
MAIN ROTOR GROUP													
0.000000	0.0	0.0	0.000000	0.0	100.0000	0.000000							
257.5000	0.0	233.0000	0.0	0.0	1.000000	0.0							
0.0	1.000000	0.000000E+00	0.0	0.0	0.000000	0.0							
0.0	0.0	9.550000	0.000000	0.0	0.0	0.0							
20.00000	0.000000	0.000000	0.000000	0.0	0.0	0.0							
0.0	0.0	0.0	0.0	0.0	0.0	0.0							
-10.00000	0.000000	0.0	0.0	0.0	0.0	0.0							
0.0	0.0	0.0	0.0	0.0	0.0	0.0							
18.25000	18.25000	18.25000	18.25000	18.25000	18.25000	18.25000							
18.25000	18.25000	18.25000	18.25000	18.25000	18.25000	18.25000							
0.0	1.800000	1.800000	1.800000	1.800000	1.800000	1.800000							
1.400000	1.200000	1.000000	0.800000	0.600000	0.400000	0.200000							
0.0	-0.200000	-0.400000	-0.600000	-0.800000	-1.000000	-1.200000							
S-67 TAIL ROTOR GROUP													
TAIL ROTOR GROUP													
0.000000	0.0	0.0	0.000000	0.0	0.0	0.000000							
111.0000	-24.00000	223.5000	0.0	0.0	0.100000	0.0							
0.0	1.000000	0.000000E+00	0.0	0.0	0.0	0.0							
0.0	0.0	45.00000	0.000000	0.0	0.0	0.0							
0.0	0.0	3.000000	0.000000	0.0	0.0	0.0							
0.0	0.0	0.0	0.0	0.0	0.0	0.0							
0.0	0.0	40.00000	0.0	0.0	0.0	0.0							
0.0	3.550000	3.550000	3.550000	3.550000	3.550000	3.550000							
7.340000	7.340000	7.340000	7.340000	7.340000	7.340000	7.340000							
7.340000	7.340000	7.340000	7.340000	7.340000	7.340000	7.340000							

TABLE III. - Concluded

S-67 WING GROUP						
			WING GROUP			
89.00000	268.0000	103.0000	121.0000	12.00000	13.00000	10.75000
7.147000	1.000000	.3460000	.0	.0	.0	.0
.0	.0	.0	.0	.0	.0	.0
.0	.0	.0	.0	.0	.0	.0
.5000000	.5000000	.0	.0	-.7999998E-01	-.7999998E-01	.2350000
-.4200000	.0	-.2500000E-01	-.1500000E-01	-.3200000	-.6000000E-01	9.000000
.7000000	.7500000	1.420000	.0	.0	.0	1.000000
.1000000	.0	.0	.0	.6800000E-02	-.3320000E-03	.4600000E-04
.4000000E-01	.1300000E-01	.1200000	.0	.0	.0	.0
.0	.0	.8200000	-.9500000E-01	.0	.0	.0
STABILIZER 1 HORIZONTAL TAIL S-67						
			STABILIZER NO. 1 GROUP			
53.00000	534.0000	.0	150.0000	-.3500000	.0	.0
4.787000	1.000000	.4800000	.0	.1400000	.0	.0
.0	.0	.0	.0	.0	.0	.0
.0	.0	.4.000000	.1400000	-.2500000E-02	.0	.0
1.400000	.0	.0	.0	.0	.0	.0
.7000000	.7500000	.8000000	.0	.0	.0	.8000000
.1000000	-.9000000E-02	.8098000E-01	.0	.8000000E-02	-.1667000E-04	.1567000E-04
-.000000E-01	.1200000E-01	.1400000	.0	.0	.0	.0
.0	.0	.0	.0	.0	.0	.0
.0	.0	.0	1.715000	.0	.0	.0
.0	.0	.0	.0	.0	.0	.0
VERTICAL TAIL S-67						
			STABILIZER NO. 2 GROUP			
81.00000	700.0000	.0	200.0000	3.800000	50.00000	37.00000
2.407000	.787000	.4590000	.0	.9000000	.0	.0
.0	.0	.0	.0	.0	.0	.0
.0	.0	.0	.0	.0	.0	.1000000
.0	.0	.0	.0	.0	.0	.0
.7000000	.7500000	.8000000	.0	.0	.0	.8000000
.1000000	-.9000000E-02	.8098000E-01	.0	.8000000E-02	-.3849999E-03	.6101999E-04
.4000000E-01	.1300000E-01	.1400000	.0	.0	.0	.0
.0	.0	.8200000	-.8999997E-01	.0	.0	.0
.0	.0	.0	.0	.0	.0	.0
.0	.0	.0	.0	.0	.0	.0
S-67 ROTOR CONTROLS GROUP						
			CONTROLS GROUP			
4.00000	1.500000	14.20000	.0	.0	.0	.0
14.00000	-.10.00000	24.00000	.0	.0	.0	.0
14.00000	-.4.00000	16.00000	.0	.0	.0	.0
.407000	-.5.00000	31.50000	.0	.0	.0	.0
S-67 ITERATION LOGIC GROUP						
			ITERATION GROUP			
25.00000	15.00000	.5000000	.5000000	.0	.0	.0
.2000000	.2000000	.0	.0	.0	.0	.0
.200.0000	.200.0000	200.0000	.200.0000	200.0000	200.0000	40.00000
FLIGHT CONSTANTS GROUP						
.0	.0	.0	.0	.0	.0	.0
50.00000	45.00000	50.00000	50.00000	.0	8.500000	.0
.0	.0	.0	.0	.0	.0	.0
.0	.0	3000.000	211.0000	15500.00	1000.000	.0
.0	.0	.0	.0	.0	3000.000	.0

COPY AVAILABLE TO YOU DOES NOT
PERMIT FULLY LEGIBLE PRODUCTION

TABLE IV. C81 PRELOADED 0012 AIRFOIL DATA

NACA 0012 AIRFOIL

CLCD DATA TABLES USED

11

ALPHA/MACH	CL	CD	CM	CL	CD	CM	CL	CD	CM	CL	CD
0.0/0.3	0.0	0.0	0.0	0.0	0.0	0.0	0.0	0.0	0.0	0.0	0.0
0.5/0.3	0.0	0.0	0.0	0.0	0.0	0.0	0.0	0.0	0.0	0.0	0.0
1.0/0.3	0.0	0.0	0.0	0.0	0.0	0.0	0.0	0.0	0.0	0.0	0.0
1.5/0.3	0.0	0.0	0.0	0.0	0.0	0.0	0.0	0.0	0.0	0.0	0.0
2.0/0.3	0.0	0.0	0.0	0.0	0.0	0.0	0.0	0.0	0.0	0.0	0.0
2.5/0.3	0.0	0.0	0.0	0.0	0.0	0.0	0.0	0.0	0.0	0.0	0.0
3.0/0.3	0.0	0.0	0.0	0.0	0.0	0.0	0.0	0.0	0.0	0.0	0.0
3.5/0.3	0.0	0.0	0.0	0.0	0.0	0.0	0.0	0.0	0.0	0.0	0.0
4.0/0.3	0.0	0.0	0.0	0.0	0.0	0.0	0.0	0.0	0.0	0.0	0.0
4.5/0.3	0.0	0.0	0.0	0.0	0.0	0.0	0.0	0.0	0.0	0.0	0.0
5.0/0.3	0.0	0.0	0.0	0.0	0.0	0.0	0.0	0.0	0.0	0.0	0.0
5.5/0.3	0.0	0.0	0.0	0.0	0.0	0.0	0.0	0.0	0.0	0.0	0.0
6.0/0.3	0.0	0.0	0.0	0.0	0.0	0.0	0.0	0.0	0.0	0.0	0.0
6.5/0.3	0.0	0.0	0.0	0.0	0.0	0.0	0.0	0.0	0.0	0.0	0.0
7.0/0.3	0.0	0.0	0.0	0.0	0.0	0.0	0.0	0.0	0.0	0.0	0.0
7.5/0.3	0.0	0.0	0.0	0.0	0.0	0.0	0.0	0.0	0.0	0.0	0.0
8.0/0.3	0.0	0.0	0.0	0.0	0.0	0.0	0.0	0.0	0.0	0.0	0.0
8.5/0.3	0.0	0.0	0.0	0.0	0.0	0.0	0.0	0.0	0.0	0.0	0.0
9.0/0.3	0.0	0.0	0.0	0.0	0.0	0.0	0.0	0.0	0.0	0.0	0.0
9.5/0.3	0.0	0.0	0.0	0.0	0.0	0.0	0.0	0.0	0.0	0.0	0.0
10.0/0.3	0.0	0.0	0.0	0.0	0.0	0.0	0.0	0.0	0.0	0.0	0.0
10.5/0.3	0.0	0.0	0.0	0.0	0.0	0.0	0.0	0.0	0.0	0.0	0.0
11.0/0.3	0.0	0.0	0.0	0.0	0.0	0.0	0.0	0.0	0.0	0.0	0.0
11.5/0.3	0.0	0.0	0.0	0.0	0.0	0.0	0.0	0.0	0.0	0.0	0.0
12.0/0.3	0.0	0.0	0.0	0.0	0.0	0.0	0.0	0.0	0.0	0.0	0.0
12.5/0.3	0.0	0.0	0.0	0.0	0.0	0.0	0.0	0.0	0.0	0.0	0.0
13.0/0.3	0.0	0.0	0.0	0.0	0.0	0.0	0.0	0.0	0.0	0.0	0.0
13.5/0.3	0.0	0.0	0.0	0.0	0.0	0.0	0.0	0.0	0.0	0.0	0.0
14.0/0.3	0.0	0.0	0.0	0.0	0.0	0.0	0.0	0.0	0.0	0.0	0.0
14.5/0.3	0.0	0.0	0.0	0.0	0.0	0.0	0.0	0.0	0.0	0.0	0.0
15.0/0.3	0.0	0.0	0.0	0.0	0.0	0.0	0.0	0.0	0.0	0.0	0.0
15.5/0.3	0.0	0.0	0.0	0.0	0.0	0.0	0.0	0.0	0.0	0.0	0.0
16.0/0.3	0.0	0.0	0.0	0.0	0.0	0.0	0.0	0.0	0.0	0.0	0.0
16.5/0.3	0.0	0.0	0.0	0.0	0.0	0.0	0.0	0.0	0.0	0.0	0.0
17.0/0.3	0.0	0.0	0.0	0.0	0.0	0.0	0.0	0.0	0.0	0.0	0.0
17.5/0.3	0.0	0.0	0.0	0.0	0.0	0.0	0.0	0.0	0.0	0.0	0.0
18.0/0.3	0.0	0.0	0.0	0.0	0.0	0.0	0.0	0.0	0.0	0.0	0.0
18.5/0.3	0.0	0.0	0.0	0.0	0.0	0.0	0.0	0.0	0.0	0.0	0.0
19.0/0.3	0.0	0.0	0.0	0.0	0.0	0.0	0.0	0.0	0.0	0.0	0.0
19.5/0.3	0.0	0.0	0.0	0.0	0.0	0.0	0.0	0.0	0.0	0.0	0.0
20.0/0.3	0.0	0.0	0.0	0.0	0.0	0.0	0.0	0.0	0.0	0.0	0.0
20.5/0.3	0.0	0.0	0.0	0.0	0.0	0.0	0.0	0.0	0.0	0.0	0.0
21.0/0.3	0.0	0.0	0.0	0.0	0.0	0.0	0.0	0.0	0.0	0.0	0.0
21.5/0.3	0.0	0.0	0.0	0.0	0.0	0.0	0.0	0.0	0.0	0.0	0.0
22.0/0.3	0.0	0.0	0.0	0.0	0.0	0.0	0.0	0.0	0.0	0.0	0.0
22.5/0.3	0.0	0.0	0.0	0.0	0.0	0.0	0.0	0.0	0.0	0.0	0.0
23.0/0.3	0.0	0.0	0.0	0.0	0.0	0.0	0.0	0.0	0.0	0.0	0.0
23.5/0.3	0.0	0.0	0.0	0.0	0.0	0.0	0.0	0.0	0.0	0.0	0.0
24.0/0.3	0.0	0.0	0.0	0.0	0.0	0.0	0.0	0.0	0.0	0.0	0.0
24.5/0.3	0.0	0.0	0.0	0.0	0.0	0.0	0.0	0.0	0.0	0.0	0.0
25.0/0.3	0.0	0.0	0.0	0.0	0.0	0.0	0.0	0.0	0.0	0.0	0.0
25.5/0.3	0.0	0.0	0.0	0.0	0.0	0.0	0.0	0.0	0.0	0.0	0.0
26.0/0.3	0.0	0.0	0.0	0.0	0.0	0.0	0.0	0.0	0.0	0.0	0.0
26.5/0.3	0.0	0.0	0.0	0.0	0.0	0.0	0.0	0.0	0.0	0.0	0.0
27.0/0.3	0.0	0.0	0.0	0.0	0.0	0.0	0.0	0.0	0.0	0.0	0.0
27.5/0.3	0.0	0.0	0.0	0.0	0.0	0.0	0.0	0.0	0.0	0.0	0.0
28.0/0.3	0.0	0.0	0.0	0.0	0.0	0.0	0.0	0.0	0.0	0.0	0.0
28.5/0.3	0.0	0.0	0.0	0.0	0.0	0.0	0.0	0.0	0.0	0.0	0.0
29.0/0.3	0.0	0.0	0.0	0.0	0.0	0.0	0.0	0.0	0.0	0.0	0.0
29.5/0.3	0.0	0.0	0.0	0.0	0.0	0.0	0.0	0.0	0.0	0.0	0.0
30.0/0.3	0.0	0.0	0.0	0.0	0.0	0.0	0.0	0.0	0.0	0.0	0.0

NACA 0012 AIRFOIL

CLCD DATA TABLES USED

CM

ALPHA/MACH	CL	CD	CM	CL	CD	CM	CL	CD	CM	CL	CD
0.0/0.3	0.0	0.0	0.0	0.0	0.0	0.0	0.0	0.0	0.0	0.0	0.0
0.5/0.3	0.0	0.0	0.0	0.0	0.0	0.0	0.0	0.0	0.0	0.0	0.0
1.0/0.3	0.0	0.0	0.0	0.0	0.0	0.0	0.0	0.0	0.0	0.0	0.0
1.5/0.3	0.0	0.0	0.0	0.0	0.0	0.0	0.0	0.0	0.0	0.0	0.0
2.0/0.3	0.0	0.0	0.0	0.0	0.0	0.0	0.0	0.0	0.0	0.0	0.0
2.5/0.3	0.0	0.0	0.0	0.0	0.0	0.0	0.0	0.0	0.0	0.0	0.0
3.0/0.3	0.0	0.0	0.0	0.0	0.0	0.0	0.0	0.0	0.0	0.0	0.0
3.5/0.3	0.0	0.0	0.0	0.0	0.0	0.0	0.0	0.0	0.0	0.0	0.0
4.0/0.3	0.0	0.0	0.0	0.0	0.0	0.0	0.0	0.0	0.0	0.0	0.0
4.5/0.3	0.0	0.0	0.0	0.0	0.0	0.0	0.0	0.0	0.0	0.0	0.0
5.0/0.3	0.0	0.0	0.0	0.0	0.0	0.0	0.0	0.0	0.0	0.0	0.0
5.5/0.3	0.0	0.0	0.0	0.0	0.0	0.0	0.0	0.0	0.0	0.0	0.0
6.0/0.3	0.0	0.0	0.0	0.0	0.0	0.0	0.0	0.0	0.0	0.0	0.0
6.5/0.3	0.0	0.0	0.0	0.0	0.0	0.0	0.0	0.0	0.0	0.0	0.0
7.0/0.3	0.0	0.0	0.0	0.0	0.0	0.0	0.0	0.0	0.0	0.0	0.0
7.5/0.3	0.0	0.0	0.0	0.0	0.0	0.0	0.0	0.0	0.0	0.0	0.0
8.0/0.3	0.0	0.0	0.0	0.0	0.0	0.0	0.0	0.0	0.0	0.0	0.0
8.5/0.3	0.0	0.0	0.0	0.0	0.0	0.0	0.0	0.0	0.0	0.0	0.0
9.0/0.3	0.0	0.0	0.0	0.0	0.0	0.0	0.0	0.0	0.0	0.0	0.0
9.5/0.3	0.0	0.0	0.0	0.0	0.0	0.0	0.0	0.0	0.0	0.0	0.0
10.0/0.3	0.0	0.0	0.0	0.0	0.0	0.0	0.0	0.0	0.0	0.0	0.0
10.5/0.3	0.0	0.0	0.0	0.0	0.0	0.0	0.0	0.0	0.0	0.0	0.0
11.0/0.3	0.0	0.0	0.0	0.0	0.0	0.0	0.0	0.0	0.0	0.0	0.0
11.5/0.3	0.0	0.0	0.0	0.0	0.0	0.0	0.0	0.0	0.0	0.0	0.0
12.0/0.3	0.0	0.0	0.0	0.0	0.0	0.0	0.0	0.0	0.0	0.0	0.0
12.5/0.3	0.0	0.0	0.0	0.0	0.0	0.0	0.0	0.0	0.0	0.0	0.0
13.0/0.3	0.0	0.0	0.0	0.0	0.0	0.0	0.0	0.0	0.0	0.0	0.0
13.5/0.3	0.0	0.0	0.0	0.0	0.0	0.0	0.0	0.0	0.0	0.0	0.0
14.0/0.3	0.0	0.0	0.0	0.0	0.0	0.0	0.0	0.0	0.0	0.0	0.0
14.5/0.3	0.0	0.0	0.0	0.0	0.0	0.0	0.0	0.0	0.0	0.0	0.0
15.0/0.3	0.0	0.0	0.0	0.0	0.0	0.0	0.0	0.0	0.0	0.0	0.0
15.5/0.3	0.0	0.0	0.0	0.0	0.0	0.0	0.0	0.0	0.0	0.0	0.0
16.0/0.3	0.0	0.0	0.0	0.0	0.0	0.0	0.0	0.0	0.0	0.0	0.0
16.5/0.3	0.0	0.0	0.0	0.0	0.0	0.0	0.0	0.0	0.0	0.0	0.0
17.0/0.3	0.0	0.0	0.0	0.0	0.0	0.0	0.0	0.0	0.0	0.0	0.0
17.5/0.3	0.0	0.0	0.0	0.0	0.0	0.0	0.0	0.0	0.0	0.0	0.0
18.0/0.3	0.0	0.0	0.0	0.0	0.0	0.0	0.0	0.0	0.0	0.0	0.0
18.5/0.3	0.0	0.0	0.0	0.0	0.0	0.0	0.0	0.0	0.0	0.0	0.0
19.0/0.3	0.0	0.0	0.0	0.0	0.0	0.0	0.0	0.0	0.0	0.0	0.0
19.5/0.3	0.0	0.0	0.0	0.0	0.0	0.0	0.0	0.0	0.0	0.0	0.0
20.0/0.3	0.0	0.0	0.0	0.0	0.0	0.0	0.0	0.0	0.0	0.0	0.0
20.5/0.3	0.0	0.0	0.0	0.0	0.0	0.0	0.0	0.0	0.0	0.0	0.0
21.0/0.3	0.0	0.0	0.0	0.0	0.0	0.0	0.0	0.0	0.0	0.0	0.0
21.5/0.3	0.0	0.0	0.0	0.0	0.0	0.0	0.0	0.0	0.0	0.0	0.0
22.0/0.3	0.0	0.0	0.0	0.0	0.0	0.0	0.0	0.0	0.0	0.0	0.0
22.5/0.3	0.0	0.0	0.0	0.0	0.0	0.0	0.0	0.0	0.0	0.0	0.0
23.0/0.3	0.0	0.0	0.0	0.0	0.0	0.0	0.0	0.0	0.0	0.0	0.0
23.5/0.3	0.0	0.0	0.0	0.0	0.0	0.0	0.0	0.0	0.0	0.0	0.0
24.0/0.3	0.0	0.0	0.0	0.0	0.0	0.0	0.0	0.0	0.0	0.0	0.0
24.5/0.3	0.0	0.0	0.0	0.0	0.0	0.0	0.0	0.0	0.0	0.0	0.0
25.0/0.3	0.0	0.0	0.0	0.0	0.0	0.0	0.0	0.0	0.0	0.0	0.0
25.5/0.3	0.0	0.0	0.0	0.0	0.0	0.0	0.0	0.0	0.0	0.0	0.0

[illegible]

59

TABLE V. SIKORSKY VERSION OF 0012 AIRFOIL DATA
IN C81 FORMAT

C1

C100 DATA TABLES USED

ALPHA/4PI	3.0	0.10000	0.10000	0.40000	0.50000	0.60000	0.70000	0.75000	0.80000	0.85000	0.90000	1.00000
-180.00000	0.0	0.0	0.0	0.0	0.0	0.0	0.0	0.0	0.0	0.0	0.0	0.0
-172.50000	0.77500	0.74000	0.71250	0.71250	0.72000	0.71750	0.76560	0.77500	0.77500	0.77500	0.77500	0.77500
-161.00000	0.70500	0.70500	0.70500	0.70500	0.70500	0.70500	0.79870	0.70500	0.70500	0.70500	0.70500	0.70500
-147.00000	1.01000	1.01000	1.01000	1.01000	1.01000	1.01000	1.01000	1.01000	1.01000	1.01000	1.01000	1.01000
-124.00000	0.94000	0.94000	0.94000	0.94000	0.94000	0.94000	0.94000	0.94000	0.94000	0.94000	0.94000	0.94000
-99.00000	-1.11000	-1.11000	-1.11000	-1.11000	-1.11000	-1.11000	-1.11000	-1.11000	-1.11000	-1.11000	-1.11000	-1.11000
-10.00000	-1.00000	-1.00000	-1.00000	-1.00000	-1.00000	-1.00000	-1.00000	-1.00000	-1.00000	-1.00000	-1.00000	-1.00000
-16.50000	-0.64000	-0.72880	-0.94870	-0.80630	-0.81500	-0.77850	-0.81200	-0.79900	-0.72300	-0.64650	-0.64650	-0.64650
-15.00000	-0.65000	-0.78000	-1.10000	-0.89750	-0.64200	-0.79000	-0.80960	-0.77500	-0.69000	-0.60500	-0.60500	-0.60500
-14.00000	-0.67900	-0.86500	-1.26000	-0.97000	-0.86000	-0.80000	-0.81410	-0.75700	-0.66400	-0.56900	-0.56900	-0.56900
-13.00000	-0.76500	-1.02500	-1.26110	-1.02500	-0.88750	-0.81670	-0.81670	-0.73900	-0.63800	-0.53800	-0.53800	-0.53800
-12.00000	-0.84000	-1.03500	-1.15750	-1.10000	-0.95500	-0.87500	-0.80840	-0.70000	-0.58000	-0.44500	-0.44500	-0.44500
-11.00000	-0.84800	-1.00000	-1.07500	-1.07000	-0.90000	-0.80000	-0.70000	-0.60000	-0.48000	-0.35000	-0.35000	-0.35000
-10.00000	-0.81000	-0.94000	-1.07500	-1.07000	-0.80000	-0.70000	-0.60000	-0.48000	-0.35000	-0.22000	-0.22000	-0.22000
-8.00000	-0.66400	-0.75200	-0.86000	-0.88440	-0.81000	-0.70000	-0.60000	-0.48000	-0.35000	-0.22000	-0.22000	-0.22000
-6.70000	-0.49800	-0.56400	-0.64500	-0.66330	-0.60000	-0.50000	-0.40000	-0.30000	-0.20000	-0.10000	-0.10000	-0.10000
-4.00000	-0.31200	-0.37600	-0.43000	-0.44720	-0.46700	-0.48330	-0.50000	-0.50000	-0.50000	-0.50000	-0.50000	-0.50000
-2.00000	-0.16600	-0.21500	-0.22110	-0.23330	-0.24170	-0.24170	-0.24170	-0.24170	-0.24170	-0.24170	-0.24170	-0.24170
0.0	0.0	0.0	0.0	0.0	0.0	0.0	0.0	0.0	0.0	0.0	0.0	0.0
2.00000	0.16600	0.21500	0.22110	0.23330	0.24170	0.24170	0.24170	0.24170	0.24170	0.24170	0.24170	0.24170
4.00000	0.31200	0.37600	0.43000	0.44720	0.46700	0.48330	0.50000	0.50000	0.50000	0.50000	0.50000	0.50000
6.70000	0.49800	0.56400	0.64500	0.66330	0.70000	0.75000	0.80000	0.80000	0.80000	0.80000	0.80000	0.80000
8.00000	0.66400	0.75200	0.86000	0.88440	0.95500	1.00000	1.00000	1.00000	1.00000	1.00000	1.00000	1.00000
10.00000	0.81000	0.94000	1.07500	1.07000	0.90000	0.80000	0.70000	0.60000	0.48000	0.35000	0.35000	0.35000
11.00000	0.84800	1.00000	1.15750	1.10000	0.95500	0.87500	0.80840	0.70000	0.58000	0.44500	0.44500	0.44500
12.00000	0.84000	1.03500	1.26000	1.26110	1.02500	0.88750	0.81670	0.73900	0.63800	0.53800	0.53800	0.53800
13.00000	0.76500	1.02500	1.26110	1.02500	0.88750	0.81670	0.81670	0.73900	0.63800	0.53800	0.53800	0.53800
14.00000	0.67900	0.86500	1.26000	0.97000	0.86000	0.80000	0.81410	0.75700	0.66400	0.56900	0.56900	0.56900
15.00000	0.65000	0.78000	1.10000	0.89750	0.84200	0.79000	0.80960	0.77500	0.69000	0.60500	0.60500	0.60500
16.50000	0.64000	0.72880	0.94870	0.80630	0.81500	0.77850	0.81200	0.79900	0.72300	0.64650	0.64650	0.64650
180.00000	0.0	0.0	0.0	0.0	0.0	0.0	0.0	0.0	0.0	0.0	0.0	0.0

C1

C100 DATA TABLES USED

ALPHA/4PI	3.0	0.10000	0.10000	0.40000	0.50000	0.60000	0.70000	0.75000	0.80000	0.85000	0.90000	1.00000
-180.00000	0.0	0.0	0.0	0.0	0.0	0.0	0.0	0.0	0.0	0.0	0.0	0.0
-170.00000	0.37200	0.35500	0.37100	0.39500	0.39000	0.39000	0.32000	0.32000	0.32000	0.32000	0.32000	0.32000
-165.00000	0.30000	0.30000	0.30000	0.30000	0.30000	0.30000	0.30000	0.30000	0.30000	0.30000	0.30000	0.30000
-150.00000	0.54670	0.54670	0.54670	0.54670	0.54670	0.54670	0.54670	0.54670	0.54670	0.54670	0.54670	0.54670
-10.00000	0.52810	0.52810	0.52810	0.52810	0.52810	0.52810	0.52810	0.52810	0.52810	0.52810	0.52810	0.52810
-30.00000	0.17280	0.17280	0.17280	0.17280	0.17280	0.17280	0.17280	0.17280	0.17280	0.17280	0.17280	0.17280
-15.00000	0.06700	0.04450	0.02550	0.01600	0.05800	0.07250	0.08050	0.08050	0.08050	0.08050	0.08050	0.08050
-14.00000	0.05600	0.02700	0.00730	-0.00330	0.04000	0.06100	0.07400	0.08200	0.08600	0.08900	0.08900	0.08900
-13.00000	0.03900	0.01130	-0.00800	-0.01990	0.01000	0.04000	0.06200	0.07500	0.08100	0.08300	0.08300	0.08300
-12.00000	0.02200	0.00220	-0.01730	-0.02650	-0.02500	0.01630	0.05000	0.06800	0.07250	0.07600	0.07600	0.07600
-11.00000	0.00100	-0.00440	-0.02100	-0.02510	-0.02920	-0.01830	0.03200	0.05200	0.05400	0.05600	0.05600	0.05600
-10.00000	-0.30200	-0.00910	-0.01450	-0.02180	-0.02900	-0.03600	0.01400	0.04100	0.05170	0.05800	0.05800	0.05800
-9.00000	-0.30180	-0.00460	-0.01250	-0.01840	-0.02550	-0.03000	0.02900	0.04200	0.05350	0.06000	0.06000	0.06000
-8.00000	-0.00180	-0.00410	-0.01050	-0.01500	-0.02200	-0.02720	-0.01590	0.01700	0.02700	0.03600	0.03600	0.03600
-7.00000	-0.30140	-0.00360	-0.00850	-0.01260	-0.01830	-0.02430	-0.01050	0.00500	0.01800	0.02800	0.02800	0.02800
-6.00000	-0.30120	-0.00310	-0.00650	-0.01030	-0.01500	-0.02050	-0.00700	0.00900	0.02300	0.03400	0.03400	0.03400
-4.00000	-0.30080	-0.00270	-0.00430	-0.00550	-0.00800	-0.01100	-0.01500	-0.02000	0.0	0.01000	0.01500	0.01500
-3.00000	-0.30060	-0.00230	-0.00320	-0.00410	-0.00600	-0.00820	-0.01120	-0.01500	0.0	0.00600	0.01000	0.01000
-2.00000	-0.30040	-0.00190	-0.00220	-0.00280	-0.00400	-0.00550	-0.00750	-0.01000	0.0	0.00300	0.00600	0.00600
-1.00000	-0.30020	-0.00150	-0.00110	-0.00140	-0.00200	-0.00280	-0.00380	-0.00500	0.0	0.00100	0.00200	0.00200
0.0	0.0	0.0	0.0	0.0	0.0	0.0	0.0	0.0	0.0	0.0	0.0	0.0
1.00000	0.30020	0.00150	0.00110	0.00140	0.00200	0.00280	0.00380	0.00500	0.00700	0.00900	0.00900	0.00900
2.00000	0.30040	0.00190	0.00220	0.00280	0.00400	0.00550	0.00750	0.01000	0.0	0.00300	0.00600	0.00600
3.00000	0.30060	0.00230	0.00320	0.00410	0.00600	0.00820	0.01120	0.01500	0.0	0.00600	0.01000	0.01000
4.00000	0.30080	0.00270	0.00430	0.00550	0.00800	0.01100	0.01500	0.02000	0.0	0.01000	0.01500	0.01500
6.00000	0.30120	0.00310	0.00650	0.01030	0.01500	0.02050	0.02500	0.03000	0.00900	0.02300	0.03400	0.03400
7.00000	0.30140	0.00360	0.00850	0.01260	0.01830	0.02430	0.03000	0.03500	0.00800	0.02200	0.03300	0.03300
8.00000	0.30160	0.00410	0.01050	0.01500	0.02200	0.02720	0.03000	0.03500	0.00700	0.02100	0.03200	0.03200
9.00000	0.30180	0.00460	0.01250	0.01840	0.02550	0.03000	0.03500	0.04000	0.00600	0.02000	0.03100	0.03100
10.00000	0.30200	0.00510	0.01450	0.02180	0.02900	0.03600	0.04100	0.04600	0.00500	0.01900	0.03000	0.03000
11.00000	0.30220	0.00560	0.01650	0.02510	0.03200	0.03900	0.04400	0.04900	0.00400	0.01800	0.02900	0.02900
12.00000	0.30240	0.00610	0.01850	0.02840	0.03500	0.04200	0.04700	0.05200	0.00300	0.01700	0.02800	0.02800
13.00000	0.30260	0.00660	0.02050	0.03170	0.03800	0.04500	0.05000	0.05500	0.00200	0.01600	0.02700	0.02700
14.00000	0.30280	0.00710	0.02250	0.03500	0.04100	0.04800	0.05300	0.05800	0.00100	0.01500	0.02600	0.02600
15.00000	0.30300	0.00760	0.02450	0.03830	0.04400	0.05100	0.05600	0.06100	0.00000	0.01400	0.02500	0.02500
16.50000	0.30320	0.00810	0.02650	0.04160	0.04700	0.05400	0.05900	0.06400	0.00000	0.01300	0.02400	0.02400
180.00000	0.0	0.0	0.0	0.0	0.0	0.0	0.0	0.0	0.0	0.0	0.0	0.0

[illegible]

61

TABLE VI. H-53 AEROELASTIC BLADE DATA USED IN C81

MAIN ROTOR AEROELASTIC BLADE DISTRIBUTIONS AND DATA									
BLADE STATION NUMBER		WEIGHT (LB/IN)	BEAMWISE INERTIA (IN-LB-SEC**2/IN)			CHORDWISE INERTIA (IN-LB-SEC**2/IN)			
		1	2	3	4	5	6	7	
		0.0	0.7850	0.0002	0.0003	0.0004	0.0041	0.0041	
		0.0	0.4830	0.0003	0.0004	0.0005	0.0046	0.0046	
		0.0	0.7020	0.0004	0.0005	0.0006	0.0053	0.0053	
		0.0	0.7780	0.0002	0.0003	0.0004	0.0041	0.0041	
		0.0	0.7580	0.0003	0.0004	0.0005	0.0041	0.0041	
		0.0	0.7550	0.0003	0.0004	0.0005	0.0046	0.0046	
		0.0	0.7190	0.0003	0.0004	0.0005	0.0046	0.0046	
		0.0	0.7540	0.0003	0.0004	0.0005	0.0046	0.0046	
		0.0	0.7770	0.0003	0.0004	0.0005	0.0053	0.0053	
		0.0	0.7660	0.0003	0.0004	0.0005	0.0055	0.0055	
		0.0	0.7610	0.0003	0.0004	0.0005	0.0057	0.0057	
		0.0	0.7610	0.0003	0.0004	0.0005	0.0057	0.0057	
		0.0	0.8000	0.0003	0.0004	0.0005	0.0062	0.0062	
		0.0	0.8210	0.0003	0.0004	0.0005	0.0062	0.0062	
		0.0	0.8070	0.0003	0.0004	0.0005	0.0061	0.0061	
		0.0	0.8070	0.0003	0.0004	0.0005	0.0061	0.0061	
		0.0	0.7900	0.0004	0.0005	0.0006	0.0067	0.0067	
		0.0	0.8670	0.0005	0.0006	0.0007	0.0066	0.0066	
		0.0	0.8520	0.0005	0.0006	0.0007	0.0069	0.0069	
TOTAL BLADE WEIGHT = 129.57 LB BLADE TIP WEIGHT = 0.0 LB FLAPPING INERTIA/BLADE = 4865.0 SLUG-FT**2									
MODE SHAPE									
MODE SHAPE FOR MODE 1			MODE SHAPE FOR MODE 2			MODE SHAPE FOR MODE 3			
STA	OUT-OF-PLANE	IN-PLANE	TORSION	OUT-OF-PLANE	IN-PLANE	TORSION	OUT-OF-PLANE	IN-PLANE	TORSION
0	0.0	0.0	0.0	0.0	0.0	0.0	0.0	0.0	0.0
1	0.0	0.0	0.0	0.0	0.0	0.0	0.0	0.0	0.0
2	0.0025	0.0	0.0	0.0025	0.0	0.0	-0.01300	0.01300	0.0
3	0.0192	0.0	0.0	0.0	0.0192	0.0	-0.02050	0.02050	0.0
4	0.0178	0.0	0.0	0.0	0.0178	0.0	-0.01100	0.01100	0.0
5	0.0135	0.0	0.0	0.0	0.0135	0.0	-0.00300	0.00300	0.0
6	0.0031	0.0	0.0	0.0	0.0031	0.0	-0.00000	0.00000	0.0
7	0.0117	0.0	0.0	0.0	0.0117	0.0	-0.00400	0.00400	0.0
8	0.0094	0.0	0.0	0.0	0.0094	0.0	-0.00300	0.00300	0.0
9	0.0210	0.0	0.0	0.0	0.0210	0.0	-0.00300	0.00300	0.0
10	0.0473	0.0	0.0	0.0	0.0473	0.0	-0.00300	0.00300	0.0
11	0.0523	0.0	0.0	0.0	0.0523	0.0	-0.00300	0.00300	0.0
12	0.0787	0.0	0.0	0.0	0.0787	0.0	-0.00300	0.00300	0.0
13	0.0514	0.0	0.0	0.0	0.0514	0.0	-0.00300	0.00300	0.0
14	0.0517	0.0	0.0	0.0	0.0517	0.0	-0.00300	0.00300	0.0
15	0.0398	0.0	0.0	0.0	0.0398	0.0	-0.00300	0.00300	0.0
16	0.0094	0.0	0.0	0.0	0.0094	0.0	-0.00300	0.00300	0.0
17	0.0021	0.0	0.0	0.0	0.0021	0.0	-0.00300	0.00300	0.0
18	0.0047	0.0	0.0	0.0	0.0047	0.0	-0.00300	0.00300	0.0
19	0.0073	0.0	0.0	0.0	0.0073	0.0	-0.00300	0.00300	0.0
20	0.0130	0.0	0.0	0.0	0.0130	0.0	-0.00300	0.00300	0.0
MODE SHAPE FOR MODE 4			MODE SHAPE FOR MODE 5			MODE SHAPE FOR MODE 6			
STA	OUT-OF-PLANE	IN-PLANE	TORSION	OUT-OF-PLANE	IN-PLANE	TORSION	OUT-OF-PLANE	IN-PLANE	TORSION
0	0.0	0.0	0.0	0.0	0.0	0.0	0.0	0.0	0.0
1	0.0	0.0	0.0	0.0	0.0	0.0	0.0	0.0	0.0
2	-0.00300	-0.01300	0.0	0.0	0.0	0.0	0.0	0.0	0.0
3	-0.00300	-0.00300	0.0	0.0	0.0	0.0	0.0	0.0	0.0
4	-0.00300	-0.00300	0.0	0.0	0.0	0.0	0.0	0.0	0.0
5	-0.01000	-0.00300	0.0	0.0	0.0	0.0	0.0	0.0	0.0
6	-0.01300	-0.01300	0.0	0.0	0.0	0.0	0.0	0.0	0.0
7	-0.01000	-0.00300	0.0	0.0	0.0	0.0	0.0	0.0	0.0
8	-0.00300	-0.00300	0.0	0.0	0.0	0.0	0.0	0.0	0.0
9	-0.00300	-0.00300	0.0	0.0	0.0	0.0	0.0	0.0	0.0
10	-0.00300	-0.00300	0.0	0.0	0.0	0.0	0.0	0.0	0.0
11	-0.00300	-0.00300	0.0	0.0	0.0	0.0	0.0	0.0	0.0
12	-0.00300	-0.00300	0.0	0.0	0.0	0.0	0.0	0.0	0.0
13	-0.00300	-0.00300	0.0	0.0	0.0	0.0	0.0	0.0	0.0
14	-0.00300	-0.00300	0.0	0.0	0.0	0.0	0.0	0.0	0.0
15	-0.00300	-0.00300	0.0	0.0	0.0	0.0	0.0	0.0	0.0
16	-0.00300	-0.00300	0.0	0.0	0.0	0.0	0.0	0.0	0.0
17	-0.00300	-0.00300	0.0	0.0	0.0	0.0	0.0	0.0	0.0
18	-0.00300	-0.00300	0.0	0.0	0.0	0.0	0.0	0.0	0.0
19	-0.00300	-0.00300	0.0	0.0	0.0	0.0	0.0	0.0	0.0
20	-0.00300	-0.00300	0.0	0.0	0.0	0.0	0.0	0.0	0.0
MODE NUMBER									
MODE TYPE									
DAMPING RATIO									
GENERALIZED INERTIA									
NATURAL FREQUENCY, REV									
CHARACTERISTIC COEFFICIENTS AT BLADE ROOT									
BEAM BENDING MOMENT, FT-LB									
CHORD BENDING MOMENT, FT-LB									
TORSIONAL MOMENT, FT-LB									
VERTICAL SHEAR, LB									
IN-PLANE SHEAR, LB									
MOMENT COEFFICIENTS AT R = 21.50 IN									
BEAM BENDING MOMENT, FT-LB									
CHORD BENDING MOMENT, FT-LB									
TORSIONAL MOMENT, FT-LB									
NATURAL FREQUENCY AT									
0.0 G/G AND 150.0 RPM, 150.0 RPM									
0.0 G/G AND 150.0 RPM, 150.0 RPM									
0.0 G/G AND 230.0 RPM, 230.0 RPM									
0.0 G/G AND 230.0 RPM, 230.0 RPM									

TABLE VI. - Concluded

TABLE VI. - Concluded										
TAIL ROTOR										
MODE SHAPE FOR MODE 1				MODE SHAPE FOR MODE 2			MODE SHAPE FOR MODE 3			
STA	OUT-OF-PLANE	INPLANE	TORSION	OUT-OF-PLANE	INPLANE	TORSION	OUT-OF-PLANE	INPLANE	TORSION	
0	0.0	0.0	0.0	0.0	0.0	0.0	0.0	0.0	0.0	
1	0.0	0.0	0.0	0.0	0.0	0.0	0.0	0.0	0.0	
2	0.0540	0.0	0.0	0.0	0.0	0.0	0.0	0.0	0.0	
3	0.1060	0.0	0.0	0.0	0.0	0.0	0.0	0.0	0.0	
4	0.1590	0.0	0.0	0.0	0.0	0.0	0.0	0.0	0.0	
5	0.2120	0.0	0.0	0.0	0.0	0.0	0.0	0.0	0.0	
6	0.2650	0.0	0.0	0.0	0.0	0.0	0.0	0.0	0.0	
7	0.3180	0.0	0.0	0.0	0.0	0.0	0.0	0.0	0.0	
8	0.3710	0.0	0.0	0.0	0.0	0.0	0.0	0.0	0.0	
9	0.4240	0.0	0.0	0.0	0.0	0.0	0.0	0.0	0.0	
10	0.4770	0.0	0.0	0.0	0.0	0.0	0.0	0.0	0.0	
11	0.5300	0.0	0.0	0.0	0.0	0.0	0.0	0.0	0.0	
12	0.5830	0.0	0.0	0.0	0.0	0.0	0.0	0.0	0.0	
13	0.6360	0.0	0.0	0.0	0.0	0.0	0.0	0.0	0.0	
14	0.6890	0.0	0.0	0.0	0.0	0.0	0.0	0.0	0.0	
15	0.7420	0.0	0.0	0.0	0.0	0.0	0.0	0.0	0.0	
16	0.7950	0.0	0.0	0.0	0.0	0.0	0.0	0.0	0.0	
17	0.8480	0.0	0.0	0.0	0.0	0.0	0.0	0.0	0.0	
18	0.9010	0.0	0.0	0.0	0.0	0.0	0.0	0.0	0.0	
19	0.9540	0.0	0.0	0.0	0.0	0.0	0.0	0.0	0.0	
20	1.0070	0.0	0.0	0.0	0.0	0.0	0.0	0.0	0.0	
MODE SHAPE FOR MODE 4				MODE SHAPE FOR MODE 5			MODE SHAPE FOR MODE 6			
STA	OUT-OF-PLANE	INPLANE	TORSION	OUT-OF-PLANE	INPLANE	TORSION	OUT-OF-PLANE	INPLANE	TORSION	
0	0.0	0.0	0.0	0.0	0.0	0.0	0.0	0.0	0.0	
1	0.0	0.0	0.0	0.0	0.0	0.0	0.0	0.0	0.0	
2	0.0	0.0	0.0	0.0	0.0	0.0	0.0	0.0	0.0	
3	0.0	0.0	0.0	0.0	0.0	0.0	0.0	0.0	0.0	
4	0.0	0.0	0.0	0.0	0.0	0.0	0.0	0.0	0.0	
5	0.0	0.0	0.0	0.0	0.0	0.0	0.0	0.0	0.0	
6	0.0	0.0	0.0	0.0	0.0	0.0	0.0	0.0	0.0	
7	0.0	0.0	0.0	0.0	0.0	0.0	0.0	0.0	0.0	
8	0.0	0.0	0.0	0.0	0.0	0.0	0.0	0.0	0.0	
9	0.0	0.0	0.0	0.0	0.0	0.0	0.0	0.0	0.0	
10	0.0	0.0	0.0	0.0	0.0	0.0	0.0	0.0	0.0	
11	0.0	0.0	0.0	0.0	0.0	0.0	0.0	0.0	0.0	
12	0.0	0.0	0.0	0.0	0.0	0.0	0.0	0.0	0.0	
13	0.0	0.0	0.0	0.0	0.0	0.0	0.0	0.0	0.0	
14	0.0	0.0	0.0	0.0	0.0	0.0	0.0	0.0	0.0	
15	0.0	0.0	0.0	0.0	0.0	0.0	0.0	0.0	0.0	
16	0.0	0.0	0.0	0.0	0.0	0.0	0.0	0.0	0.0	
17	0.0	0.0	0.0	0.0	0.0	0.0	0.0	0.0	0.0	
18	0.0	0.0	0.0	0.0	0.0	0.0	0.0	0.0	0.0	
19	0.0	0.0	0.0	0.0	0.0	0.0	0.0	0.0	0.0	
20	0.0	0.0	0.0	0.0	0.0	0.0	0.0	0.0	0.0	
MODE NUMBER										
MODE TYPE										
INDEPENDENT										
DAMPING RATIO										
GENERALIZED INERTIA										
NATURAL FREQUENCY, REV										
CHARACTERISTIC COEFFICIENTS AT BLADE ROOT										
BEAM BENDING MOMENT, FT-LB										
CHORD BENDING MOMENT, FT-LB										
TORSIONAL MOMENT, FT-LB										
VERTICAL SHEAR, LB										
INPLANE SHEAR, LB										
MOMENT COEFFICIENTS AT R = 0.0 IN.										
BEAM BENDING MOMENT, FT-LB										
CHORD BENDING MOMENT, FT-LB										
TORSIONAL MOMENT, FT-LB										
NATURAL FREQUENCY AT										
0.0 COLL AND 712.0 RPM, / 712.0 RPM										
30.0 COLL AND 712.0 RPM, / 712.0 RPM										
0.0 COLL AND 870.0 RPM, / 870.0 RPM										
10.0 COLL AND 870.0 RPM, / 870.0 RPM										
TAIL ROTOR ALPHALANTIC BLADE DISTRIBUTIONS AND DATA										
BLADE STATION NUMBER	WEIGHT (LB/IN)	BLADEWISE INERTIA (IN-LB-SEC**2/IN)	CHORDWISE INERTIA (IN-LB-SEC**2/IN)							
1	0.0	0.0	0.0							
2	0.9810	0.0	0.0106							
3	1.1680	0.0	0.0106							
4	2.2750	0.0	0.0106							
5	1.6610	0.0	0.0106							
6	1.1800	0.0	0.0106							
7	0.9120	0.0	0.0106							
8	0.3530	0.0	0.0106							
9	0.2930	0.0	0.0106							
10	0.2600	0.0	0.0106							
11	0.2440	0.0	0.0106							
12	0.2520	0.0	0.0106							
13	0.2490	0.0	0.0106							
14	0.2600	0.0	0.0106							
15	0.2690	0.0	0.0106							
16	0.2740	0.0	0.0106							
17	0.2690	0.0	0.0106							
18	0.2680	0.0	0.0106							
19	0.3150	0.0	0.0106							
20	0.3250	0.0	0.0106							
TOTAL BLADE WEIGHT = 64.30 LB										
BLADE TIP WEIGHT = 0.0 LB										
FLAPPING INERTIA/BLADE = 20.7 SLUG-FT**2										

TABLE VII. S-67 AEROELASTIC BLADE DATA USED IN C81

MAIN ROTOR AEROELASTIC BLADE DISTRIBUTIONS AND DATA			
BLADE STATION NUMBER	WEIGHT (LB/IN)	BEAMWISE INERTIA (IN-LB-SEC**2/IN)	CHORDWISE INERTIA (IN-LB-SEC**2/IN)
1	1.0590	0.0130	3.3210
2	3.3290	0.0130	0.0650
3	1.4950	0.0020	0.0385
4	0.5073	0.0020	0.0244
5	0.4850	0.0020	0.0251
6	0.4800	0.0020	0.0253
7	0.5130	0.0020	0.0245
8	0.5300	0.0020	0.0243
9	0.5330	0.0020	0.0243
10	0.5312	0.0020	0.0242
11	0.5200	0.0020	0.0239
12	0.5032	0.0020	0.0235
13	0.5030	0.0020	0.0234
14	0.5060	0.0020	0.0241
15	0.5020	0.0020	0.0238
16	0.5000	0.0020	0.0239
17	0.5030	0.0020	0.0234
18	0.5100	0.0020	0.0240
19	0.4900	0.0020	0.0240
20	0.4200	0.0020	0.0240

TOTAL BLADE WEIGHT = 269.70 LB BLADE TIP WEIGHT = 3.0 LB FLAPPING INERTIA/BLADE = 1849.3 SLUG-FT**2

MAIN ROTOR

MODE SHAPE FOR MODE 1				MODE SHAPE FOR MODE 2			MODE SHAPE FOR MODE 3		
STA	OUT-OF-PLANE	INPLANE	TORSION	OUT-OF-PLANE	INPLANE	TORSION	OUT-OF-PLANE	INPLANE	TORSION
0	0.0	0.0	0.0	0.0	0.0	0.0	0.0	0.0	0.0
1	0.0200	0.0	0.0	0.0	0.0200	0.0	0.0	0.0	0.0
2	0.0720	0.0	0.0	0.0	0.0720	0.0	0.0	0.0	0.0
3	0.1240	0.0	0.0	0.0	0.1240	0.0	0.0	0.0	0.0
4	0.1750	0.0	0.0	0.0	0.1750	0.0	0.0	0.0	0.0
5	0.2240	0.0	0.0	0.0	0.2240	0.0	0.0	0.0	0.0
6	0.2800	0.0	0.0	0.0	0.2800	0.0	0.0	0.0	0.0
7	0.3320	0.0	0.0	0.0	0.3320	0.0	0.0	0.0	0.0
8	0.3840	0.0	0.0	0.0	0.3840	0.0	0.0	0.0	0.0
9	0.4350	0.0	0.0	0.0	0.4350	0.0	0.0	0.0	0.0
10	0.4880	0.0	0.0	0.0	0.4880	0.0	0.0	0.0	0.0
11	0.5400	0.0	0.0	0.0	0.5400	0.0	0.0	0.0	0.0
12	0.5920	0.0	0.0	0.0	0.5920	0.0	0.0	0.0	0.0
13	0.6440	0.0	0.0	0.0	0.6440	0.0	0.0	0.0	0.0
14	0.6950	0.0	0.0	0.0	0.6950	0.0	0.0	0.0	0.0
15	0.7480	0.0	0.0	0.0	0.7480	0.0	0.0	0.0	0.0
16	0.8000	0.0	0.0	0.0	0.8000	0.0	0.0	0.0	0.0
17	0.8520	0.0	0.0	0.0	0.8520	0.0	0.0	0.0	0.0
18	0.9040	0.0	0.0	0.0	0.9040	0.0	0.0	0.0	0.0
19	0.9550	0.0	0.0	0.0	0.9550	0.0	0.0	0.0	0.0
20	1.0000	0.0	0.0	0.0	1.0000	0.0	0.0	0.0	0.0

MODE SHAPE FOR MODE 4				MODE SHAPE FOR MODE 5			MODE SHAPE FOR MODE 6		
STA	OUT-OF-PLANE	INPLANE	TORSION	OUT-OF-PLANE	INPLANE	TORSION	OUT-OF-PLANE	INPLANE	TORSION
0	0.0	0.0	0.0	0.0	0.0	0.0	0.0	0.0	0.0
1	0.0	0.0	0.0	0.0	0.0	0.0	0.0	0.0	0.0
2	0.0	0.0	0.0	0.0	0.0	0.0	0.0	0.0	0.0
3	0.0	0.0	0.0	0.0	0.0	0.0	0.0	0.0	0.0
4	0.0	0.0	0.0	0.0	0.0	0.0	0.0	0.0	0.0
5	0.0	0.0	0.0	0.0	0.0	0.0	0.0	0.0	0.0
6	0.0	0.0	0.0	0.0	0.0	0.0	0.0	0.0	0.0
7	0.0	0.0	0.0	0.0	0.0	0.0	0.0	0.0	0.0
8	0.0	0.0	0.0	0.0	0.0	0.0	0.0	0.0	0.0
9	0.0	0.0	0.0	0.0	0.0	0.0	0.0	0.0	0.0
10	0.0	0.0	0.0	0.0	0.0	0.0	0.0	0.0	0.0
11	0.0	0.0	0.0	0.0	0.0	0.0	0.0	0.0	0.0
12	0.0	0.0	0.0	0.0	0.0	0.0	0.0	0.0	0.0
13	0.0	0.0	0.0	0.0	0.0	0.0	0.0	0.0	0.0
14	0.0	0.0	0.0	0.0	0.0	0.0	0.0	0.0	0.0
15	0.0	0.0	0.0	0.0	0.0	0.0	0.0	0.0	0.0
16	0.0	0.0	0.0	0.0	0.0	0.0	0.0	0.0	0.0
17	0.0	0.0	0.0	0.0	0.0	0.0	0.0	0.0	0.0
18	0.0	0.0	0.0	0.0	0.0	0.0	0.0	0.0	0.0
19	0.0	0.0	0.0	0.0	0.0	0.0	0.0	0.0	0.0
20	0.0	0.0	0.0	0.0	0.0	0.0	0.0	0.0	0.0

MODE NUMBER	1	2	3	4	5	6
MODE TYPE	INDEPENDENT	INDEPENDENT	NOT USED	NOT USED	NOT USED	NOT USED
DAMPING RATIO	0.0	0.0	0.0	0.0	0.0	0.0
GENERALIZED INERTIA	0.18875E+01	0.18875E+01	0.0	0.0	0.0	0.0
NATURAL FREQUENCY, /PEV	0.10300E+01	0.23500E+00	0.0	0.0	0.0	0.0
CHARACTERISTIC COEFFICIENTS AT BLADE ROOT						
BEAM BENDING MOMENT, FT-LB	0.17520E+04	0.0	0.0	0.0	0.0	0.0
CHORD BENDING MOMENT, FT-LB	0.0	0.15895E+04	0.0	0.0	0.0	0.0
TORSIONAL MOMENT, FT-LB	0.0	0.0	0.0	0.0	0.0	0.0
VERTICAL SHEAR, LB	0.15318E+04	0.0	0.0	0.0	0.0	0.0
INPLANE SHEAR, LB	0.0	0.15236E+04	0.0	0.0	0.0	0.0
MOMENT COEFFICIENTS AT R = 0.0 IN.						
BEAM BENDING MOMENT, FT-LB	0.17520E+04	0.0	0.0	0.0	0.0	0.0
CHORD BENDING MOMENT, FT-LB	0.0	0.15895E+04	0.0	0.0	0.0	0.0
TORSIONAL MOMENT, FT-LB	0.0	0.0	0.0	0.0	0.0	0.0
NATURAL FREQUENCY AT						
0.0 COLL AND 183.0 RPM / 183.0 RPM	0.10273E+01	0.23552E+00	0.0	0.0	0.0	0.0
20.0 COLL AND 183.0 RPM / 183.0 RPM	0.10273E+01	0.23552E+00	0.0	0.0	0.0	0.0
0.0 COLL AND 223.0 RPM / 223.0 RPM	0.10269E+01	0.23229E+00	0.0	0.0	0.0	0.0
20.0 COLL AND 223.0 RPM / 223.0 RPM	0.10269E+01	0.23229E+00	0.0	0.0	0.0	0.0

TABLE VII. - Concluded

TAIL ROTOR									
MODE SHAPE FOR MODE 1			MODE SHAPE FOR MODE 2			MODE SHAPE FOR MODE 3			
STA	OUT-OF-PLANE	INPLANE	TORSION	OUT-OF-PL	INPLANE	TORSION	OUT-OF-PLANE	INPLANE	TORSION
0	0.0	0.0	0.0	0.0	0.0	0.0	0.0	0.0	0.0
1	0.0	0.0	0.0	0.0	0.0	0.0	0.0	0.0	0.0
2	0.0400	0.0	0.0	0.0	0.0	0.0	0.0	0.0	0.0
3	0.0900	0.0	0.0	0.0	0.0	0.0	0.0	0.0	0.0
4	0.1500	0.0	0.0	0.0	0.0	0.0	0.0	0.0	0.0
5	0.2000	0.0	0.0	0.0	0.0	0.0	0.0	0.0	0.0
6	0.2500	0.0	0.0	0.0	0.0	0.0	0.0	0.0	0.0
7	0.3100	0.0	0.0	0.0	0.0	0.0	0.0	0.0	0.0
8	0.3700	0.0	0.0	0.0	0.0	0.0	0.0	0.0	0.0
9	0.4200	0.0	0.0	0.0	0.0	0.0	0.0	0.0	0.0
10	0.4700	0.0	0.0	0.0	0.0	0.0	0.0	0.0	0.0
11	0.5200	0.0	0.0	0.0	0.0	0.0	0.0	0.0	0.0
12	0.5600	0.0	0.0	0.0	0.0	0.0	0.0	0.0	0.0
13	0.5900	0.0	0.0	0.0	0.0	0.0	0.0	0.0	0.0
14	0.6200	0.0	0.0	0.0	0.0	0.0	0.0	0.0	0.0
15	0.6500	0.0	0.0	0.0	0.0	0.0	0.0	0.0	0.0
16	0.6700	0.0	0.0	0.0	0.0	0.0	0.0	0.0	0.0
17	0.6900	0.0	0.0	0.0	0.0	0.0	0.0	0.0	0.0
18	0.7100	0.0	0.0	0.0	0.0	0.0	0.0	0.0	0.0
19	0.7300	0.0	0.0	0.0	0.0	0.0	0.0	0.0	0.0
20	0.7500	0.0	0.0	0.0	0.0	0.0	0.0	0.0	0.0
MODE SHAPE FOR MODE 4			MODE SHAPE FOR MODE 5			MODE SHAPE FOR MODE 6			
STA	OUT-OF-PLANE	INPLANE	TORSION	OUT-OF-PLANE	INPLANE	TORSION	OUT-OF-PLANE	INPLANE	TORSION
0	0.0	0.0	0.0	0.0	0.0	0.0	0.0	0.0	0.0
1	0.0	0.0	0.0	0.0	0.0	0.0	0.0	0.0	0.0
2	0.0	0.0	0.0	0.0	0.0	0.0	0.0	0.0	0.0
3	0.0	0.0	0.0	0.0	0.0	0.0	0.0	0.0	0.0
4	0.0	0.0	0.0	0.0	0.0	0.0	0.0	0.0	0.0
5	0.0	0.0	0.0	0.0	0.0	0.0	0.0	0.0	0.0
6	0.0	0.0	0.0	0.0	0.0	0.0	0.0	0.0	0.0
7	0.0	0.0	0.0	0.0	0.0	0.0	0.0	0.0	0.0
8	0.0	0.0	0.0	0.0	0.0	0.0	0.0	0.0	0.0
9	0.0	0.0	0.0	0.0	0.0	0.0	0.0	0.0	0.0
10	0.0	0.0	0.0	0.0	0.0	0.0	0.0	0.0	0.0
11	0.0	0.0	0.0	0.0	0.0	0.0	0.0	0.0	0.0
12	0.0	0.0	0.0	0.0	0.0	0.0	0.0	0.0	0.0
13	0.0	0.0	0.0	0.0	0.0	0.0	0.0	0.0	0.0
14	0.0	0.0	0.0	0.0	0.0	0.0	0.0	0.0	0.0
15	0.0	0.0	0.0	0.0	0.0	0.0	0.0	0.0	0.0
16	0.0	0.0	0.0	0.0	0.0	0.0	0.0	0.0	0.0
17	0.0	0.0	0.0	0.0	0.0	0.0	0.0	0.0	0.0
18	0.0	0.0	0.0	0.0	0.0	0.0	0.0	0.0	0.0
19	0.0	0.0	0.0	0.0	0.0	0.0	0.0	0.0	0.0
20	0.0	0.0	0.0	0.0	0.0	0.0	0.0	0.0	0.0
MODE NUMBER									
MODE TYPE									
DAMPING RATIO									
GENERALIZED INERTIA									
NATURAL FREQUENCY, /REV									
CHARACTERISTIC COEFFICIENTS AT BLADE ROOT									
BEAM BENDING MOMENT, FT-LB									
CHORD BENDING MOMENT, FT-LB									
TORSIONAL MOMENT, FT-LB									
VERTICAL SHEAR, LB									
INPLANE SHEAR, LB									
MOMENT COEFFICIENTS AT R = 0.0 IN.									
BEAM BENDING MOMENT, FT-LB									
CHORD BENDING MOMENT, FT-LB									
TORSIONAL MOMENT, FT-LB									
NATURAL FREQUENCY AT									
0.0 COL AND 119.0 RPM, /1119.0 RPM									
0.0 COL AND 119.0 RPM, /1119.0 RPM									
0.0 COL AND 136.0 RPM, /1367.0 RPM									
0.0 COL AND 136.0 RPM, /1367.0 RPM									
TAIL ROTOR AEROLASTIC BLADE DISTRIBUTIONS AND DATA									
BLADE STATION NUMBER	WEIGHT (LB/IN)	BLADEWISE INERTIA (IN-LB-SEC**2/IN)	CHORDWISE INERTIA (IN-LB-SEC**2/IN)						
1	0.0	0.0	0.0						
2	1.2080	0.0	0.0010						
3	1.5370	0.0	0.0012						
4	1.5370	0.0	0.0010						
5	1.1920	0.0	0.0007						
6	0.3140	0.0	0.0005						
7	0.2540	0.0	0.0004						
8	0.1770	0.0	0.0003						
9	0.1110	0.0	0.0002						
10	0.1270	0.0	0.0003						
11	0.1130	0.0	0.0002						
12	0.1350	0.0	0.0003						
13	0.1310	0.0	0.0003						
14	0.0970	0.0	0.0002						
15	0.1040	0.0	0.0002						
16	0.1340	0.0	0.0003						
17	0.1340	0.0	0.0003						
18	0.1170	0.0	0.0002						
19	0.1070	0.0	0.0002						
20	0.1070	0.0	0.0002						
TOTAL BLADE WEIGHT = 24.07 LB				BLADE TIP WEIGHT = 0.0 LB		FLAPPING INERTIA/BLADE = 2.0 SLUG-FT**2			

TABLE VIII. C81 PROGRAM VALIDATION DATA CASES

Topic of Analysis	Flight Condition	Aircraft	Speed, Kt	Gross Weight, lb	Fuselage Station Center-of-Gravity, in.	Source of Baseline Data
Trim	Level flight	CH-53D	0 to 160	35,000	328	Reference 10
Trim	Level flight	CH-53D	0 to 160	35,000	336	Reference 10
Trim	Level flight	CH-53D	0 to 160	35,000	352	Reference 10
Trim	Level flight	S-67	0 to 180	16,500	272.3	Unpublished
Trim	Level flight	S-67	0 to 180	17,300	258	Reference 9
Trim	Level flight	CH-53A	100	33,500	348	Reference 11
Trim	Right Side-ward	CH-53D	0 to 30	42,000	328	Reference 10
Trim	Left Side-ward	CH-53D	0, 10	42,000	328	Reference 10
Trim	Rearward	CH-53D	0-20	46,000	328.3	Reference 10
Trim	Coordinated turn (3 g-levels; right, left turns	CH-53D	75	46,000	328.3	Reference 10
Performance	Level flight	CH-53A	0	Various	336	Reference 12
Performance	Level flight	CH-53A	70 to 160	42,000	336	Reference 12
Performance	Level flight	S-67	85 to 200	16,500	272.3	Unpublished
Performance	MR whirl stand	CH-53D	0	--	--	Unpublished
Performance	TR whirl stand	CH-53A	0	--	--	Reference 13

TABLE VIII. - Continued						
Topic of Analysis	Flight Condition	Aircraft	Speed, kt	Gross Weight, lb	Fuselage Station Center-of-Gravity, in.	Source of Baseline Data
Performance	Climb (at 4500 ft altitude)	HH-53C	60, 80	35,000	340	Reference 14
Performance	Climb (at 14,000 ft altitude)	HH-53C	40	35,000	340	Reference 14
Performance	Autorotation	HH-53C	60 to 100	35,000	340	Reference 14
Stability	Level flight	CH-53A	0, 100, 150	33,500	348	Reference 11
Stability	Level flight	CH-53A	100, 150	35,000	352	Reference 15
Stability	Level flight	S-67	100, 140, 180	14,800	276	Reference 16
Time history	Longitudinal pulse	CH-53A	0, 100, 150	33,500	347	Reference 11
Time history	Longitudinal, lateral, directional pulses	HH-53C	0	31,000	328	Reference 14
Time history	Longitudinal, lateral, directional steps	HH-53C	0	31,000	328	Reference 14
Time history	Longitudinal, lateral, directional steps	HH-53C	113	41,000	328	Reference 14
Time history	Symmetrical pull-up	S-67	180	14,800	276	Reference 16

TABLE VIII. - Concluded						
Topic of Analysis	Flight Condition	Aircraft	Speed, Kt	Gross Weight, lb	Fuselage Station Center-of-Gravity, in.	Source of Baseline Data
Time history	Longitudinal pulse	S-67	140	14,800	276	Reference 16
Time history	Directional doublet	S-67	140	14,800	276	Reference 16
Rotor loads	Level flight	CH-53A	0	33,070	336	Reference 7
Rotor loads	Level flight	CH-53A	159	34,120	336	Reference 7
Rotor loads	Level flight	CH-53A	137	40,650	336	Reference 7

TABLE IX. CH-53A TRIM AT 100 KT,
33,500 LB, 348 FSCG, CALCULATED
BY THE C81 AND THE GENHEL ANALYSES

Trim Parameters	GENHEL	C81
ϕ_b , deg	-1.59	-1.08
θ_b , deg	2.56	4.09
ψ_b , deg	0	0
MR Thrust, lb	34,186.	33,267.
MR X-force, lb	-490.	-1199.
MR side force, lb	620.	-1090.
MR Roll moment, ft-lb	-4194.	-8900.
MR Pitch moment, ft-lb	-15,064.	-1743.
MR Torque, ft-lb	67,373.	69,080.
$\theta_{.75MR}$, deg	7.01	6.68
B_{1S} , deg	5.86	6.38
A_{1S} , deg	-0.95	-1.68
$\theta_{.75TR}$, deg	4.0	2.59
α_F , deg	-0.11	4.09
a_{OMR} , deg	4.66	--
a_{1MR} , deg	-2.12	-2.78
b_{1MR} , deg	-0.11	-0.07

TABLE X. COORDINATED TURN TRIM FOR THE CH-53D AT 46,000 LB, 328.3 FSCG, 104% N_r, TEST DATA COMPARISON TO C81 ANALYSIS

Speed kt	Density altitude ft	Turn direction	Load factor g's	Control angles, deg								Attitude, deg			
				$\theta_{.75MR}$		B_{1S}		A_{1S}		$\phi_{.75TR}$		ψ_b			
				Test	C81	Test	C81	Test	C81	Test	C81	Test	C81	Test	C81
75	2000	Left	1.04	8.0	8.1	2.6	1.6	-2.8	-2.6	7.0	6.9	-17.0	-16.0	0.3	-0.6
77	2000	Left	1.12	7.8	8.5	2.6	1.7	-3.3	-2.6	6.4	7.8	-30.3	-27.0	3.7	-2.1
72	160	Left	1.21	8.9	8.9	1.8	0.9	-3.7	-2.8	7.0	8.7	-43.8	-34.8	0.5	-3.7
75	160	Right	1.07	8.6	8.1	3.1	1.6	-2.6	-2.5	6.1	5.6	13.9	21.3	1.2	3.1
77	2000	Right	1.13	8.1	9.0	2.9	1.9	-2.2	-2.5	7.0	6.7	29.6	28.4	2.9	4.2
82	160	Right	1.32	9.7	10.2	3.9	2.2	-2.8	-2.3	5.8	7.8	43.6	41.5	6.0	5.2

TABLE XI. ROTOR AND BODY STABILITY DERIVATIVES
OBTAINED FROM THE C81 AND

Variable Degree of freedom	u ft/sec	v ft/sec	w ft/sec	p rad/sec	q rad/sec	r rad/sec	$\dot{\phi}$ rad	$\dot{\theta}$ rad	$\dot{\psi}$ rad
\ddot{u} , ft/sec ²	-.049 (-.005)	.017 (.0004)	.14 (.094)	1.27 (-.126)	-10.8 (-9.97)	-1.12 (.865)	0 (0)	-32.1 (-32.2)	-
\ddot{v} , ft/sec ²	.003 (.016)	-.182 (-.057)	-.06 (.0022)	9.85 (6.63)	.194 (-.659)	-174. (-167.)	32.1 (32.2)	0 (.054)	(
\ddot{w} , ft/sec ²	.151 (-.124)	-.05 (-.007)	-1.21 (-.744)	-7.55 (-6.12)	168. (193.)	4.3 (4.4)	.607 (.89)	-2.3 (-1.44)	(
\ddot{p} , rad/sec ²	.0006 (-.001)	-.034 (-.016)	-.015 (-.010)	-.56 (-.172)	-.15 (.017)	1.30 (.443)	0 (0)	0 (0)	
\ddot{q} , rad/sec ²	.0014 (-.0005)	-.0014 (.0023)	.0003 (.0016)	-.054 (-.006)	-.294 (-.121)	.049 (.0045)	0 (0)	0 (0)	
\ddot{r} , rad/sec ²	-.0012 (-.0016)	.025 (.008)	-.006 (-.0002)	.177 (.111)	.172 (.06)	-1.43 (-.728)	0 (0)	0 (0)	
\ddot{a}_{1MR} , rad/sec ²	-.042 (-.089)	.181 (.071)	-.021 (-.038)	36.5 (8.46)	26.1 (18.8)	2.22 (-.156)	0 (0)	0 (0)	
\ddot{b}_{1MR} , rad/sec	.10 (.065)	.0925 (.051)	.471 (.094)	27.4 (15.2)	-36.6 (-12.1)	4.19 (.72)	0 (0)	0 (0)	(
\ddot{a}_{1TR} , rad/sec ²	-.068	.212	-.717	-154.	-30.2	-49.0	0	0	
\ddot{b}_{1TR} , rad/sec ²	-.726	3.1	-.09	-11.5	1.86	23.9	0	0	
MR coning \ddot{a}_{0MR} , rad/sec ²	(-.029)	(-.0005)	(-.432)	(-.495)	(3.97)	(3.96)	(0)	(0)	

Stability derivatives in parentheses are from GENHEL analysis.

ROTOR AND BODY STABILITY DERIVATIVES FOR THE CH-53A AT 100 KT, 33,500 LB, 348 FSCG,
OBTAINED FROM THE C81 AND THE GENHEL ANALYSES

r rad/sec	i rad	q rad	a _{1MR} rad	q̇ _{1MR} rad/sec	b _{1MR} rad	q̇ _{1MR} rad/sec	a _{1TR} rad	q̇ _{1TR} rad/sec	b _{1TR} rad	q̇ _{1TR} rad/sec	q̇ _{MR} rad
-1.12 (.865)	0 (0)	-32.1 (-32.2)	-26.4 (-24.)	1.08 (2.51)	16.6 (-1.91)	.964 (-.49)	1.01	-.006	-.37	-.003	76. (26.5)
-174. (-167.)	32.1 (32.2)	0 (.054)	16.8 (4.32)	.195 (-.21)	17.5 (25.8)	-1.13 (.923)	1.19	-.009	-.67	-.122	-34.2 (-.71)
4.3 (4.4)	.607 (.89)	-2.3 (-1.4)	30.9 (-11.1)	.37 (3.78)	16.6 (11.7)	-6.33 (-4.49)	-.18	-.009	-1.31	.002	-595. (-269.)
1.30 (.443)	0 (0)	0 (0)	4.68 (-4.56)	-.002 (-.472)	16.7 (17.8)	-.252 (1.07)	.353	-.002	-.89	-.035	-9.9 (3.45)
.049 (.0045)	0 (0)	0 (0)	3.75 (3.84)	-.058 (.30)	-.95 (1.0)	-.011 (.104)	-.123	-.002	-.294	.0012	-.315 (.66)
-1.43 (-.728)	0 (0)	0 (0)	-1.08 (-.83)	.131 (-.053)	.645 (1.84)	-.078 (.08)	-.512	.0025	.191	.036	3.46 (4.7)
2.22 (-.156)	0 (0)	0 (0)	10.6 (47.)	24.1 (19.4)	475. (161.)	35.8 (23.7)	0	0	0	0	-6.04 (-30.7)
4.19 (.72)	0 (0)	0 (0)	-445. (-154.)	-38.7 (-22.8)	1.95 (48.7)	25.3 (17.6)	0	0	0	0	397. (84.)
-49.0	0	0	0	0	0	0	24.7	38.7	3270.	166.	.122
23.9	0	0	0	0	0	0	-3095.	-166.	20.6	40.	-.108
(3.96)	(0)	(0)	(-19.)	(-1.0)	(16.8)	(.59)					(-231.)

lysis.

0 LB, 348 FSCG,

θ_{TR} rad	$\dot{\theta}_{TR}$ rad/sec	b_{TR} rad	\dot{b}_{TR} rad/sec	θ_{MR} rad	A_{IS} rad	B_{IS} rad	θ_{TR} rad	$\dot{\theta}_{MR}$ rad	$\dot{\theta}_{MR}$ rad/sec
.01	-.006	-.37	-.003	76. (26.5)	-24.1 (-4.92)	-13.3 (-7.92)	-1.925 (-.48)	(25.1)	(.042)
1.19	-.009	-.67	-.122	-34.2 (-.71)	20.3 (11.9)	26.4 (12.0)	48.3 (6.67)	(-10.1)	(-.38)
-.18	-.009	-1.31	.002	-595. (-269.)	36.4 (17.1)	232. (124.)	.187 (.534)	(-218.)	(.80)
.353	-.002	-.89	-.035	-9.9 (3.45)	5.98 (3.33)	5.55 (.913)	13.7 (3.85)	(-.52)	(-.01)
-.123	-.002	-.294	.0012	-.315 (.66)	1.005 (-.080)	-.713 (-.352)	.112 (.008)	(-.064)	(-.042)
-.512	.0025	.191	.036	3.46 (4.7)	-2.24 (-.543)	2.66 (-.09)	-14.2 (-5.17)	(-1.4)	(-.015)
0	0	0	0	-6.04 (-30.7)	-515. (-163.)	90.2 (117.)	.05 (.53)	(-89.5)	(-3.32)
0	0	0	0	397. (84.)	-98.6 (-110.)	-578. (-163.)	-.004 (-.29)	(8.31)	(-1.56)
24.7	38.7	3270.	166.	.122	.129	.121	-184.		
-3095.	-166.	20.6	40.	-.108 (-231.)	-.10 (-9.82)	-.127 (64.2)	-2640. (1.94)	(168.)	(13.7)

TABLE XII. BODY STABILITY DERIVATIVES FOR THE CH-53A AT 100 KT, 33,500 LB, 348 FSCG,
OBTAINED FROM THE C81 AND THE GENHEL ANALYSES

Variable Degree of freedom	\dot{u} ft/sec	\dot{v} ft/sec	\dot{w} ft/sec	\dot{p} rad/sec	\dot{q} rad/sec	\dot{r} rad/sec	\ddot{u} rad	\ddot{v} rad	\ddot{w} rad	\ddot{p} rad	\ddot{q} rad	\ddot{r} rad
\dot{u} , ft/sec ²	-.049 (-.046)	.017 (.002)	.14 (.074)	-.018 (-1.76)	-9.44 (-5.54)	-1.44 (-.53)	0 (0)	-32.1 (-32.2)	52.4 (24.2)	-6.0 (-.21)	19.9 (20.9)	-2.82 (-.19)
\dot{v} , ft/sec ²	.003 (.007)	-.182 (-.081)	-.06 (-.008)	8.46 (5.22)	-2.17 (-2.49)	-164.3 (-166.5)	32.1 (32.2)	0 (0)	-19.2 (-2.19)	39.4 (35.1)	1.41 (-1.72)	47.2 (18.4)
\dot{w} , ft/sec ²	.151 (.052)	-.05 (-.027)	-1.21 (-.88)	-8.90 (-4.58)	164.5 (167.3)	4.48 (3.67)	-.007 (.904)	-2.3 (-1.42)	-568. (-410.)	54.5 (22.5)	188.5 (14.)	.26 (.14)
\dot{p} , rad/sec ²	.0006 (.0017)	-.034 (-.023)	-.015 (.003)	-1.89 (-1.59)	-1.43 (-1.02)	1.25 (.40)	0 (0)	0 (0)	-5.76 (3.64)	22.4 (22.5)	-3.25 (-2.58)	13.3 (3.90)
\dot{q} , rad/sec ²	.0014 (.0017)	-.0014 (-.0018)	.0003 (.006)	.004 (.21)	-.565 (-.58)	.082 (.012)	0 (0)	0 (0)	-3.04 (4.28)	-.035 (-.30)	-5.51 (-5.51)	.20 (.33)
\dot{r} , rad/sec ²	-.0012 (-.0014)	.025 (.007)	-.006 (-.002)	.14 (-.025)	.23 (-.073)	-1.44 (-.74)	0 (0)	0 (0)	5.49 (3.63)	-1.54 (1.50)	3.98 (.41)	-13.8 (-5.14)

First derivatives are derived from the C81 analysis
Second derivatives (in parentheses) are from GENHEL analysis.

TABLE XIII. CH-53A MAIN ROTOR BLADE FLAPPING MODE SHAPES AND MASS DISTRIBUTION USED IN INVESTIGATORY C81 ROTOR LOADS SOLUTION RUNS

C81 Blade Input Locations			Blade Rigid Flapping Normal Mode Shapes		Blade Mass Distribution, lb/in	
Segment Number	Station Number	% Radius	Exact Linear (5% Offset)	Approximate Linear (5.56% Offset)	Actual Non-uniform	Uniform Approximation
1	0	Tip	0	0	0	0
2	1	5	0	0	4.785	1.2916
3	2	10	0.0526	0.04	5.383	1.2916
4	3	15	0.1052	0.09	1.702	1.2916
5	4	20	0.1578	0.14	0.778	1.2916
6	5	25	0.2105	0.19	0.758	1.2916
7	6	30	0.2631	0.24	0.755	1.2916
8	7	35	0.3157	0.29	0.719	1.2916
9	8	40	0.3684	0.34	0.754	1.2916
10	9	45	0.4210	0.39	0.770	1.2916
11	10	50	0.4736	0.44	0.766	1.2916
12	11	55	0.5263	0.49	0.761	1.2916
13	12	60	0.5789	0.54	0.761	1.2916
14	13	65	0.6315	0.59	0.80	1.2916
15	14	70	0.6842	0.64	0.821	1.2916
16	15	75	0.7368	0.69	0.807	1.2916
17	16	80	0.7894	0.74	0.807	1.2916
18	17	85	0.8421	0.80	0.790	1.2916
19	18	90	0.8947	0.87	0.867	1.2916
20	19	95	0.9473	0.93	0.956	1.2916
	20	100	1.0	1.0		

TABLE XIV. COMPARISON OF C81 MAIN ROTOR TRIM PARAMETERS FOR FREE AIRCRAFT AND SHAFT - FIXED SOLUTIONS WITH FLIGHT TEST DATA FOR THE CH-53A WITH NEUTRAL (336 FSCG) CENTER OF GRAVITY LOCATION

Main Rotor Trim Parameters	Hover, 34,120 lb Gross Weight				159 Kt, 33,070 lb Gross Weight				137 Kt, 40,650 lb Gross Weight			
	Flight Test	C81			Flight Test	C81			Flight Test	C81		
		Free Aircraft Solution		Shaft - Fixed Solution (2 Bending Modes)		Free Aircraft Solution		Shaft - Fixed Solution (2 Bending Modes)		Free Aircraft Solution		Shaft - Fixed Solution (2 Bending Modes)
		5 Bending Modes	2 Bending Modes	Control Inputs Specified	Tip Path Plane Specified	5 Bending Modes	2 Bending Modes	Tip Path Plane Specified		5 Bending Modes	2 Bending Modes	Tip Path Plane Specified
9.75 4R, deg	9.40	9.51	8.78	8.90	8.90	13.70	11.0	10.80	10.40	9.54		
A, deg	-1.04	-1.07	-1.18	-1.05	-0.31	-0.48	-1.16	-5.05	-5.25	-0.72		
B, deg	-0.77	0.89	0.80	-0.77	-0.63	6.12	8.0	9.91	9.10	5.15		
0 4R, deg	4.06	--	--	--	--	--	--	--	4.87	--		
A, 1 4R, deg	3.70	-0.39	-0.68	0.94	0.69	-1.17	-0.37	-0.69	-0.89	0.01		
B, 1 4R, deg	-0.21	-1.40	-1.31	-0.99	-0.24	-0.92	-0.16	-0.06	0.19	-0.06		
4R Horsepower	4300.	4150.	4157.	4262.	4260.	4894.	5185.	5104.	4270.	3908.		

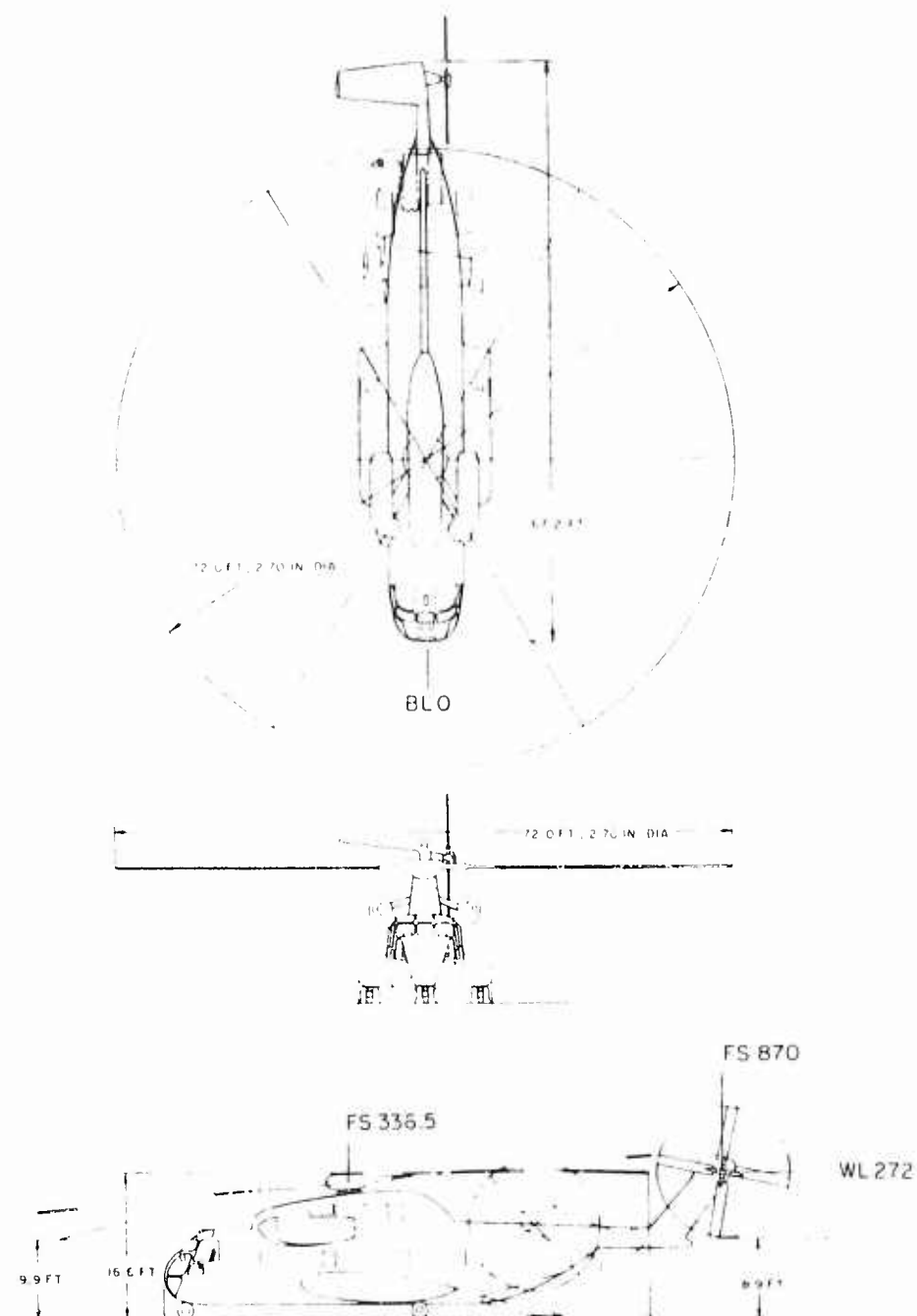


Figure 1. CH-53A Articulated-Rotor Helicopter.

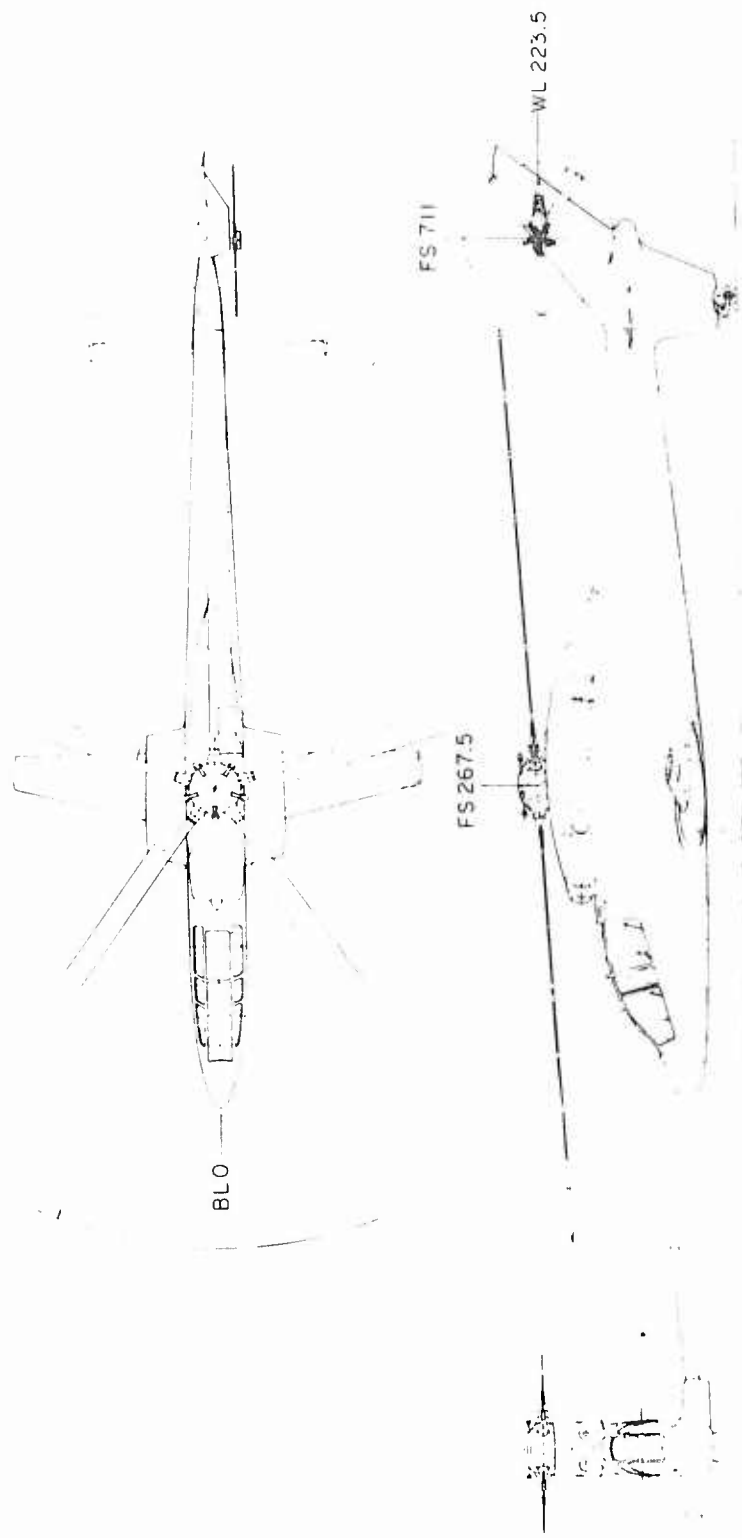


Figure 2. S-67 Articulated-Rotor Helicopter.

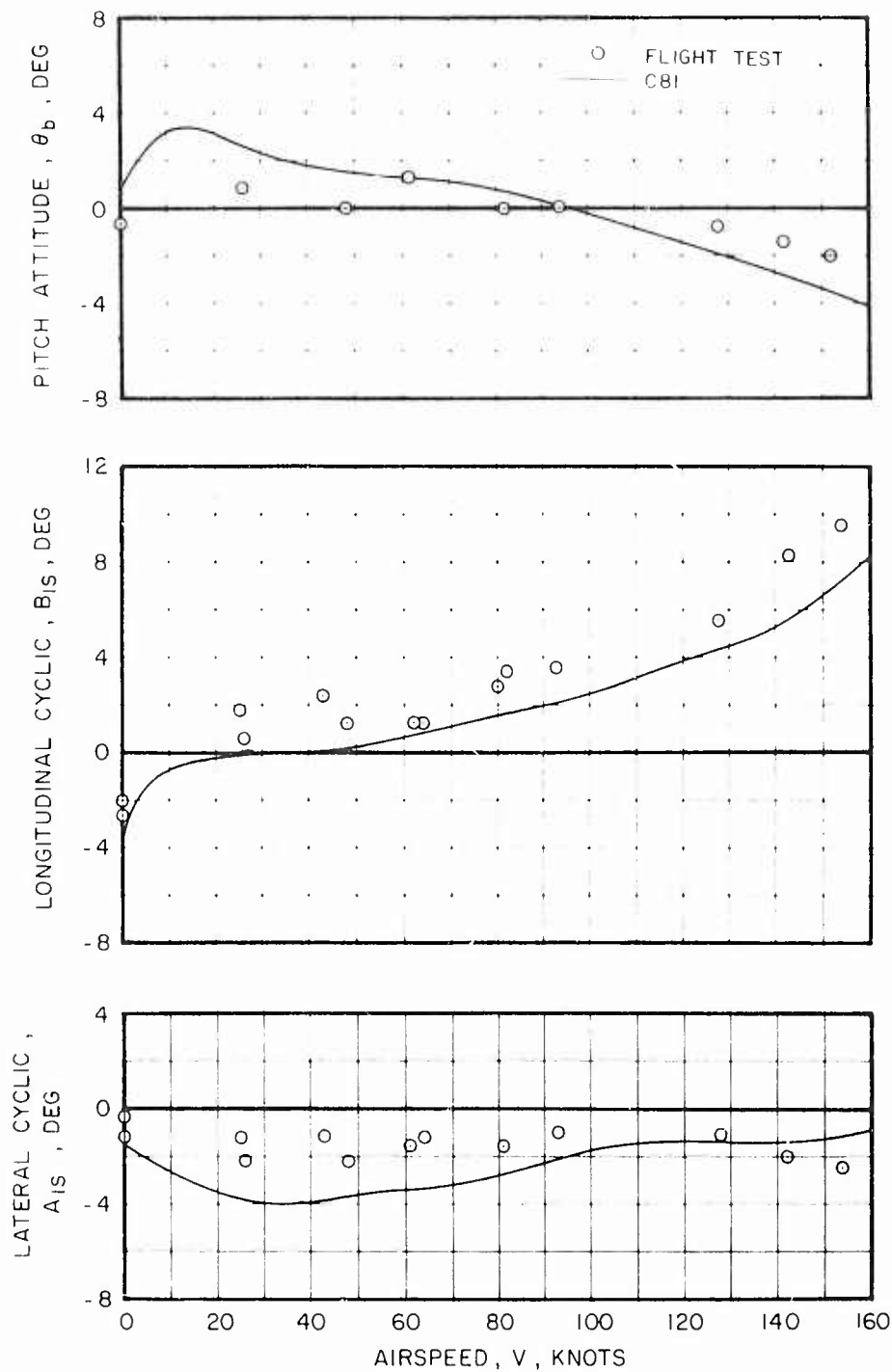


Figure 3. C81 Level Flight Trim vs Airspeed, Compared With Flight Test Data for the CH-53D at 35,000 Lb, Forward FSCG = 328 (100% N_r , $h_d = 2000$ Ft).

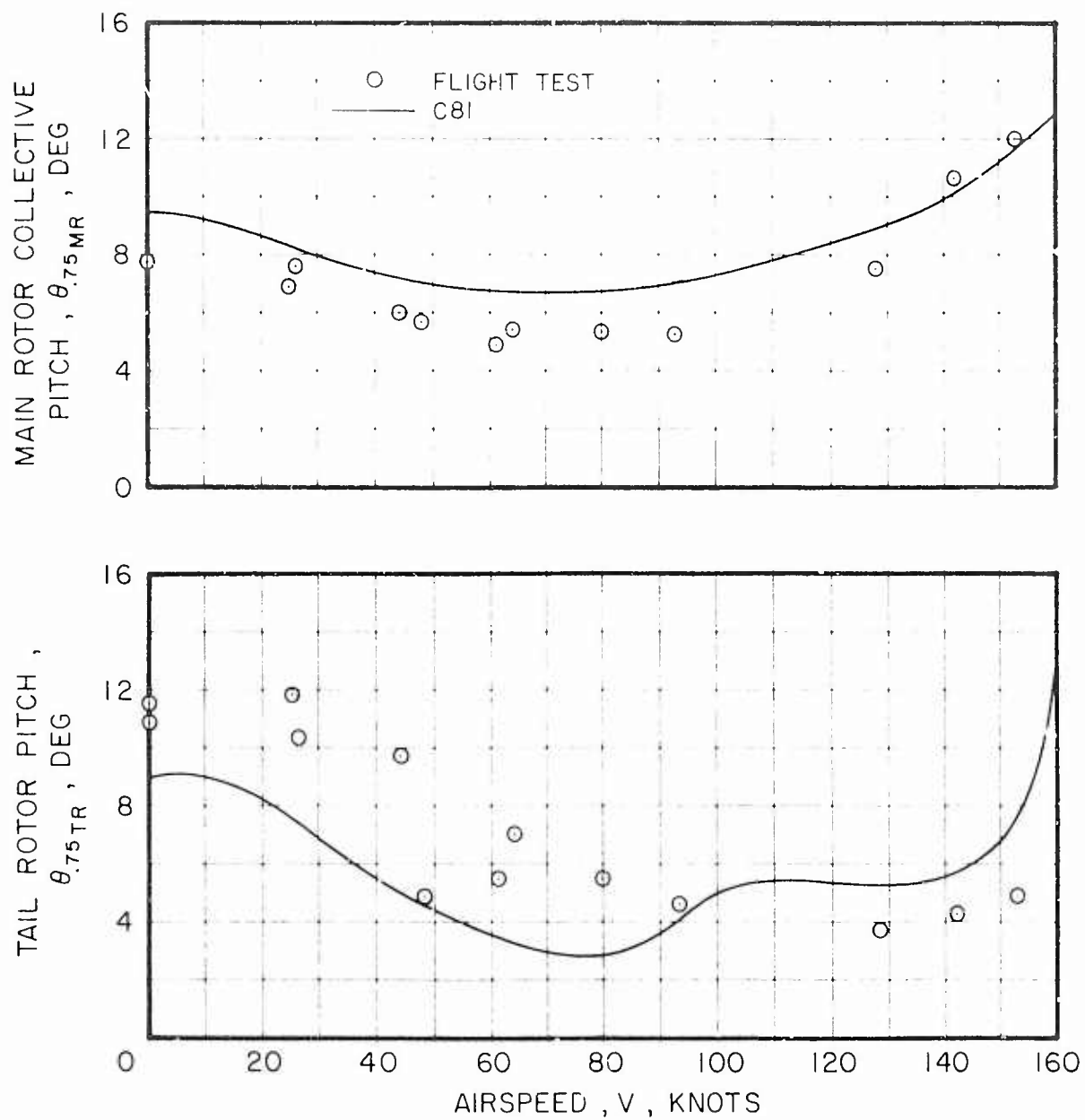


Figure 3. Concluded.

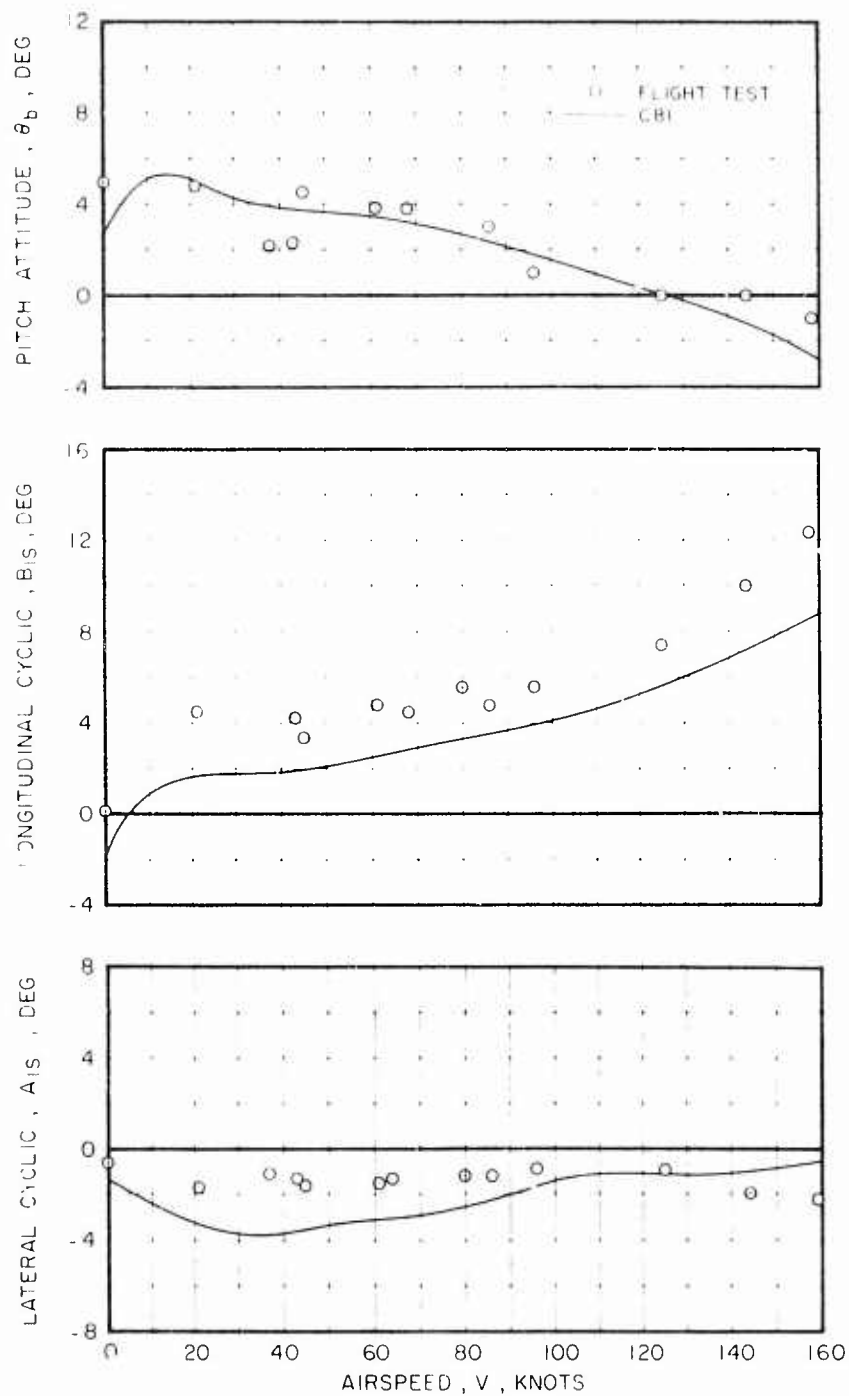


Figure 4. C81 Level Flight Trim vs Airspeed, Compared With Flight Test Data for the CH-53D at 35,000 Lb, Mid FSCG = 336 (100% N_T , h_d = 2000 Ft).

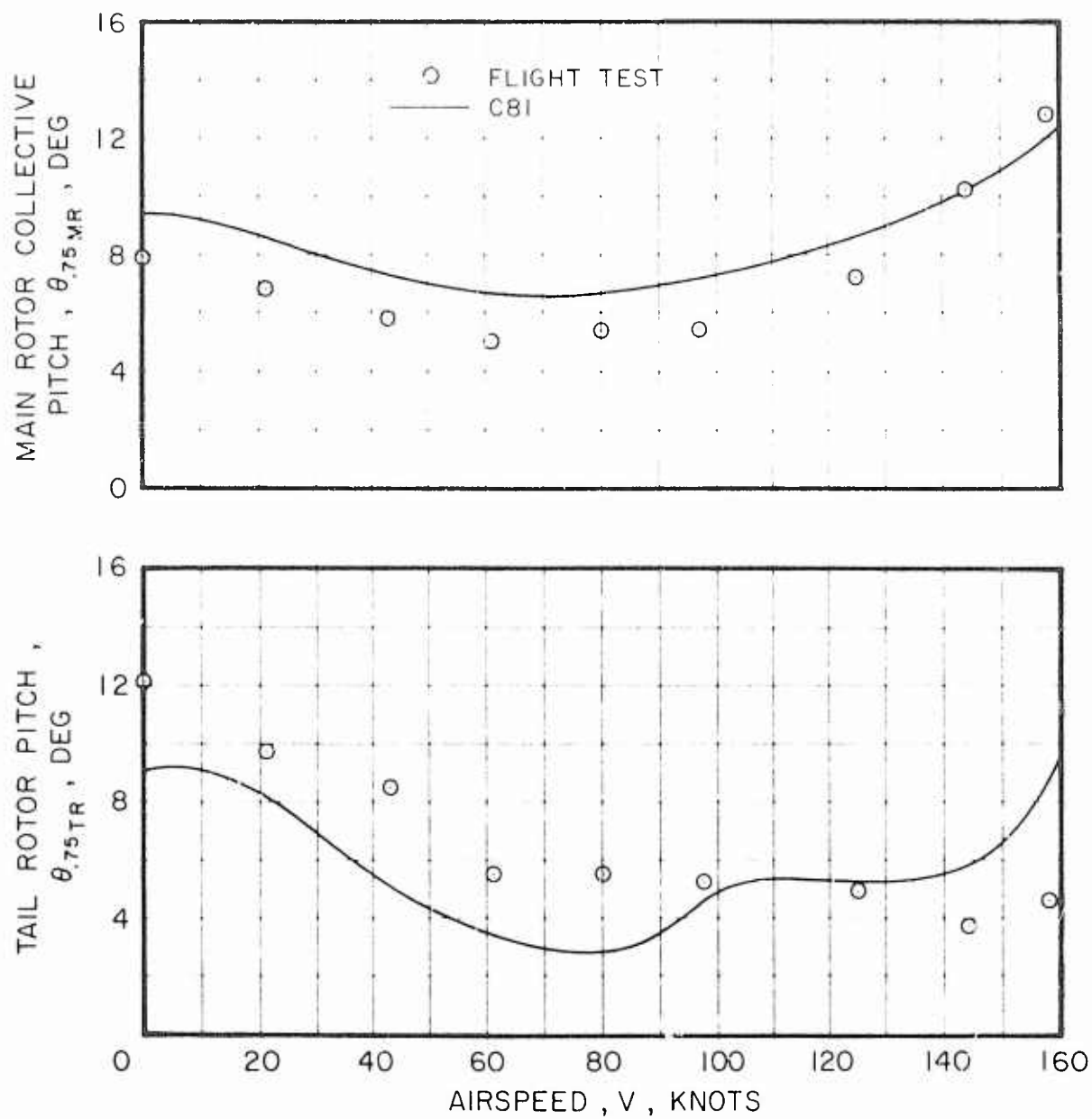


Figure 4. Concluded.

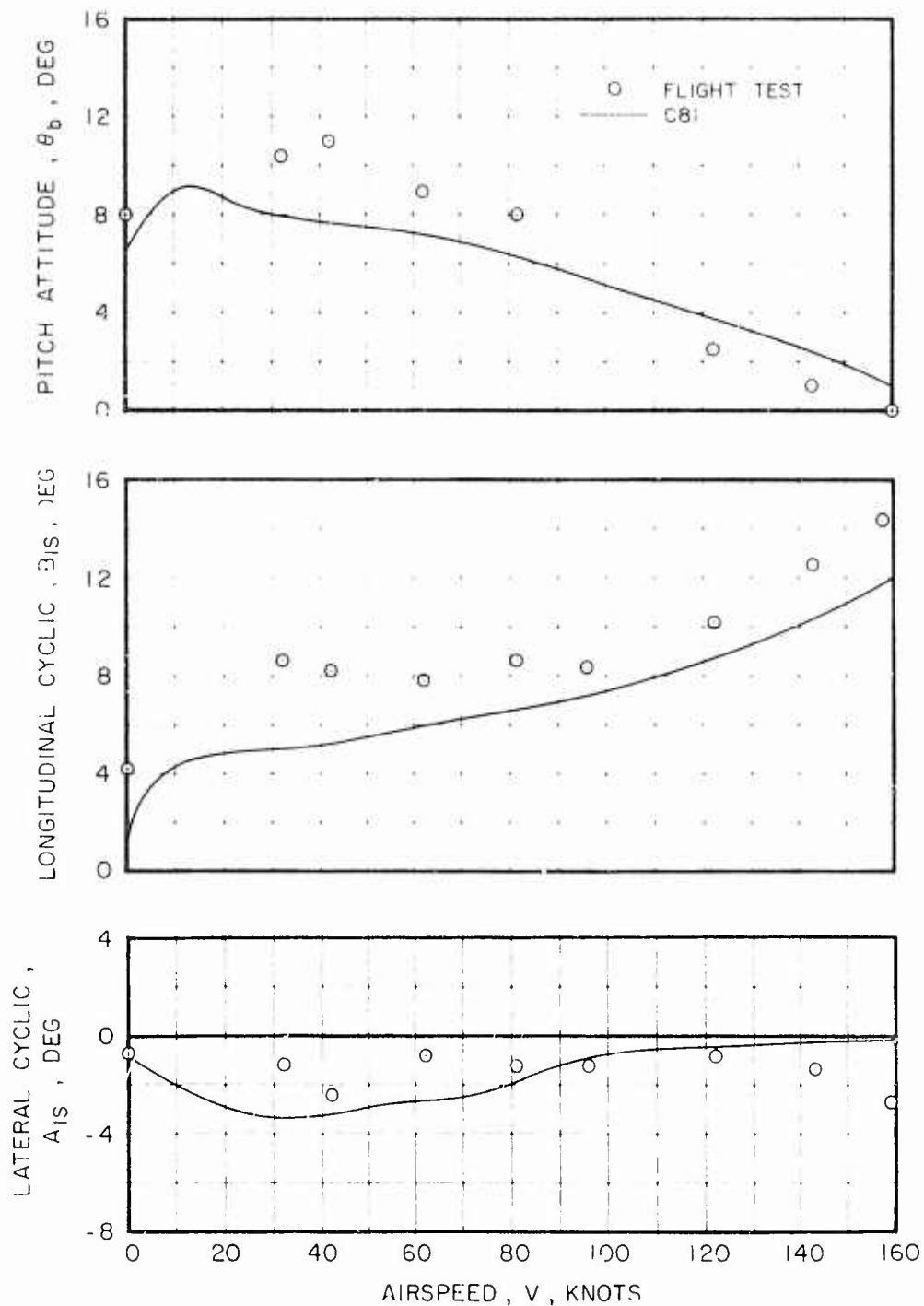


Figure 5. C81 Level Flight Trim vs Airspeed, Compared With Flight Test Data for the CH-53D at 35,000 Lb, Aft FSCG = 352 (100% N_x , h_d = 2000 Ft).

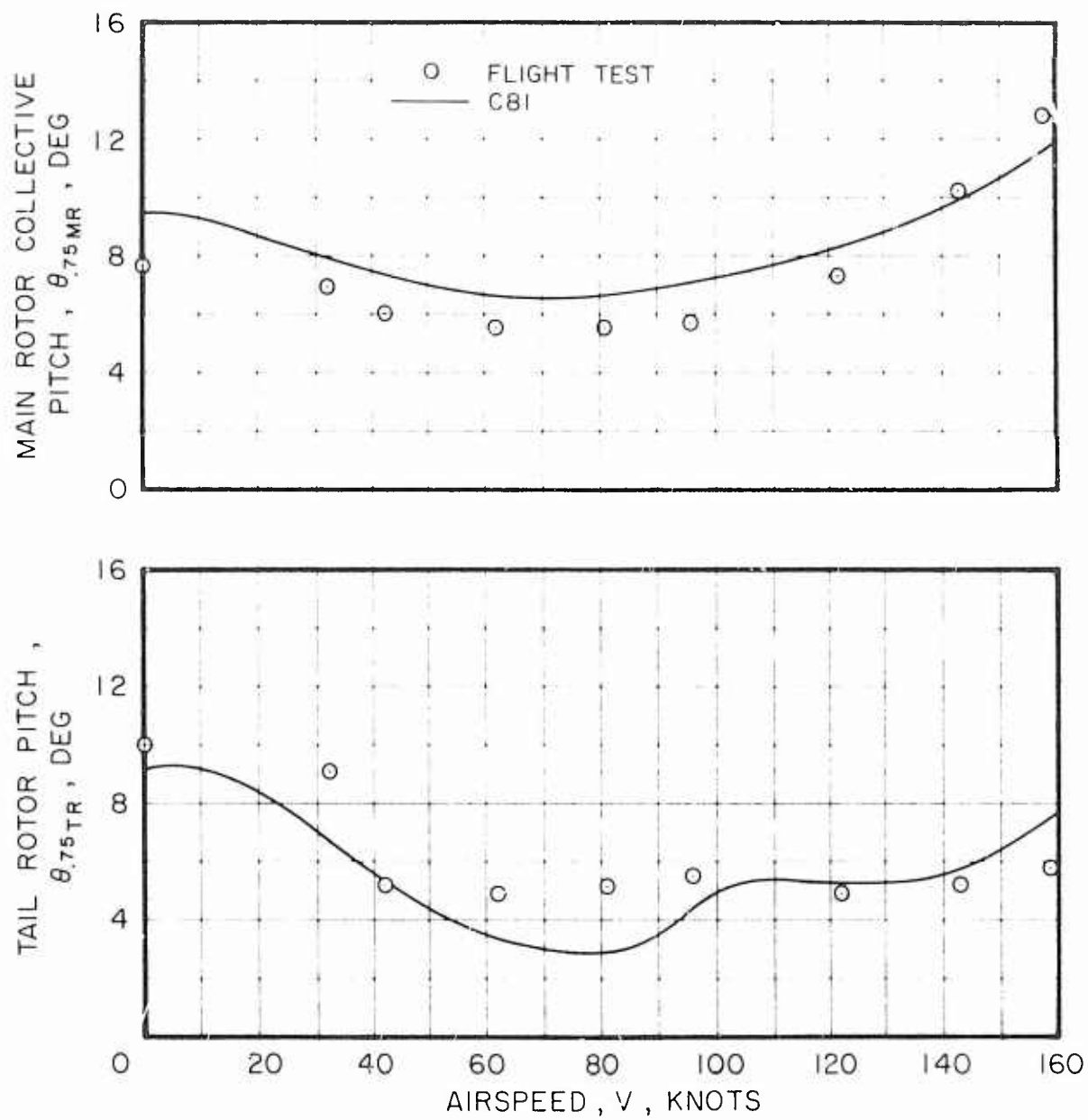


Figure 5. Concluded.

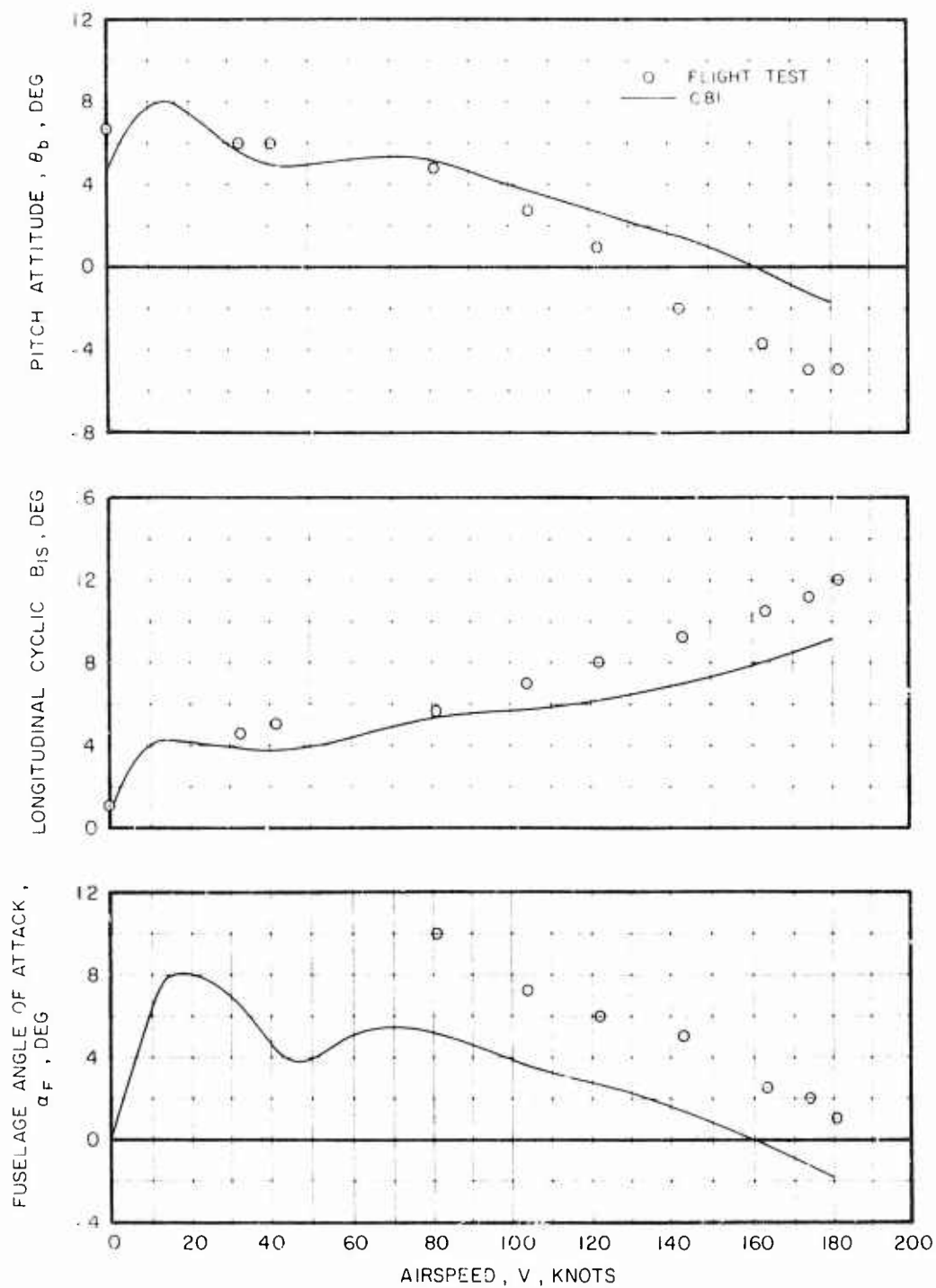


Figure 6. C81 Level Flight Trim vs Airspeed, Compared With Flight Test Data for the S-67 at 16,500 Lb, Mid FSCG = 272 (104% N_T , h_d = 3000 Ft).

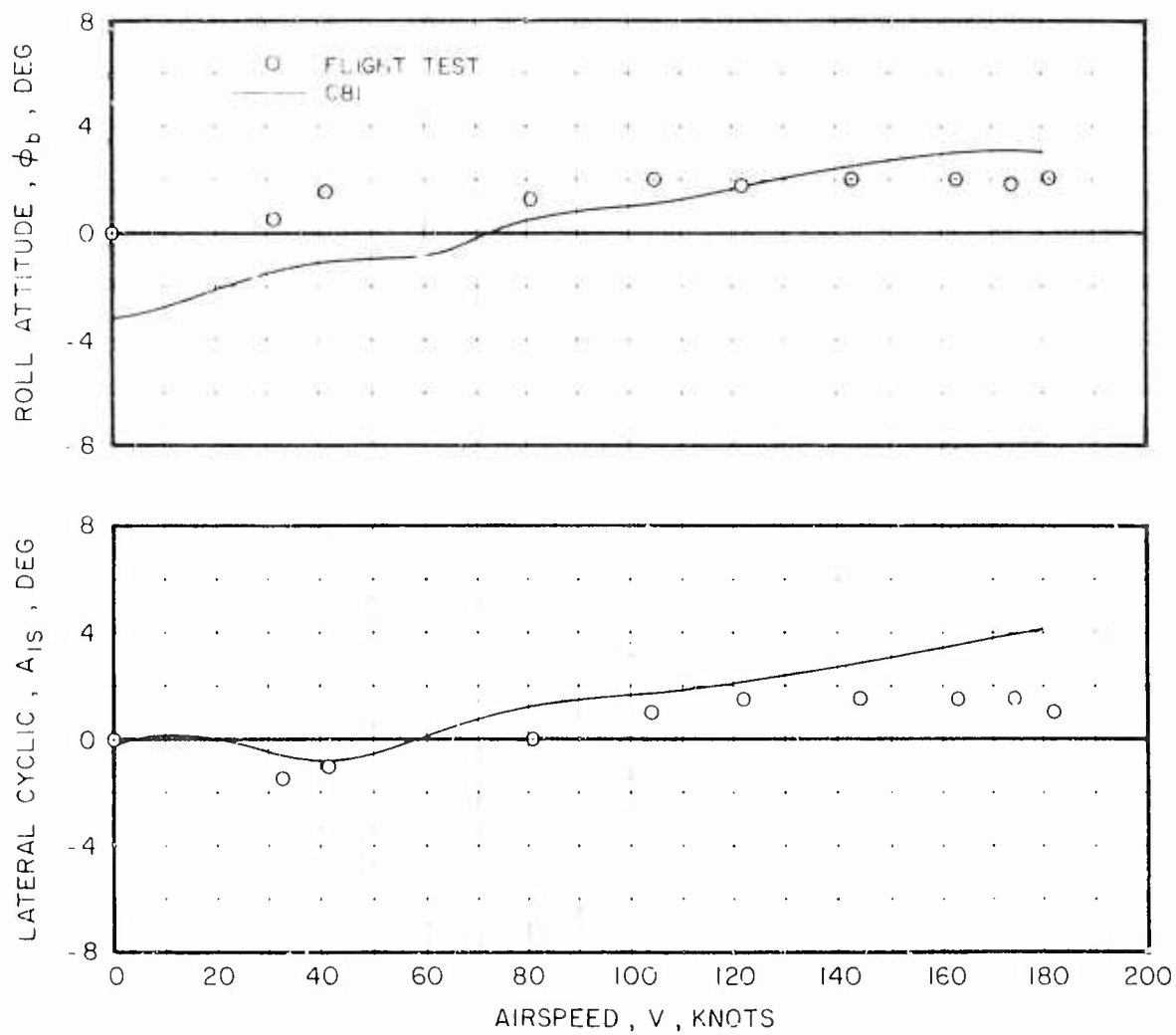


Figure 6. Continued.

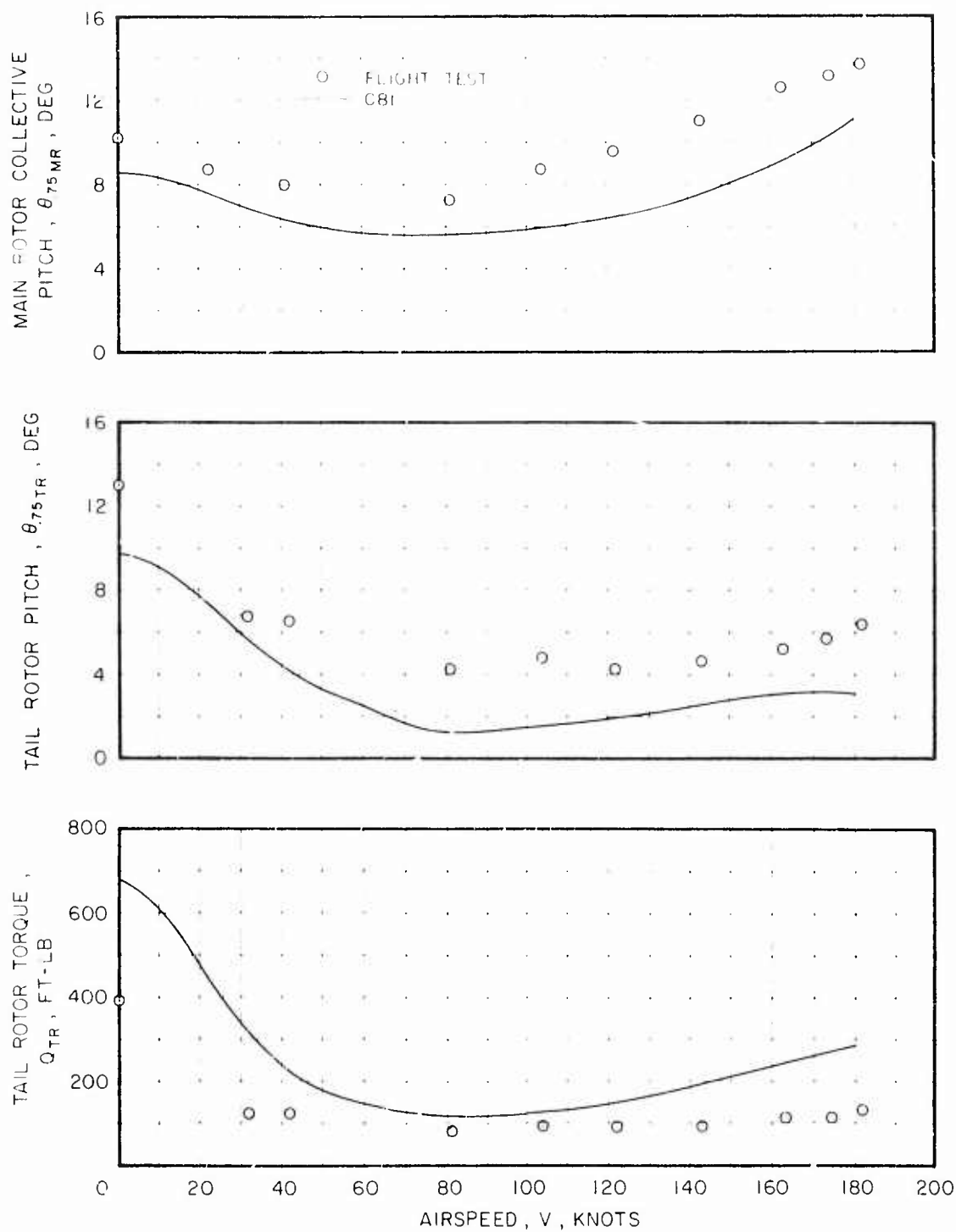


Figure 6. Concluded.

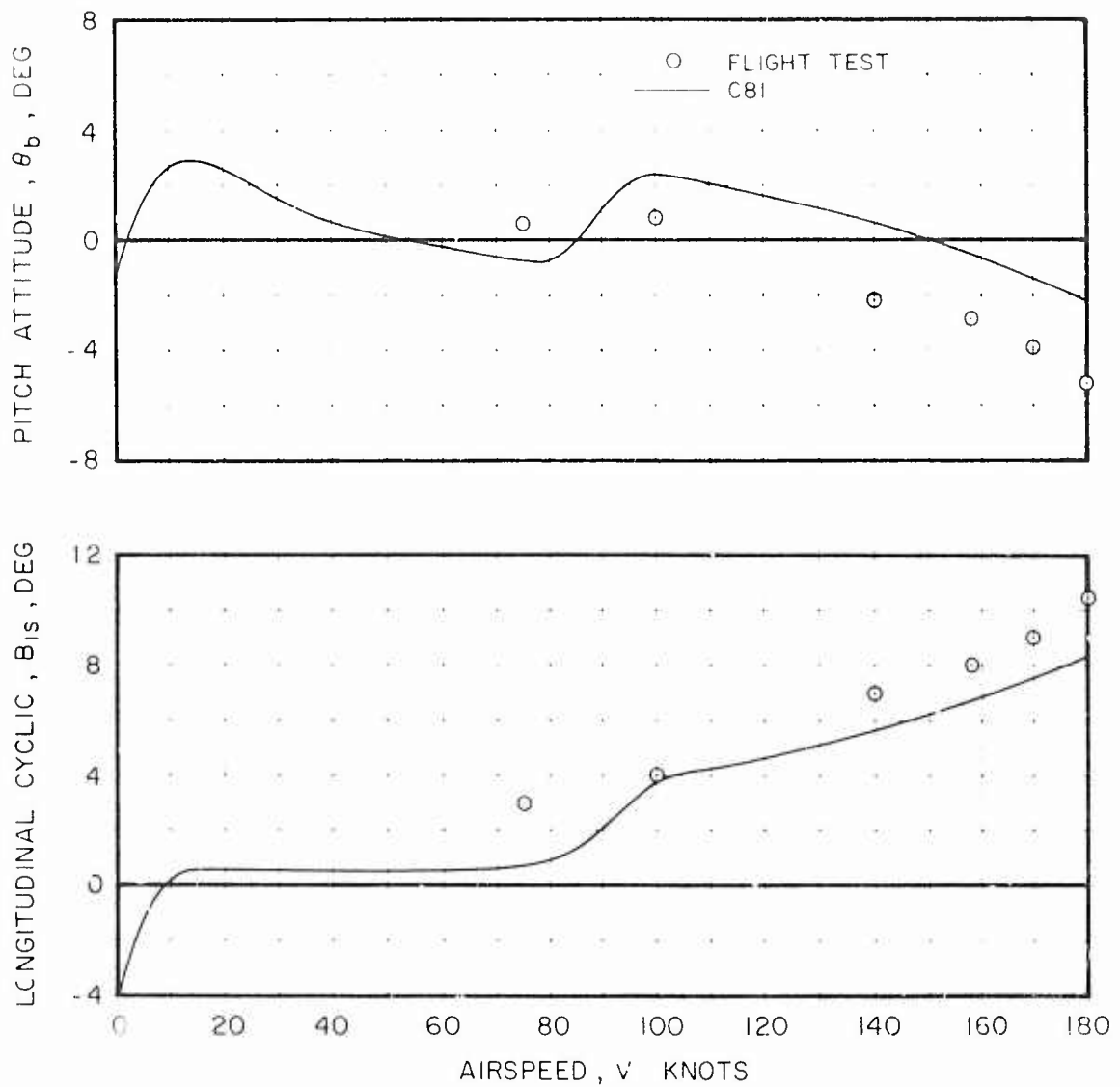


Figure 7. C81 Level Flight Trim vs Airspeed, Compared With Flight Test Data for the S-67 at 17,300 Lb, Forward FSCG = 258 (104% N_T , h_d = 3000 Ft).

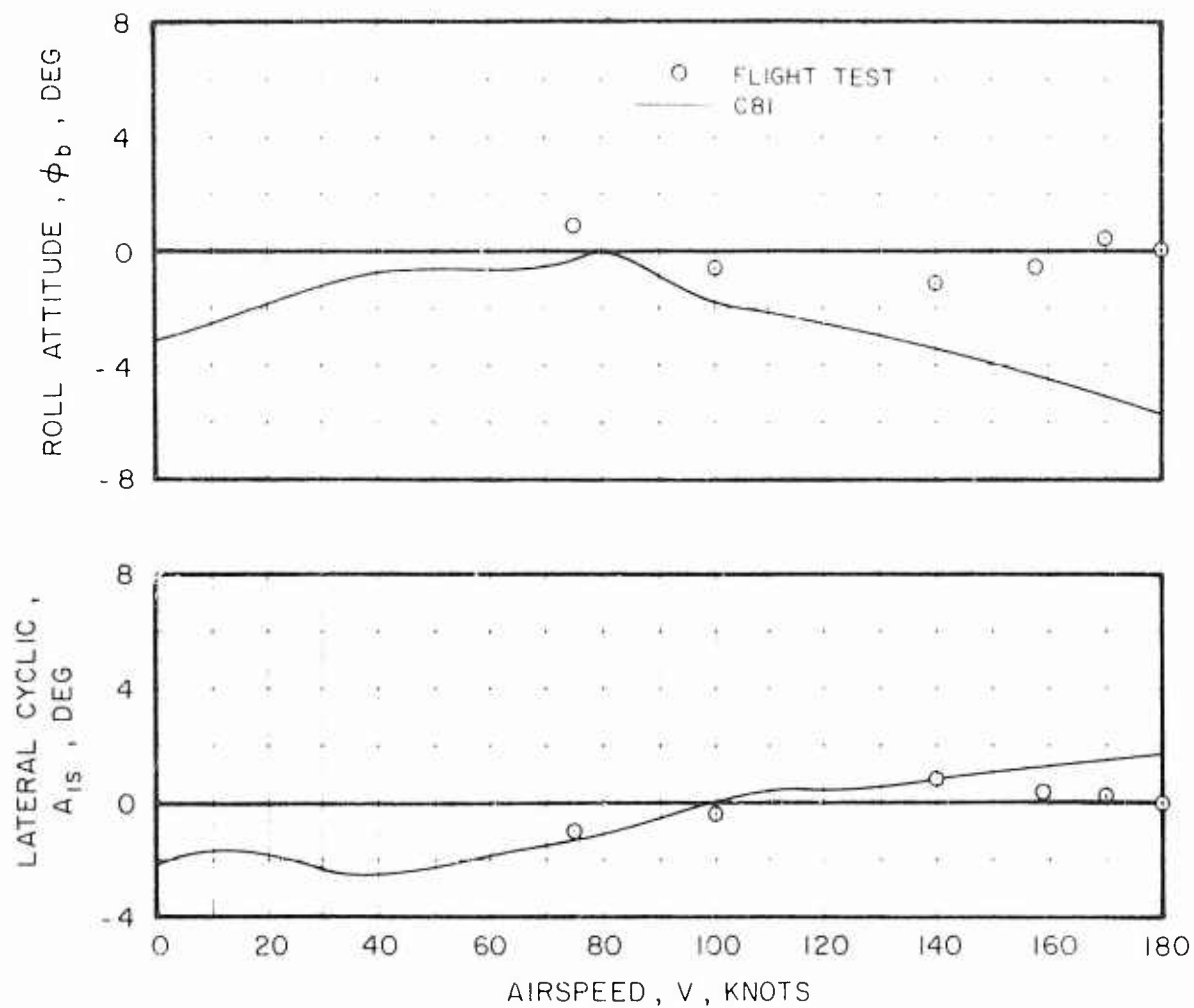


Figure 7. Continued.

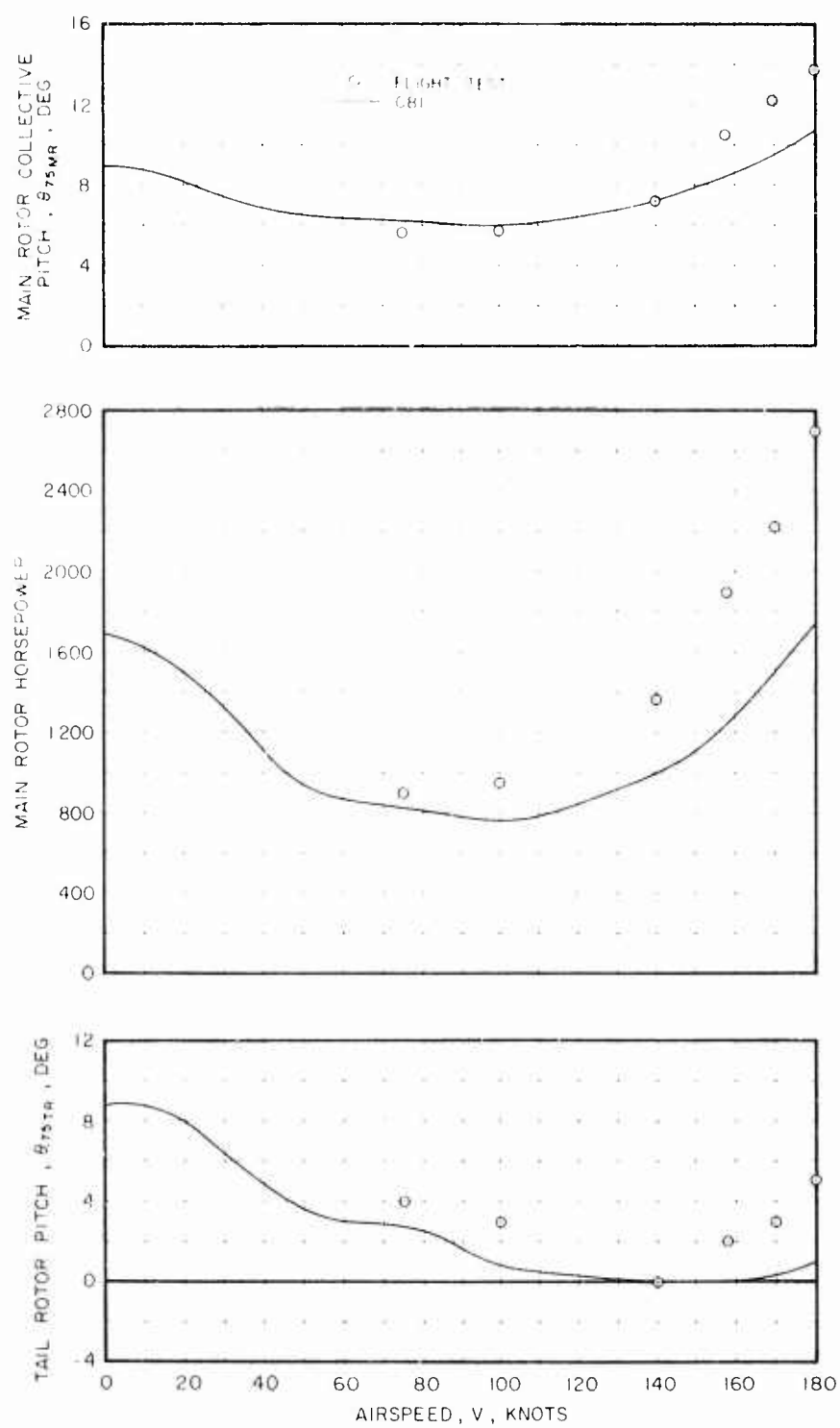


Figure 7. Concluded.

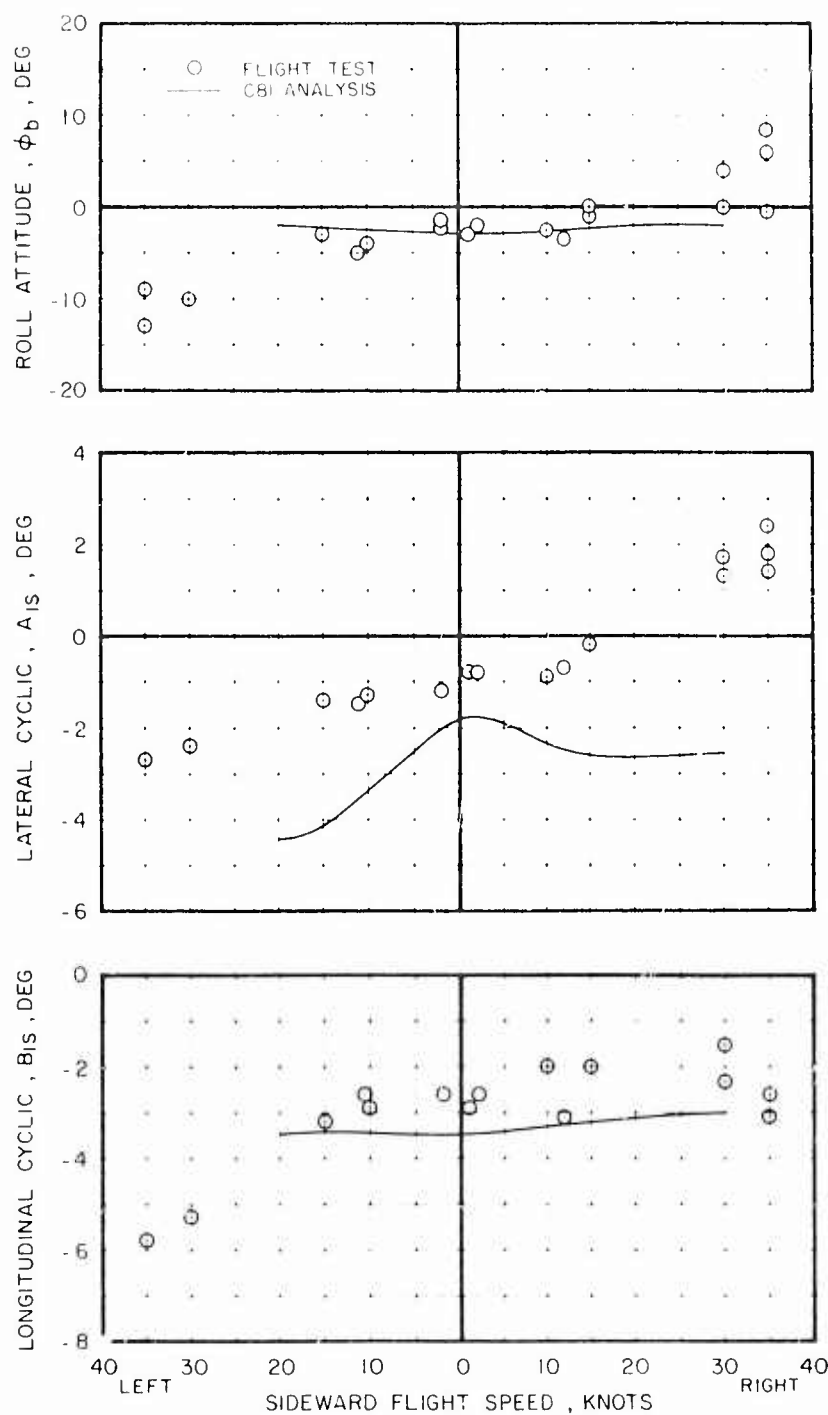


Figure 8. C81 Sideward Flight Trim vs Airspeed, Compared With Flight Test Data for the CH-53D at 42,000 Lb, Forward FSCG = 328 (100% N_T , $h_d = 0$ Ft).

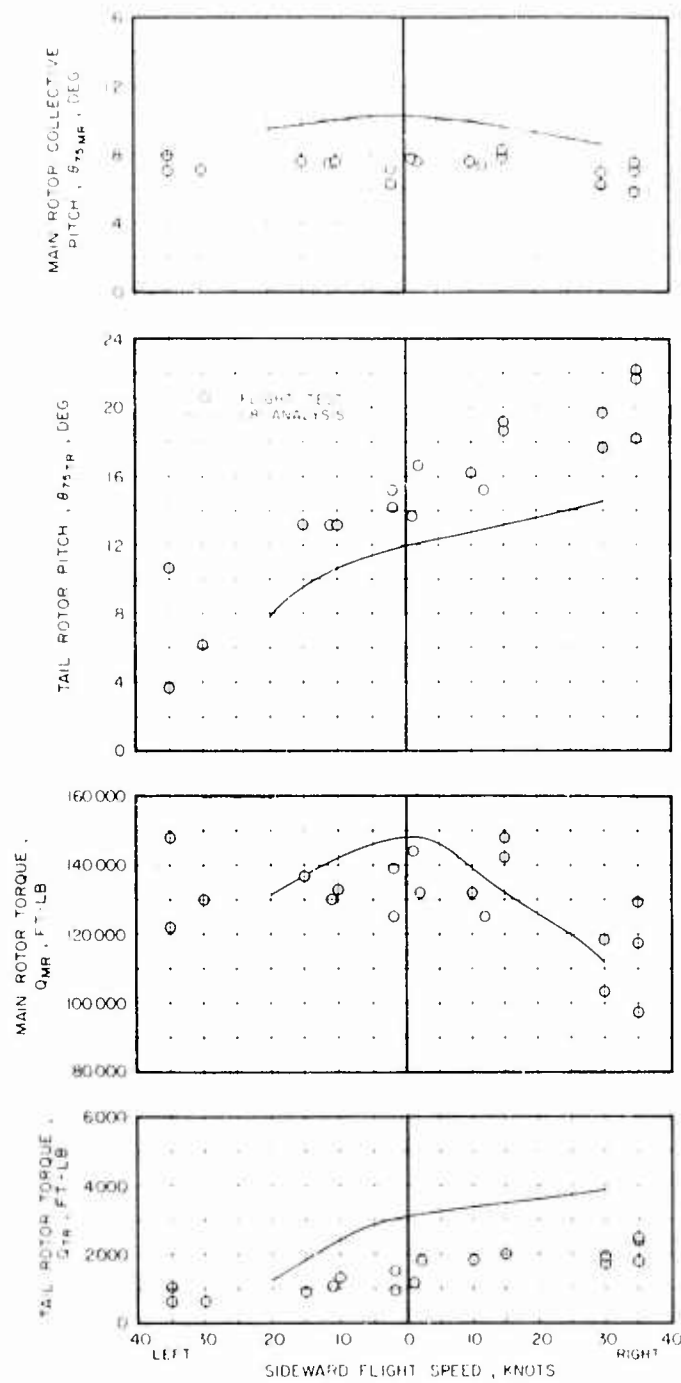


Figure 8. Concluded.

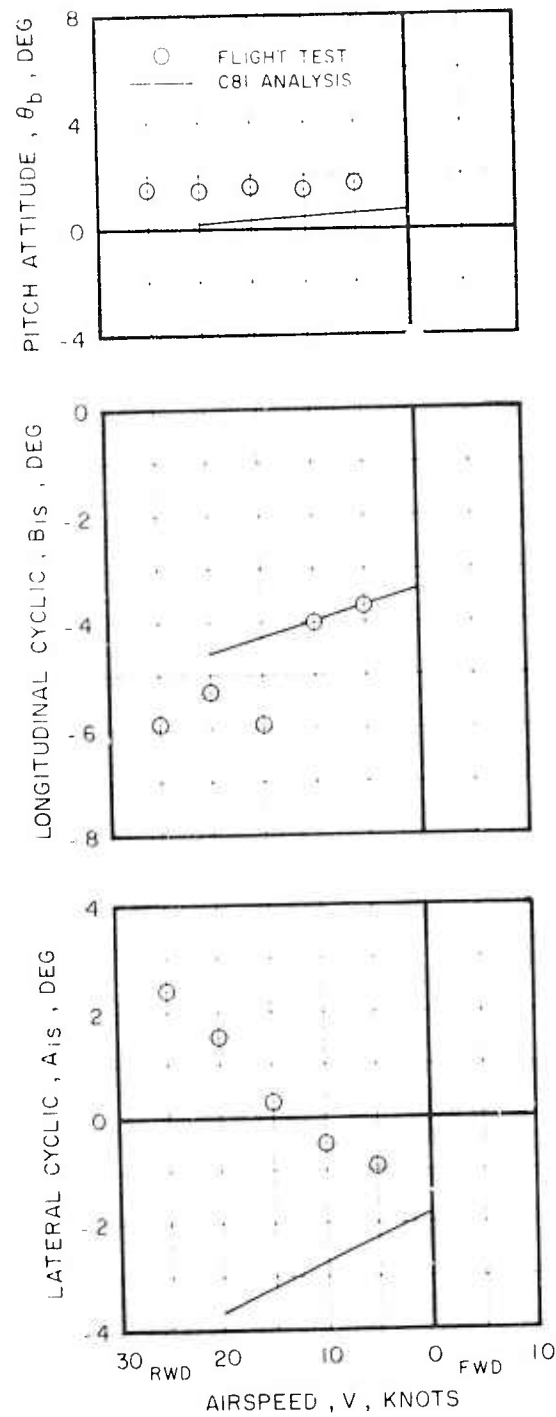


Figure 9. C81 Rearward Flight Trim vs Airspeed, Compared With Flight Test Data for the CH-53D at 46,000 Lb, Forward FSCG = 328.3 (104% N_r , h_d = 2000 Ft).

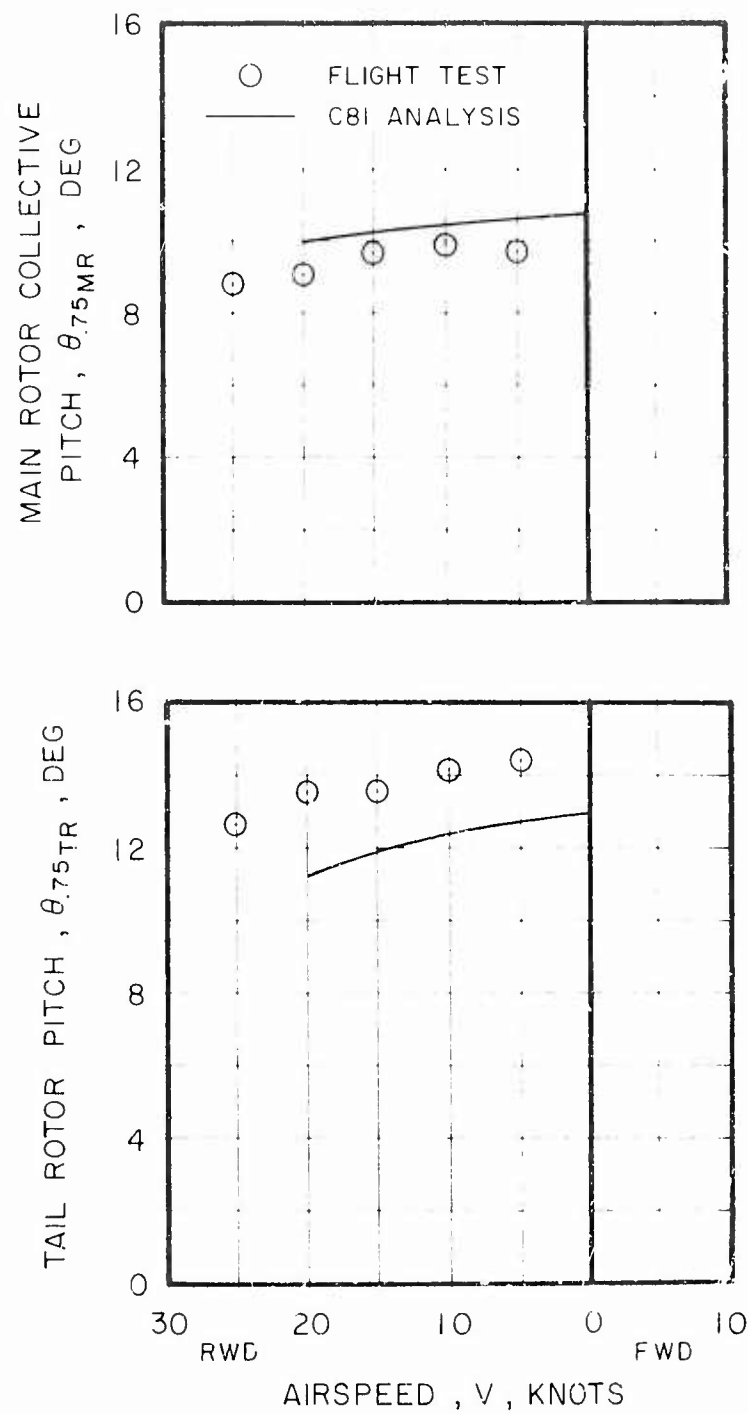


Figure 9. Concluded.

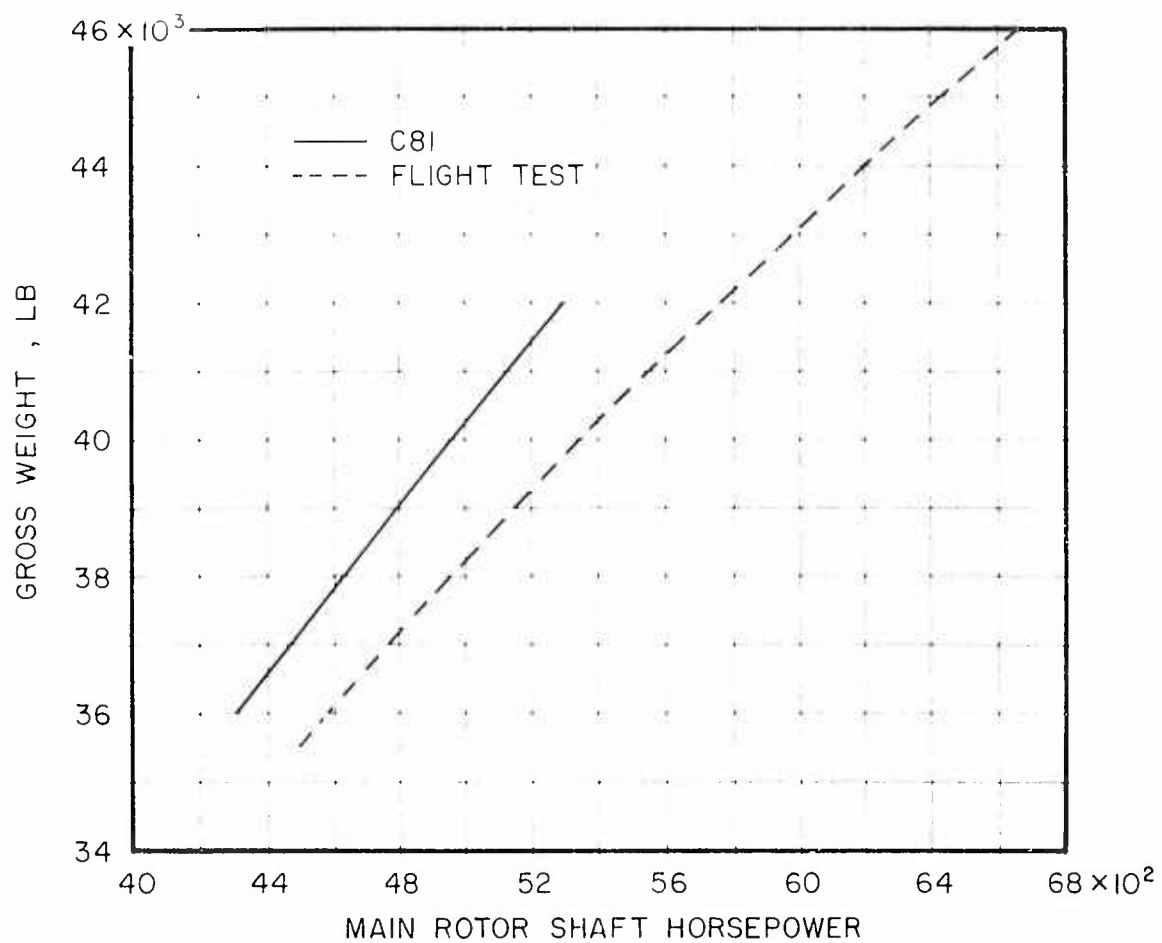


Figure 10. C81 Hover Gross Weight vs Power Requirement, Compared With Flight Test Data for the CH-53A at 105% N_r and at Standard Sea Level Conditions (FSCG = 336).

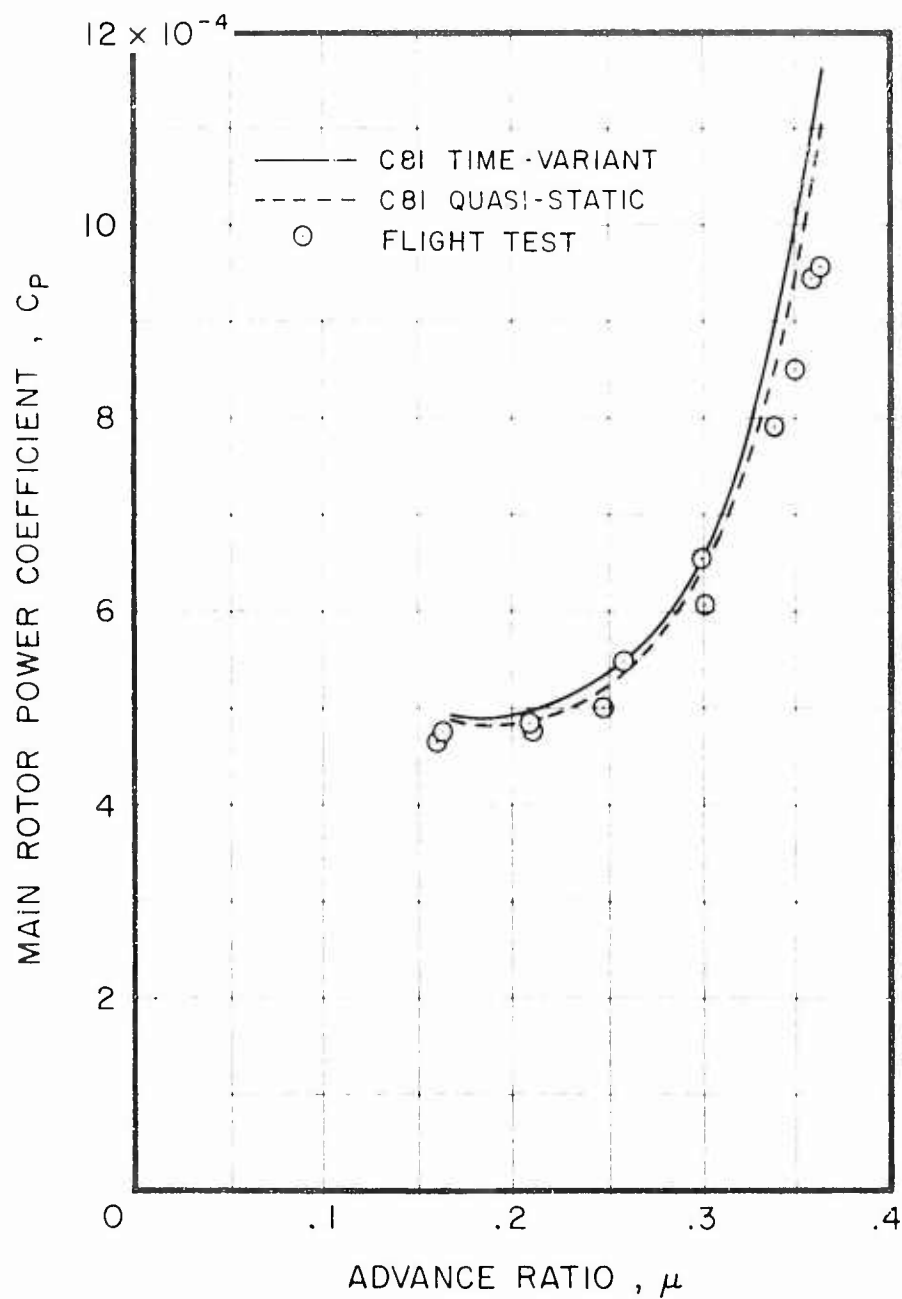


Figure 11. C81 Level Flight Power Requirement vs Advance Ratio, Compared With Flight Test Data for the CH-53A at 42,000 Lb, 105% N_r , $h_d = 2130$ Ft (FSCG = 328, $C_W = 0.0088$).

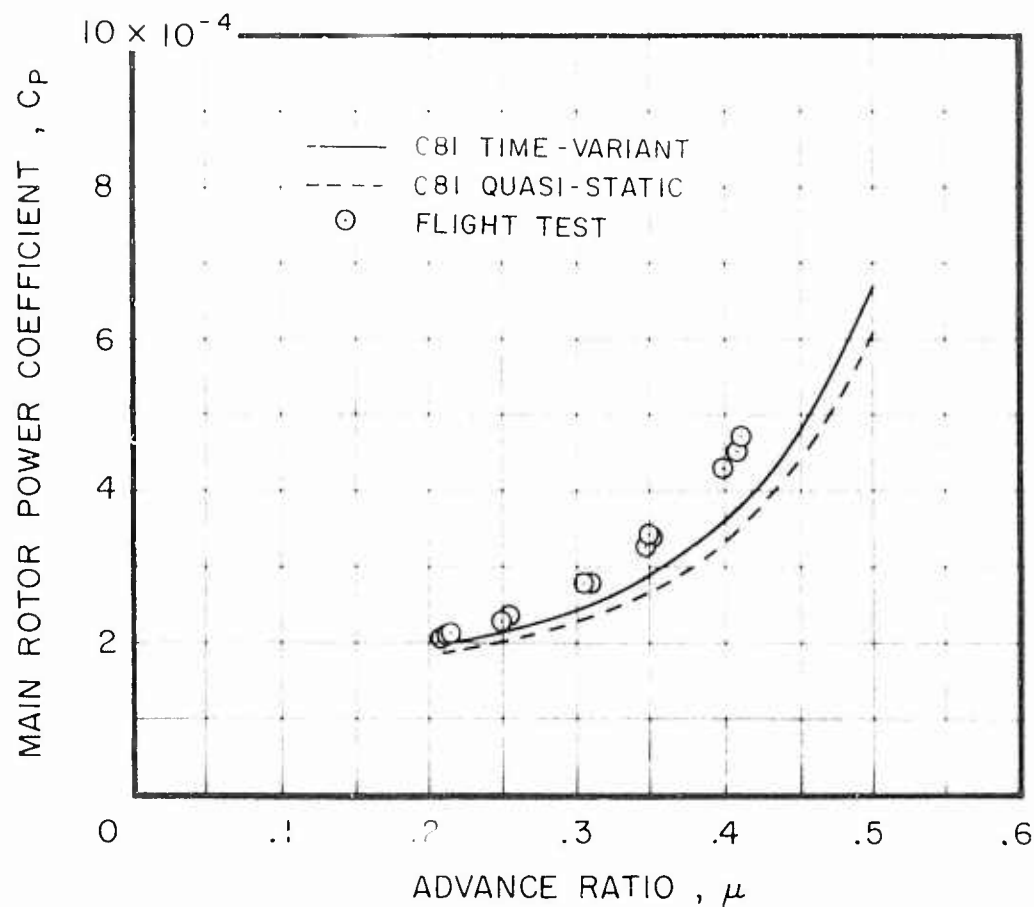


Figure 12. C81 Level Flight Power Requirement vs Advance Ratio, Compared With Flight Test Data for the S-67 at 16,500 Lb, 102.5% N_T , $h_d = 0$ Ft (FSCG = 272.3, $C_W = 0.00505$).

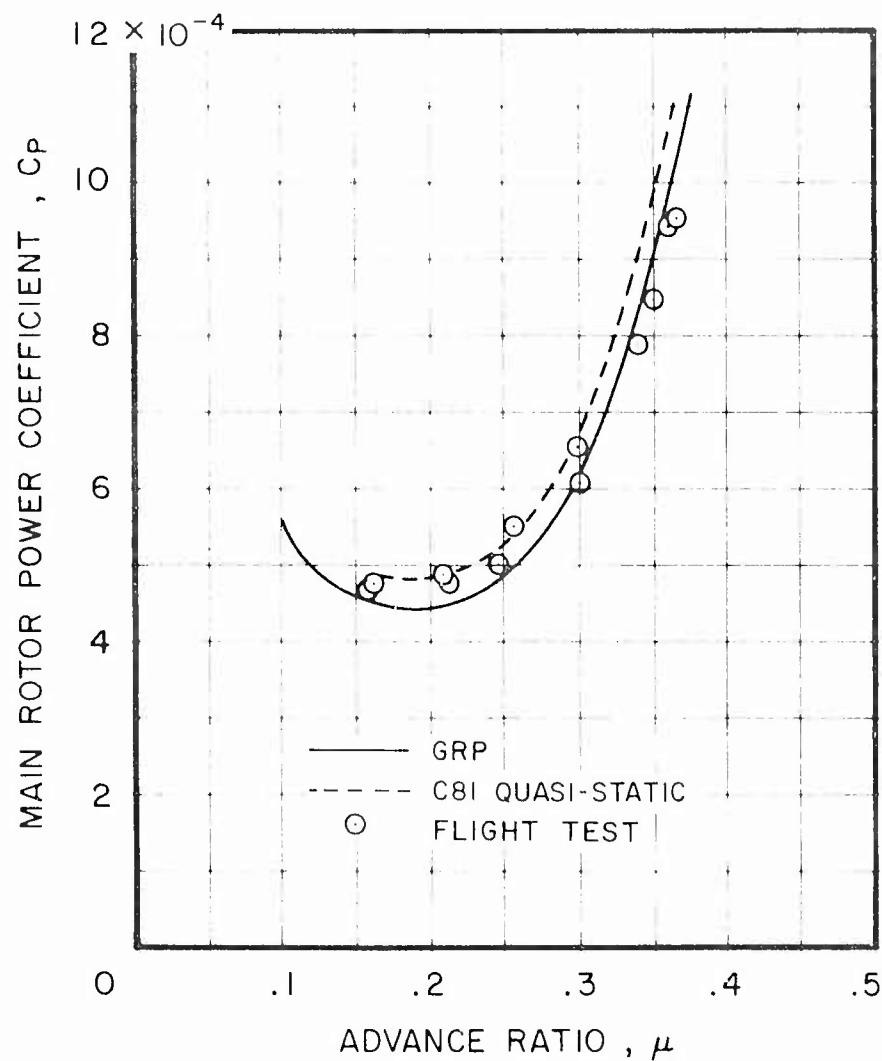


Figure 13. C81 Level Flight Power Requirement vs Advance Ratio, Compared With GRP Analysis and Flight Test Data for the CH-53A at 42,000 Lb, 105% N_r , $h_d = 2130$ Ft (FSCG = 328, $C_w = 0.0088$).

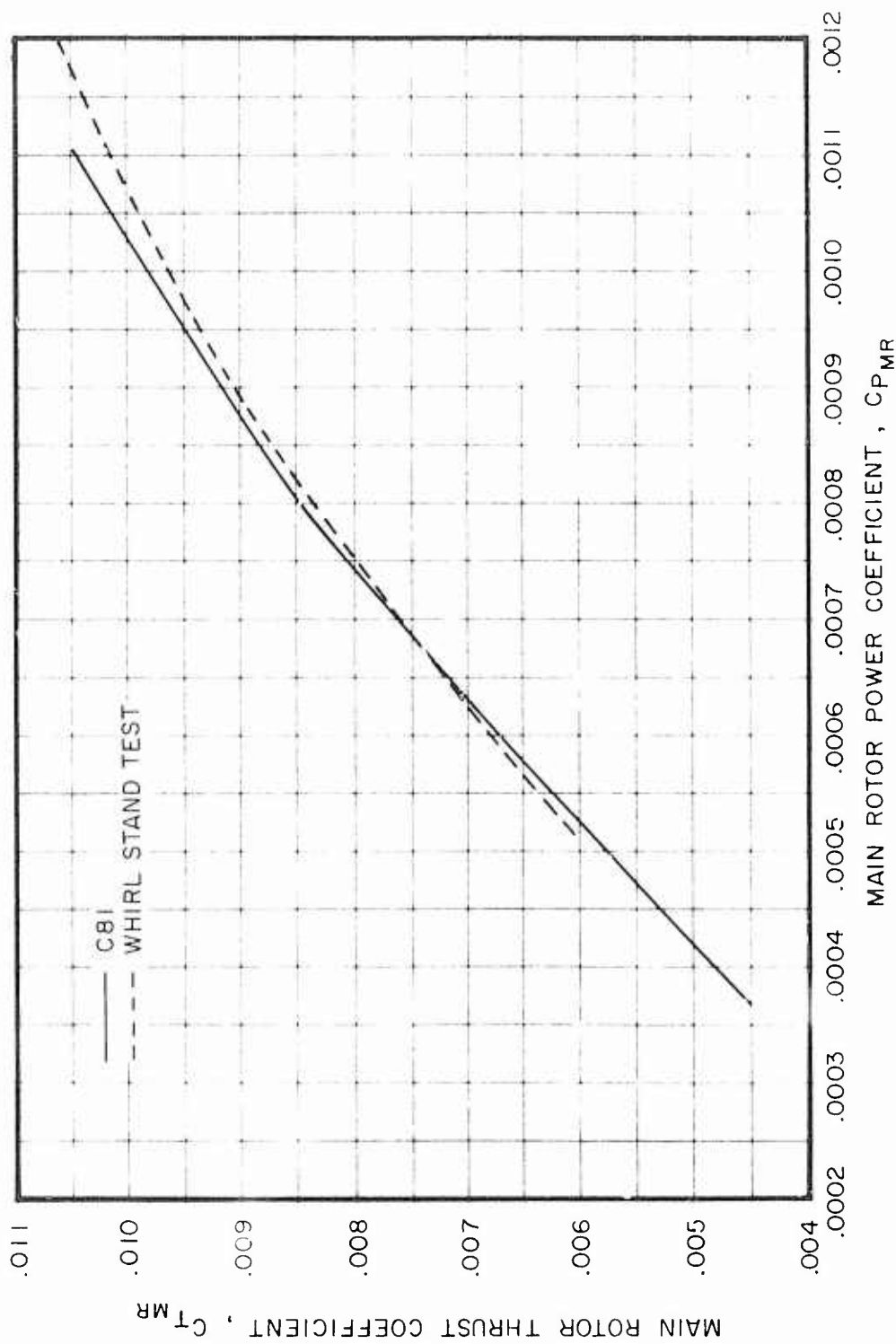


Figure 14. C81 Prediction of Main Rotor Thrust Coefficient vs Power Coefficient, Compared With Whirl Stand Test Data for the CH-53D Main Rotor Out of Ground Effect, at 100% N_r , and at Standard Sea Level Conditions.

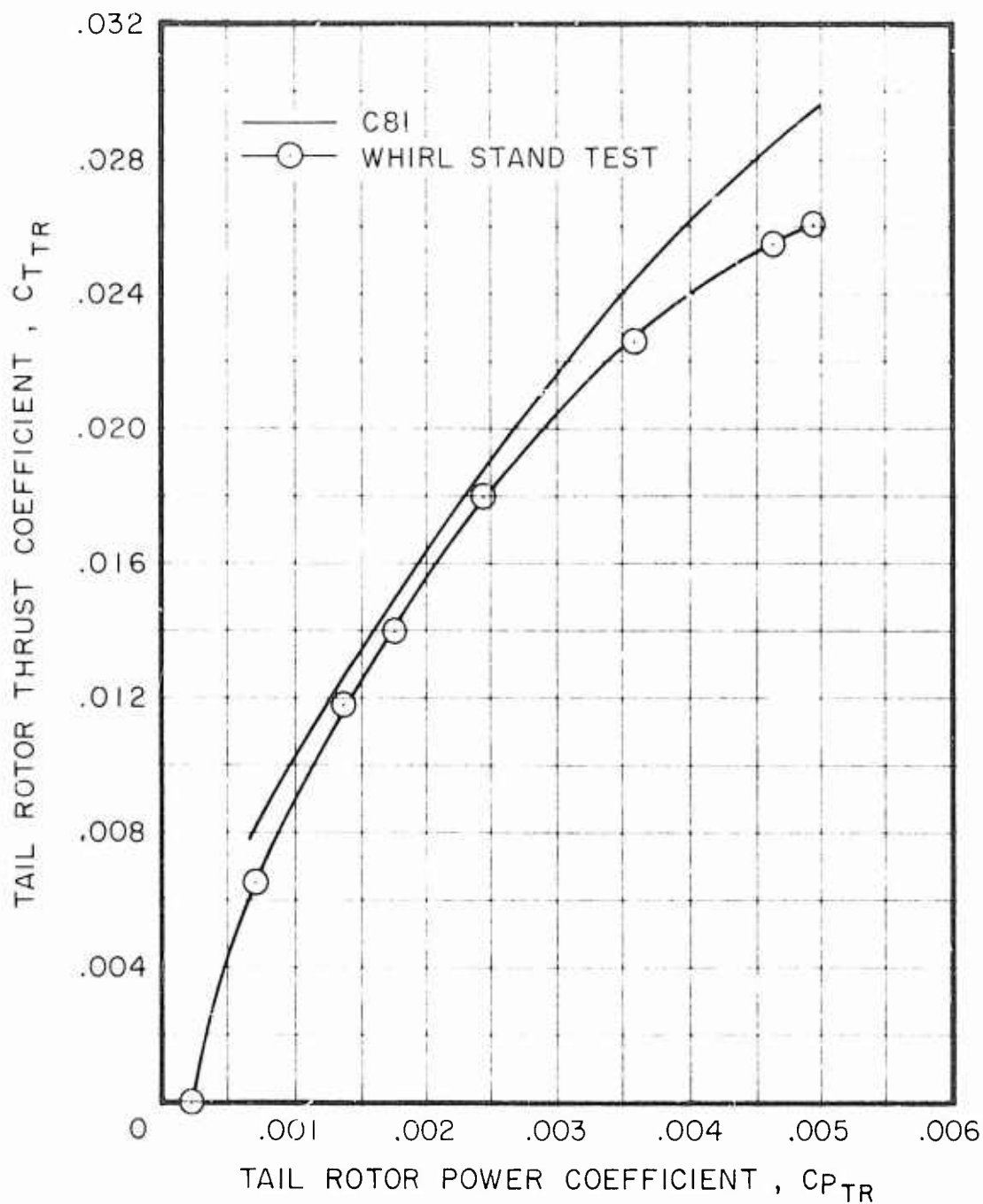


Figure 15. C81 Prediction of Tail Rotor Thrust Coefficient vs Power Coefficient, Compared With Whirl Stand Test Data for the CH-53A Tail Rotor Out of Ground Effect, at 100% N_r , and at Standard Sea Level Conditions.

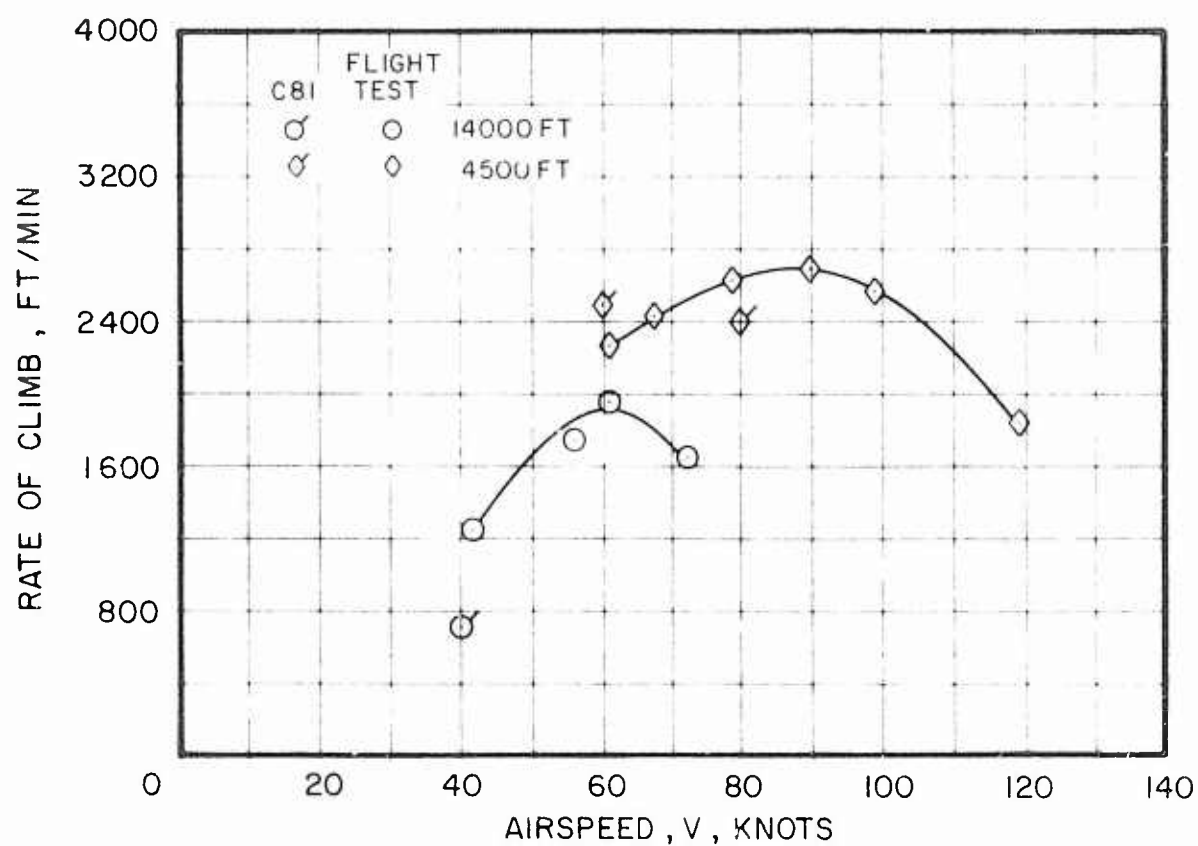


Figure 16. C81 Maximum Rate of Climb Performance vs Airspeed, Compared With Flight Test Data for the HH-53C at 35,000 Lb at Various Density Altitudes (100% N_r , FSCG = 340).

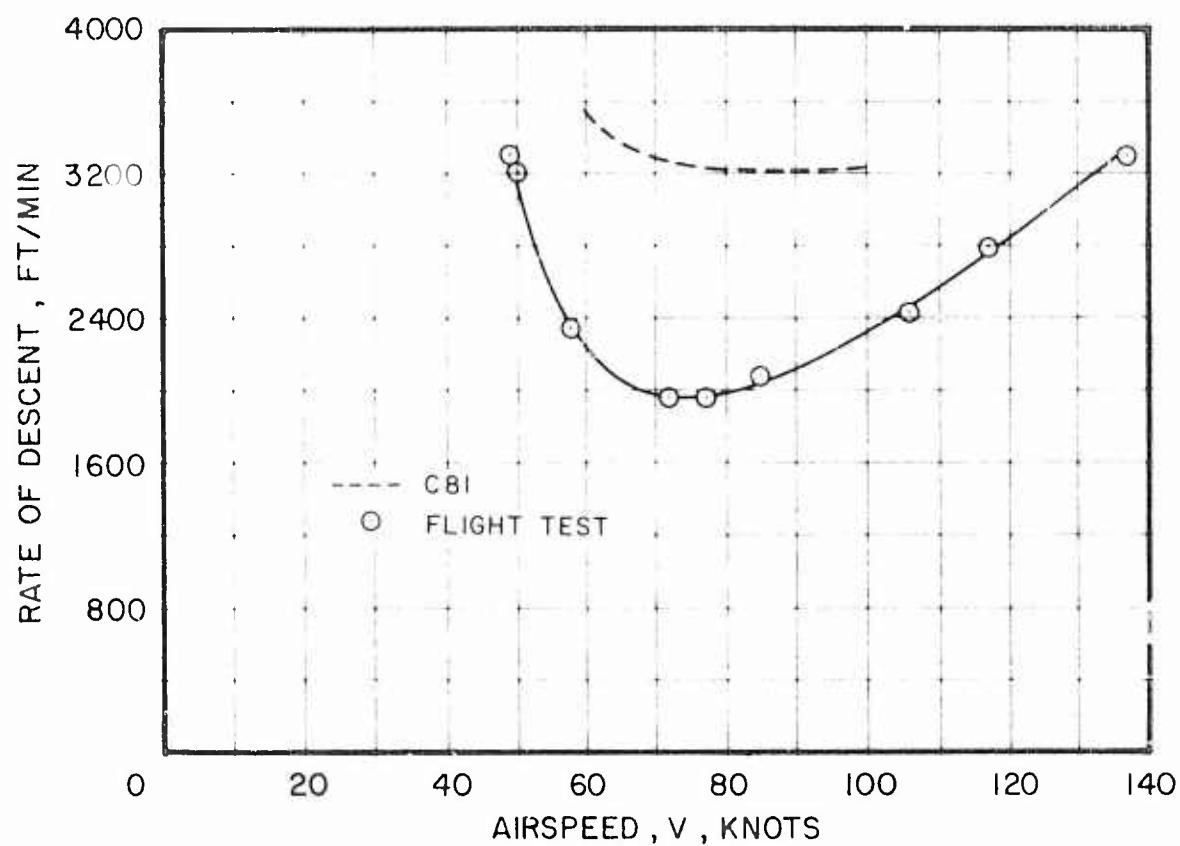


Figure 17. C81 Maximum Rate of Descent in Autorotation vs Airspeed, Compared With Flight Test Data for the HH-53C at 35,000 Lb, 100% N_r , $h_d = 4500$ Ft (FSCG = 340).

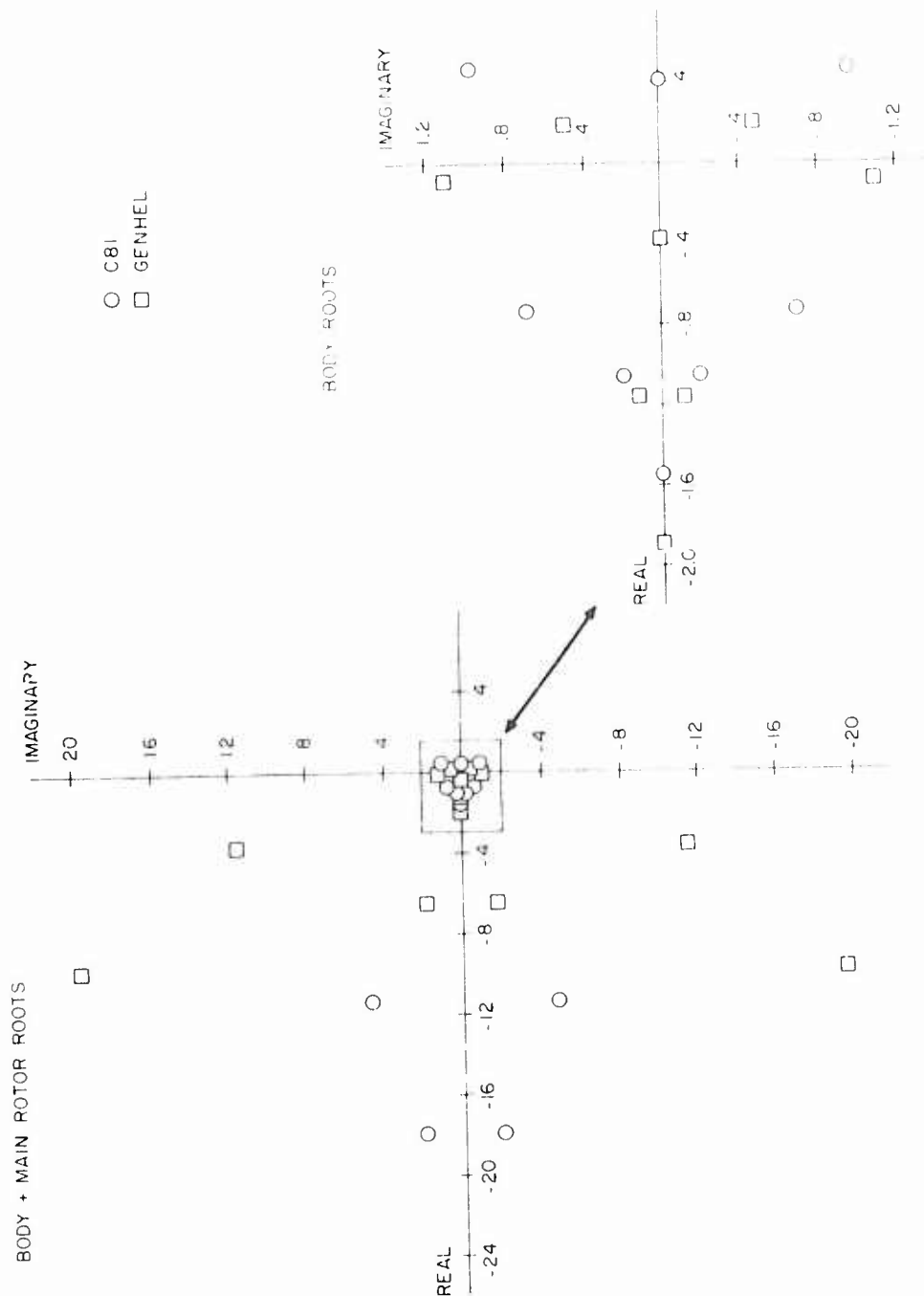


Figure 18. C81 Main Rotor and Body Root Locus, Compared With GENHEL Analysis Data for the CH-53A in Hover (33,500 Lb, FSCG = 348).

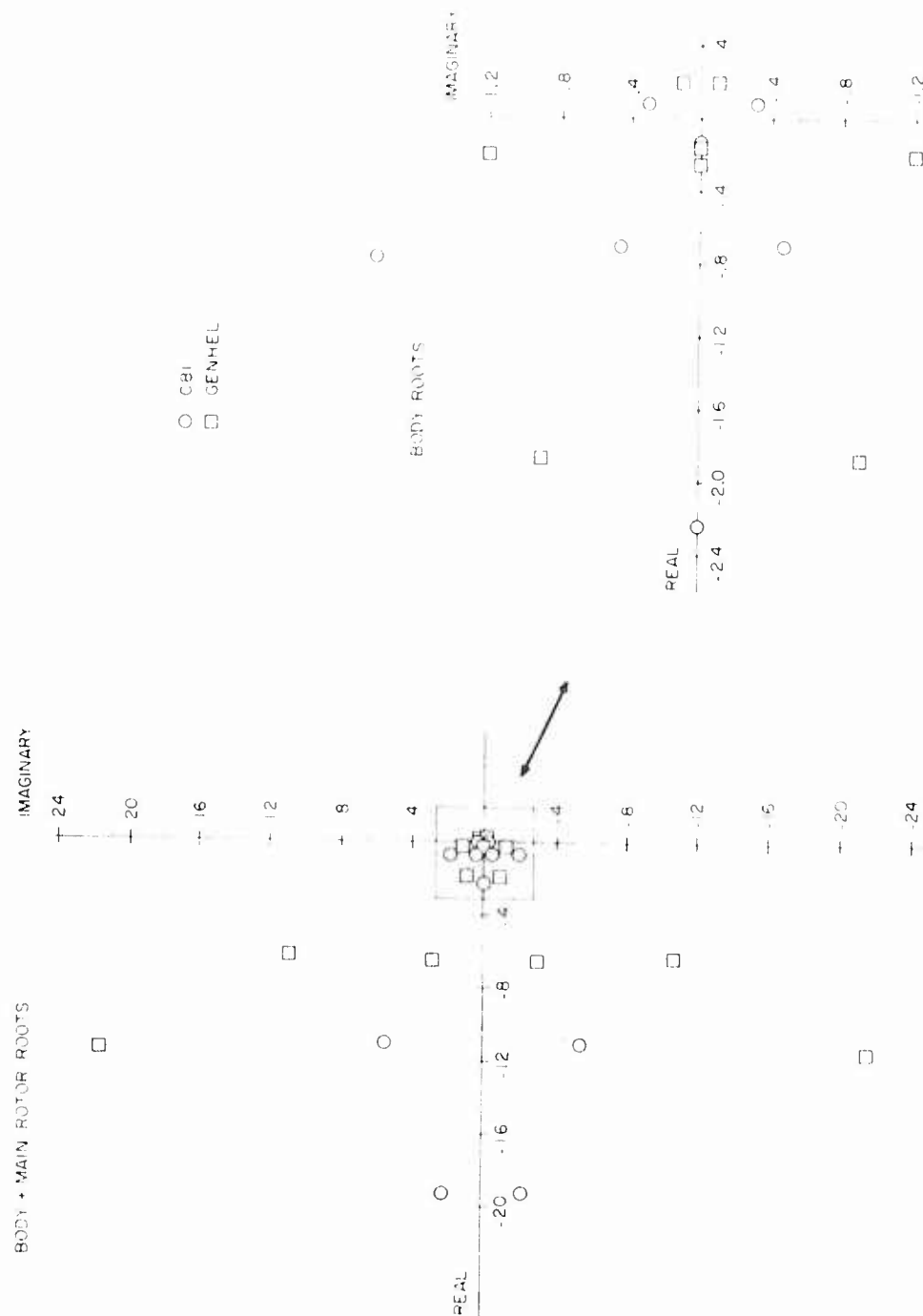


Figure 19. C81 Main Rotor and Body Root Locus, Compared With GENHEL Analysis Data for the CH-53A at 100 Kt (33,500 Lb, FSCG = 348).

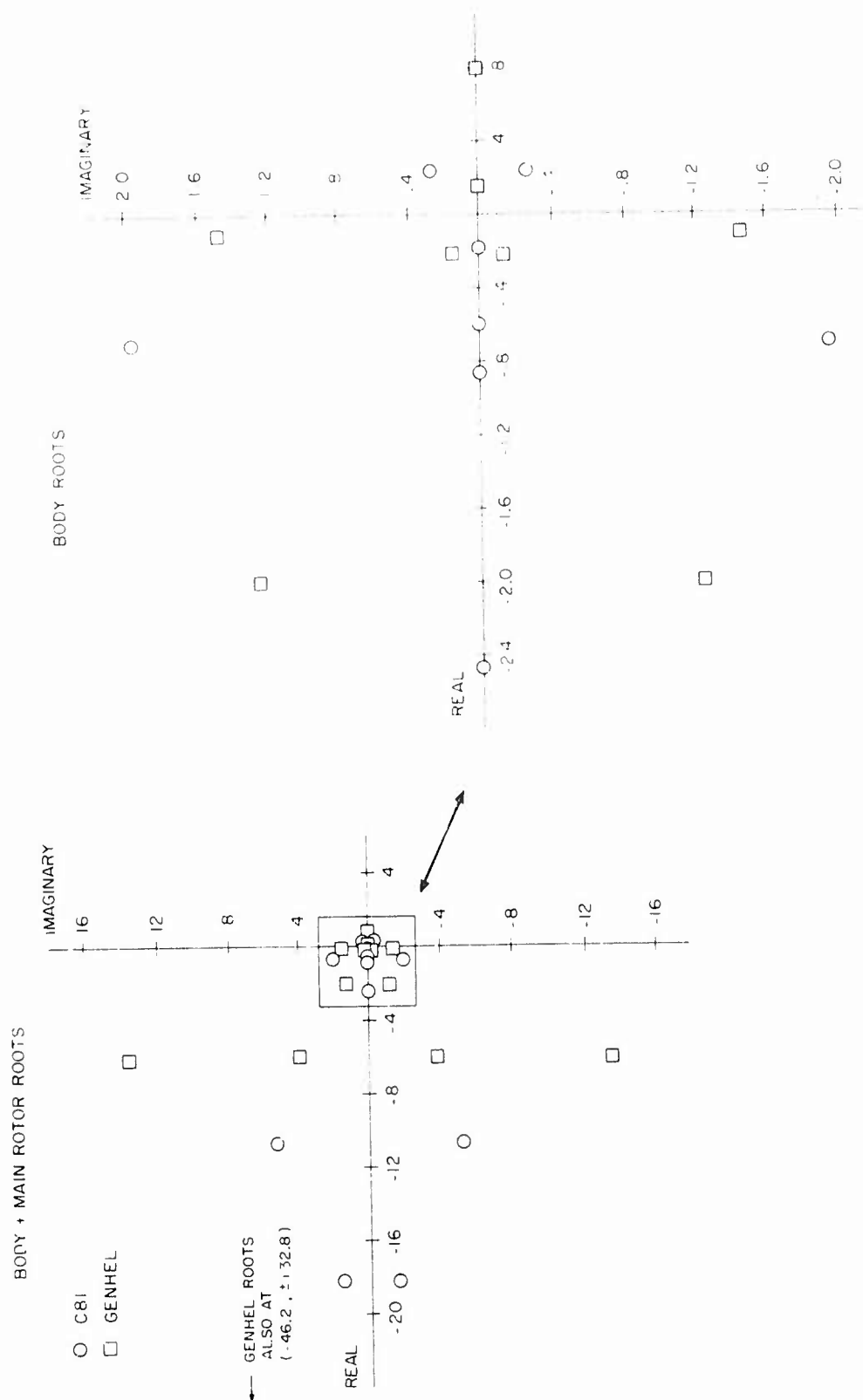


Figure 20. C81 Main Rotor and Body Root Locus, Compared With GENHEL Analysis Data for the CH-53A at 150 Kt (33,500 Lb, FSCG = 348).

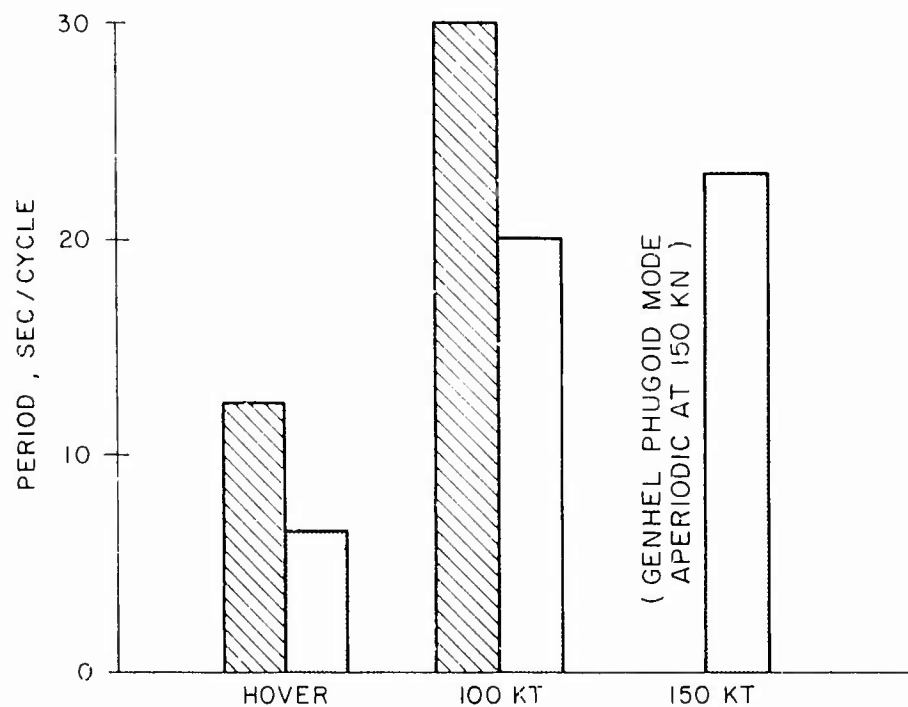
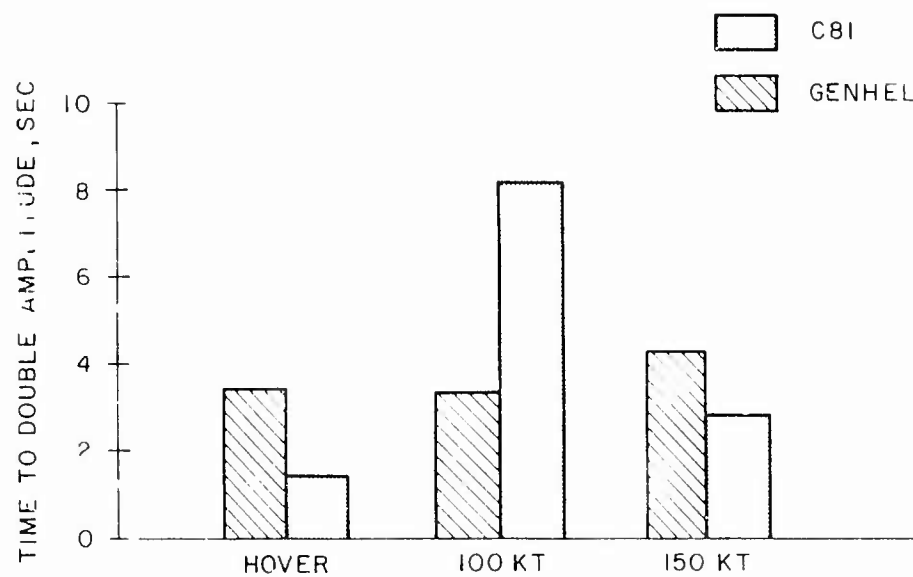


Figure 21. C81 Prediction of Time to Double Amplitude and Period of Phugoid Modes, Compared With GENHEL Data for the CH-53A at Various Speeds (33,500 Lb, FSCG = 348).

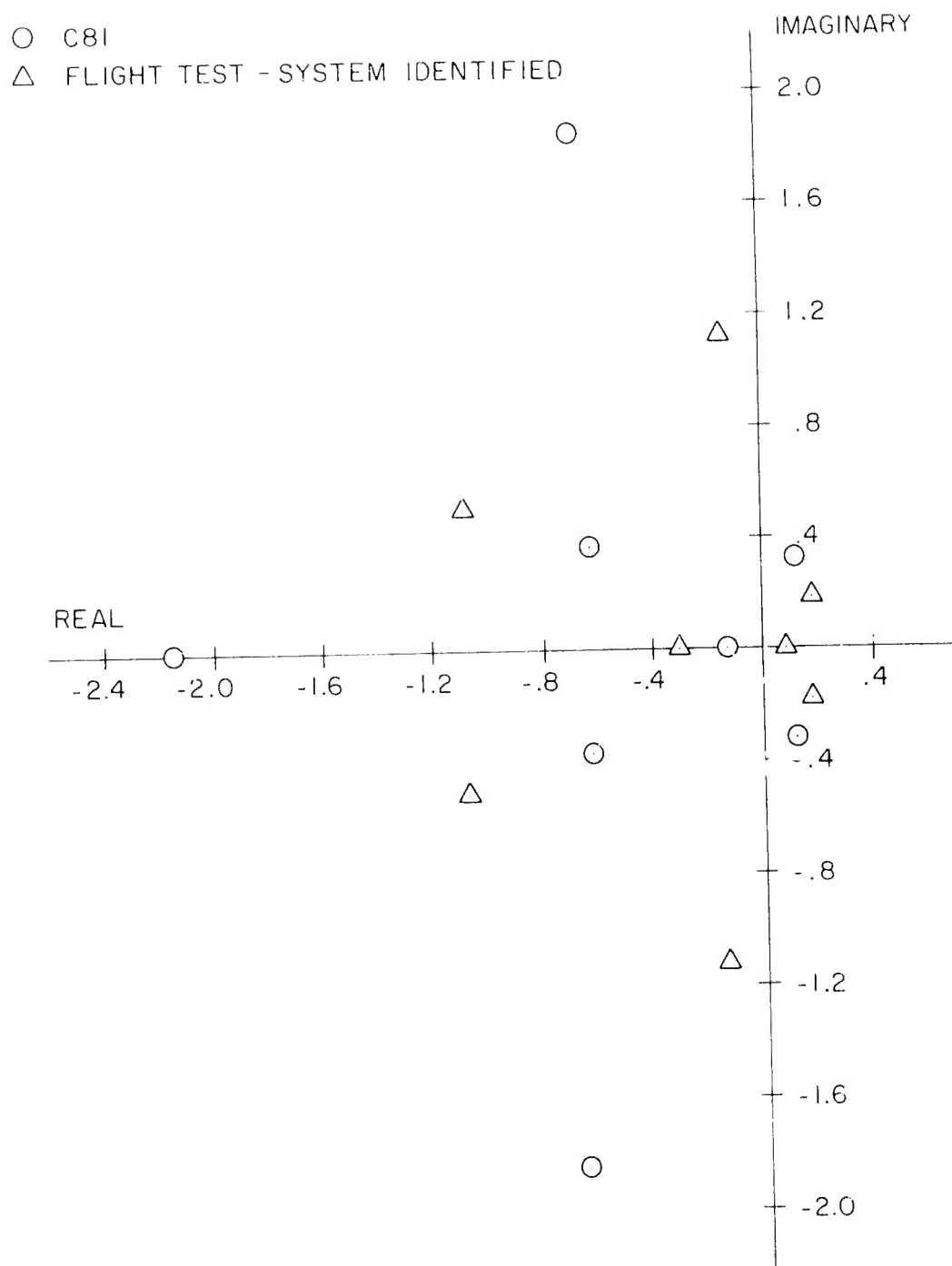


Figure 22. C81 Body Root Locus Compared With Flight Test System-Identified Data for the CH-53A at 100 Kt (35,000 Lb, FSCG = 352).

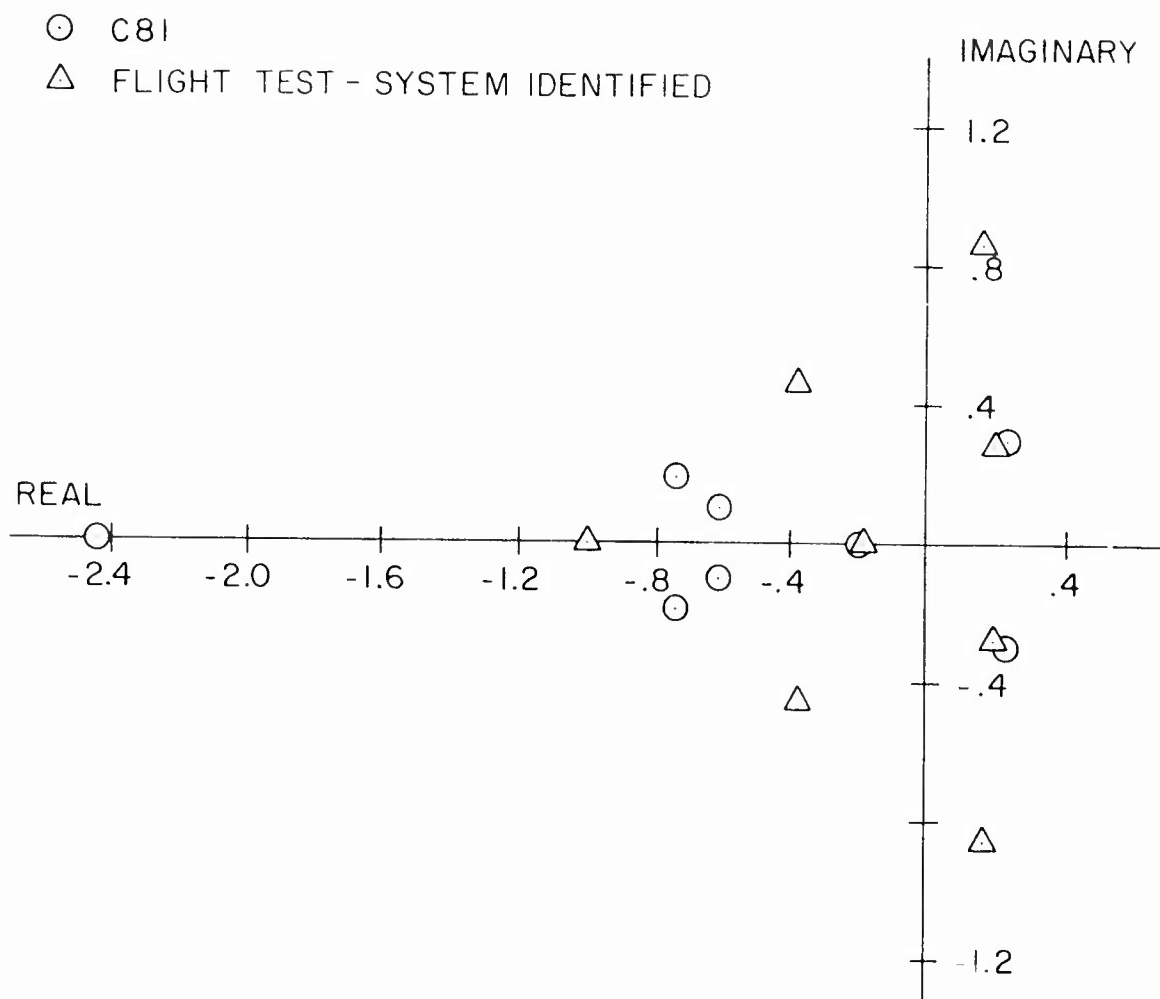


Figure 23. C81 Body Root Locus Compared With Flight Test System-Identified Data for the CH-53A at 150 Kt (35,000 Lb, FSCG = 352).

○ C81

◇ FLIGHT TEST - TIME HISTORY FIT

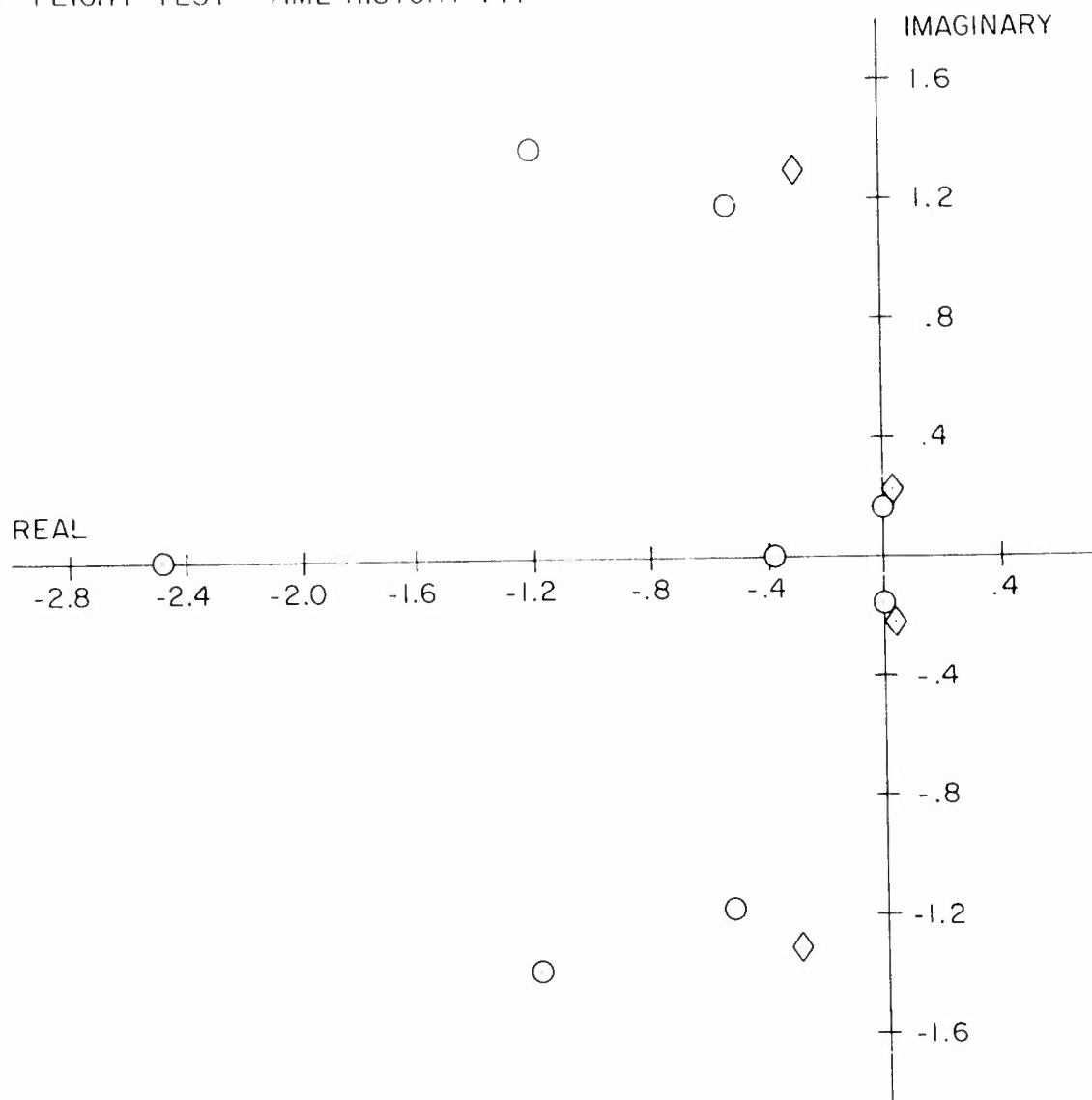


Figure 24. C81 Body Root Locus Compared With Flight Test Time-History-Fitted Data for the S-67 at 100 Kt (14,800 Lb, FSCG = 276).

○ C81
 ◇ FLIGHT TEST - TIME HISTORY FIT

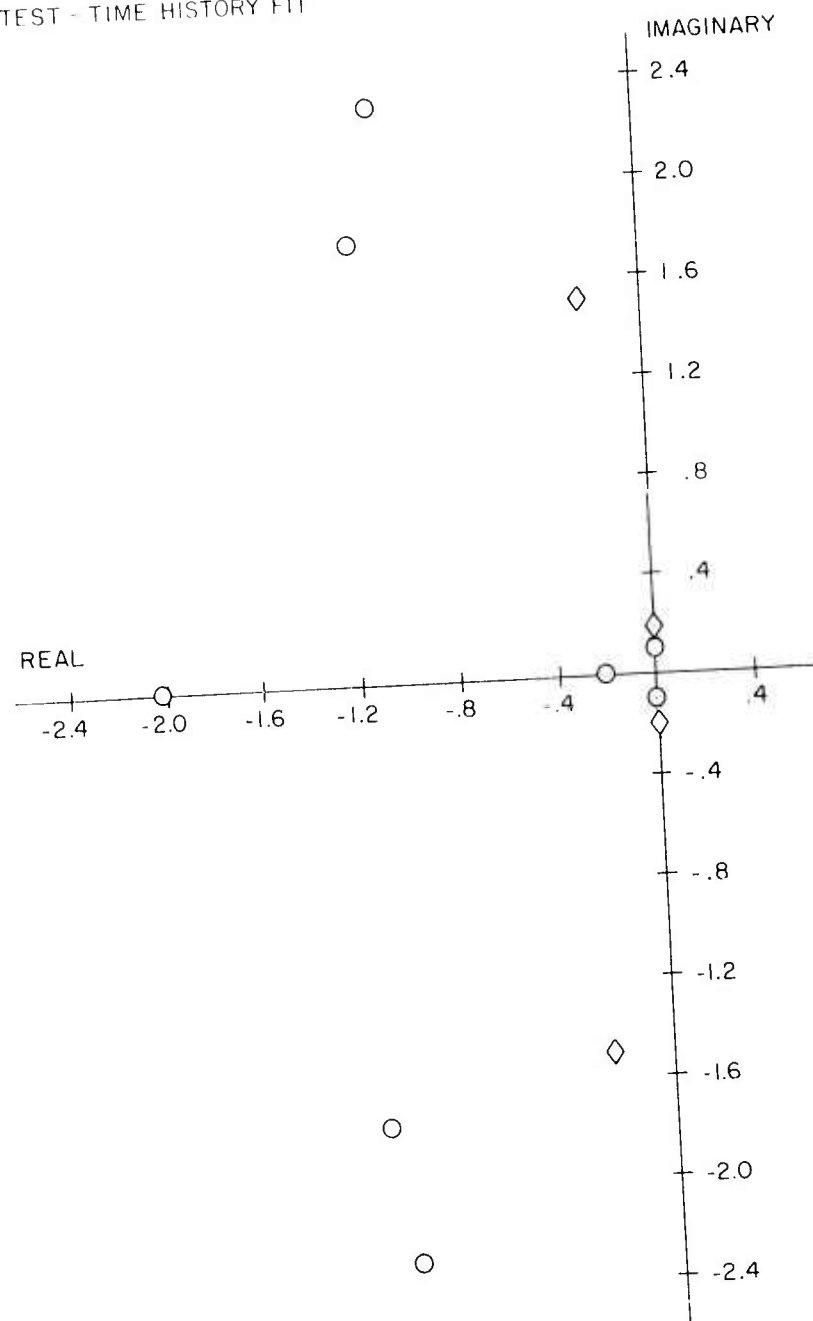


Figure 25. C81 Body Root Locus Compared With Flight Test Time-History-Fitted Data for the S-67 at 140 Kt (14,800 Lb, FSCG = 276).

○ C81
 ◇ FLIGHT TEST - TIME HISTORY FIT

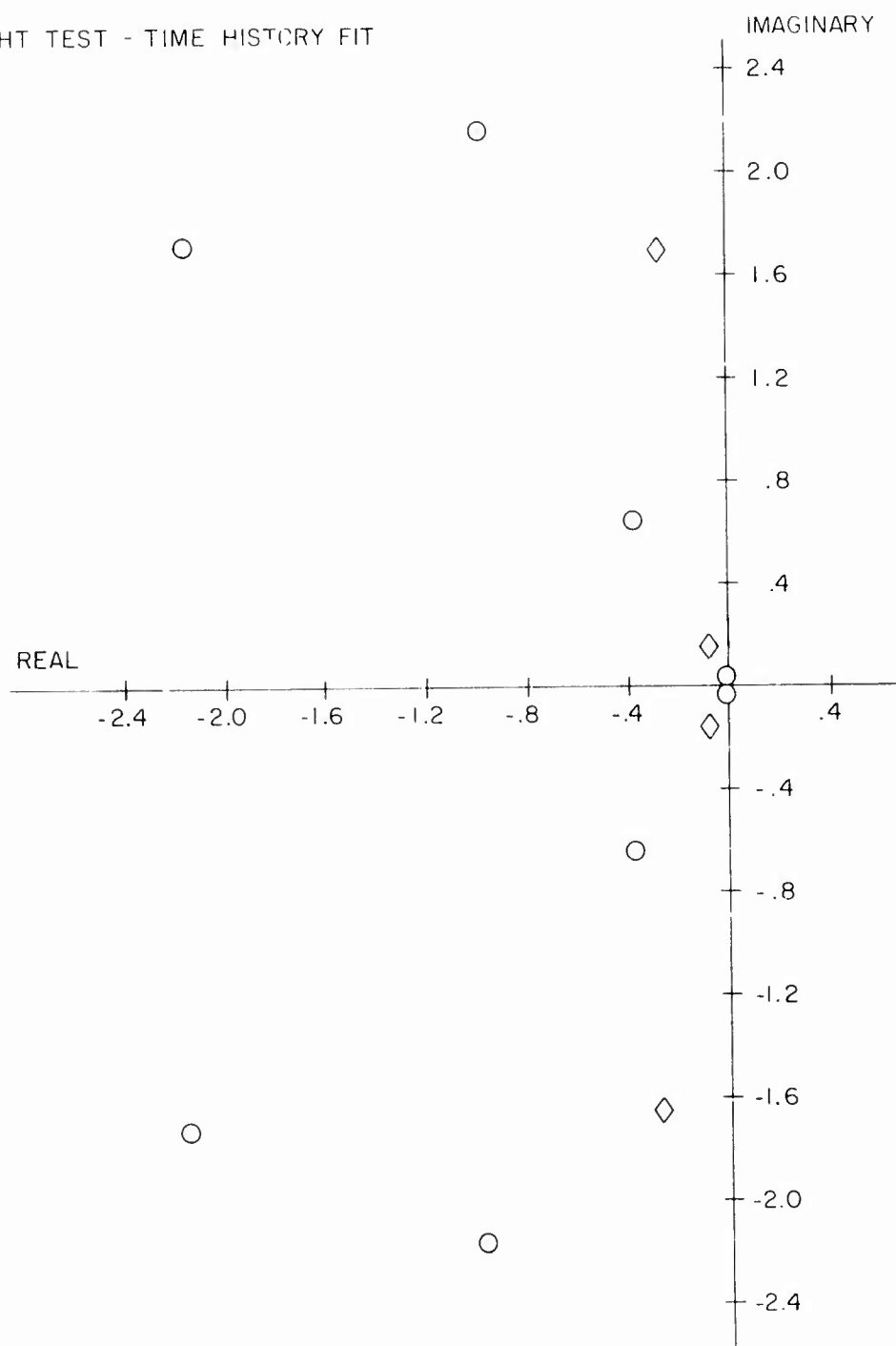


Figure 26. C81 Body Root Locus Compared With Flight Test Time-History-Fitted Data for the S-67 at 180 Kt (14,800 Lb, FSCG = 276).

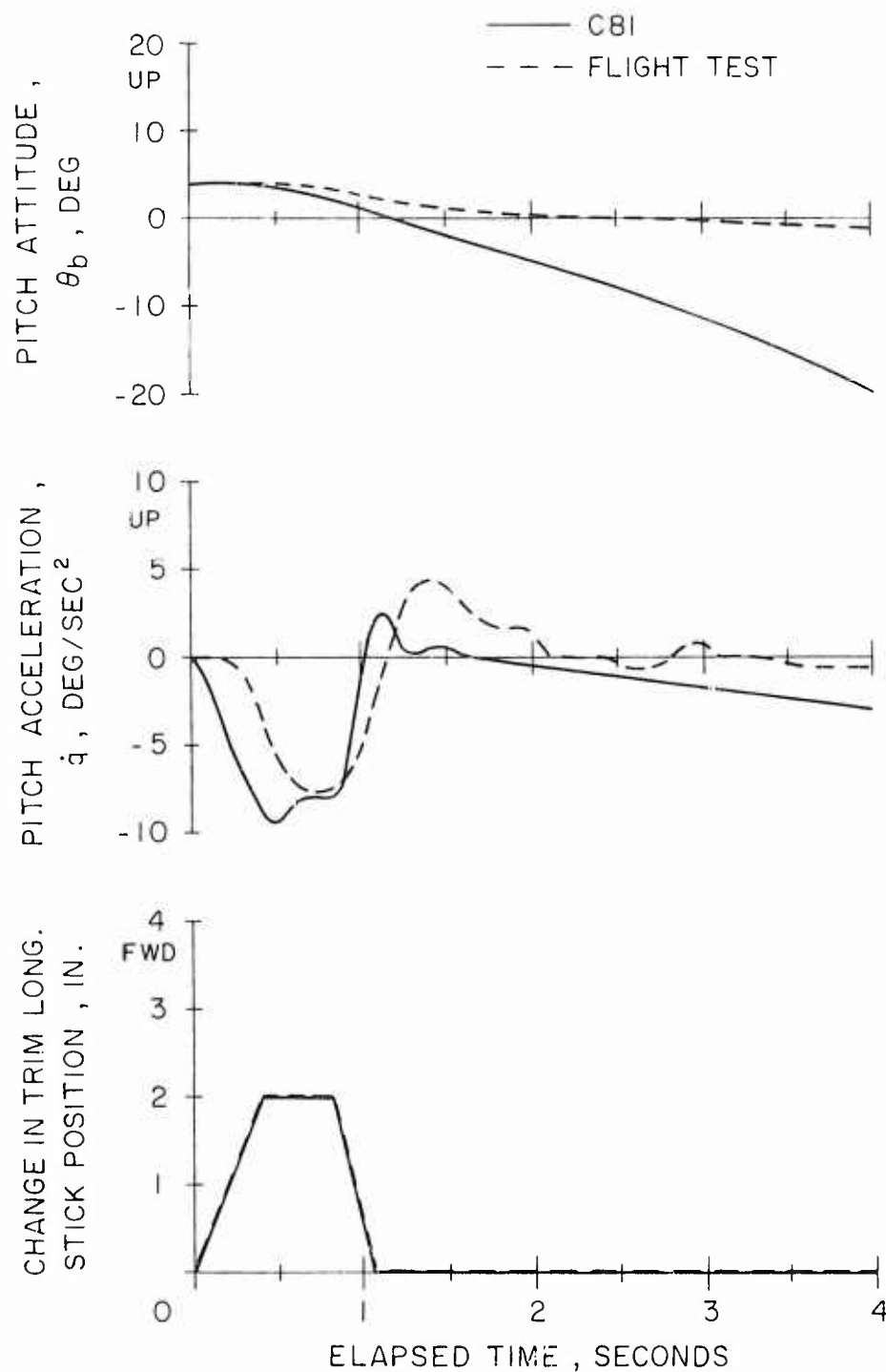


Figure 27. C81 Maneuver Response Time History Comparison With Flight Test Data for the CH-53A at 100 Kt, Following a Forward Stick Pulse Input (33,539 Lb, FSCG = 347.7).

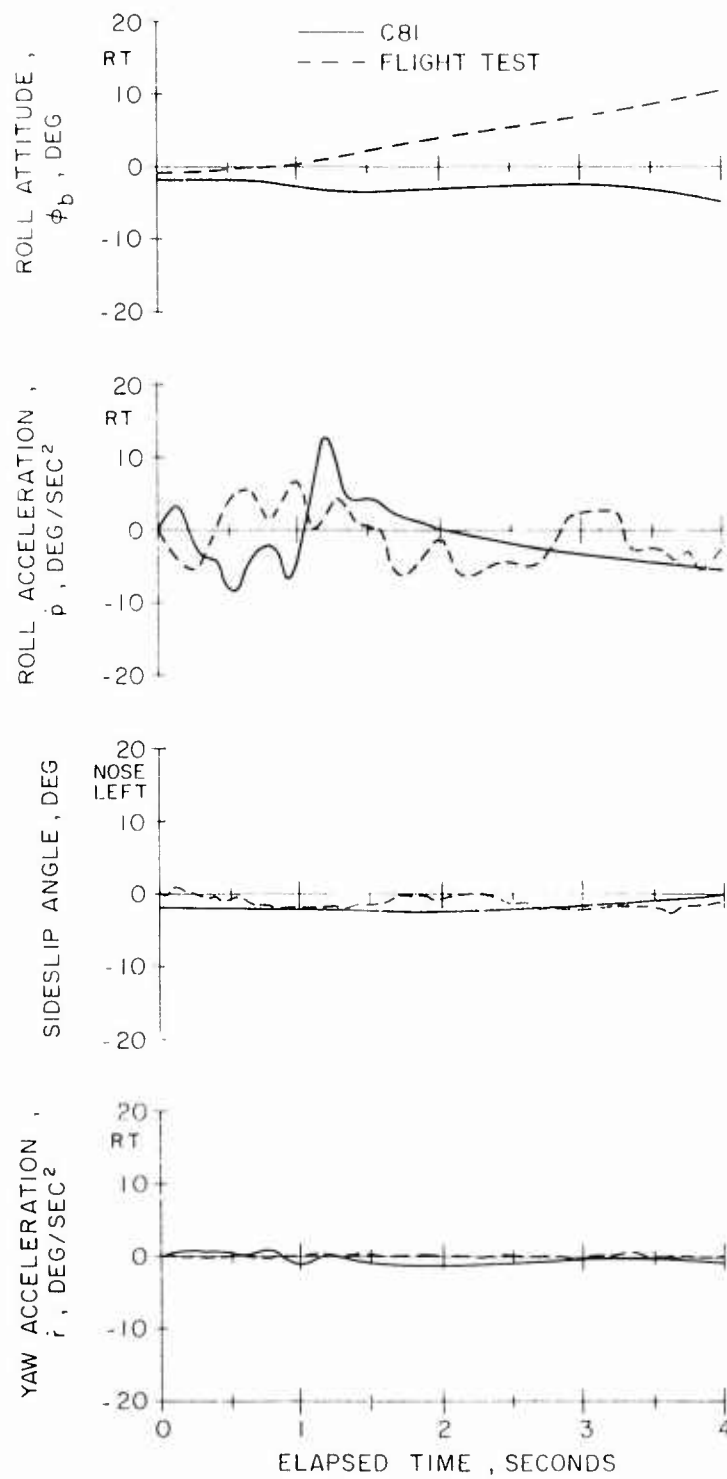


Figure 27. Continued.

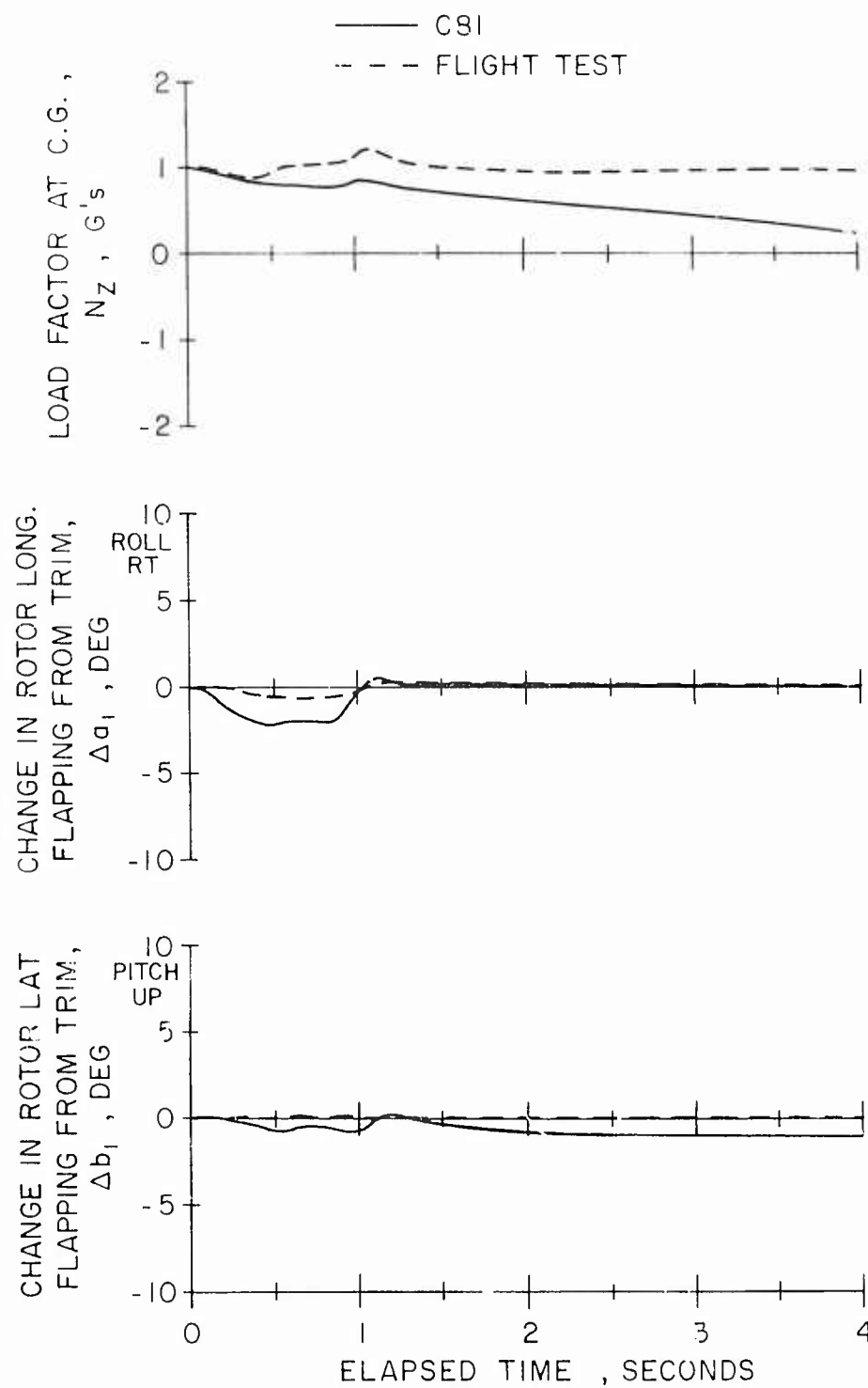


Figure 27. Concluded.

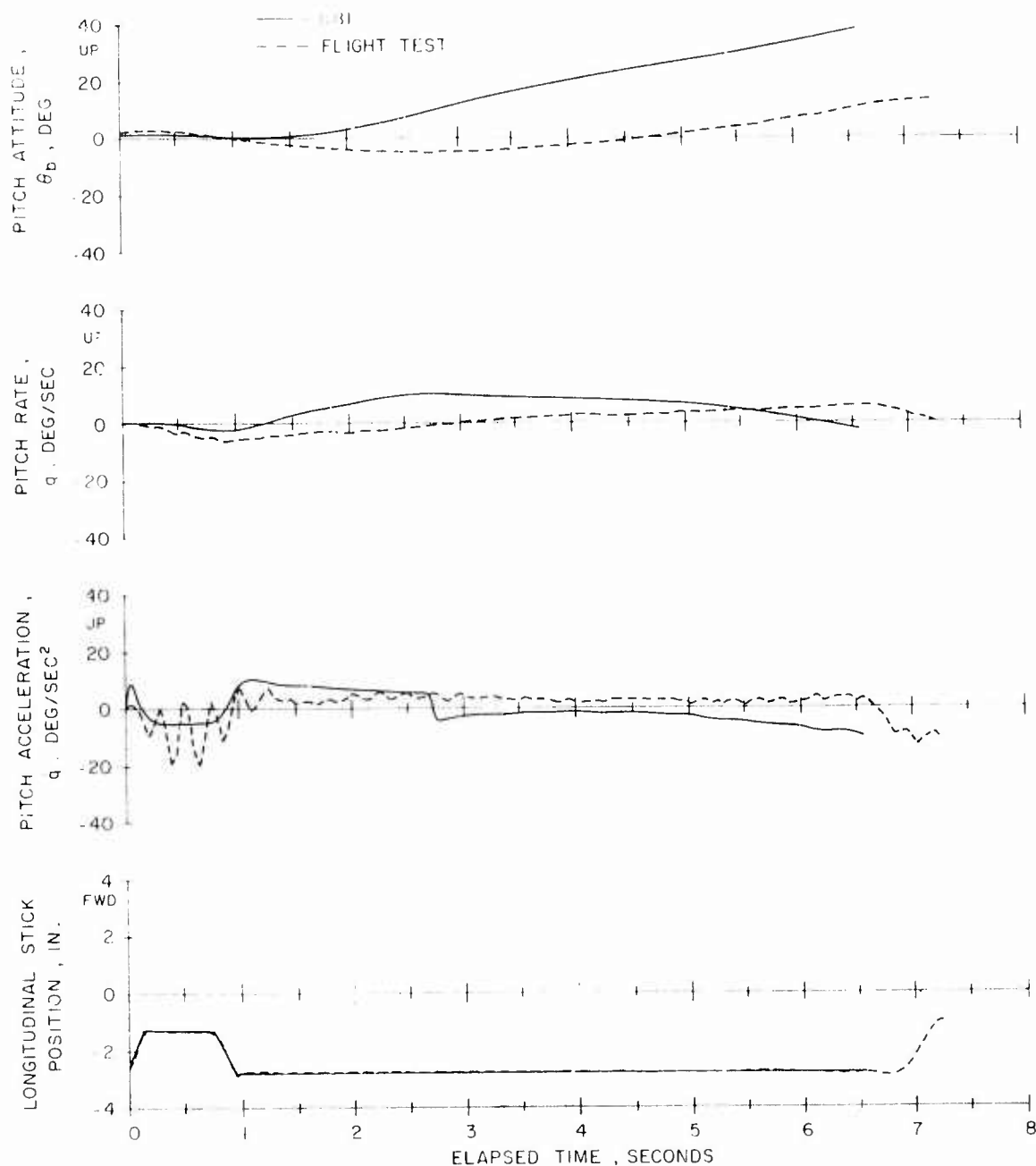


Figure 28. C81 Maneuver Response Time History Comparison With Flight Test Data for the HH-53C in Hover, Following a Forward Stick Pulse Input (31,000 Lb, FSCG = 328).

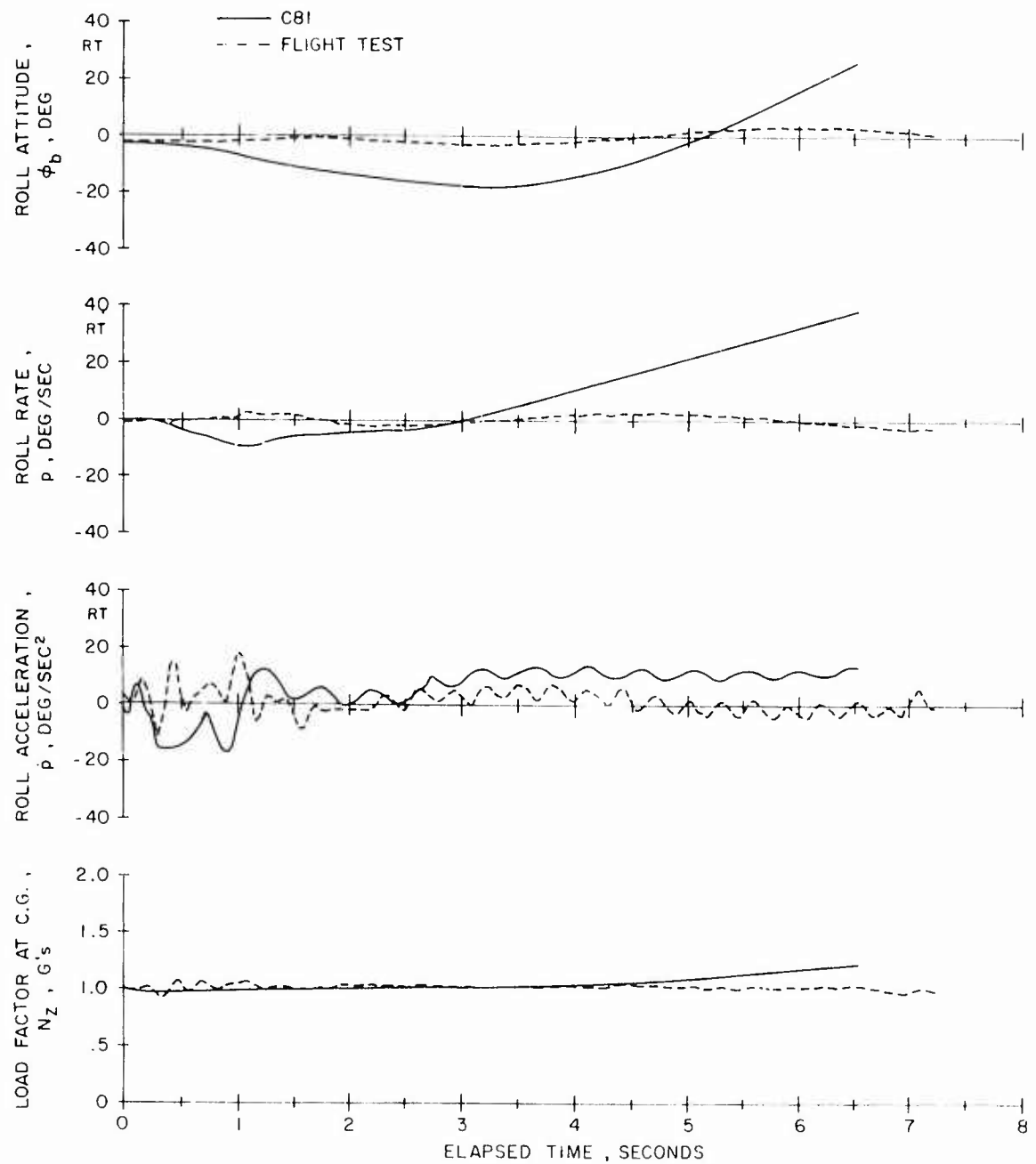


Figure 28. Continued.

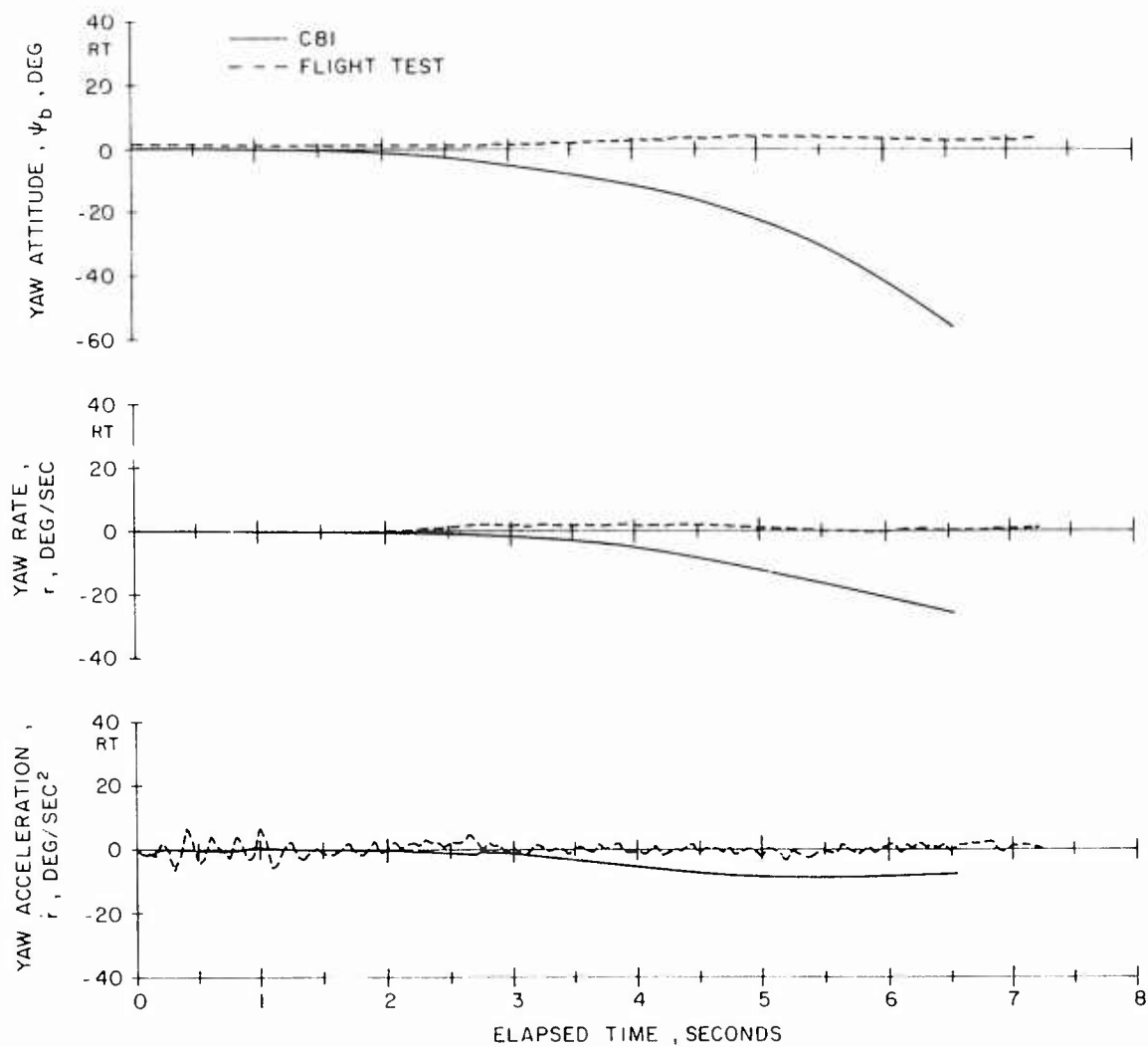


Figure 28. Concluded.

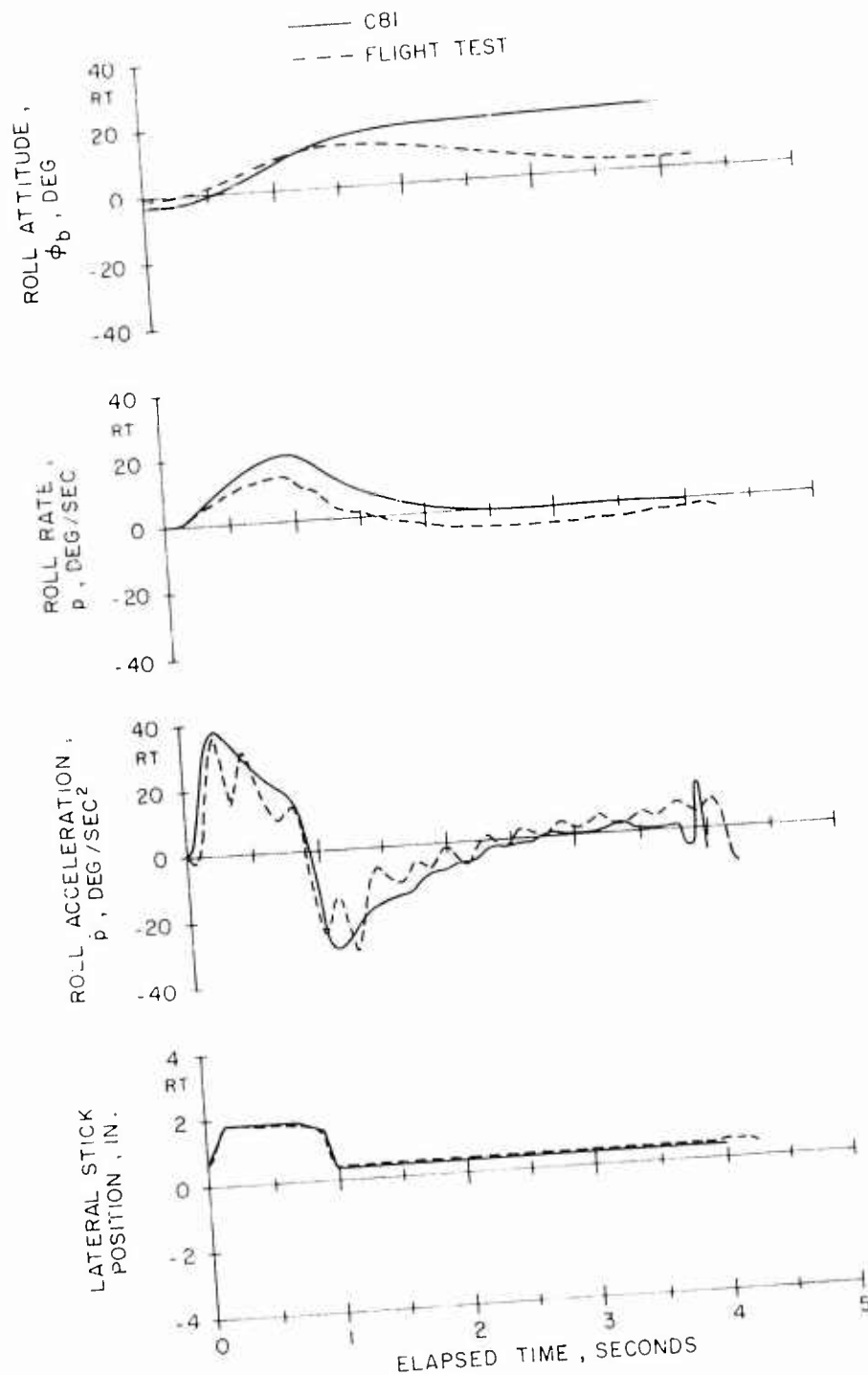


Figure 29. C81 Maneuver Response Time History Comparison With Flight Test Data for the HH-53C in Hover, Following a Right Lateral Stick Pulse Input (31,000 Lb, FSCG = 129).

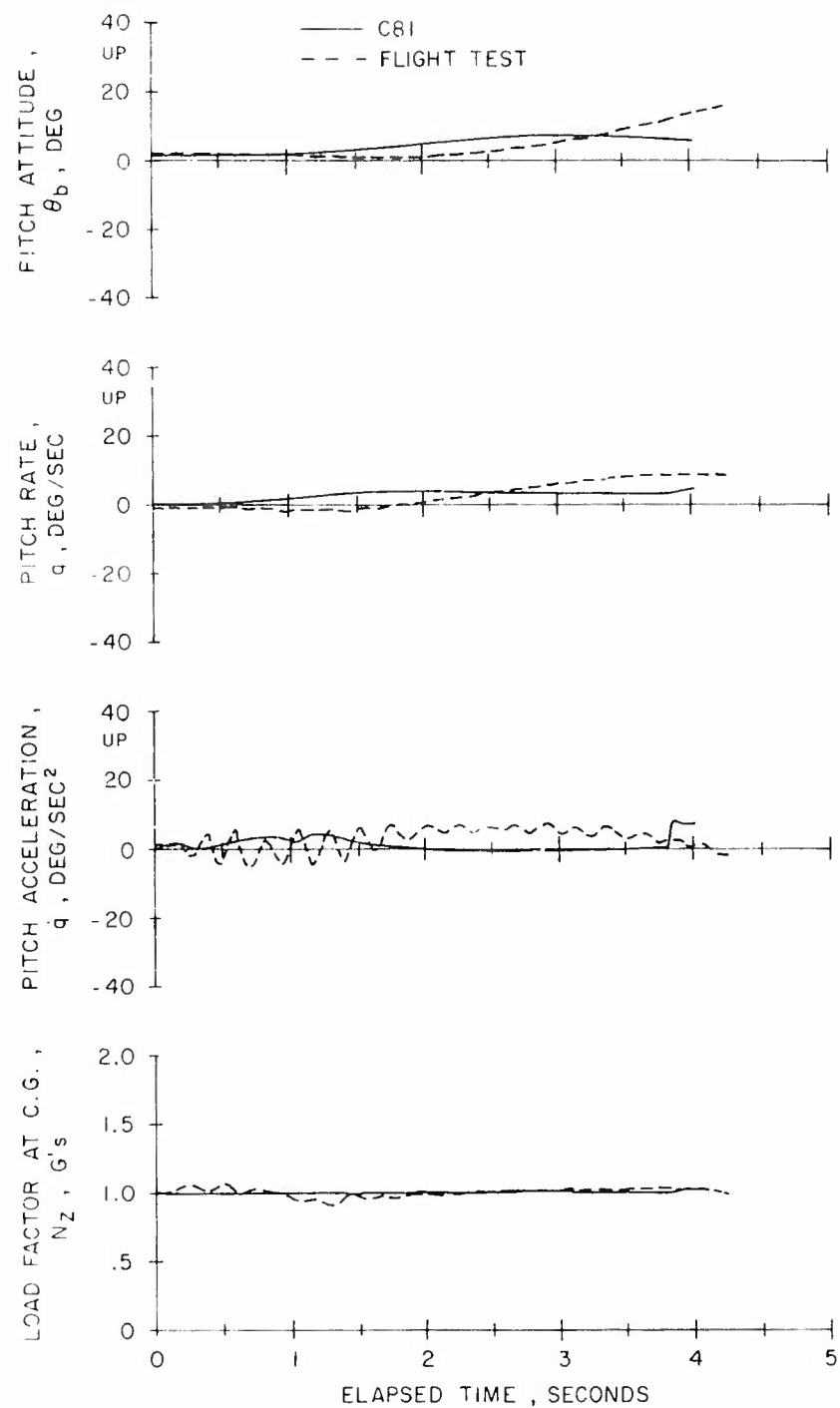


Figure 29. Continued.

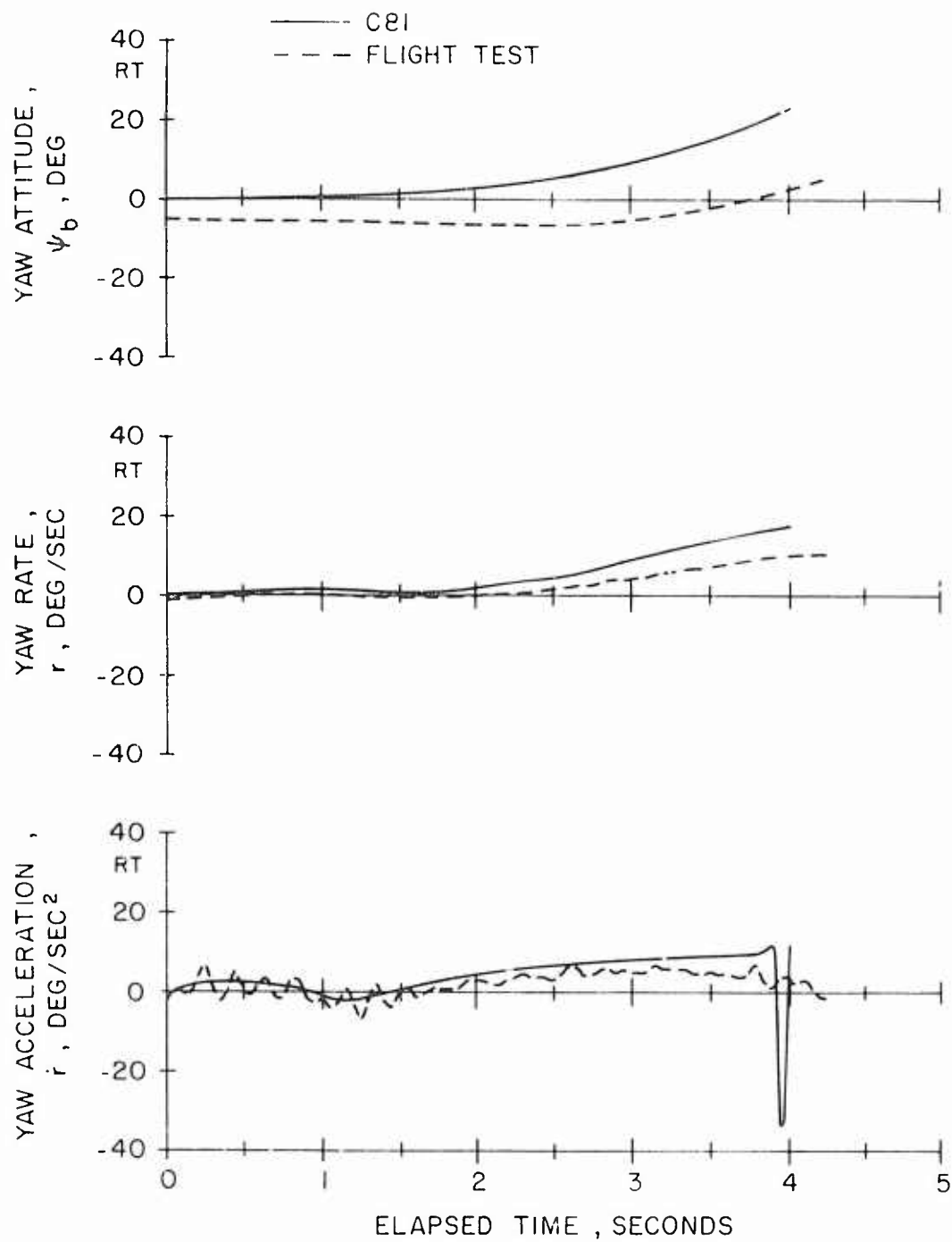


Figure 29. Concluded.

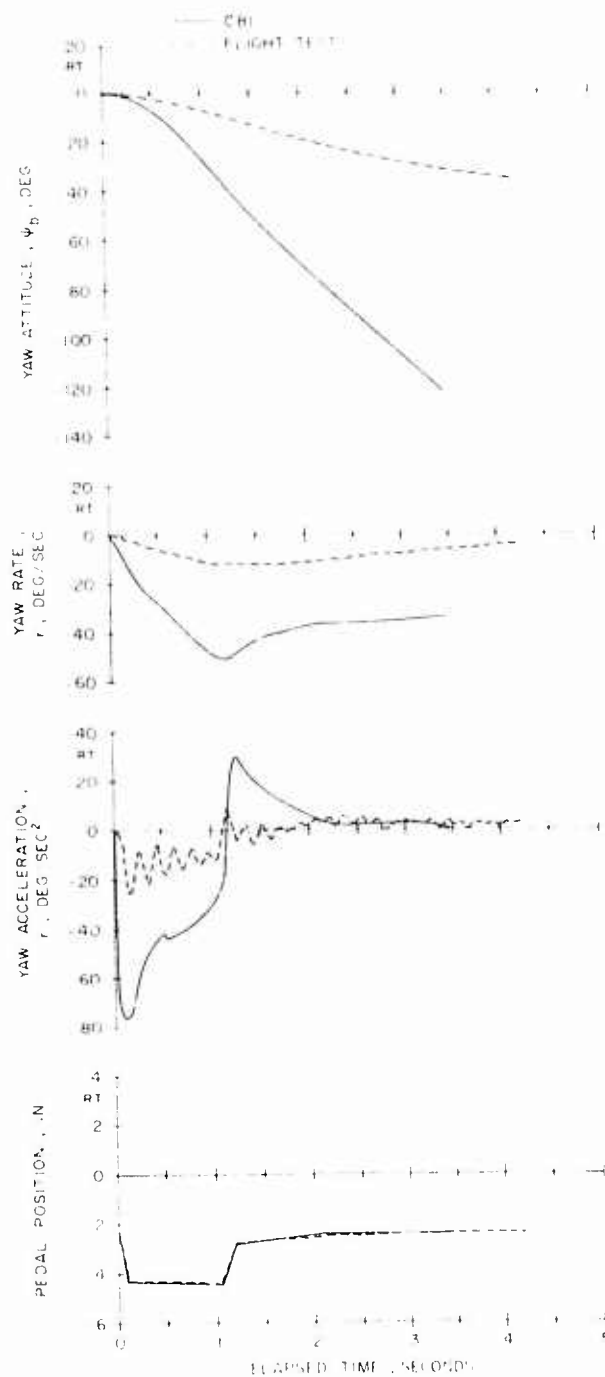


Figure 30. C81 Maneuver Response Time History Comparison With Flight Test Data for the HH-53C in Hover, Following a Left Pedal Pulse Input (31,000 Lb, FSCG = 328).

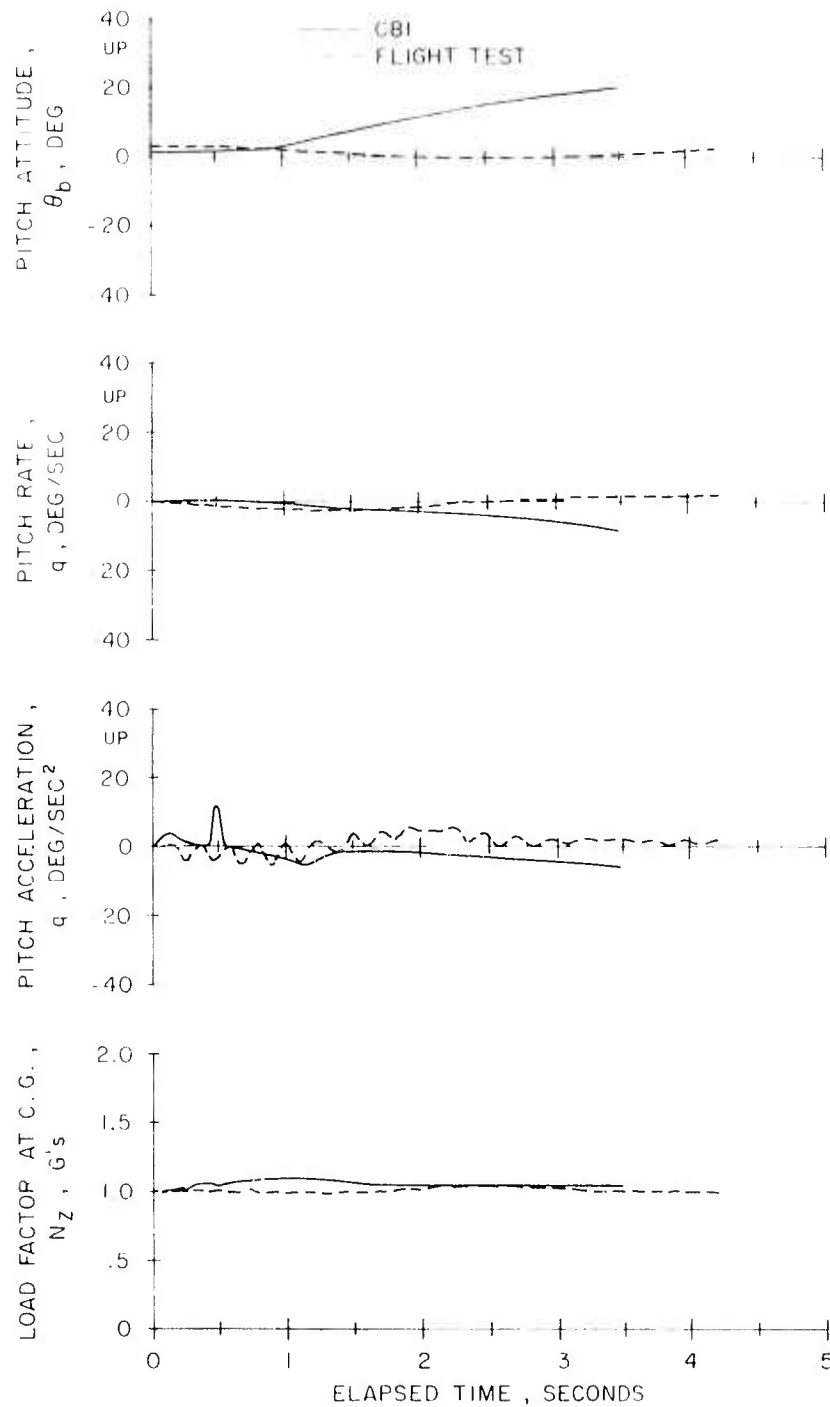


Figure 30. Continued.

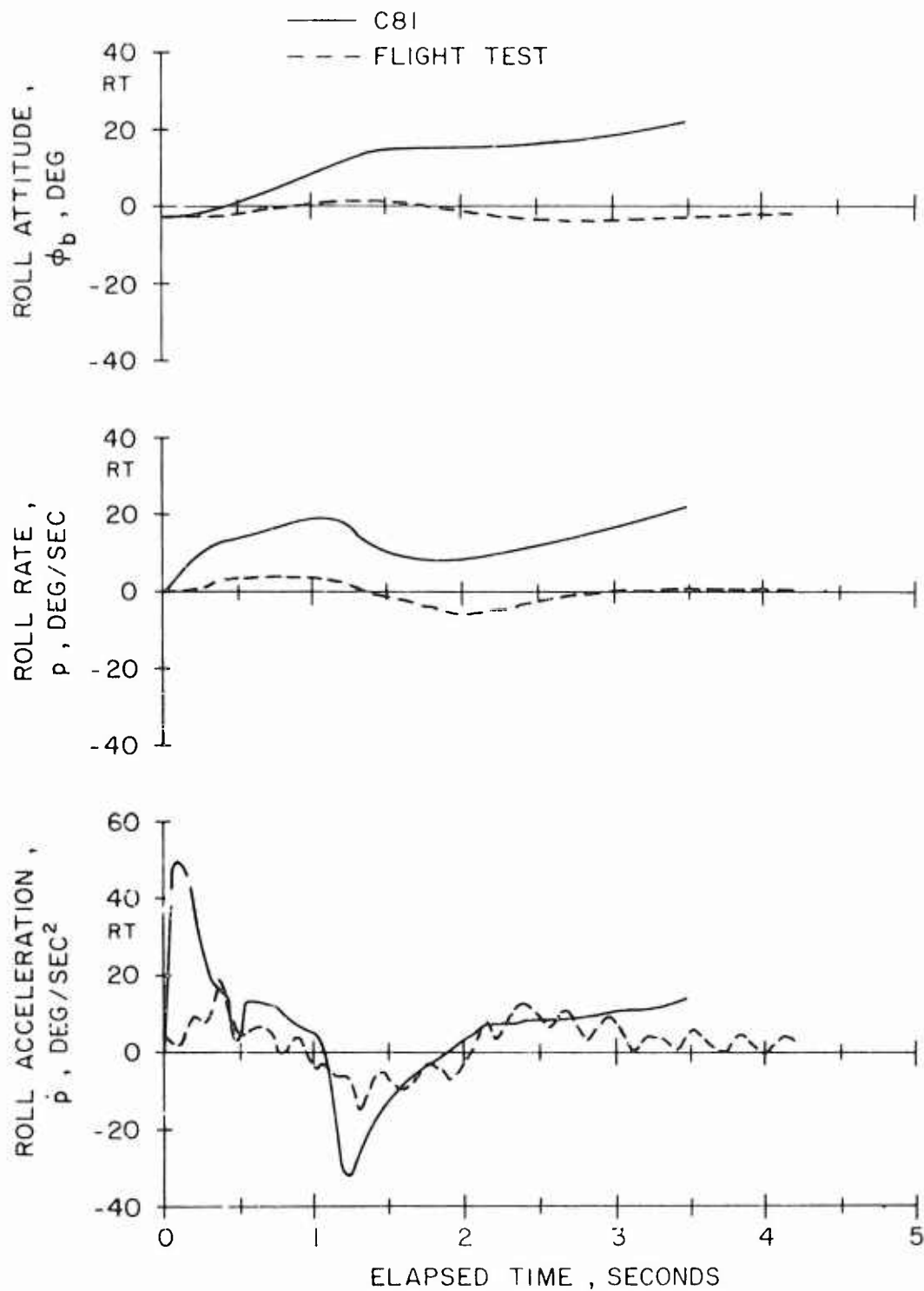


Figure 30. Concluded.

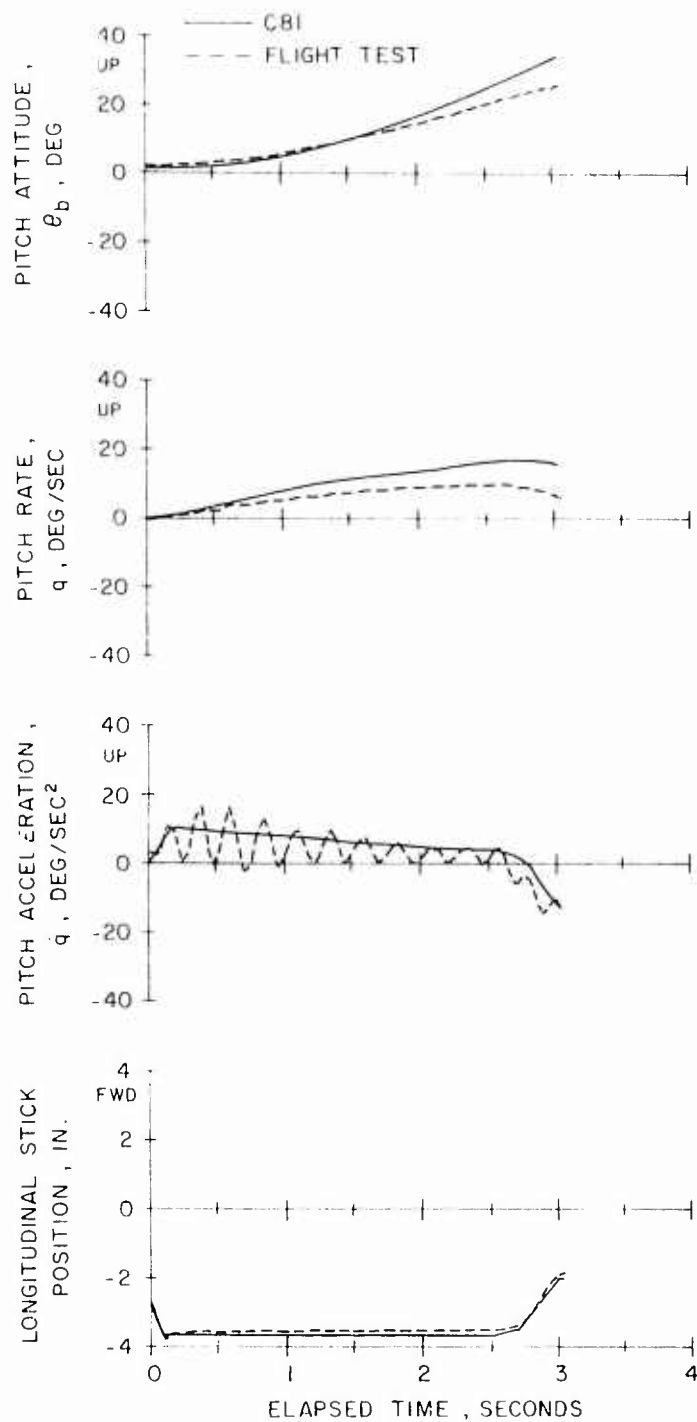


Figure 31. C81 Maneuver Response Time History Comparison With Flight Test Data for the HH-53C in Hover, Following an Aft Stick Step Input (31,000 Lb, FSCG = 328).

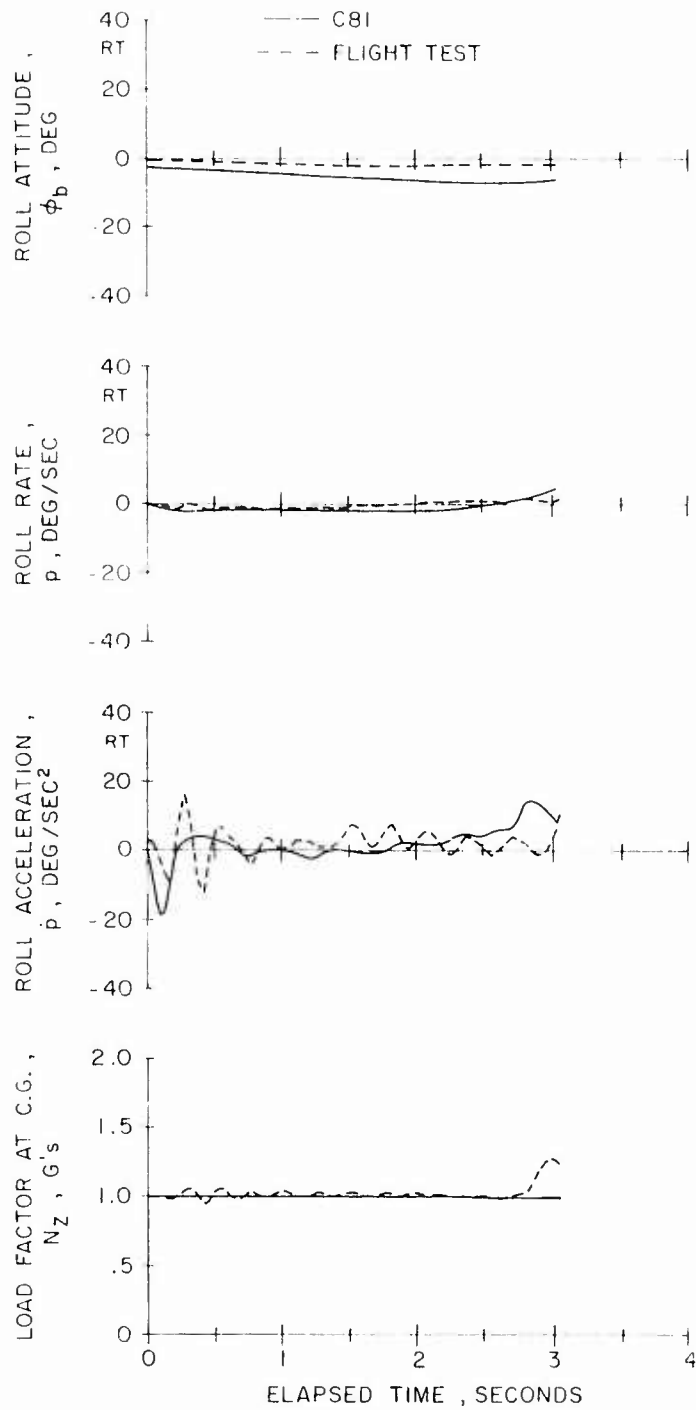


Figure 31. Continued.

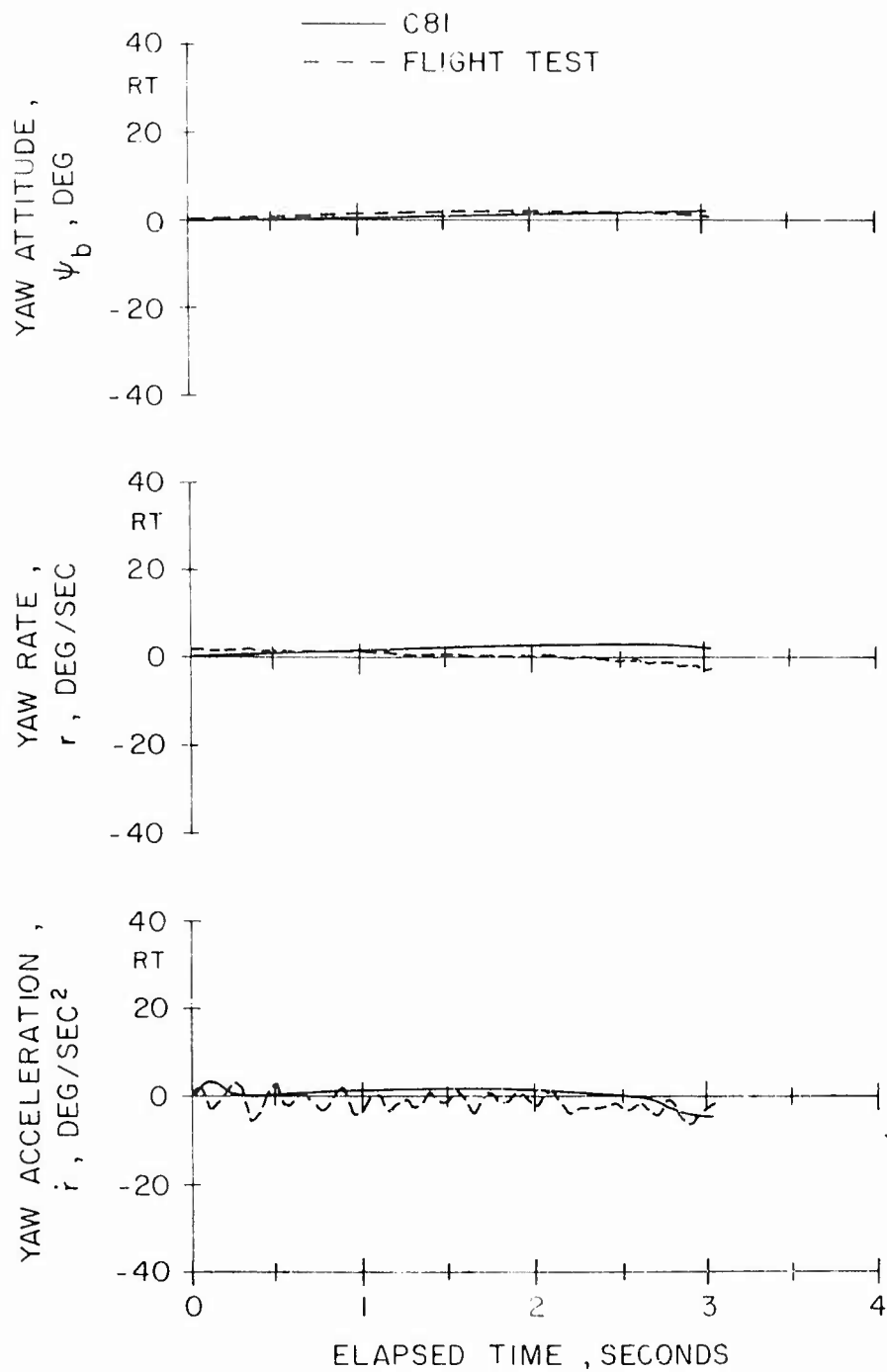


Figure 31. Concluded.

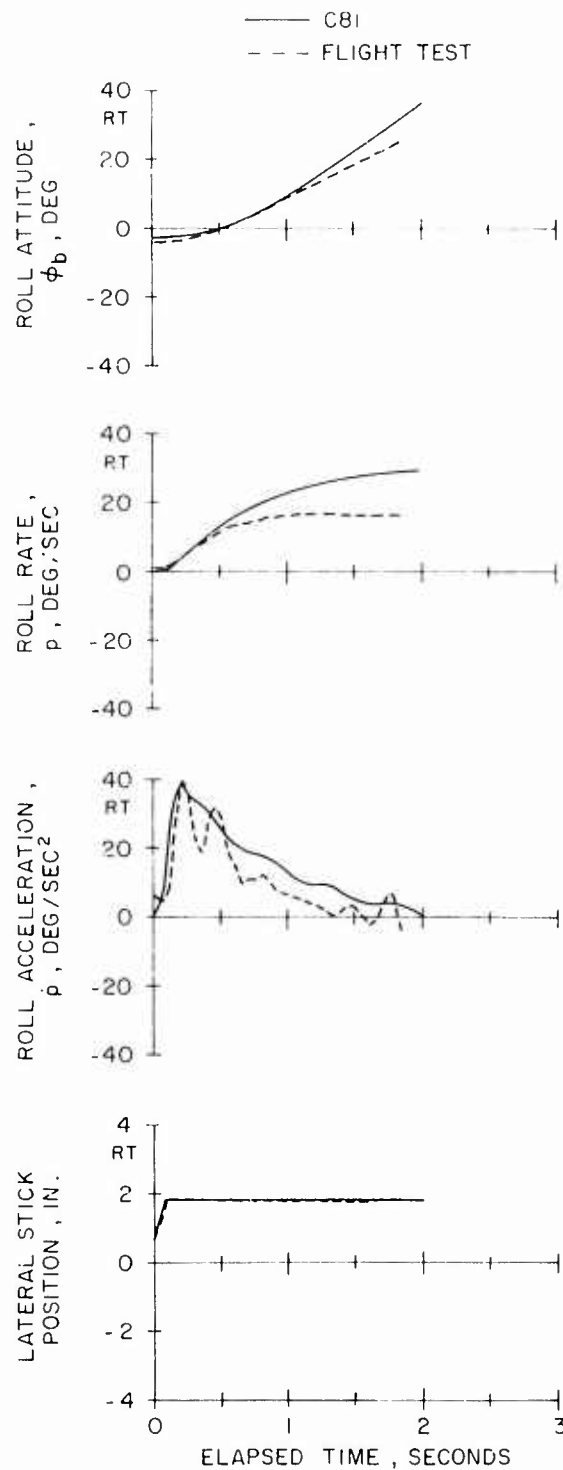


Figure 32. C81 Manuever Response Time History Comparison With Flight Test Data for the HH-53C in Hover, Following a Right Lateral Stick Step Input (31,000 Lb, FSCG = 328).

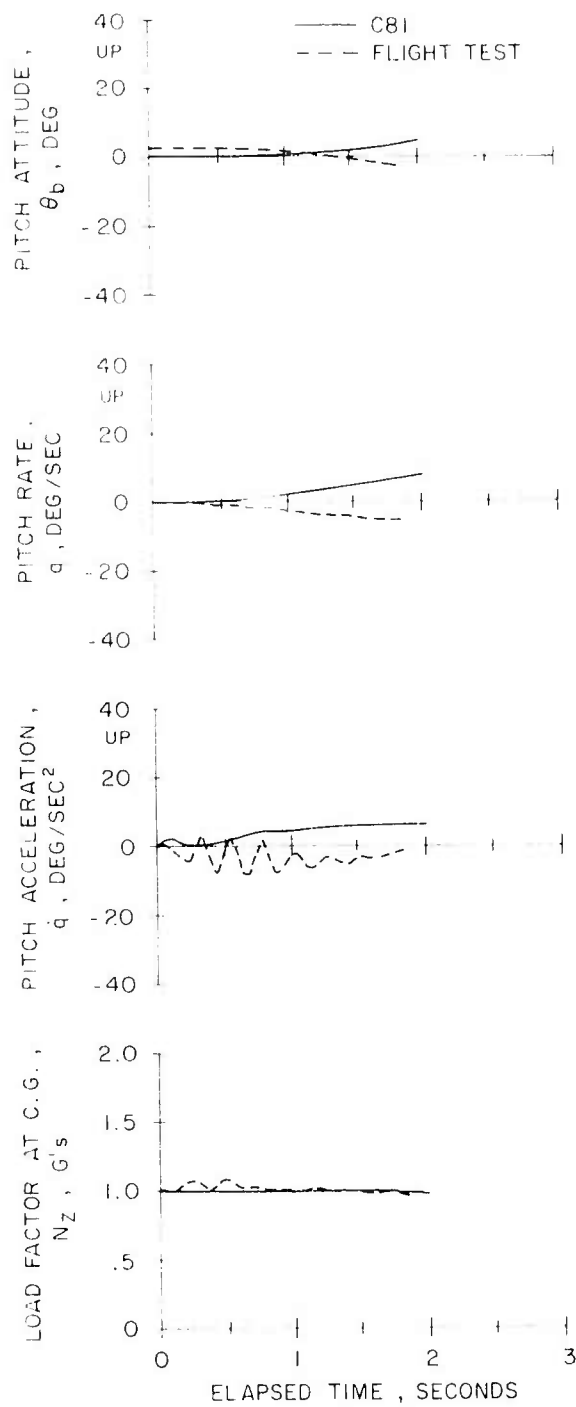


Figure 32. Continued.

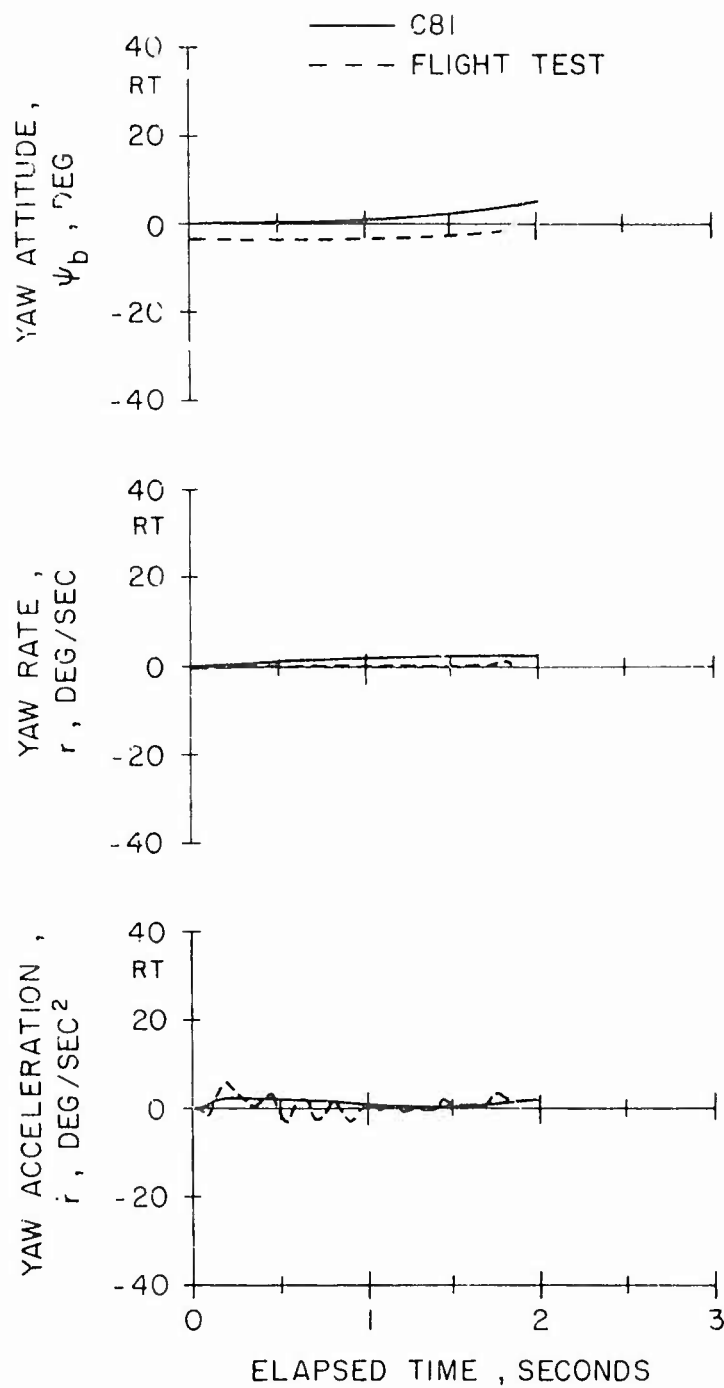


Figure 32. Concluded.

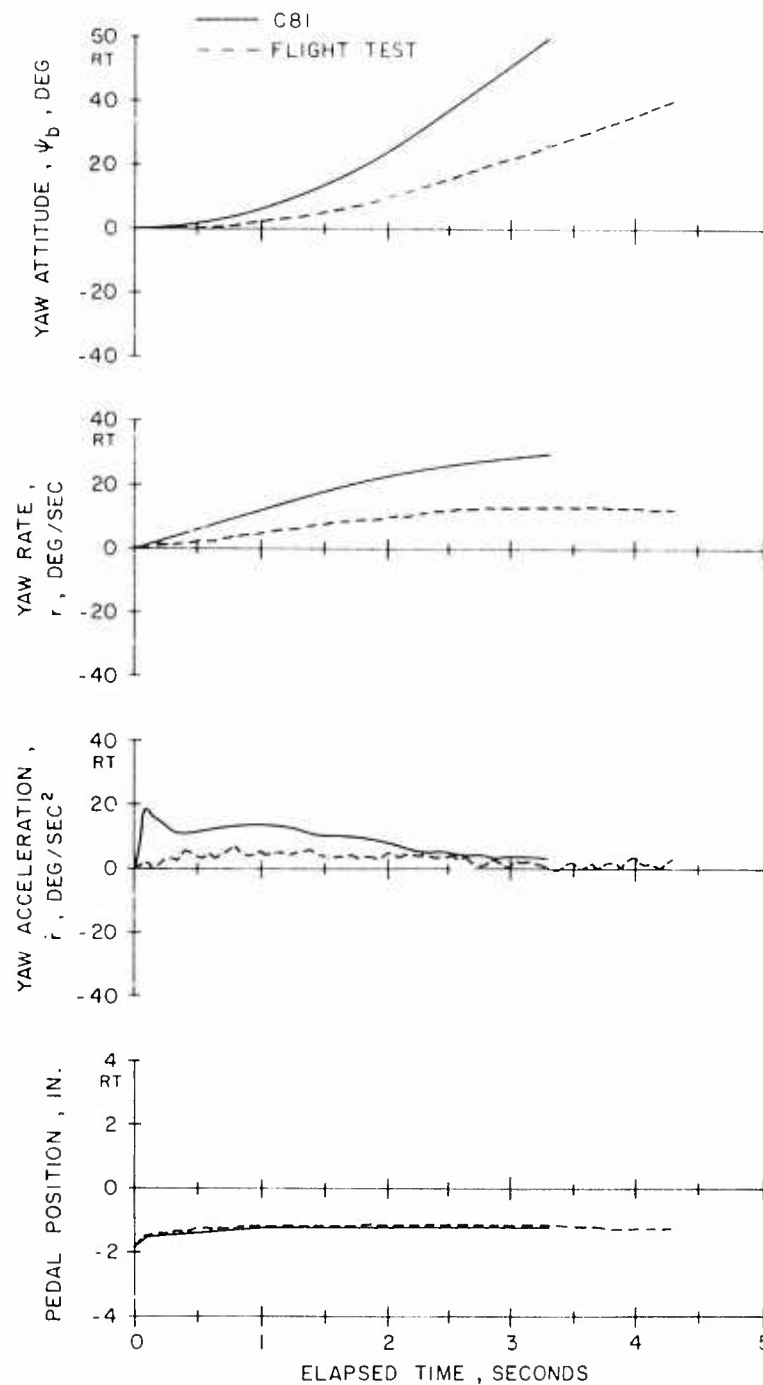


Figure 33. C81 Maneuver Response Time History Comparison With Flight Test Data for the KH-53C in Hover, Following a Right Pedal Step Input (31,000 Lb, FSCG = 328).

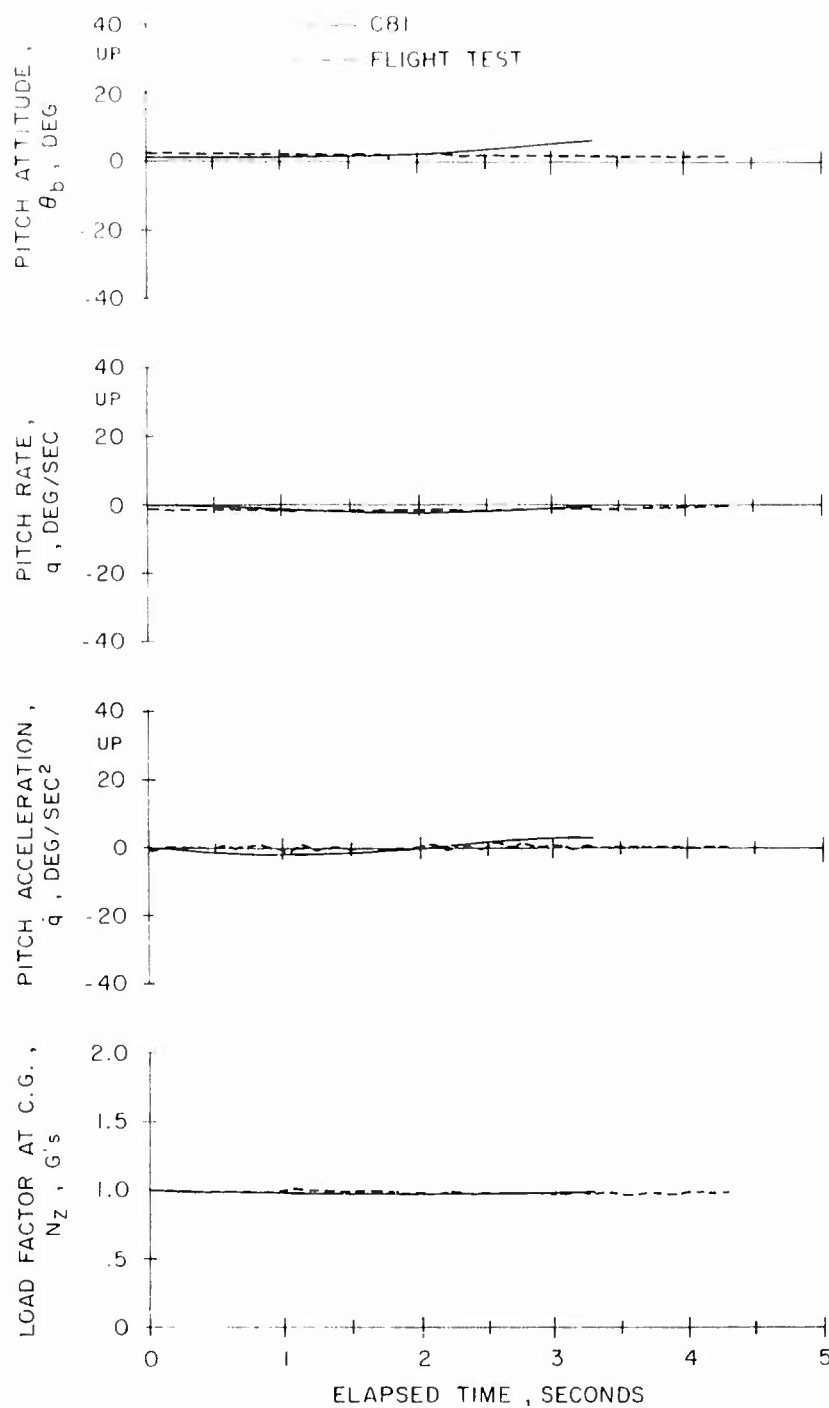


Figure 33. Continued.

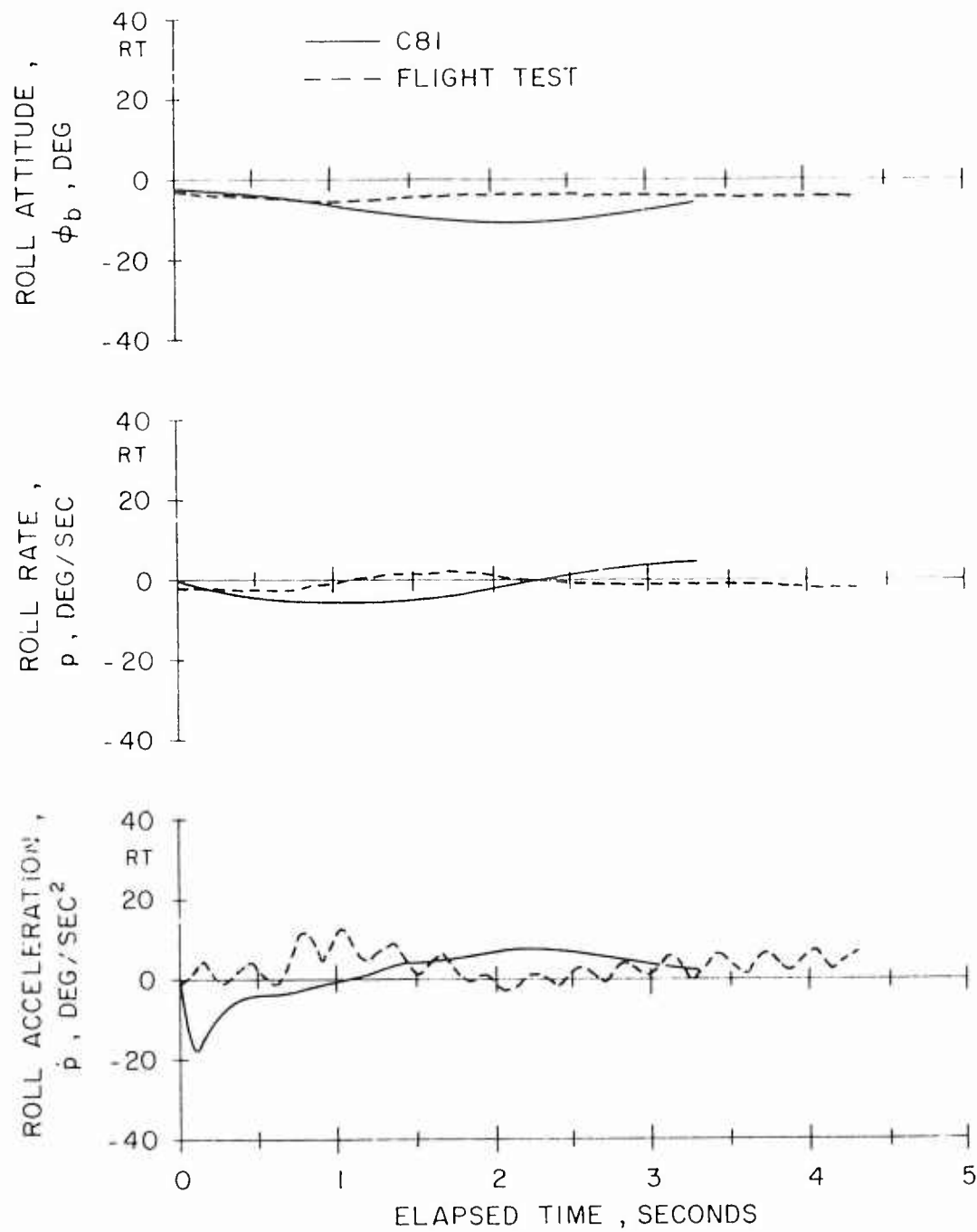


Figure 33. Concluded.

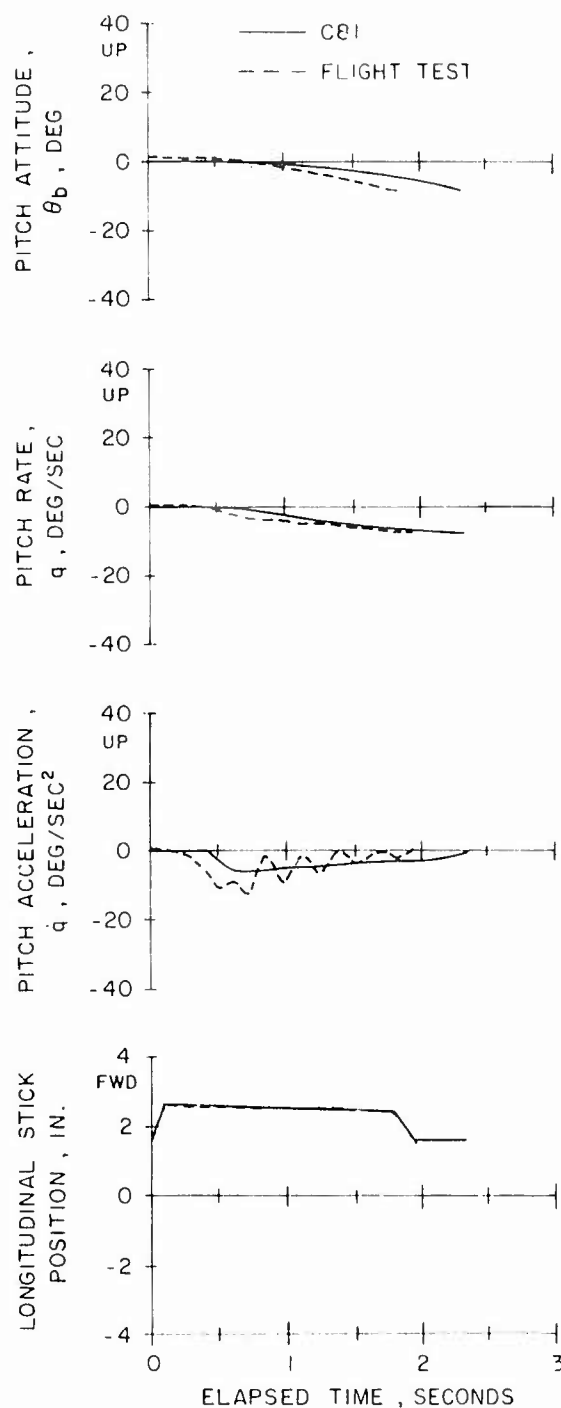


Figure 34. C81 Maneuver Response Time History Comparison With Flight Test Data for the HH-53C at 113 Kt, Following a Forward Stick Step Input (41,000 Lb, FSCG = 328).

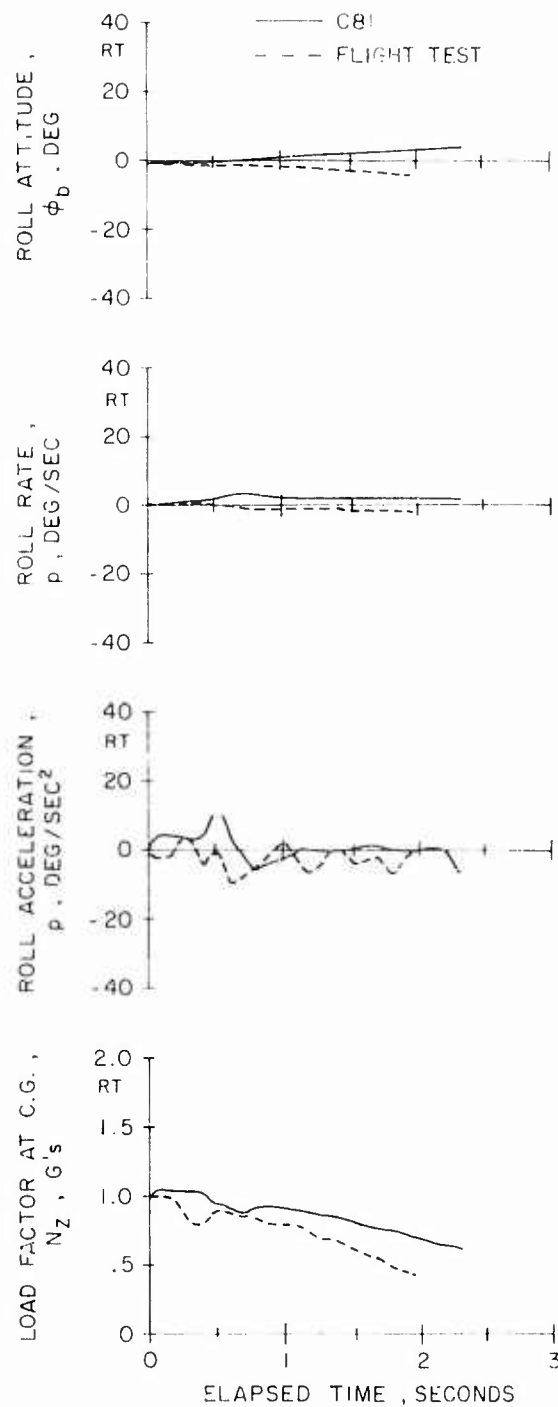


Figure 34. Continued.

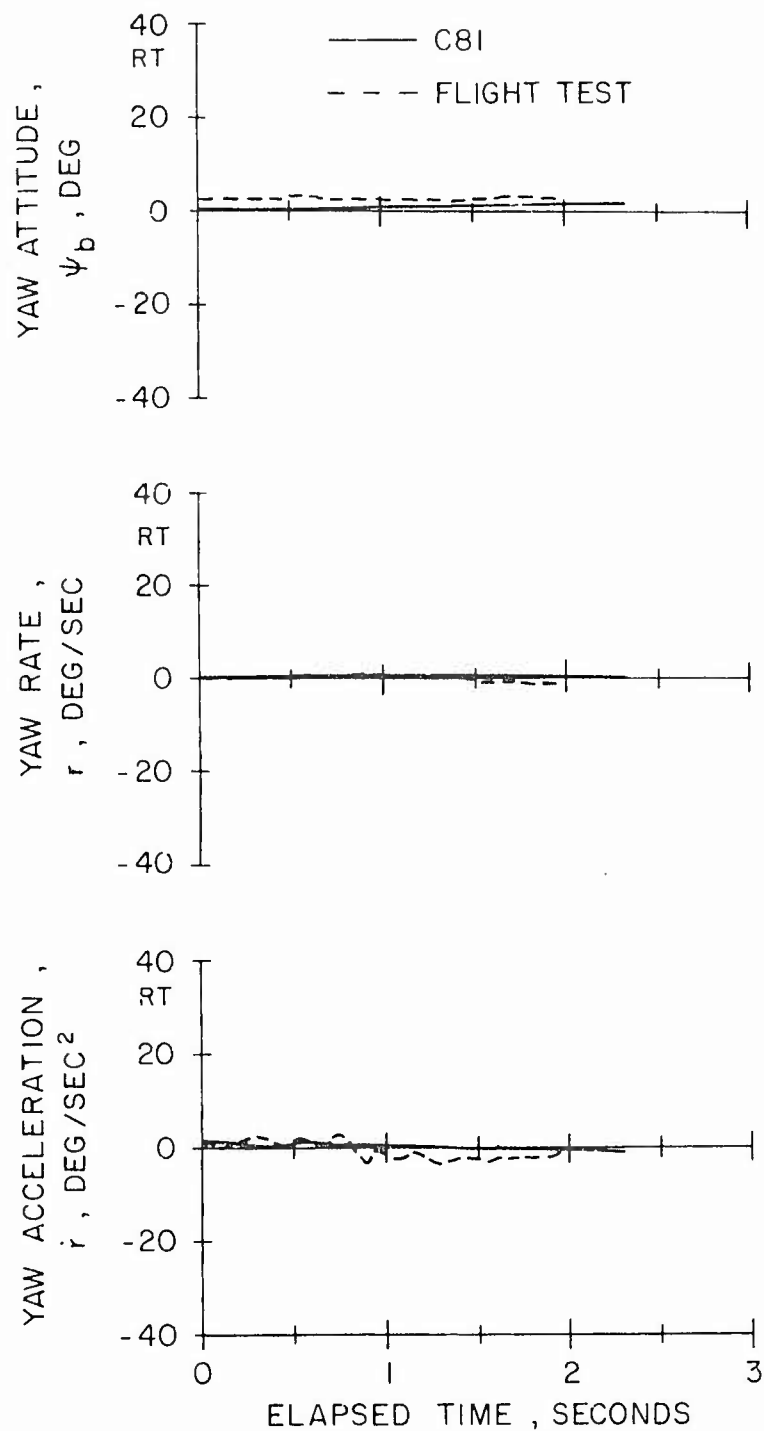


Figure 34. Concluded.

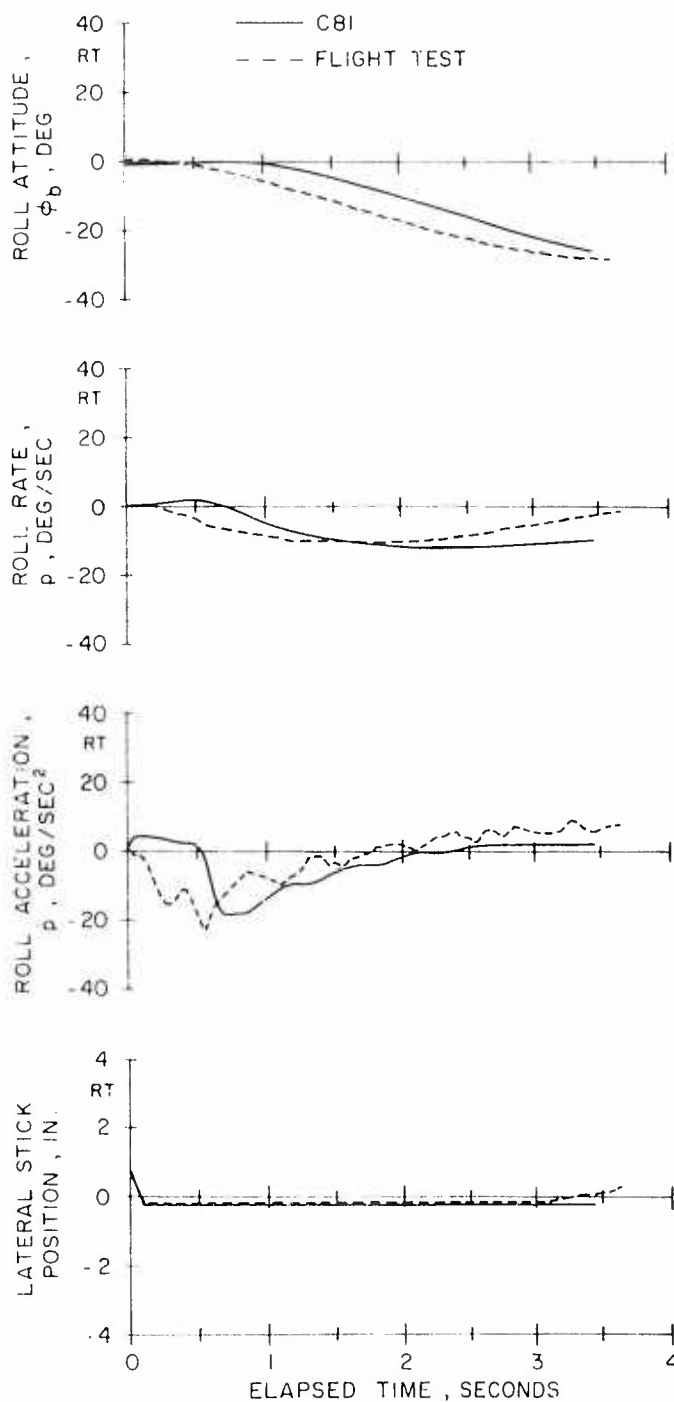


Figure 35. C81 Maneuver Response Time History Comparison With Flight Test Data for the HH-53C at 113 Kt, Following a Left Lateral Stick Step Input (41,000 Lb, FSCG = 328).

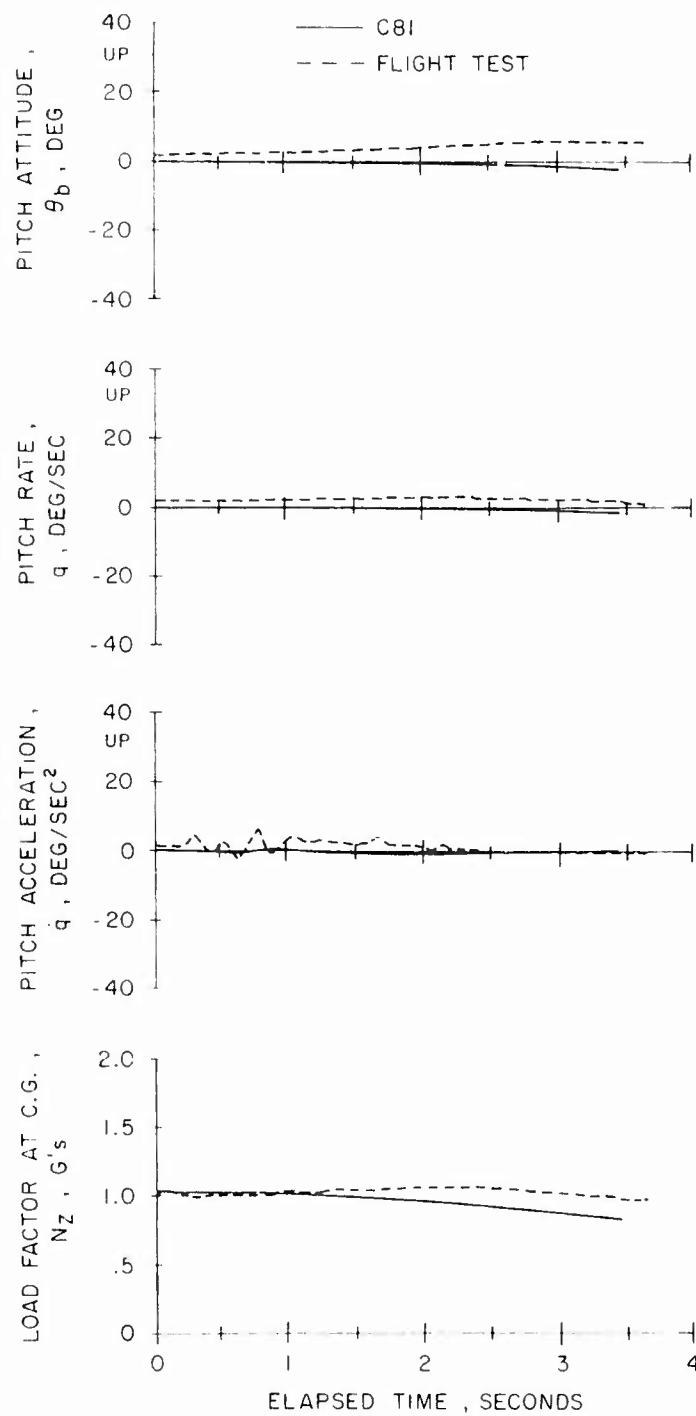


Figure 35. Continued.

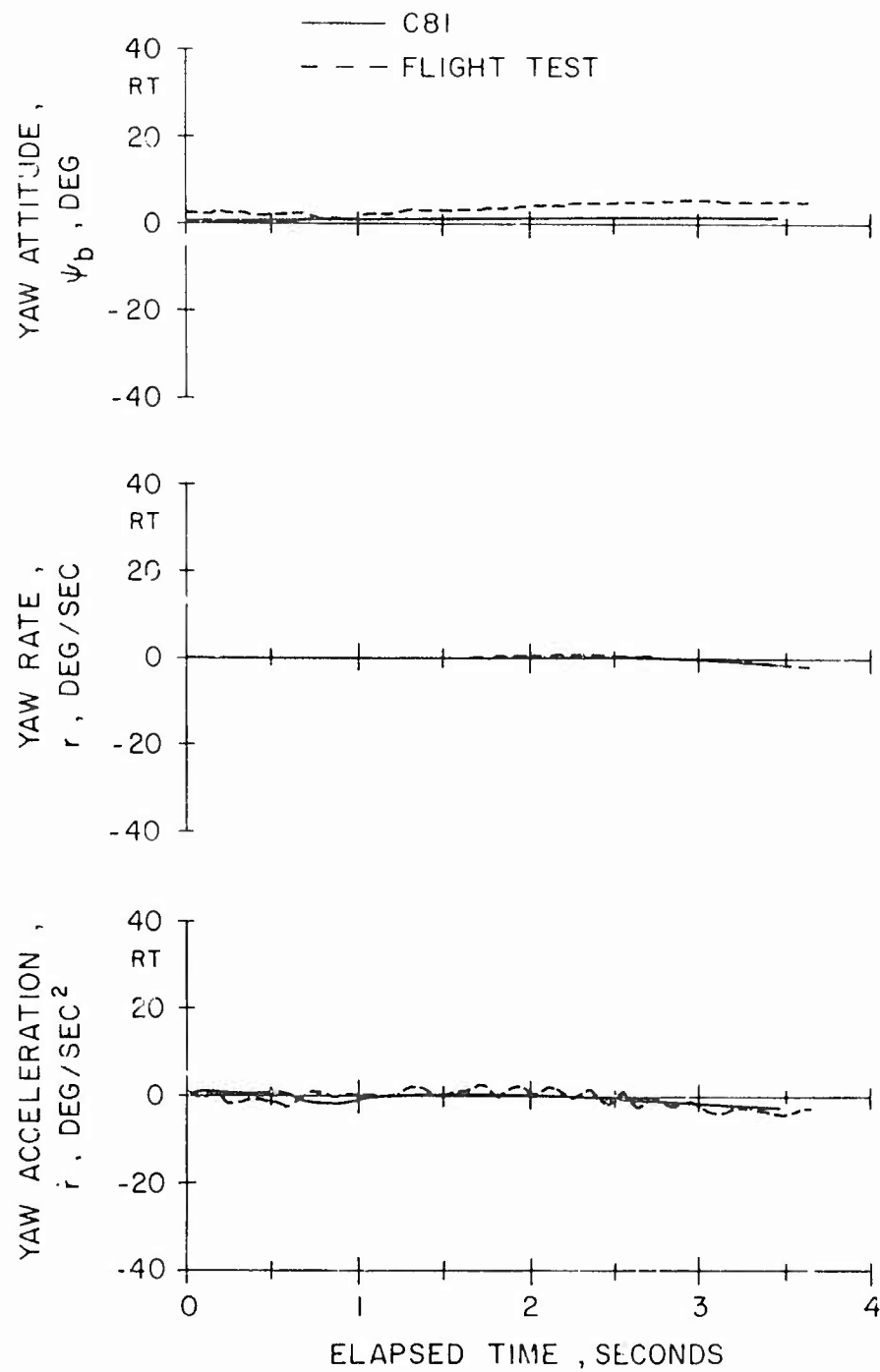


Figure 35. Concluded.

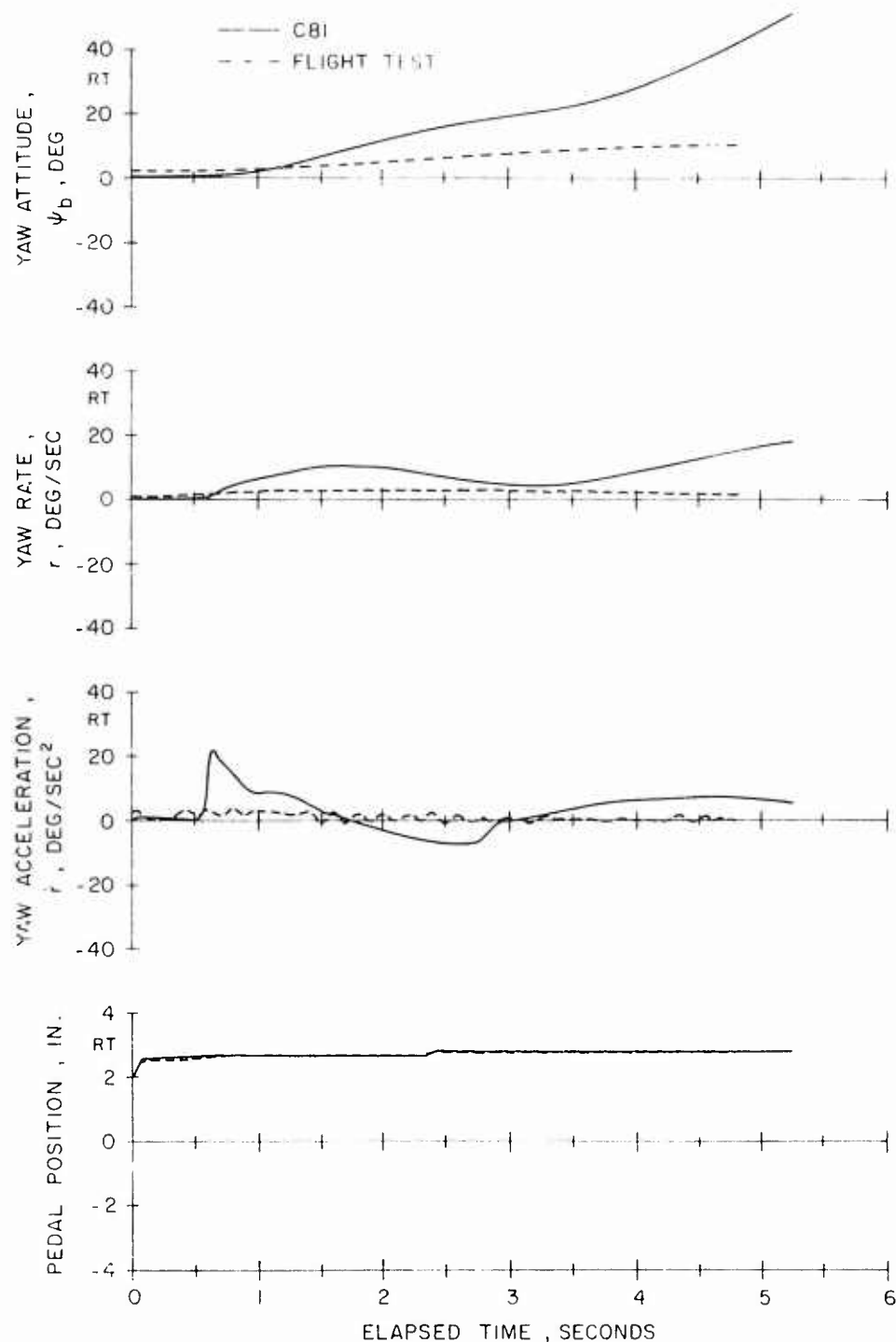


Figure 36. C81 Maneuver Response Time History Comparison With Flight Test Data for the HH-53C at 113 Kt, Following a Right Pedal Step Input (41,000 Lb, FSCG = 328).

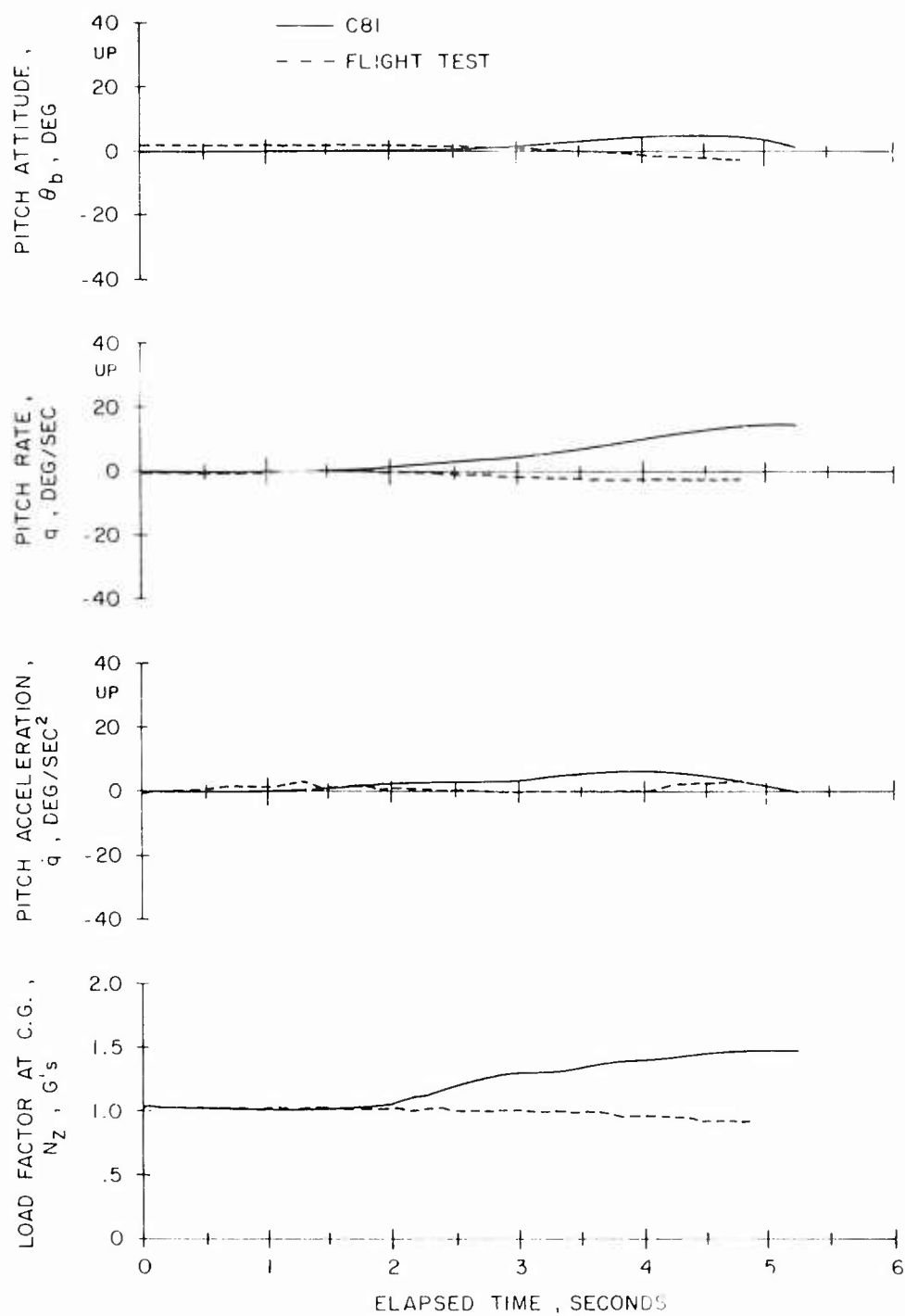


Figure 36. Continued.

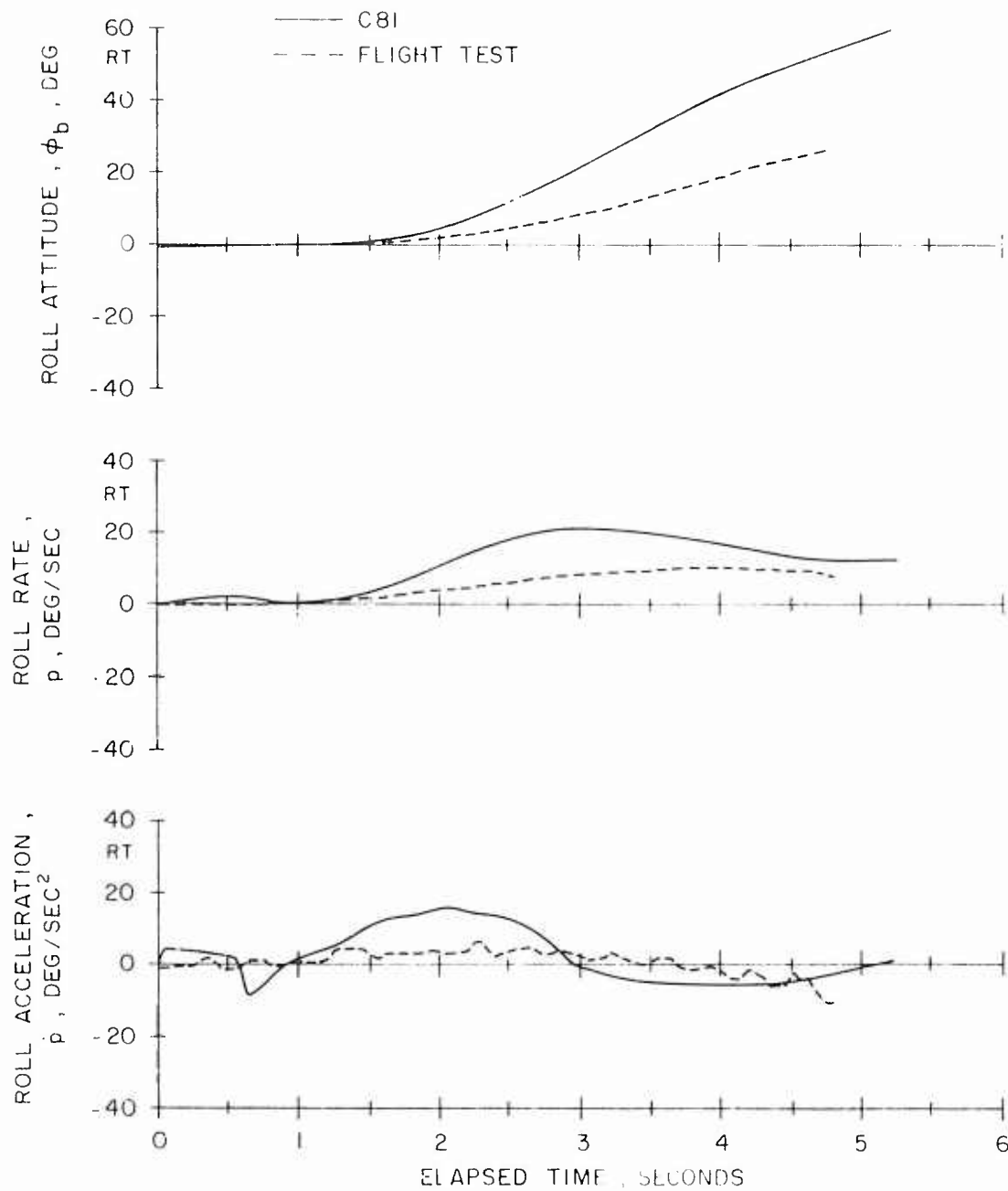


Figure 36. Concluded.

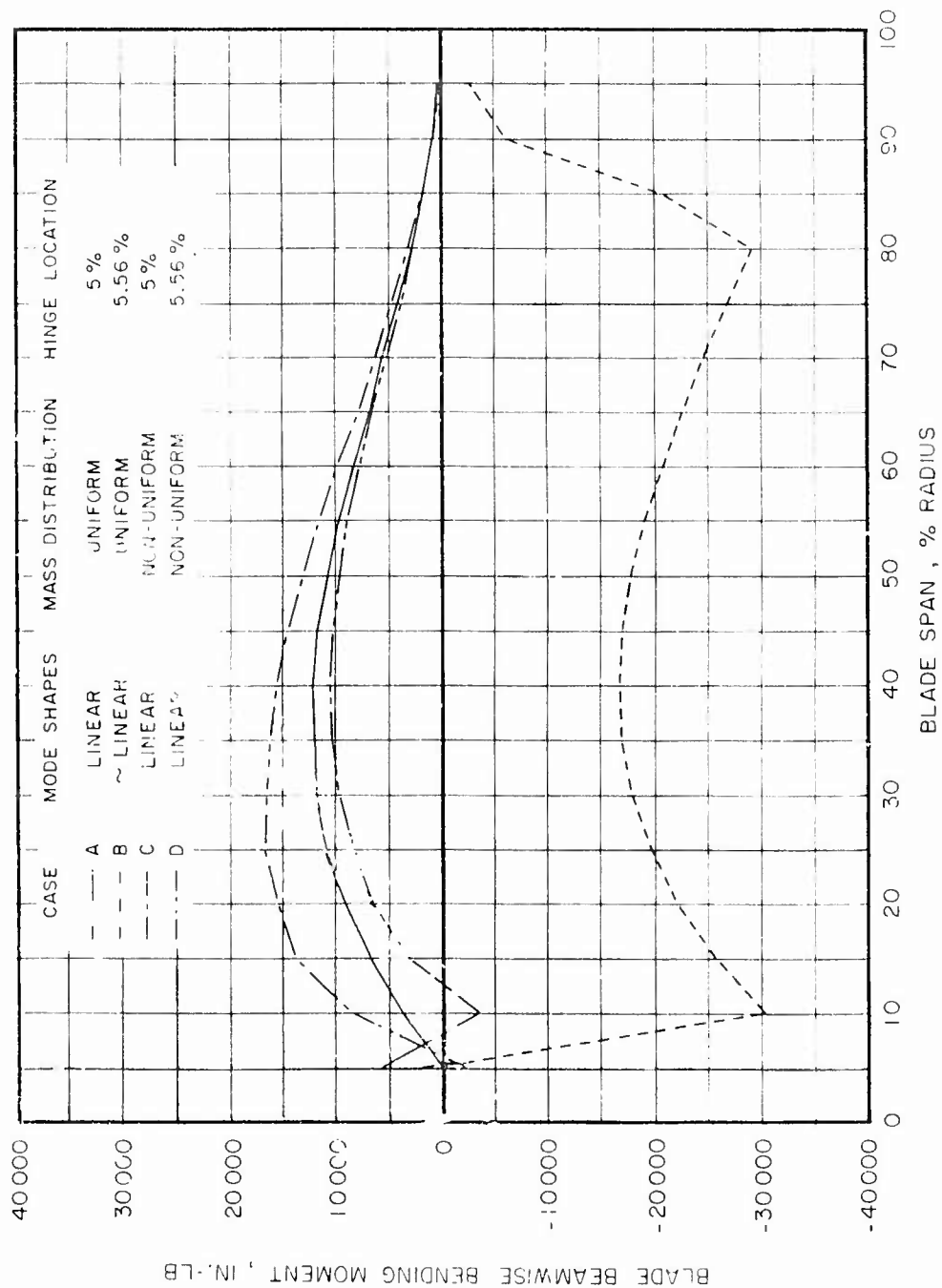


Figure 37. C81 Solutions of Blade Beamwise Bending Moment vs Span at $\psi_{MR} = 60$ Deg as Functions of Mode Shape, Hinge Offset, and Mass Distribution for the CH-53A in Hover at 32,550 Lb.

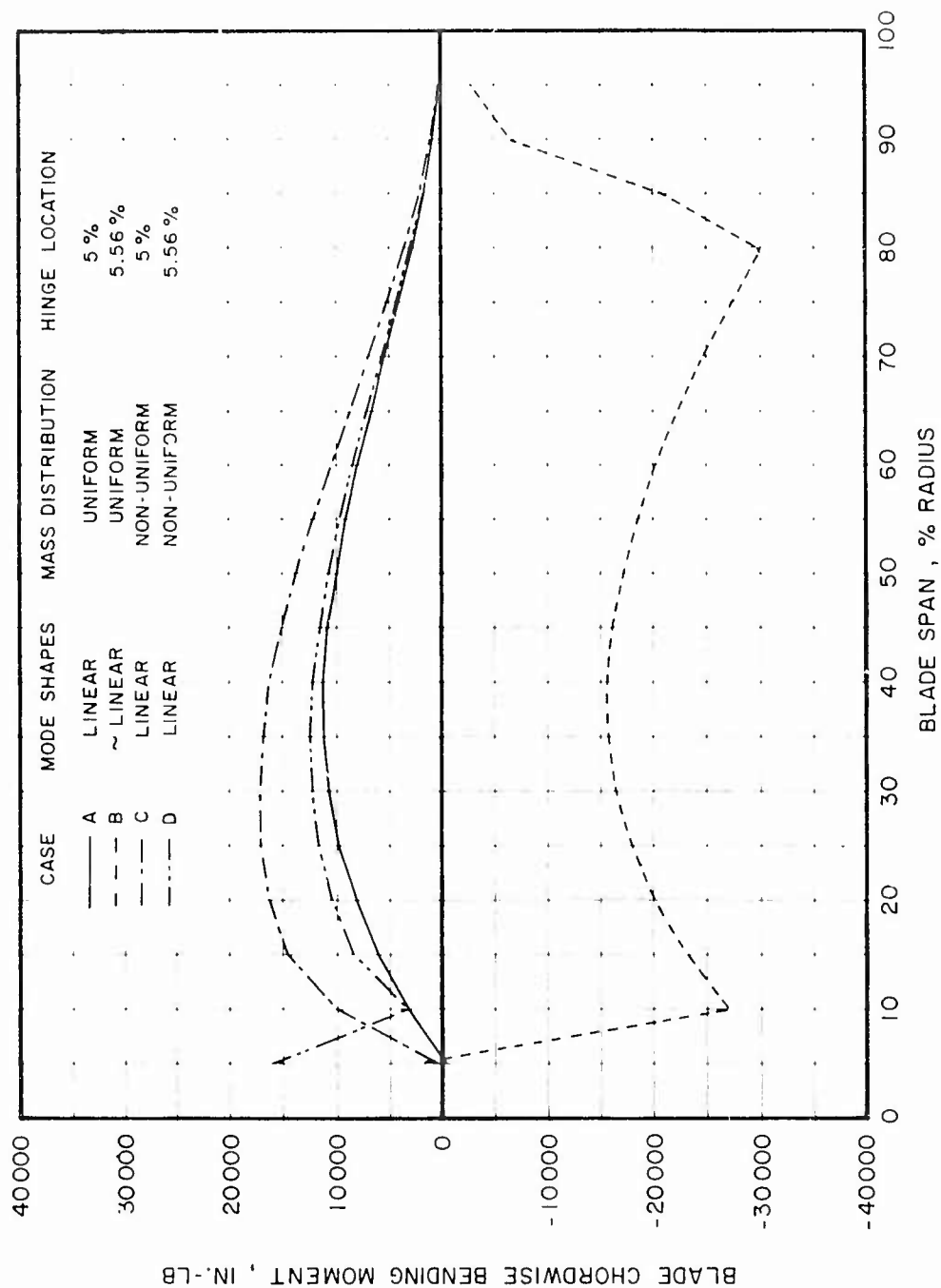


Figure 38. C81 Solutions of Blade Chordwise Bending Moment vs Span at $\psi_{MP} = 60$ Deg as Functions of Mode Shape, Hinge Offset, and Mass Distribution for the CH-53A in Hover at 32,550 Lb.

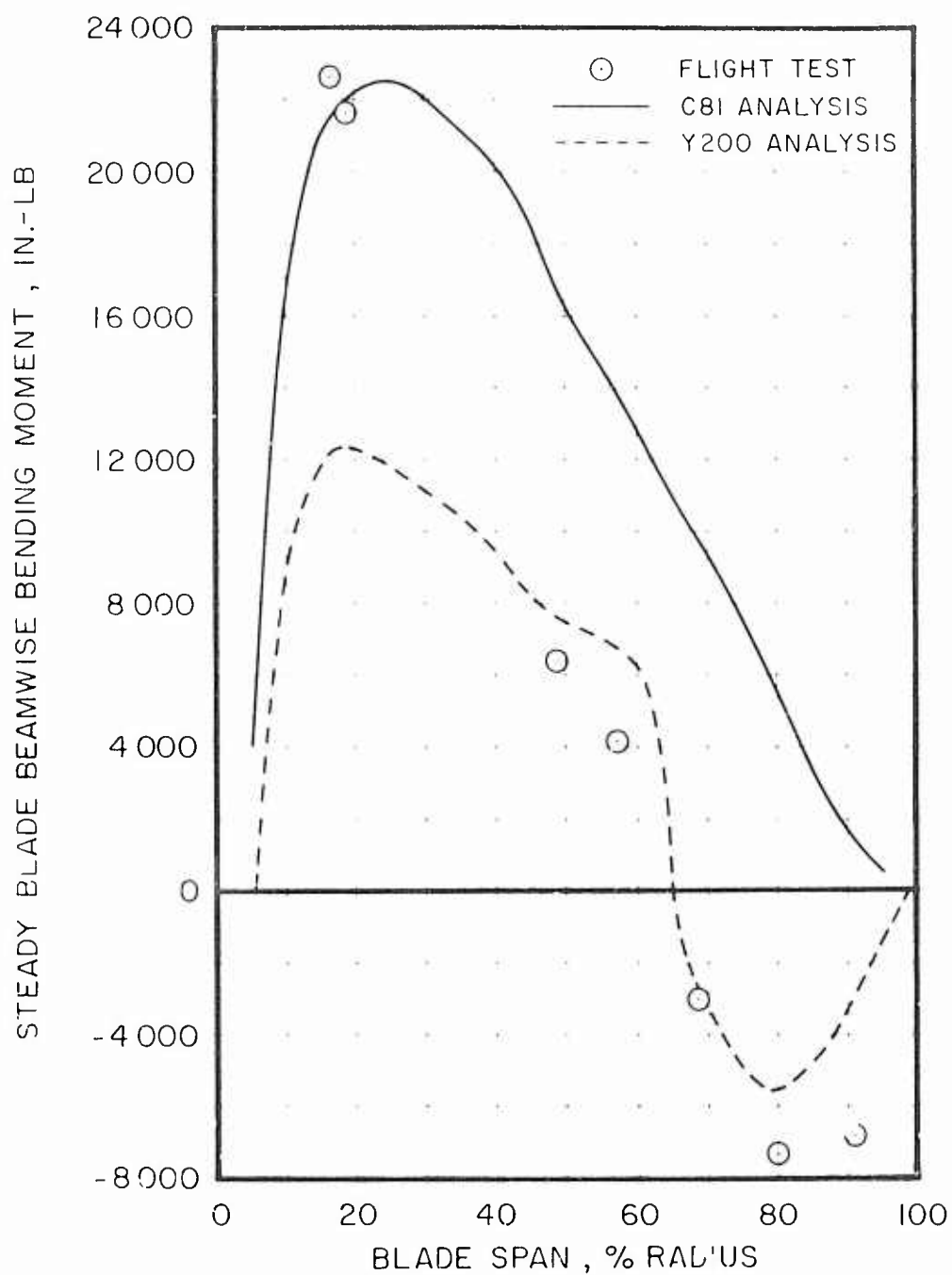


Figure 39. C81 Rotor Loads Solution of Blade Steady Beamwise Bending Moment vs Span, Compared With Flight Test and Y200 Analysis Data for the CH-53A at 159 Kt, 33,070 Lb (103% N_r , $h_d = 3000$ Ft, FSCG = 336, Level Flight).

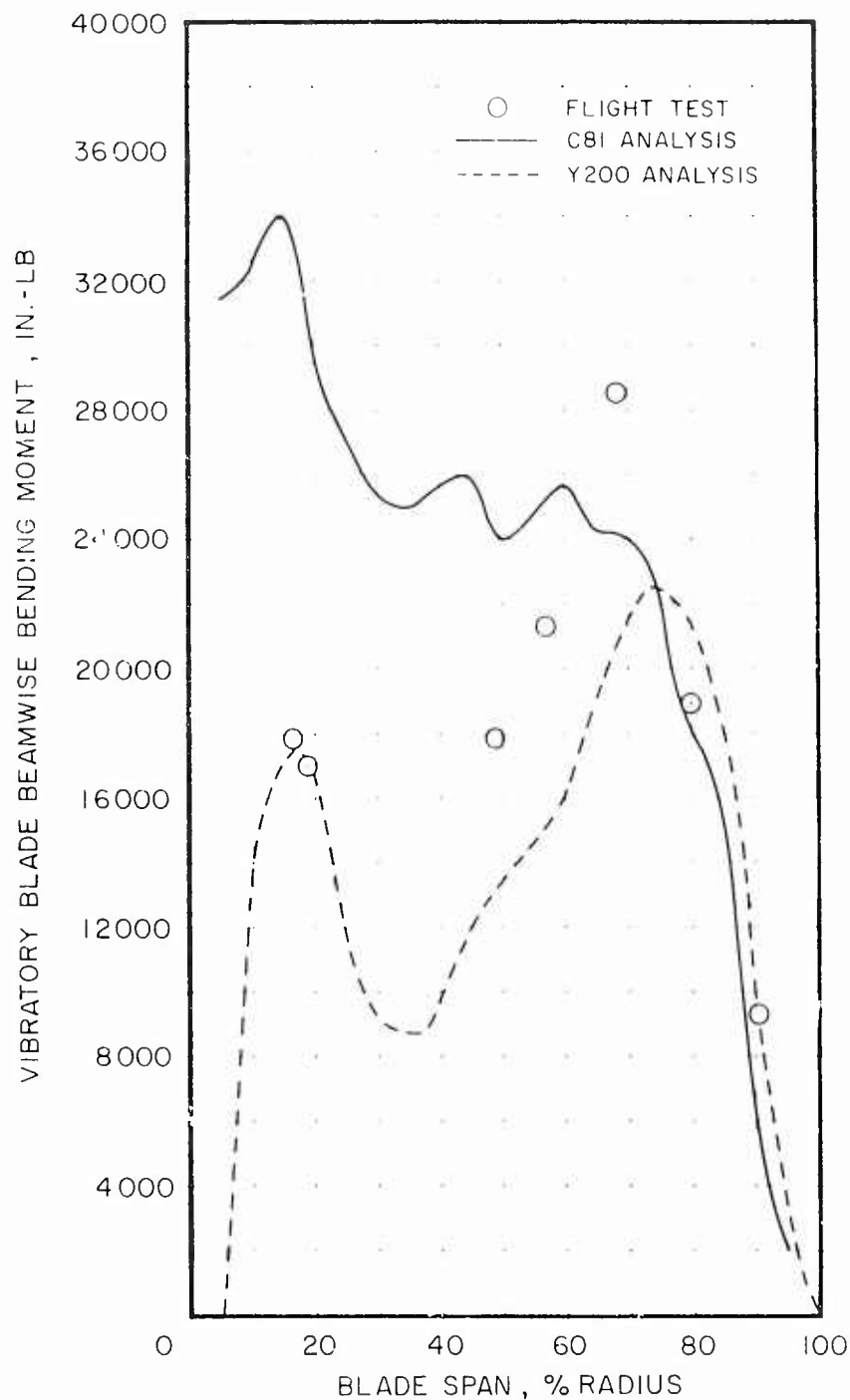


Figure 40. C81 Rotor Loads Solution of Blade Vibratory Beamwise Bending Moment vs Span, Compared With Flight Test and Y200 Analysis Data for the CH-53A at 159 Kt, 33,070 Lb (103% N_r , $h_d = 3000$ Ft, FSCG = 336, Level Flight).

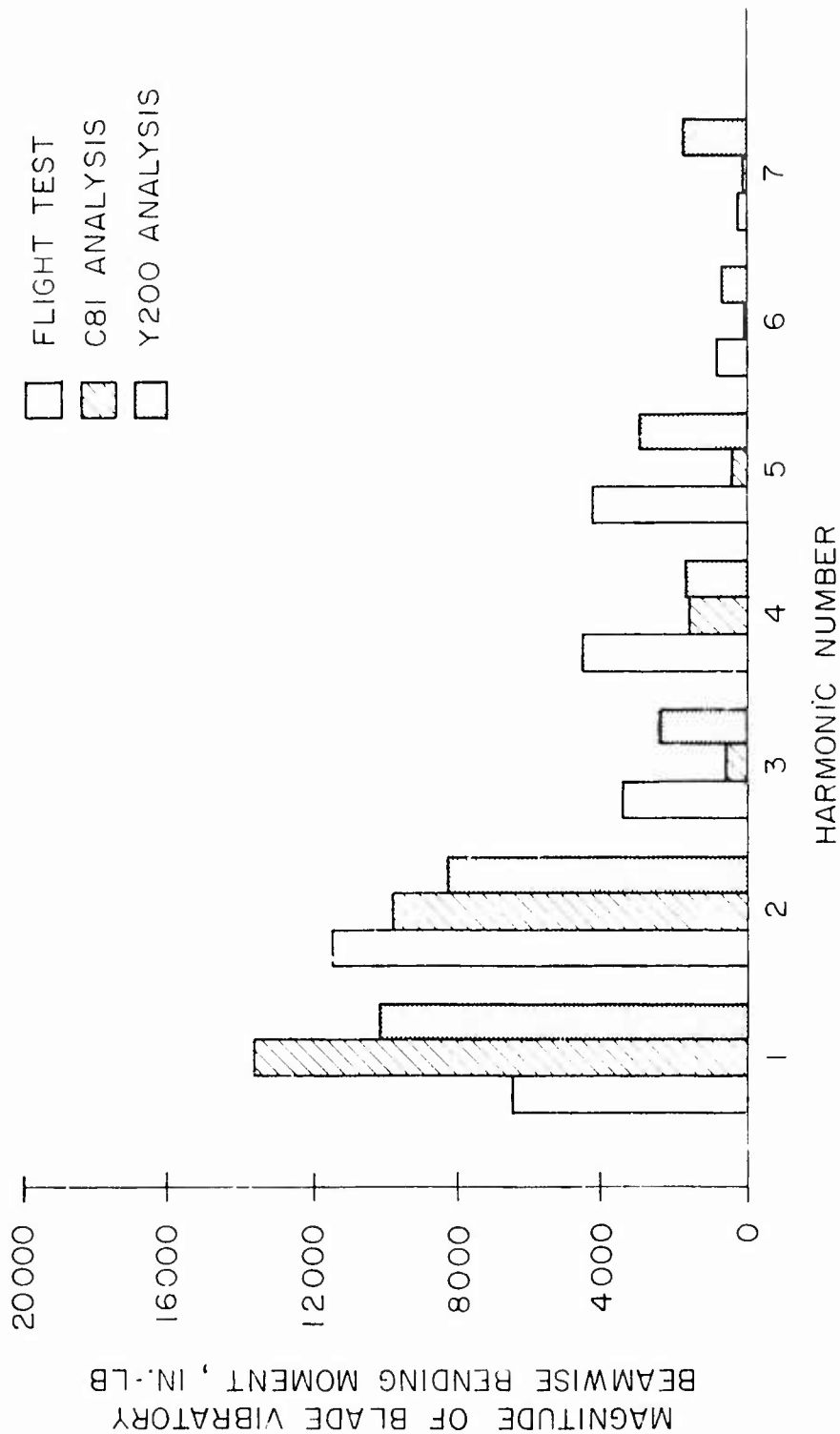


Figure 41. C81 Rotor Loads Solution of Harmonic Content of Blade Vibratory Beamwise Bending Moment at Approximately 80% Blade Span, Compared With Flight Test and Y200 Analysis Data for the CH-53A at 159 Kt, 33,070 Lb (103% N_r , $h_d = 3300$ Ft, FSCG = 336, Level Flight).

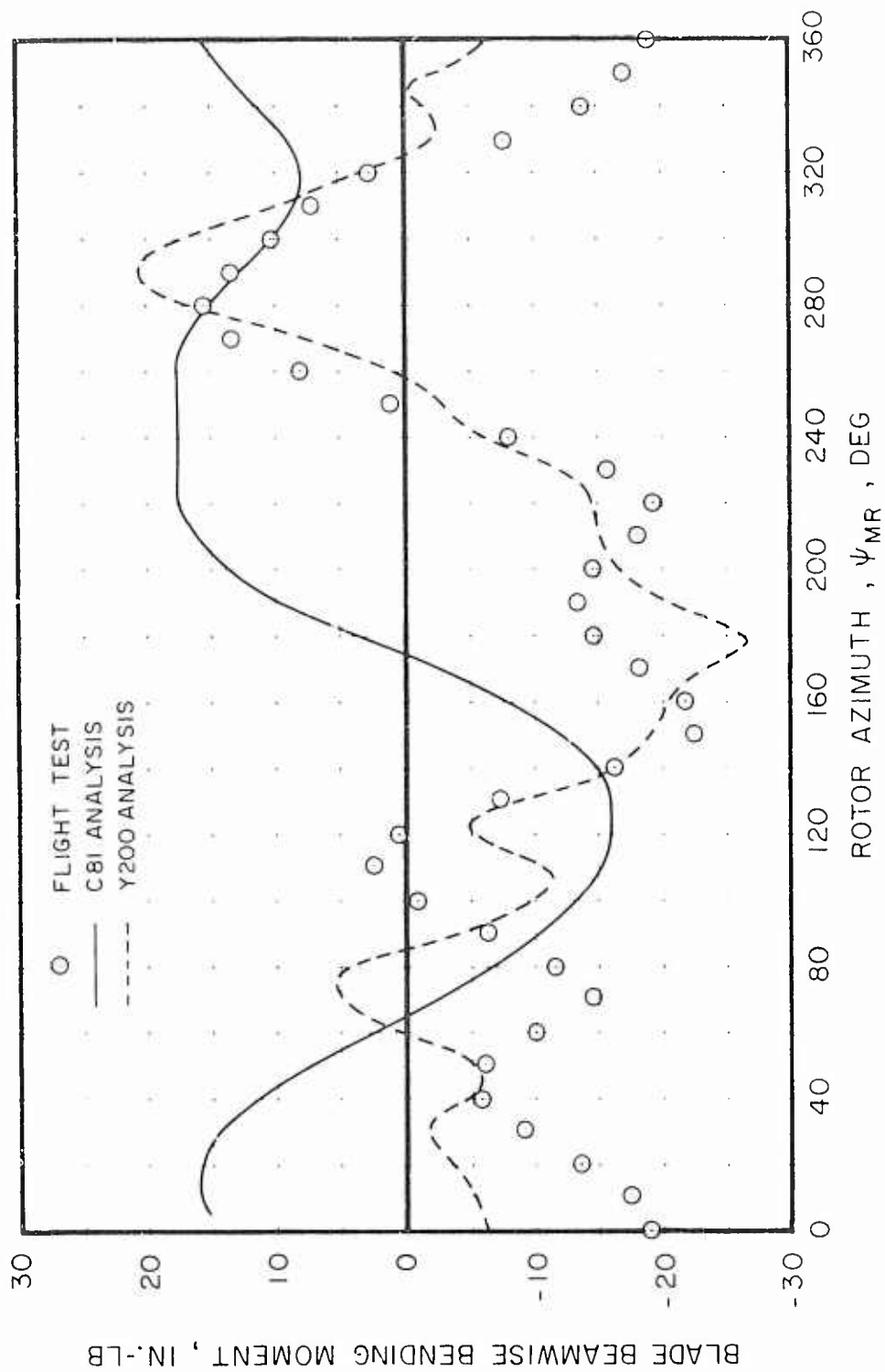


Figure 42. C81 Rotor Loads Time History Solution of Total Blade Beamwise Bending Moment at Approximately 80% Blade Span, Compared With Flight Test and Y200 Analysis Data for the CH-53A at 159 Kt, 33,070 Lb (103% N_r , $h_d = 3000$ Ft, FSCG = 336, Level Flight).

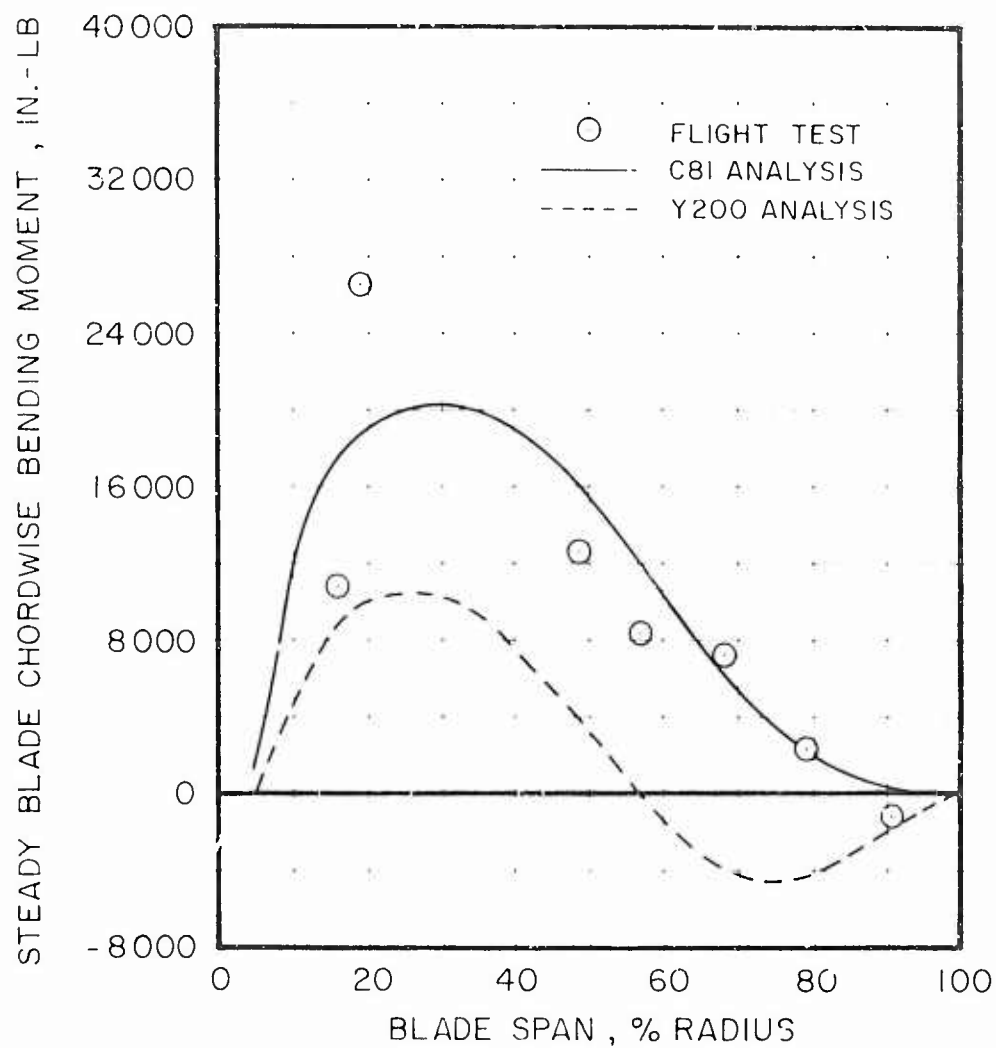


Figure 43. C81 Rotor Loads Solution of Blade Steady Chordwise Bending Moment vs Span, Compared With Flight Test and Y200 Analysis Data for the CH-53A at 159 Kt, 33,070 Lb (103% N_r , $h_d = 3000$ Ft, FSCG = 336, Level Flight).

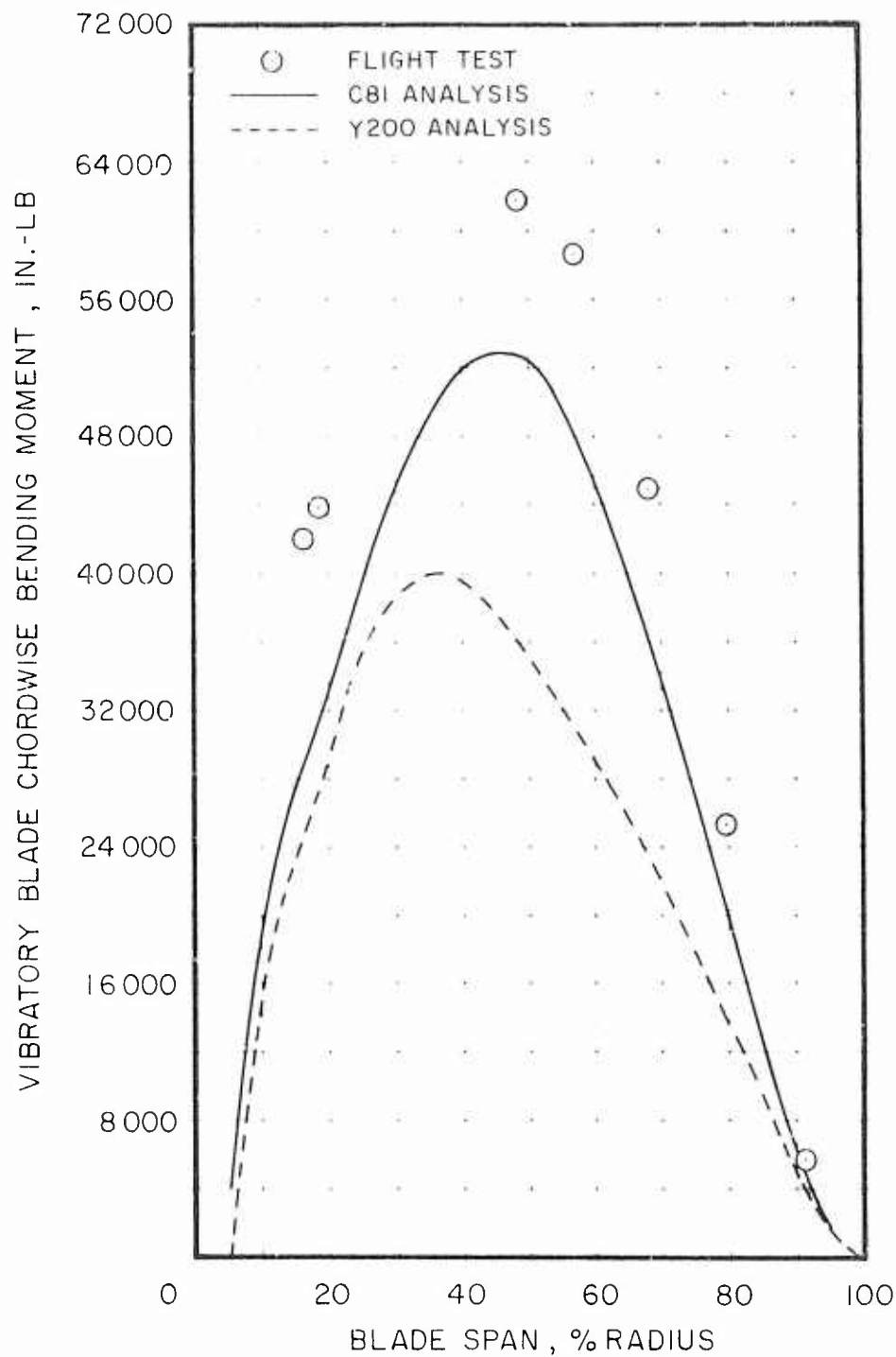


Figure 44. C81 Rotor Loads Solution of Blade Vibratory Chordwise Bending Moment vs Span, Compared With Flight Test and Y200 Analysis Data for the CH-53A at 159 Kt, 33,070 Lb (103% N_R , h_d = 3000 Ft, FSCG = 336, Level Flight).

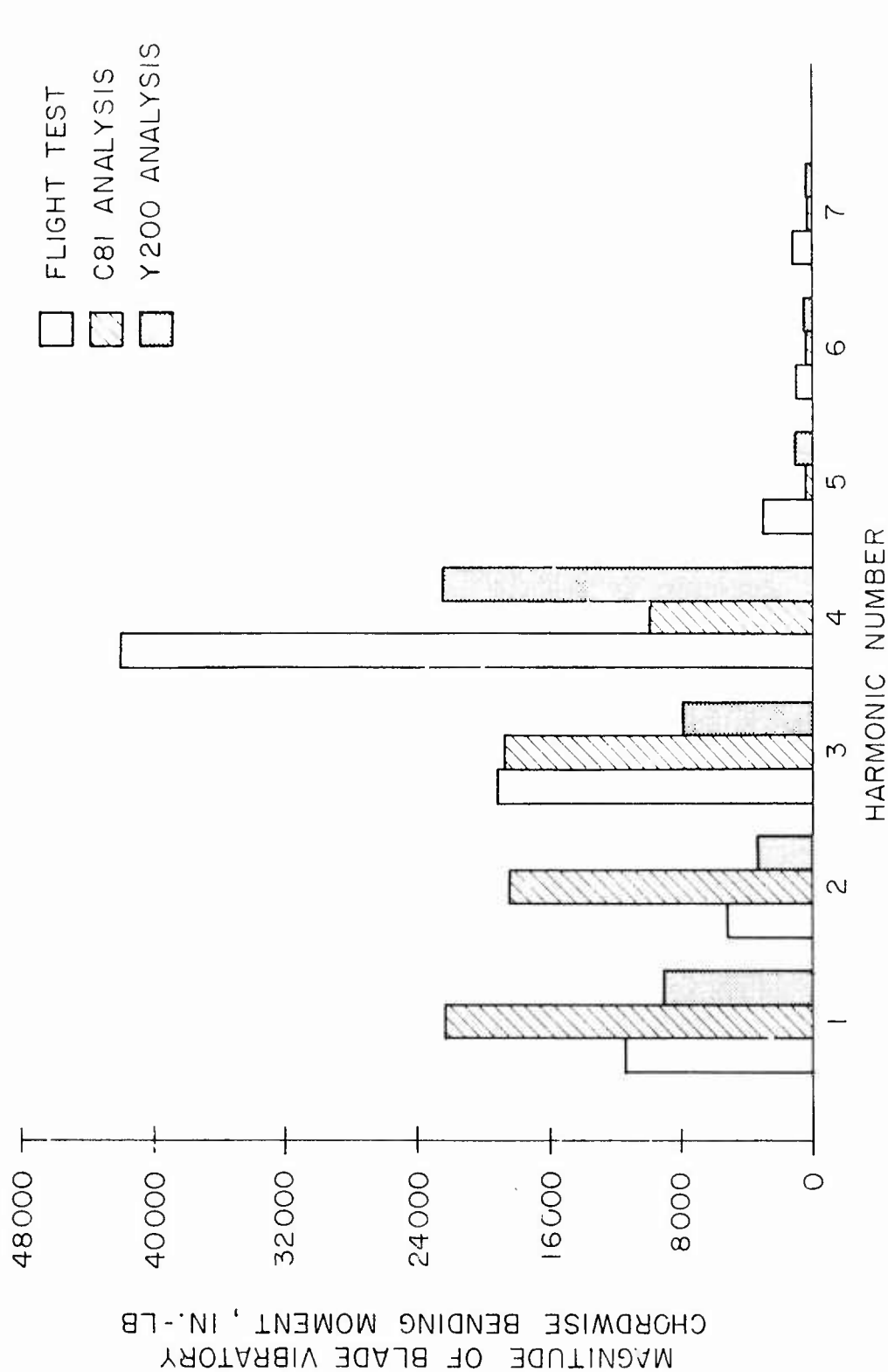


Figure 45. C81 Rotor Loads Solution of Harmonic Content of Blade Vibratory Chordwise Bending Moment at Approximately 55% Blade Span, Compared With Flight Test and Y200 Analysis Data for the CH-53A at 159 Kt, 33,070 Lb (103% N_r , $h_d = 3000$ Ft, FSCG = 336, Level Flight).

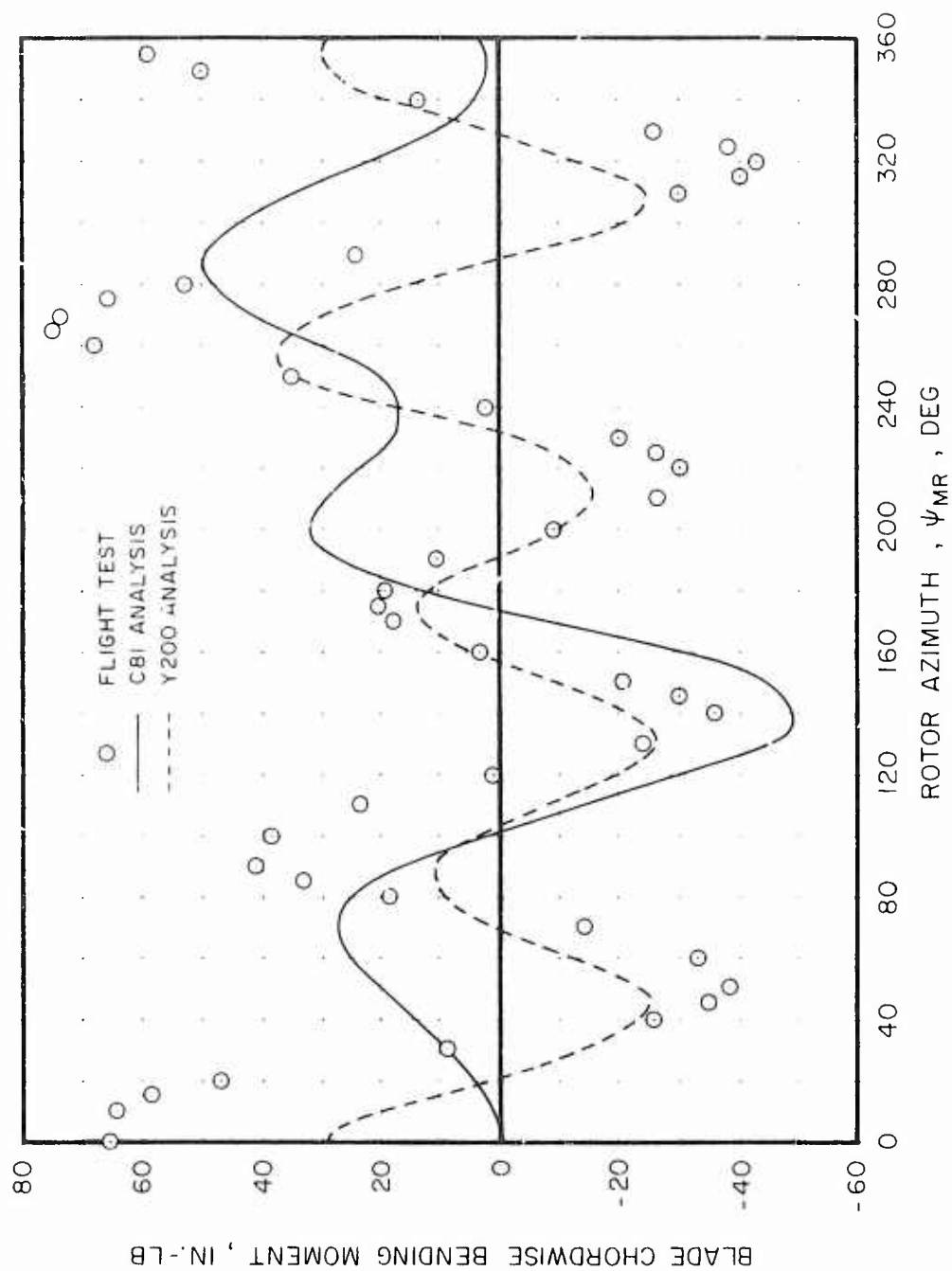


Figure 46. C81 Rotor Loads Time History Solution of Total Blade Chordwise Bending Moment at Approximately 55% Blade Span, Compared With Flight Test and Y200 Analysis Data for the CH-53A at 159 Kt, 33,070 Lb (103% N_r , $h_d = 3000$ Ft, FSCG = 336, Level Flight).

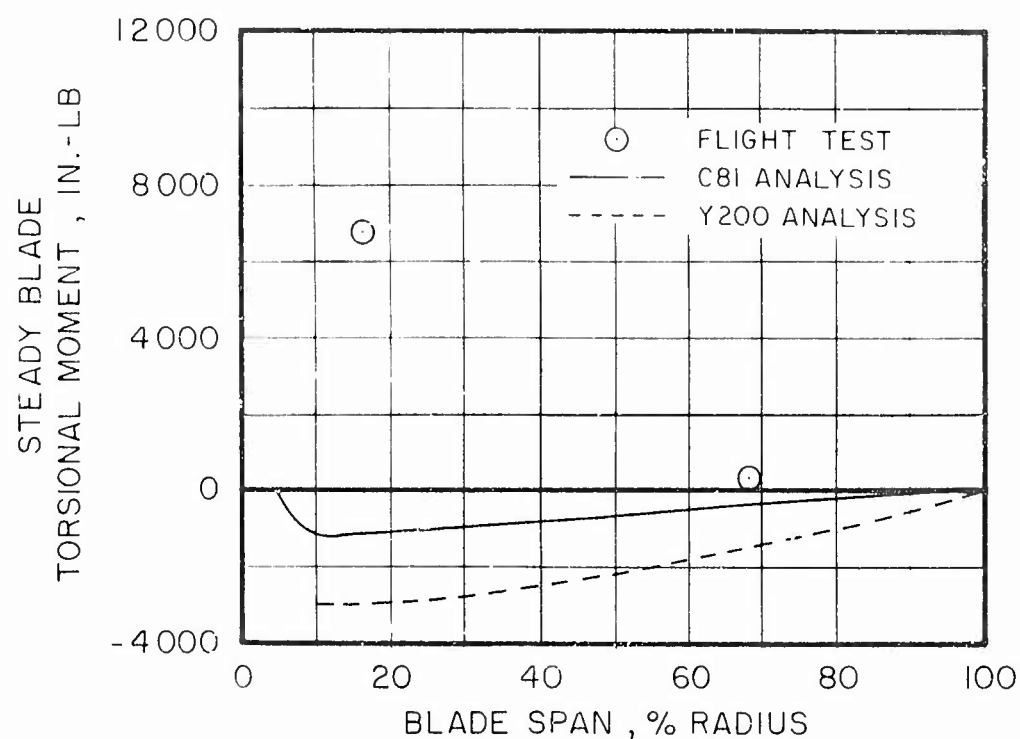


Figure 47. C81 Rotor Loads Solution of Blade Steady Torsional Moment vs Span, Compared With Flight Test and Y200 Analysis Data for the CH-53A at 159 Kt, 33,070 Lb (103% N_r , $h_d = 3000$ Ft, FSCG = 336, Level Flight).

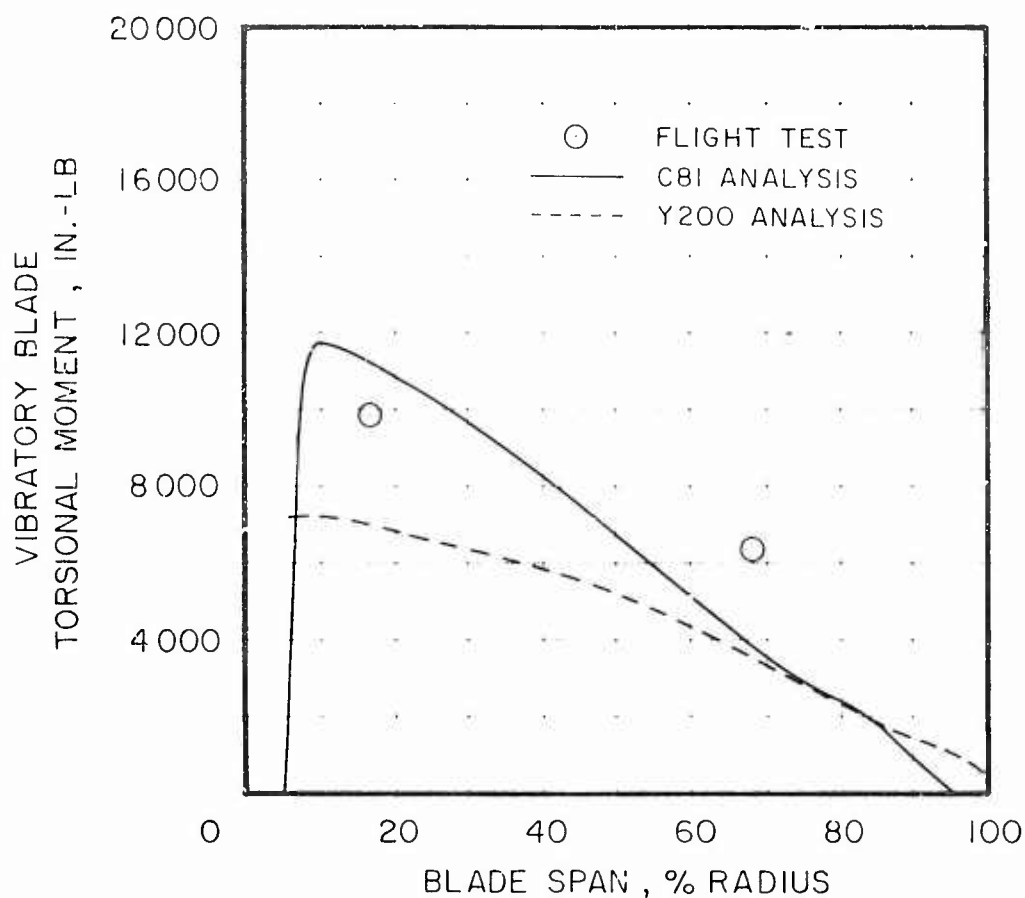


Figure 48. CBI Rotor Loads Solution of Blade Vibratory Torsional Moment vs Span, Compared With Flight Test and Y200 Analysis Data for the CH-53A at 159 Kt, 33,070 Lb (103% N_r , $h_d = 3000$ Ft, FSCG = 336, Level Flight).

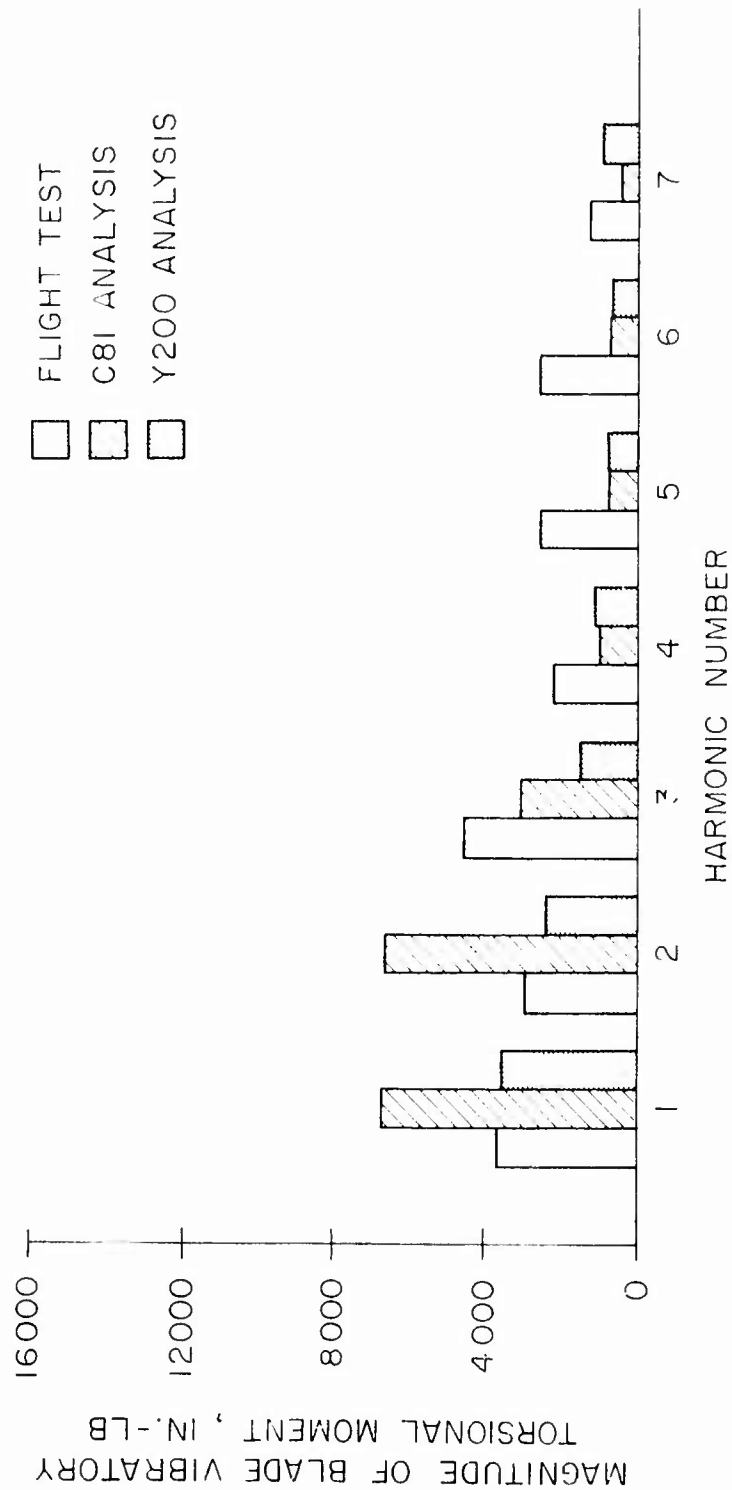


Figure 49. C81 Rotor Loads Solution of Harmonic Content of Blade Vibratory Torsional Moment at Approximately 15% Blade Span, Compared With Flight Test and Y200 Analysis Data for the CH-53A at 159 Kt, 33,070 Lb (103% N_r , h_d = 3000 Ft, FSCG = 336, Level Flight).

LIST OF SYMBOLS

a_o	rotor coning angle, deg
A_{1s}	main rotor lateral cyclic control, deg
a_1	rotor longitudinal flapping angle, deg
B_{1s}	main rotor longitudinal cyclic control, deg
b_1	rotor lateral flapping angle, deg
BL	buttline, in.
CG	center-of-gravity
C_p	rotor power coefficient
C_T	rotor thrust coefficient
C_W	rotor loading (weight) coefficient
FS	stationline (fuselage station), in.
FSCG	fuselage station center-of-gravity location relative to a fixed reference, in.
h_d	density altitude, ft
MR	main rotor
N_r	actual rotor speed referred to design rotor speed, pct
N_z	normal load factor at helicopter center of gravity, g's
n	notation for normal load factor in velocity - load factor plots, g's
p	helicopter roll angular velocity, deg/sec
Q	torque, ft-lb
q	helicopter pitch angular velocity, deg/sec
r	helicopter yaw angular velocity, deg/sec
TR	tail rotor
u	helicopter longitudinal velocity, ft/sec

V	helicopter total velocity, kt
v	helicopter lateral velocity, ft/sec
WL	waterline, in.
w	helicopter normal velocity, ft/sec
X	helicopter longitudinal body axis
Y	helicopter lateral body axis
Z	helicopter vertical body axis
α_F	fuselage angle of attack, deg
θ	helicopter body pitch attitude, deg
θ_{MR}	main rotor collective blade pitch control, deg
θ_{TR}	tail rotor blade pitch control, deg
μ	advance ratio: helicopter velocity over main rotor tip speed
ϕ	helicopter body roll attitude, deg
ψ	helicopter body yaw attitude, deg
ψ_{MR}	main rotor azimuth location of reference blade, deg
$(^\circ)$	denotes first derivative with respect to time
$(^{\circ\circ})$	denotes second derivative with respect to time
$()_{.75}$	denotes blade pitch angle at 75% rotor radius
$()_b$	denotes a parameter referenced to the helicopter body axis system
$()_{MR}$	denotes a main rotor parameter
$()_{TR}$	denotes a tail rotor parameter
$\Delta()$	denotes a change from the trim value of a parameter